PLACE IN RETURN BOX to remove this checkout from your record. **TO AVOID FINES** return on or before date due. **MAY BE RECALLED** with earlier due date if requested.

DATE DUE	<u>DATE DUE</u>	<u>DATE DUE</u>

6/01 c:/CIRC/DateDue.p65-p.15

A COMBINED CONVECTION COOKING AND SALMONELLA INACTIVATION MODEL FOR GROUND MEAT AND POULTRY PRODUCTS

by

Adam Edward Watkins

A DISSERTATION

Submitted to
Michigan State University
In partial fulfillment of the requirements
for the degree of

DOCTOR OF PHILOSOPHY

Department of Biosystems and Agricultural Engineering

2004

ABSTRACT

A COMBINED CONVECTION COOKING AND SALMONELLA INACTIVATION MODEL FOR GROUND MEAT AND POULTRY PRODUCTS

By

Adam Edward Watkins

A predictive model for moist-air impingement cooking of ground-and-formed meat and poultry products was developed. A coupled heat and mass transfer model incorporating the effects of fat transfer was combined with a model for *Salmonella* inactivation, to produce a complete prediction tool for meat and poultry processors. The model utilized the finite element method to numerically solve separate equations for heat, moisture, and fat transport. These equations were coupled through boundary conditions and interdependent thermo-physical property relationships. An enthalpy formulation for heat transfer was utilized to avoid discontinuities related to solid-to-liquid phase changes of water and fat within the product. Boundary conditions unique to moist-air impinging flow were incorporated into the model. These boundary conditions accounted for the additional heating effects of surface condensation that are common within moist air impingement systems.

To complete the fat transport component of the model, laboratory experiments were conducted to determine the fat holding capacity of ground beef as a function of temperature and initial fat content. Fat holding capacities ranged from 0.05 to 0.6 g fat/g nonfat dry matter, and a polynomial model was parameterized to those data.

Additionally, laboratory-scale, moist-air convection cooking tests were conducted to confirm the importance of fat transport. Species and initial fat content significantly affected (P<0.05) cooking time, yield, and fat loss for ground beef, pork, and turkey. The heating time required to reach 85°C varied by as much as 217 seconds between different fat contents of the same species. Differences in cooking yield of up to 18% were measured between different fat contents. Fat transport was responsible for up to 28% yield loss in high fat products.

Finally, cooking experiments using an industrial moist-air impingement cooking system were used to validate the temperature, moisture, and yield predictions of the complete cooking model. The cooking model predicted transient patty center temperatures with a standard error of prediction of 8.0°C for 54 cooking tests. At temperatures above 45°C, the standard error of the prediction was 5.8°C. The standard error for final moisture content predictions was 2.3% wet basis. Standard error for final cooking yield predictions was 6%. Additional comparisons were conducted between the cooking model and published data collected from moist-air impingement ovens. Data from published sources were used to perform a verification of the *Salmonella* inactivation predictions of the model. The standard error of prediction for *Salmonella* inactivation was 1.3 logs (CFU/g).

ACKNOWLEDGEMENTS

Funding for this project was provided by the United States Department of Agriculture National Needs Graduate Fellowship Program. Additional assistance was provided by the United States Department of Agriculture CSREES National Food Safety Initiative. Access to the JSO-IV impingement oven was provided by FMC FoodTech of Sandusky, OH. I would like to thank Mr. Bob Swackhamer, Dr. Nahed Kotrola, and Mr. Todd Gerold for assistance in arranging for and conducting tests with the JSO-IV oven. Of course this project would not have been possible without the support of my major professor, Dr. Brad Marks, the members of my committee, the members of our research team, and all of the people that have helped me here or there along the way. Special thanks go out to my family and friends who stood by me through the past four years.

TABLE OF CONTENTS

L	IST OF	TAI	BLES	viii
L	IST OF	FIG	URES	x
K	EY TO	SYN	MBOLS	xviii
1		INT	RODUCTION AND OBJECTIVES	1
	1.1	Bacl	kground	1
	1.2	Obje	ectives	4
2		REV	/IEW OF LITERATURE	5
	2.1	Intro	oduction	5
	2.2	Intro	oduction to cooking	5
	2.3	Heat	t and mass transfer in meat during cooking	6
	2.4	Mod	leling the cooking process	8
	2.4.	1	Empirical models	10
	2.4.	2	Models based upon heat and mass transfer principles	12
	2.4.	3	Contact cooking	14
	2.4.	4	Frying	20
	2.4.	5	Convection cooking	23
	2.4.	6	Other types of cooking	28
	2.5	Ther	rmal and physical properties required for modeling	31
	2.6	Mici	robial models	33
	2.6.	1	Primary models	34
	2.6.	2	Secondary models	35
	2.6.	3	Tertiary models	37
	2.7	Com	nbined models	38
	2.8	Limi	itations of models	40
	2.9	Sum	mary	41
3		MA	TERIALS AND EXPERIMENTAL METHODS	42
	3.1	Ove	rview	42
	3.2	Labo	oratory oven cooking tests	42

	3.2	.1 Experimental procedure	42
	3.2	.2 Statistical analysis	47
	3.3	Measurement of fat holding capacity	48
	3.3	.1 Experimental procedure	48
	3.3	.2 Statistical analysis	51
	3.4	Industrial oven cooking tests	52
	3.4	.1 Experimental procedure	52
	3.4	.2 Statistical analysis	56
	3.5	Cooking model validation	56
	3.5	.1 Cooking model	56
	3.5	.2 Experimental data	57
	3.5	.3 Comparisons with literature data	58
	3.6	Salmonella inactivation model validation	59
4		MODEL DEVELOPMENT	61
	4.1	Introduction	61
	4.2	Heat and mass transfer model	64
	4.2	.1 Heat transfer solution	64
	4.2	.2 Moisture transfer solution	67
	4.2	.3 Fat transfer solution	70
	4.2	.4 Heat and mass transfer coefficients – Array of slot nozzles	71
	4.2	.5 Heat and mass transfer coefficients – array of round nozzles	74
	4.3	Microbial inactivation model	76
	4.4	Finite element formulation	77
	4.4	.1 Introduction	77
	4.4	.2 Finite element basics	77
	4.4	.3 Governing equations	79
	4.4	.4 Finite difference time solution	86
	4.4	.5 Application of FEM solution	87
	4.4	.6 User interface	88
5		RESULTS AND DISCUSSION	
	5.1	Overview	
	5.2	Laboratory oven cooking tests	

5.	2.1	Cooking time	90
5.	2.2	Cooking yield	95
5.	2.3	Fat loss	99
5.	2.4	Volume change	103
5.3	Fat l	nolding capacity experiments	107
5.	3.1	Low fat samples (5.6% initial fat wet basis)	108
5.	3.2	High fat samples (15% initial fat wet basis)	114
5.	3.3	Summary	123
5.4	Indu	strial cooking tests	124
5.	4.1	Cooking time	124
5.	4.2	Cooking yield	129
5.	4.3	Fat loss	130
5.	4.4	Volume change	132
5.5	Cool	king model validation	134
5.	5.1	Finite element mesh	134
5.	5.2	Temperature profile-experimental data	135
5.	5.3	Temperature profile-published data	143
5.	5.4	Moisture content- experimental data	145
5.	5.5	Cooking yield – experimental data	146
5.	5.6	Cooking yield – published data	148
5.6	Leth	ality model validation	148
5.7	Illus	tration of model utility	151
	CON	ICLUSIONS	155
	FUT	URE WORK	158
	APP	ENDICES	161
8.1	Mod	el and experimental temperature versus time curves for moist-air	
	impi	ngement cooking of ground beef patties	162
8.2	Deri	vation of cooking-air thermo-physical property equations	189
8.3		uct thermo-physical properties	
8.4	Scre	en shots from Visual Basic cooking model user interface	201
8.5	Visu	al Basic model code	203
	BIBI	JOGRAPHY	255

9

LIST OF TABLES

Table 3.1. Treatment conditions utilized for model validation experiments54
Table 5.1 – Analysis of variance for cooking time of ground turkey patties as affected by temperature and fat content
Table 5.2 - Analysis of variance for cooking time of ground beef patties as affected by temperature and fat content
Table 5.3 - Analysis of variance for cooking time of ground pork patties as affected by temperature and fat content
Table 5.4 – Analysis of variance of yield as a function of center temperature and fat content for ground turkey patties
Table 5.5 - Analysis of variance of yield as a function of center temperature and fat content for ground beef patties96
Table 5.6 - Analysis of variance of yield as a function of center temperature and fat content for ground pork patties
Table 5.7 – Analysis of variance for fat loss as functions of center temperature and fat content for ground turkey patties
Table 5.8 – Analysis of variance for fat loss as functions of center temperature and fat content for ground beef patties
Table 5.9 – Analysis of variance for fat loss as functions of center temperature and fat content for ground pork patties
Table 5.10 – Analysis of variance for effects of temperature and initial fat content on volume change for ground turkey patties cooked in a laboratory convection oven103
Table 5.11 – Analysis of variance for effects of temperature and initial fat content on volume change for ground beef patties cooked in a laboratory convection oven104
Table 5.12 – Analysis of variance for effects of temperature and initial fat content on volume change for ground pork patties cooked in a laboratory convection oven106
Table 5.13 – Results from regression of fat holding capacity as functions of time and holding temperature for 5.6% fat ground beef.

Table 5.14 – Results from regression of fat holding capacity versus holding temperature for 5.6% fat ground beef
Table 5.15 – Results from regression of fat holding versus time and holding temperature for 15% fat ground beef
Table 5.16 – Results of regression of fat holding capacity versus holding temperature for 15% fat ground beef
Table 5.17 – Linear regression of fat holding capacity as functions of heating temperature, holding time, and initial fat content
Table 5.18 - Linear regression of holding capacity as a function of holding temperature and fat content
Table 5.19 – Linear regression of patty center temperature as functions of oven temperature, steam content, cooking time, and oven airflow
Table 5.20 – Regression parameters for cooking yield as a function of oven temperature, steam content, cooking time, and airflow
Table 5.21 – Regression parameters for cooking yield as a function of oven temperature, steam content, cooking time, and airflow
Table 5.22 – Standard error of prediction for the entire trial (SEP) and for data above 45°C (SEP _{T>45°C}) for center temperature of beef patties142
Table 5.23. Standard error of prediction for transient center temperature of ground chicken breast patties predicted by the model and by the regression equation of Murphy et al. (2001a)
Table 5.24 – Difference between measured and predicted moisture content for each oven condition. Experiment numbers correspond to the conditions listed in Table 3.1145
Table 5.25 – Difference between measured and predicted cooking yields for each oven condition. Experiment numbers correspond to the conditions in Table 3.1146

LIST OF FIGURES

Figure 3.1 – General arrangement of the laboratory convection oven showing directions of steam and airflow	43
Figure 3.2 - Interior of laboratory oven showing conditioning chamber	43
Figure 3.3 - Interior of laboratory oven showing fan, ducts, and sample chamber (located at left)	44
Figure 3.4 – (a) Picture and (b) schematic of jig used to place thermocouples into meat patties during cooking experiments	46
Figure 3.5 – Schematic of tube setup used for centrifuging	50
Figure 3.6 – Schematic of the centrifuge tube after centrifuging showing the two distinct layers that formed within the tube. In this schematic the heating tube has been removed.	51
Figure 3.7 – Stein model JSO-IV moist-air impingement oven	
1 igure 5.7 — Stein model 350-1 v moist-an impingement oven	55
Figure 4.1 - Illustration of the airflow within an impingement oven in relation to the product.	62
Figure 4.2 – Geometry of a patty illustrating radial coordinate system	65
Figure 4.3 - Geometry of a ground meat patty with the modeled region and element mesh indicated	78
Figure 4.4 - Illustration of the finite element mesh utilized for the model	78
Figure 4.5 – Illustration of a triangular element showing counterclockwise node numbering	81
Figure 5.1 – Center temperature as a function of cooking time for ground turkey patties cooked in a laboratory convection oven: means of 5 replicates	90
Figure 5.2 – Center temperature as a function of cooking time for ground beef patties cooked in a laboratory convection oven: means of 5 replicates	91
Figure 5.3 – Center temperature as a function of cooking time for ground beef patties cooked in a laboratory convection oven: means of 5 replicates	91

Figure 5.4 – Yield as a function of endpoint center temperature for ground turkey patties of two fat contents: means of 5 replicates96
Figure 5.5 - Yield as a function of endpoint center temperature for ground beef patties of two fat contents: means of 5 replicates
Figure 5.6 - Yield as a function of endpoint center temperature for ground pork patties of two fat contents: means of 5 replicates98
Figure 5.7 – Fat loss as a function of temperature for ground turkey patties of two fat contents: means of 5 replicates
Figure 5.8 - Fat loss as a function of temperature for ground beef patties of two fat contents: means of 5 replicates
Figure 5.9 - Fat loss as a function of temperature for ground pork patties of two fat contents: means of 5 replicates
Figure 5.10 – Relationship between product temperature and volume change for ground turkey patties cooked in a laboratory convection oven: means of 5 replicates
Figure 5.11 – Relationship between product temperature and volume change for ground beef patties cooked in a laboratory convection oven: means of 5 replicates
Figure 5.12 – Relationship between product temperature and volume change for ground pork patties cooked in a laboratory convection oven: means of 5 replicates
Figure 5.13 – Fat holding capacity as a function of temperature for 5.6% fat ground beef heated for 2 minutes at temperatures from 30 to 90°C: means of 5 replicates
Figure 5.14 – Fat holding capacity as a function of temperature for 5.6% fat ground beef heated for 5 minutes at temperatures from 30 to 90°C: means of 5 replicates
Figure 5.15 – Fat holding capacity as a function of temperature for 5.6% fat ground beef heated for 10 minutes at temperatures from 30 to 90°C: means of 5 replicates
Figure 5.16 – Fat holding capacity as a function of temperature for 5.6% fat ground beef heated for 15 minutes at temperatures from 30 to 90°C: means of 5 replicates

Figure 5.17 – Comparison of fat holding capacity calculated from regression model versus experimental values: means of 5 replicates
Figure 5.18 – Fat holding capacity as a function of temperature for 15% fat ground beef heated for 2 minutes at temperatures from 30 to 90°C: means of 5 replicates
Figure 5.19 - Fat holding capacity as a function of temperature for 15% fat ground beef heated for 5 minutes at temperatures from 30 to 90°C: means of 5 replicates
Figure 5.20 – Fat holding capacity as a function of temperature for 15% fat ground beef heated for 10 minutes at temperatures from 30 to 90°C: means of 5 replicates
Figure 5.21 – Fat holding capacity as a function of temperature for 15% fat ground beef heated for 15 minutes at temperatures from 30 to 90°C: means of 5 replicates
Figure 5.22 - Comparison of fat holding capacity calculated from regression model versus experimental values (15% fat): means of 5 replicates
Figure 5.23 – Comparison of fat holding capacity calculated from regression model versus experimental values: means of 5 replicates
Figure 5.24 – Bottom and center temperature versus time for ground beef patties cooked at (a) oven temperature: 121°C, oven steam content: 50% by volume, oven airflow: 11.4 m/s and (b) oven temperature: 232°C, oven steam content: 50% by volume, oven airflow: 16.8 m/s
Figure 5.25 - Cooking yield as a function of endpoint center temperature for ground beef patties cooked in a Stein JSO-IV industrial moist air impingement oven129
Figure 5.26 - Yield loss not accounted for by moisture loss as a function of endpoint temperature for ground beef patties cooked in a Stein JSO-IV industrial moist-air impingement oven
Figure 5.27 – Reduction in diameter during cooking as a function of cooking yield for ground beef patties cooked in a Stein JSO-IV industrial moist-air impingement oven
Figure 5.28 – Example comparison of experimental temperature data with data generated by the model (oven temperature=121°C, steam content=50%, air velocity =11.4 m/s)

Figure 5.29 – Example comparison of experimental temperature data with data generated by the model (oven temperature=121°C, steam content=70%, air velocity =11.4 m/s)
Figure 5.30 – Example comparison of experimental temperature data with data generated by the model (oven temperature=121°C, steam content=88%, air velocity =11.4 m/s)
Figure 5.31 – Comparison between model Salmonella Senftenberg lethality predictions and data points published by Murphy et al. (2002)148
Figure 5.32 – Comparison between model <i>Listeria innocua</i> lethality predictions and data points published by Murphy et al. (2002)
Figure 8.1 – Oven temperature: 121°C, oven steam content: 50% by volume, oven airflow: 11.4 m/s (Experiment 1a)
Figure 8.2 – Oven temperature: 121°C, oven steam content: 50% by volume, oven airflow: 11.4 m/s (Experiment 1b)
Figure 8.3 – Oven temperature: 121°C, oven steam content: 50% by volume, oven airflow: 16.8 m/s (Experiment 6a)
Figure 8.4 – Oven temperature: 121°C, oven steam content: 50% by volume, oven airflow: 16.8 m/s (Experiment 6b)
Figure 8.5 – Oven temperature: 121°C, oven steam content: 50% by volume, oven airflow: 21.8 m/s (Experiment 8a)
Figure 8.6 - Oven temperature: 121°C, oven steam content: 50% by volume, oven airflow: 21.8 m/s (Experiment 8b)
Figure 8.7 – Oven temperature: 121°C, oven steam content 70% by volume, oven airflow: 11.4 m/s (Experiment 11a)
Figure 8.8 – Oven temperature: 121°C, oven steam content 70% by volume, oven airflow: 11.4 m/s (Experiment 11b)
Figure 8.9 – Oven temperature: 121°C, oven steam content: 70% by volume, oven airflow: 16.8 m/s (Experiment 13a)
Figure 8.10 – Oven temperature: 121°C, oven steam content: 70% by volume, oven airflow: 16.8 m/s (Experiment 13b)
Figure 8.11 – Oven temperature: 121°C, oven steam content: 70% steam volume, oven airflow: 21.8 m/s (Experiment 18a)

Figure 8.12 – Oven temperature: 121°C, oven steam content: 70% steam volume, oven airflow: 21.8 m/s (Experiment 18b)
Figure 8.13 - Oven temperature: 121°C, oven steam content: 88% by volume, oven airflow: 11.4 m/s (Experiment 21a)
Figure 8.14 - Oven temperature: 121°C, oven steam content:88% by volume, oven airflow: 11.4 m/s (Experiment 21b)
Figure 8.15 – Oven temperature: 121°C, oven steam content: 78% by volume, oven airflow: 16.8 m/s (Experiment 23a)
Figure 8.16 – Oven temperature: 121°C, oven steam content: 78% by volume, oven airflow: 16.8 m/s (Experiment 23b)
Figure 8.17 – Oven temperature: 121°C, oven steam content: 78% by volume, oven airflow: 21.8 m/s (Experiment 25a)
Figure 8.18 – Oven temperature: 121°C, oven steam content: 78% by volume, oven airflow: 21.8 m/s (Experiment 25b)
Figure 8.19 - Oven temperature: 177°C, oven steam content: 50% by volume, oven airflow: 11.4 m/s (Experiment 30a)
Figure 8.20 - Oven temperature: 177°C, oven steam content: 50% by volume, oven airflow: 11.4 m/s (Experiment 30b)
Figure 8.21 – Oven temperature: 177°C, oven steam content: 50% by volume, oven airflow: 16.8 m/s (Experiment 32a)
Figure 8.22 – Oven temperature: 177°C, oven steam content: 50% by volume, oven airflow: 16.8 m/s (Experiment 32b)
Figure 8.23 - Oven temperature: 177°C, oven steam content: 50% by volume, oven airflow: 21.8 m/s (Experiment 34a)
Figure 8.24 - Oven temperature: 177°C, oven steam content: 50% by volume, oven airflow: 21.8 m/s (Experiment 34b)
Figure 8.25 – Oven temperature: 177°C, oven steam content: 70% by volume, oven airflow: 11.4 m/s (Experiment 37a)
Figure 8.26 – Oven temperature: 177°C, oven steam content: 70% by volume, oven airflow: 11.4 m/s (Experiment 37b)

Figure 8.27 - Oven temperature: 177°C, oven steam content: 83% by volume, oven airflow: 11.4 m/s (Experiment 47a)
Figure 8.28 - Oven temperature: 177°C, oven steam content: 83% by volume, oven airflow: 11.4 m/s (Experiment 47b)
Figure 8.29 - Oven temperature: 177°C, oven moisture content: 84% by volume, oven airflow: 16.8 m/s (Experiment 49a)
Figure 8.30 - Oven temperature: 177°C, oven moisture content: 84% by volume, oven airflow: 16.8 m/s (Experiment 49b)
Figure 8.31 - Oven temperature: 177°C, oven steam content: 86% by volume, oven airflow: 16.8 m/s (Experiment 50a)
Figure 8.32 - Oven temperature: 177°C, oven steam content: 86% by volume, oven airflow: 16.8 m/s (Experiment 50b)
Figure 8.33 - Oven temperature: 177°C, oven steam content: 86% by volume, oven airflow: 21.8 m/s (Experiment 54a)
Figure 8.34 - Oven temperature: 177°C, oven steam content: 86% by volume, oven airflow: 21.8 m/s (Experiment 54b)
Figure 8.35 – Oven temperature: 232°C, oven steam content: 50% by volume, oven airflow: 11.4 m/s (Experiment 56a)
Figure 8.36 – Oven temperature: 232°C, oven steam content: 50% by volume, oven airflow: 11.4 m/s (Experiment 56b)
Figure 8.37 - Oven temperature: 232°C, oven steam content: 50% by volume, oven airflow: 16.8 m/s (Experiment 58a)
Figure 8.38 - Oven temperature: 232°C, oven steam content: 50% by volume, oven airflow: 16.8 m/s (Experiment 58b)
Figure 8.39 - Oven temperature: 232°C, oven steam content: 50% by volume, oven airflow: 21.8 m/s (Experiment 63a)
Figure 8.40 - Oven temperature: 232°C, oven steam content: 50% by volume, oven airflow: 21.8 m/s (Experiment 63b)
Figure 8.41 - Oven temperature: 232°C, oven steam content: 70% by volume, oven airflow: 11.4 m/s (Experiment 66a)

Figure 8.42 - Oven temperature: 232°C, oven steam content: 70% by volume, oven airflow: 11.4 m/s (Experiment 66b)
Figure 8.43 - Oven temperature: 232°C, oven steam content: 70% by volume, oven airflow: 16.8 m/s (Experiment 68a)
Figure 8.44 - Oven temperature: 232°C, oven steam content: 70% by volume, oven airflow: 16.8 m/s (Experiment 68b)
Figure 8.45 - Oven temperature: 232°C, oven steam content: 70% by volume, oven airflow: 21.8 m/s (Experiment 70a)
Figure 8.46 - Oven temperature: 232°C, oven steam content: 70% by volume, oven airflow: 21.8 m/s (Experiment 70b)
Figure 8.47 - Oven temperature: 232°C, oven steam content: 82% by volume, oven airflow: 11.4 m/s (Experiment 73a)
Figure 8.48 - Oven temperature: 232°C, oven steam content: 82% by volume, oven airflow: 11.4 m/s (Experiment 73b)
Figure 8.49 – Oven temperature: 232°C, oven steam content: 82% by volume, oven airflow: 11.4 m/s (Experiment 75a)
Figure 8.50 – Oven temperature: 232°C, oven steam content: 82% by volume, oven airflow: 11.4 m/s (Experiment 75b)
Figure 8.51 – Oven temperature: 232°C, oven steam content: 82% by volume, oven airflow: 16.8 m/s (Experiment 78a)
Figure 8.52 – Oven temperature: 232°C, oven steam content: 82% by volume, oven airflow: 16.8 m/s (Experiment 78b)
Figure 8.53 – Oven temperature: 232°C, oven steam content: 82% by volume, oven airflow: 21.8 m/s (Experiment 80a)
Figure 8.54 – Oven temperature: 232°C, oven steam content: 82% by volume, oven airflow: 21.8 m/s (Experiment 80b)
Figure 8.55 - Latent heat of vaporization for water as a function of temperature
(From tabular data: Geankoplis, 1993)189
Figure 8.56 - Viscosity of air as a function of temperature (From tabular data: Geankoplis, 1993)190

Figure 8.57 - Viscosity of steam as a function of temperature (From tabular data: Geankoplis, 1993)	.191
Figure 8.58 - Density of air as a function of temperature (from tabular data:	
Geankoplis, 1993)	.193
Figure 8.59 - Density of saturated steam as a function of temperature (From tabular data: Geankoplis, 1993)	194
Figure 8.60 - Density of steam at 101.35 kPa as a function of temperature (From	
tabular data: Geankoplis, 1993)	195
Figure 8.61 - Thermal conductivity of air as a function of temperature (From tabular data: Geankoplis, 1993)	.196
Figure 8.62 - Thermal conductivity of steam as a function of temperature (From tabular data: Geankoplis, 1993)	.197
Figure 8.63 – Input screen of cooking model user interface	201
Figure 8.64 – Output screen of cooking model user interface	.202

KEY TO SYMBOLS

Lower-case letters

a	Equation constant
b	Equation constant
c	Equation constant
C _m	Mass capacity (g/g)
C_p	Heat capacity (J/g.°C)
ď	Equation constant (Equation [2.2])
d	Diameter (cm)
e	Equation constant
f	Equation constant
h_{eff}	Effective heat transfer coefficient (W/cm ² .°C)
h _m	Mass transfer coefficient (cm/s)
\mathbf{h}_{T}	Heat transfer coefficient (W/cm ² °C)
k	Inactivation rate constant (1/s)
k_f	Fat conductivity (g/s·cm)
k _m	Moisture conductivity (g/s·cm)
\mathbf{k}_{T}	Thermal conductivity (W/cm·K)
1	Length (cm)
m	Moisture content – decimal dry basis
n	Mass flux (g/s·cm ²)
n	Normal direction (cm) (Equation [4.4])
q	Heat flux (W/cm ²)
r	Length, r-direction (radial coordinates) (cm)
S	Position (cm)
t	Time (s)
v	Air velocity (cm/s)
w	Slot width (cm)
X	Length, x-direction (cm)
у	Length, y-direction (cm)
Z	Length, z-direction (cm)
Z	Microbial z-value (°C)

Upper-case letters

Α	Area (cm ²)
C	Concentration (g/cm ³)
D	Decimal reduction time (s)
\mathbf{D}_{AB}	Diffusivity of A in B (cm ² /s)
$D_{cap,fat}$	Fat capillary diffusivity (cm ² /s)
D_{m}	Mass diffusivity (cm ² /s)
\mathbf{D}_{ref}	Decimal reduction value at reference temperature
E.	Activation energy (J/gmol)

Dry-basis fat content (g fat/g dry matter) F F_0 Initial dry-basis fat content (g fat/g dry matter) Fat:protein ratio (g fat/g protein) FP Enthalpy (J/g) Η Slot height (cm) H_{slot} M Mass (g) Number of microorganisms (CFU/g) N Initial number of microorganisms (CFU/g) N_0 P Pressure (Pa) Saturation pressure (Pa) P_{sat} Partial pressure of water vapor (Pa) Ideal gas constant (cm³·Pa/g mol·K) $P_{\mathbf{w}}$ R_g S N/N_0 RH Relative humidity (%) T Temperature (°C) Melting temperature (°C) T_{m} Reference temperature (°C) Tref Saturation temperature (°C) T_{sat} Volume (cm³) V W Slot width (cm) Mass fraction (decimal)

Dimensionless groups

Nu	Nusselt number $(h_{T} \cdot x/k_{T})$
Pr	Prandtl number $(c_p \cdot \mu/k_T)$
Re	Reynolds number $(D \cdot v \cdot \rho/\mu)$
Sc	Schmidt number ($\mu/\rho \cdot D_{AB}$)
Sh	Sherwood number $(h_m \cdot x/D_{AB})$

Greek letters

X

α	Thermal diffusivity (cm ² /s)
ε	Emissivity (-)
3	Error term
λ	Latent heat (J/g)
ρ	Density (g/cm ³)
σ	Stefan-Boltzmann constant (5.676·10 ⁻¹² W/cm ² ·K ⁴)
μ	Specific growth rate (1/s)
μ	Viscosity (Pa·s)

1 INTRODUCTION AND OBJECTIVES

1.1 Background

Impingement cooking is used for manufacturing many fully and partially cooked meat and poultry products. Impingement ovens utilize a type of convection in which cooking air is directed normal to the product surface at high velocities (>10 m/s). This is generally accomplished by forcing the cooking air through an array of slots or nozzles. Impinging airflow allows for heat transfer rates an order of magnitude higher than those that occur in conventional convection ovens (Gardon and Akfirat, 1966).

Moist-air impingement ovens combine impinging airflow with high humidity cooking air. In moist-air ovens, humidity can exceed 90% moisture by volume. The use of high moisture cooking air creates a condensing condition on the surface of the product. Condensing conditions dramatically increase the rate of cooking by taking advantage of the release of latent heat from steam in the cooking air. High moisture cooking air also suppresses product moisture loss during cooking. This results in cooking yields higher than those achieved when cooking with dry air. In meat cooking systems, a second cooking section with lower air moisture content is often utilized to aid in surface browning of the product.

Development of a computerized model for moist-air impingement cooking of meat products is of interest for two major reasons. First, cooking models can be used as tools for optimizing cooking processes. Heat and mass transfer models can be utilized to optimize processes in terms of product temperature, yield, and quality. Optimizing the cooking process can have major economic significance. In the United States alone, there

are 76 manufacturing facilities producing ground beef and poultry patties. The value of production from these plants exceeds \$520 million per year (FSIS, 2001). Even modest increases in cooking yield stand to increase profits significantly. A one percent increase in yield could potentially increase annual profits by over \$5 million. Reducing energy costs and wasted line capacity due to overcooking stands to improve profits even further. Reducing overcooking also stands to improve product quality characteristics such as color, flavor, and texture.

The second and more important reason for modeling the cooking process is to ensure microbial safety of the cooked product. The Food Safety and Inspection Service (FSIS) has proposed regulations that would shift the emphasis of cooking regulations for ground meat and poultry products from a system of time-temperature standards to a system of performance standards (FSIS, 2001). Such regulations have already been enacted for whole muscle meat products (FSIS, 1999). The new performance standards are based upon a 7-log₁₀ reduction in viable *Salmonella* for ready-to-eat (RTE) poultry products and a 6.5-log₁₀ reduction in *Salmonella* for RTE beef, roast beef, and corned beef products.

The new standards are designed to give processors the flexibility to develop customized, science-based processing strategies. However, it will be the duty of the processor to demonstrate that the process meets the required reductions in *Salmonella*. Unfortunately, adequate scientific tools are not currently available for processors to reliably and confidently verify compliance with the *Salmonella* performance standards.

Processors need a tool that will allow them to determine the effects of processing on the reduction of Salmonella. Due to safety concerns, it is neither feasible nor

desirable for manufacturers to conduct microbial challenge studies in the factory environment. Experiments can be conducted in the laboratory using microbial pathogens including *Salmonella* and *Listeria* monocytogenes in model food systems, but these results often do not correspond well with actual processing conditions. The use of mathematical models is an alternative to conducting microbial chellenge studies.

Although mathematical models are not a substitute for the judgment of an experienced microbiologist, FSIS has indicated that mathematical models based on heat transfer equations can be used to demonstrate the effects of processing on bacterial inactivation (FSIS, 2002).

Descriptive mathematical models for cooking processes would be of great value to processors and would allow for continuing innovation in the processed meat industry. Unfortunately, the development of cooking models is limited, with current models not accounting for the unique surface heat and mass transfer conditions present in moist-air impingement ovens (Chapter 2). Few existing models account for variations in product composition which can have significant effects on heat transfer and cooking yield. In most cases, yield loss is modeled solely as a function of moisture changes in the product during cooking. Although exceptions exist, most of the available cooking models have not been coupled with models for microbial inactivation.

To be of maximum utility, cooking models should include all variables that affect microbial lethality, including product size, density, specific heat, thermal conductivity, product composition, humidity, and strain of the organism (FSIS, 2001). Models should be flexible and applicable to various cooking conditions without the need for generation of empirical data sets. Mass losses due to both moisture and fat loss during cooking

should be considered. Finally, models should be validated against actual process data, including microbial inactivation data from inoculated challenge studies.

1.2 Objectives

The overall goal of this study was to develop a cooking model that would meet the above criteria, as well as provide a graphical tool for illustrating the effects of processing to manufacturing plant personnel. The specific objectives of this study were to:

- Develop a coupled heat and mass transfer model incorporating the transient effects of moisture and fat transfer during moist-air impingement cooking of ground beef patties.
- 2. Incorporate Salmonella inactivation models into the heat and mass transfer model and combine with a user interface to produce a tertiary cooking model.
- 3. Validate the heat and mass transfer model using data collected from an industrial moist-air impingement oven.
- 4. Validate the *Salmonella* inactivation models using data collected from inoculated challenge studies in a pilot-scale moist-air impingement oven.
- Develop the user interface as a tool than can be used to illustrate the effects of cooking parameters on yield and microbial safety to non-technical personnel, including oven operators.

2 REVIEW OF LITERATURE

2.1 Introduction

From the perspective of the processor, the most important output variables of cooking are temperature profile, cooking yield, and microbial inactivation. Cooking models can be used as a powerful tool for estimating these parameters. To model the reduction in pathogens such as *Salmonella* during cooking, it is first necessary to model the cooking process itself. The temperature history of the meat during cooking is the most important factor for modeling microbial reduction. As a result, heat transfer has been the focus of many models for cooking processes. However, in terms of profitability, the most important factor for processors to consider is cooking yield. Therefore, mass transfer is also an important factor to consider when modeling cooking processes.

The first portion of this chapter summarizes previous research in the area of cooking models. The thermo-physical properties required for modeling are also discussed. The final portion of the chapter addresses microbial modeling and previous work combining microbial models with models for meat cooking.

2.2 Introduction to cooking

Cooking and other heat treatments are among the most important unit operations in the food processing industry. Heat treatments during processing vary widely, depending upon the type of product. Foods may be fully or partially cooked, blanched to inactivate enzymes, dried to extend shelf life, pasteurized to kill unwanted microorganisms, or simply heated as part of the manufacturing process (Fellows, 1988).

The types of devices used for cooking and heating are nearly as numerous as the number of products that can be produced. Examples include heat exchangers, deep-fat fryers, contact-cooking systems, convection ovens, microwaves, and infrared ovens.

As a result of their ubiquity in the food industry, heating and cooking systems are of great interest to the food engineer. Ovens and other heating systems must be properly designed to ensure safe foods of the highest quality. Under-cooking may result in foods that are not safe to eat due to surviving pathogenic microorganisms. Over-cooked products may not have the quality characteristics demanded by customers. In addition to affecting product quality, overcooking can also be wasteful to the processor in terms of energy consumption and reduced product yield.

Most engineering analyses of cooking processes are aimed at determining the temperature and/or moisture profiles of the product undergoing cooking. Meat products are generally cooked prior to packaging. During cooking of unpackaged products, heat is transferred into the product, resulting in increased temperatures and thermal gradients within the meat. At the same time, moisture is transported out of the product, resulting in moisture gradients and yield loss (with the exception of boiling, in which case moisture may be added to the product). Fat losses during cooking can also be significant (Young et al., 1991; Pan and Singh, 2001; Badiani et al., 2002).

2.3 Heat and mass transfer in meat during cooking

Numerous studies have described heat transfer during cooking of meat (Dagerskog and Bengtsson, 1974; Dagerskog, 1979a and b; Skjöldebrand, 1980; Skjöldebrand and Hallström, 1980; Housová and Topinka, 1985; Thorvaldsson and

Skjöldebrand, 1995; Pan and Singh, 2001; Shilton et al., 2002). Virtually every analysis presumes that the dominant mechanism of heat transfer within meat products is conduction. However, Shilton et al. (2002) proposed that for high fat ground meat, heat transfer may be related to both conduction and internal convection within the melted fat phase.

Mass transport of water within meat products has also received considerable attention (Dagerskog and Bengtsson, 1974; Hung et al., 1978; Dagerskog, 1979a and b; Skjöldebrand, 1980; Skjöldebrand and Hallstrom, 1980; Mittal et al., 1982; Mittal et al., 1983; Hallström, 1990; Thorvaldsson and Skjöldebrand, 1995; Pan and Singh, 2001). Most cooking models assume that mass transport of water is primarily the result of molecular diffusion to a drying product surface (Huang and Mittal, 1995; Ngadi et al., 1997; Zanoni et al., 1997; Chen et al., 1999; Mittal and Zhang, 2000; Mittal and Zhang, 2001; Shilton et al., 2002).

Hung et al. (1978) proposed a different mechanism for water transport during convection cooking of bovine semitendinosus muscles in which it was determined water loss during cooking of these muscles was most likely due to pressure forces caused by fiber shrinkage. Furthermore, water loss was only weakly dependent on oven temperature and appeared to depend primarily on the amount of muscle shortening during cooking. For samples cooked directly from the frozen state, an initial period of drip loss was observed. The water lost during this period was believed to be due to the melting of ice crystals within the muscle. During this initial drip period, sample orientation affected the amount of loss; with samples having muscle fibers oriented vertically producing the highest losses. In this period, gravity was believed to contribute to the water loss. For

samples thawed before cooking, no such initial drip period existed. Thorvaldsson and Skjöldebrand (1995) also noted that water transport was up to 25% faster in the direction parallel to muscle fibers than across muscle fibers during oven roasting of bovine semitendinosus muscles.

Some authors have taken to expressing moisture transport in meat in terms of "water holding capacity" (Dagerskog, 1979a and b; Pan et al., 2000). This represents the amount of water that a type of meat will contain, given a certain temperature history. Upon heating, the water holding capacity of meat products generally decreases, resulting in water losses. Although this type of analysis does not truly describe a mechanistic process of water transport, it coincides with the knowledge that protein releases water upon denaturing (Bodwell and McClain, 1978).

Combined with the fiber squeezing mechanism described by Hung et al. (1978), the water holding capacity model provides a reasonable approximation of water transport during some cooking processes. However, this technique does not account for resistance to moisture transport within the product. This a significant weakness for most processes, since moisture diffusivity within meats is known to be low (Zanoni et al., 1997). Models that do not account for moisture diffusivity must be inherently empirical, as the mechanisms for transport within the product are not described based upon first principles.

2.4 Modeling the cooking process

Models for cooking processes can be divided into two categories. They are either based solely on data from experimental studies (empirical models) or derived from theoretical formulas of heat and mass transfer (Hayakawa, 1970). Empirical models can

be developed for cooking processes using data collected under the conditions of interest.

These models require less rigorous mathematical analysis and can provide good predictive capability for a limited range of conditions. Additionally, empirical models do not generally require the researcher to have accurate thermal property data to get good results. The weakness of empirical models is that they are not generally applicable to situations that are different from the conditions for which the model was developed. Slight changes in the system, such as changes in product size or geometry, require an entirely new set of experimental tests to generate new model parameters. Although it is theoretically possible to construct empirical models with an unlimited number of input parameters, the number of inputs that can be meaningfully included in the model is limited in practice.

Models based on theoretical principles are generally more robust than empirical models. Fundamental heat and mass transfer equations can be used to produce models that are much more general in nature than can be accomplished through experimental methods. By changing the boundary conditions of the model equations, a single model can often be used for several different types of cooking processes. However, models based on theoretical principles have their own drawbacks. Differential equations for heat and mass transfer quickly become too cumbersome to solve using analytical techniques. Thus, numerical methods are typically applied to cooking models. In order to produce models based upon transport equations, accurate knowledge of thermal and physical properties of the product must be known. In situations where properties are not accurately known, theoretical models end up being semi-empirical in nature, as the model

constants must be adjusted to fit experimental process data. A number of different empirical and theoretical models are described in the following sections.

2.4.1 Empirical models

Empirical models can be effective for predicting the temperature and moisture history of products during cooking. Bengtsson et al. (1976) developed a model for heat and mass transfer during oven roasting of meat. In the cooking process that was modeled, the meat was placed on a metal rack inside of an oven chamber with walls maintained at a fixed temperature. The mechanisms of heat transfer in this type of cooking are primarily natural convection and radiation. A plot consisting of a dimensionless temperature term $(T_{air}-T_{center})/(T_{air}-T_{initial})$ as a function of a dimensionless time term $(\lambda t)/(\rho c_p l^2)$ on a semi-log plot was used to develop simulation equations. From the diagram, a prediction equation for meat temperature as a function of time was developed. Results of the comparison between predicted and experimental results were good; however, quantitative results were not given.

Sarkin (1978) used a technique nearly identical to that of Bengtsson et al. (1976) to produce a computer cooking simulation for meat products. An equation for the linear portion of the heating curve was developed (Equation [2.1]).

$$\log\left(\frac{T_{air} - T}{T_{air} - T_{initial}}\right) = a + b \cdot t$$
 [2.1]

Coefficients a and b are constants and were determined by regression. The model had errors between the predicted and experimental temperatures of 0.2°C or less for cooking times of up to 10 hours. These results show the close predictions that are possible with empirical models.

Erdogdu et al. (1999) developed an empirical model for predicting the yield loss of shrimp during immersion cooking. Shrimp were cooked isothermally for varying periods in water at temperatures between 65 and 95°C. After heating, the yield losses were measured, and an equation for yield loss was determined by multiple linear regression (Equation [2.2]).

$$\% YieldLoss = a + b \cdot T + c \cdot T^2 + d \cdot t^2 + e \cdot t + f \cdot T \cdot t$$
 [2.2]

The terms a, b, c, d, e, and f were regression constants. The error between experimental and predicted yield losses ranged from 0.15 to 2.6% yield. This again shows the potential for empirical models to produce very close approximations of experimental data.

The primary drawback to each of the empirical models is that they are only valid for a specific set of cooking conditions. Although the error of the models is very low, this is to be expected, as the same data that were used for model development were used for error calculation. The models are not applicable to conditions other than those used in the regression. The cooking models of Bengtsson et al. (1976) and Sarkin (1978) only allow for meat temperature to be predicted as a function of cooking time. No provision is made for predicting yield, and processing conditions are not considered, thereby limiting the usefulness of the models as tools for processors. The yield model of Erdogdu (1999)

allows yield to be calculated as a function of time and temperature, but temperature profile is neglected. All three models ignore the effects of product composition. In addition, the models are not readily adaptable to products of different sizes or geometries from those used for model development. The weaknesses illustrated by these models show the underlying reason that empirical models cannot be utilized as general models for the varying processing conditions that occur in industry.

2.4.2 Models based upon heat and mass transfer principles

Most cooking models reported in the literature are based on theoretical heat and mass transfer equations. Models based on transport principles are generally more flexible than those developed through purely empirical methods. The equations that govern heat and mass transfer are not product specific and are generally accurate for a wide range of conditions.

During cooking of most meat products, the predominant mechanism of heat transfer within the product is conduction. The governing equation for conductive heat transfer in rectangular coordinates is derived from an energy balance (Bird et al., 1960).

$$\rho \cdot c_p \cdot \frac{\partial T}{\partial t} = \frac{\partial}{\partial x} \left(k_{T,x} \cdot \frac{\partial T}{\partial x} \right) + \frac{\partial}{\partial y} \left(k_{T,y} \cdot \frac{\partial T}{\partial y} \right) + \frac{\partial}{\partial z} \left(k_{T,z} \cdot \frac{\partial T}{\partial z} \right)$$
 [2.3]

Various cooking processes can be simulated using the conduction equation. Most cooking processes transfer heat to the product via the food surface. As a result, different cooking types can be modeled by changing the surface boundary conditions as

appropriate for the type of cooking to be modeled. Models for conductive, convective, and radiative cooking can be constructed by including the appropriate heat flux boundary conditions. The flux equations for conduction, convection, and radiation heat transfer are well known and are given by Equations [2.4], [2.5], and [2.6] respectively.

$$\frac{\mathbf{q}}{\mathbf{A}} = \mathbf{k}_{\mathrm{T}} \cdot \frac{\partial \mathbf{T}}{\partial \mathbf{x}} \big|_{\mathrm{surface}}$$
 [2.4]

$$\frac{q}{A} = h_T \cdot (T_{\infty} - T_{\text{surface}})$$
 [2.5]

$$\frac{q}{A} = \varepsilon \cdot \sigma \cdot \left(T_{\text{surface}}^{4} - T_{\text{heat source}}^{4} \right)$$
 [2.6]

Most mass transfer models are based upon transport by diffusion. The governing equation for diffusion is similar in form to the equation for conduction (Bird et al., 1960).

$$\frac{\partial C}{\partial t} = \frac{\partial}{\partial x} \left(D_m \cdot \frac{\partial C}{\partial x} \right) + \frac{\partial}{\partial y} \left(D_m \cdot \frac{\partial C}{\partial y} \right) + \frac{\partial}{\partial z} \left(D_m \cdot \frac{\partial C}{\partial z} \right)$$
 [2.7]

Treatments of surface mass transfer vary, but are typically modeled using a convective mass transfer boundary condition and/or a term for evaporation. The equation

for mass transfer by convection is analogous to convective heat transfer and is usually given by Equation [2.8].

$$n = h_m \cdot (C_{\text{equilibrium}} - C)$$
 [2.8]

Numerous authors have published theoretical models for meat cooking. Models have been developed for contact cooking (Dagerskog, 1979a and b; Ikediala et al., 1996; Pan et al., 2000), immersion frying (Ngadi et al., 1997; Farkas et al., 1995a and b; Vijayan and Singh, 1997; Mittal and Zhang, 2001), convection cooking (Mittal and Blaisedell, 1982; Mittal et al., 1983; Holtz and Skjöldebrand, 1986; Huang and Mittal, 1995; Zanoni et al, 1997; Chen et al., 1999; Mittal and Zhang, 2000), oven roasting (Singh et al., 1984), microwave cooking (Mallikarjunan et al., 1996), and infrared cooking (Shilton et al., 2002). The following sections describe models for each of these types of cooking.

2.4.3 Contact cooking

Contact cooking is one of the simplest mechanisms of cooking. During contact cooking, products are placed in direct contact with a heating surface, resulting in heat transfer by conduction. The rate of cooking is limited by the temperature gradient between the product and heating surface and by the surface resistance of the product/heating element interface. This type of cooking is common in the fast food industry, particularly for ground beef patties.

Dagerskog (1979a) developed an early model for contact cooking of meat patties. The model was based on a one-dimensional formulation of the conduction equation with a term added to incorporate the latent heat of evaporation of water. This equation was solved numerically using a finite difference technique.

Transfer of moisture out of the meat was calculated based upon experimental measurements of water holding capacity. The capacity of meat to store water under varying times and temperatures was determined experimentally. Experimental determination of water holding capacity was conducted by heating 10 g samples enclosed in sealed plastic pouches in an isothermal water bath. Water content of the samples was measured after they had been heated and allowed to drain for 1 minute on absorbent paper. Water holding capacities were then plotted as functions of temperature and time. For each time step in the model, it was assumed that the free water released due to the change in water holding capacity was transported out of the meat. Heat and mass transport equations were used to determine the amount of water that exited the meat due to evaporation. A second water loss equation was formulated using a mass balance based on changing water holding capacity. The difference in water loss due to changing water holding capacity and water lost by evaporation was attributed to drip loss. Differences between the experimental and simulated water losses ranged from 0.2 to 2.7% loss for a pan temperature of 140°C and from 0.3 to 2.9% loss for a pan temperature of 180°C. Predictions of the center temperature ranged from 0 to 2°C of the experimental values at cooking times of up to 6 minutes.

The water holding capacity model has an advantage over other methods, in that it accounts for the varying water binding capacities of different products. It also has the

benefit of easily describing the drip loss phenomenon. Weaknesses of the water holding capacity model are that it is highly empirical and does not account for internal resistance to moisture transfer. Because it does not account for internal resistance to moisture transfer, the water holding capacity model is expected to decrease in accuracy with increasing product thickness. The water holding capacity model is also product specific, as different products have much different water binding properties.

Ikediala et al. (1996) developed a model for single-side pan-frying of meat patties that was not based on the water holding capacity model, but rather a two-dimensional Fourier conduction equation formulated in radial coordinates with an added term for the evaporation of water.

$$\frac{\partial \left(\rho \cdot c_{p} \cdot T\right)}{\partial t} = \frac{1}{r} \cdot \frac{\partial}{\partial r} \left(r \cdot k_{T} \cdot \frac{\partial T}{\partial r}\right) + \frac{\partial}{\partial z} \left(k_{T} \cdot \frac{\partial T}{\partial z}\right) + \lambda \cdot \rho \cdot \frac{dm_{ave}}{dt}$$
 [2.9]

A contact heat transfer coefficient was used to describe heat transfer at the patty/grill interface. The same thermal properties reported by Dagerskog (1979a) were used for calculations. The primary difference between the heat transfer component of this model and the model of Dagerskog (1979a) was the expansion of the conduction equation into two dimensions. This allowed for the temperature distribution in the patty during cooking to be modeled in two dimensions, resulting in a more complete description of the temperature profile. Deviations between experimental and predicted center temperatures were less than 4°C.

Ikediala et al. (1996) modeled moisture loss in the patty slightly differently than Dagerskog (1979a). The average moisture content of the patties was modeled using an exponential decay model.

$$m_{ave} = m_{ave,initial} \cdot exp(-(a+b\cdot T)\cdot t)$$
 [2.10]

The constants a and b for the mass transfer equation were determined using regression of experimental values. The use of an exponential decay function for moisture transfer is completely empirical and represents a total deviation from first-principles. The result is that the model is specific for the product and conditions tested and lacks robustness.

Pan et al. (2000) used a technique similar to that of Dagerskog (1979a) and Ikediala et al. (1996) to model cooking of hamburgers by two-sided contact cooking. Heat transfer was modeled using a one-dimensional formulation of the Fourier conduction equation. However, the conduction equation was written in terms of enthalpy, rather than temperature.

$$\frac{\partial H}{\partial t} = \frac{\partial}{\partial x} \left(k_T(H) \cdot \frac{\partial T(H)}{\partial x} \right)$$
 [2.11]

Use of the enthalpy formulation allowed cooking from the frozen state to be modeled without discontinuities related to the phase change from ice to liquid water. Relationships between enthalpy and temperature were used to produce temperature history curves.

Enthalpy of frozen hamburger was calculated using a food property computer program (Singh and Mannapperuma, 1994). Enthalpy of unfrozen hamburger was calculated using an empirical equation (Equation [2.12]).

$$H_{\text{nonfrozen}} = H_{\text{ref}} + \rho \cdot \{ (1600 + 2600 \cdot X_{W} + 15 \cdot X_{f} \cdot T) \cdot (T - T_{\text{ref}}) \}$$
 [2.12]

The changes in moisture and fat contents, independent of position, were determined using Equations [2.13] and [2.14].

$$\frac{\partial m}{\partial t} = -h_{m} \cdot (m - m_{equilibrium})$$
 [2.13]

$$\frac{\partial m_f}{\partial t} = -h_f \cdot (F - F_{\text{equilibrium}})$$
 [2.14]

The model assumed that no transport of water or fat occurred below specified threshold temperatures. The temperature dependence of the water and fat equilibrium concentrations was given by Equations [2.15] and [2.16].

$$m_{equilibrium} = m_{initial} \cdot e^{(-\delta_{\mathbf{w}}(T-T_{initial}))}$$
 [2.15]

The previous equations were solved at each node for every time step, giving moisture and fat contents as functions of temperature. A finite difference technique was used for solving the heat transfer and mass equations. As in the model by Dagerskog (1979a), this method treats water and fat content as "state" variables (i.e., functions of just temperature rather than results of transport processes). The δ_w and δ_f terms are related to the water and fat holding capacities of the meat and were determined experimentally with whole patties.

This model (Pan et al., 2000) is one of the most complete models for cooking available in the literature. Differences between predicted and center temperatures were small, although differences of up to 10°C occurred in the temperature range between 0 and 40°C. Differences between measured and predicted yields were less than 3%. Inclusion of fat transport as a separate mechanism sets the model apart from any of the prior contact-cooking models. In addition, utilization of the enthalpy formulation for heat transfer represents an important step in the simulation of temperature profiles for products that may originate in the frozen state. However, the empirical nature of the water and fat holding capacity models limits robustness. Water and fat holding capacity were determined using whole patties. In this way, internal resistance to moisture and fat transfer was accounted for indirectly. However, this approach limits the utility of the model to products of the same composition and geometry that was used to develop the model parameters.

2.4.4 Frying

Frying is another operation that is commonly used to cook meat products.

Immersion (deep fat) frying is typically modeled as a moving boundary problem (Singh, 2000). Products undergoing frying are described as consisting of an inner core region surrounded by a dry crust region. As cooking proceeds, the boundary between the crust and core regions moves towards the product center.

Vijayan and Singh (1997) developed a model for heat transfer during frying of frozen foods. Frying was modeled as a moving boundary problem. Separate transport equations were utilized for the crust and core regions. Heat transfer in the crust was modeled using a one-dimensional formulation of the Fourier conduction equation. A convective boundary condition was used to describe heat transfer at the oil-product interface. The position of the crust-core interface at a given time was given by Equation [2.17].

$$s_{j+1} = s_j + \left[q_{crust} - q_{core}\right] \cdot \frac{\Delta \cdot t}{(\lambda \cdot \rho \cdot m)}$$
 [2.17]

In the core of the product, heat transfer was modeled using an enthalpy formulation of the conduction equation (see Equation [2.11]). Differences between simulated and measured center temperatures ranged from 1 to 6°C over a range of 0 to 75°C. The model did not account for mass transfer. Therefore, although useful for predicting temperature, this model cannot be used for yield predictions.

A model for moisture transport during deep fat frying of chicken drums was developed by Ngadi et al.(1997). A two-dimensional diffusion equation formulated in radial coordinates was used to describe moisture transfer in the product (Equation [2.18]).

$$\frac{\partial C}{\partial t} = \frac{1}{r} \cdot \frac{\partial}{\partial r} \left(r \cdot D_m \cdot \frac{\partial C}{\partial r} \right) + \frac{\partial}{\partial z} \left(D_m \cdot \frac{\partial C}{\partial z} \right)$$
 [2.18]

The two-dimensional formulation of the conduction equation allows for modeling of non-spherical products. This is useful not only for chicken drums, but for other products such as chicken strips.

An exponential function was used for the surface mass transfer boundary condition. This resulted in an empirical relationship similar to that used by Ikediala et al. (1996).

$$C = C_{initial} \cdot exp((-a + b \cdot T_{oil}) \cdot t)$$
 [2.19]

The constants a and b were determined by regression of experimental data and were equal to -0.045 and 4.167·10⁻⁴ respectively. The utilization of an empirical boundary condition greatly limits the robustness of the model.

The finite element grid was broken up into elements representing the bone, bone marrow, cartilage, and muscle portions of the chicken drumstick. The moisture diffusivity of the muscle portion of the drumstick was modeled as a function of cooking oil temperature and moisture content using an equation developed in separate

experiments (Equation [2.20]); (Ngadi and Correia, 1995). Constant diffusivities were used for the other components.

$$D_{m} = 8.35 \cdot 10^{-6} \cdot \exp\left(-\frac{2930}{T_{oil}} - 0.561 \cdot C + 0.092 \cdot C^{2}\right)$$
 [2.20]

This model represents a good tool for determining moisture distributions in a complex system undergoing cooking, although moisture predictions were off by up to 30% for some conditions. Unfortunately, this was not combined with a model for heat transfer. Nonetheless, the usefulness of the finite element method for modeling systems with multiple physical properties and complex geometries was demonstrated.

Mittal and Zhang (2001) developed a model for deep fat frying using a different approach. An artificial neural network (ANN) was used to predict temperature, moisture, and fat content in meatballs during deep fat frying. Input parameters included fat diffusivity, moisture diffusivity, thermal diffusivity, heat transfer coefficient, fat conductivity, and oil temperature, as well as frying time, meatball radius, and initial temperature. The data used to train the artificial neural network were generated from validated mathematical models. Heat, moisture, and fat concentration were modeled using one-dimensional transport equations formulated in radial coordinates. The maximum errors between modeled and experimental temperature, moisture, and fat content were 1.9°C, 0.004% dry basis, and 0.016% dry basis, respectively, for the optimum ANN design.

Artificial neural networks have several advantages over other types of modeling for predicting temperature and moisture distributions during cooking. ANN's can "learn" from new data to increase accuracy of prediction. This allows experimental data to be combined with simulation data from models. Neural networks can often generate results faster than mathematical models, which is useful in optimization studies where many data sets must be analyzed. However, in many cases where artificial neural networks are generated from simulation data, the question exists whether the actual simulation data would be more accurate than the data generated from the ANN. In this case, it would seem to make more sense to use the data of the original simulation rather than the ANN. In addition, theoretical models can be more readily adapted to new conditions.

2.4.5 Convection cooking

Forced-air convection cooking is an important method for commercial cooking of meat products. Huang and Mittal (1995) developed a computer model for forced convection cooking, broiling, and boiling of meatballs. Heat and moisture transfer were modeled using one-dimensional conduction and diffusion equations formulated in radial coordinates.

An energy balance at the surface of the meatball was used for the heat transfer boundary condition. This equation accounted for convective heat gain, latent heat of evaporating water, and conduction at the meatball surface.

$$k_T \cdot \frac{\partial T}{\partial r}|_{surface} = h_T \cdot (T_{air} - T_{surface}) + D_m \cdot \rho \cdot \lambda \cdot \frac{\partial m}{\partial r}|_{surface}$$
 [2.21]

Boundary conditions for the moisture transport equation were based upon moisture content equilibrium between the surface and the environment. The transport equations were solved using the finite difference method. Constant transport properties were used in the simulation. Surface heat transfer coefficients for each type of cooking were determined using analysis of the center temperatures of aluminum spheres heated under the conditions of interest. The thermal and mass diffusivity values were estimated by minimizing the root-mean-square deviations between the observed and predicted temperature and moisture histories. This was conducted using only one set of cooking data and validated using four other data sets. The average root mean square errors for temperature and mass prediction versus experimental results were 3-5.1°C and 0.04-0.19 g respectively. The strength of this model is that it was derived entirely from transport equations. Although an empirical technique was used to fit thermal and mass diffusivity values, a similar technique is often used to determine the published values that are available for those constants.

Chen et al. (1999) developed a model for convection cooking of chicken patties. The finite element method was used to solve heat and mass transfer equations based on transport principles. Cooking was modeled using two-dimensional transport equations formulated in radial coordinates. The use of two-dimensional formulations allowed for complete description of the temperature and moisture distributions in the patties.

$$\rho \cdot \frac{\partial T}{\partial t} = \left(\frac{1}{r} \cdot \frac{\partial}{\partial r} \left(r \cdot \frac{k_T}{c_p} \cdot \frac{\partial T}{\partial r} \right) + \frac{\partial}{\partial z} \left(\frac{k_T}{c_p} \cdot \frac{\partial T}{\partial z} \right) \right)$$
 [2.22]

$$\rho \cdot \frac{\partial m}{\partial t} = \left(\frac{1}{r} \cdot \frac{\partial}{\partial r} \left(r \cdot \frac{k_m}{c_m} \cdot \frac{\partial m}{\partial r} \right) + \frac{\partial}{\partial z} \left(\frac{k_m}{c_m} \cdot \frac{\partial m}{\partial z} \right) \right)$$
 [2.23]

The two-dimensional formulation of the heat and mass transfer equations made it possible to model cylindrical patties as axis-symmetric bodies. The boundary condition for the heat transfer equation consisted of both a convective heat transfer term and a latent heat term for surface evaporation.

$$k_T \cdot \frac{\partial T}{\partial n} = h_T \cdot (T_{air} - T) + D_m \cdot \rho \cdot \lambda \cdot \frac{\partial m}{\partial n}$$
 [2.24]

The boundary condition for the mass transfer equation was based upon convective mass transfer at the surface.

$$k_m \cdot \frac{\partial m}{\partial n} = h_m \cdot (m_{we} - m)$$
 [2.25]

The equilibrium moisture term used in the mass transfer boundary condition was calculated using the equation developed by Huang and Mittal (1995).

$$RH = \exp\left(\frac{-5222.47}{R_g \cdot T_{air}} \cdot m_{equilibrium}^{-1.0983}\right)$$
 [2.26]

Based on previous research, heat capacity and thermal conductivity were modeled as functions of temperature and moisture content respectively (Murphy et al., 1998; Murphy and Marks, 1999). This decreased standard error of prediction for center temperature from 5.5 to 3.7°C, as compared to using constant values for c_p and k.

$$c_p = 3017.2 + 2.05 \cdot T + 0.24 \cdot T^2 + 0.002 \cdot T^3$$
 [2.27]

$$k_T = 0.194 + 0.436 \cdot m$$
 [2.28]

Singh et al. (1984) developed a heat and mass transfer model for oven roasting of meat. Heat transfer within the meat was modeled using a two-dimensional conduction equation.

$$\frac{\partial T}{\partial t} = \alpha \cdot \left(\frac{\partial^2 T}{\partial x^2} + \frac{\partial^2 T}{\partial y^2} \right)$$
 [2.29]

A convective boundary condition with a term for evaporation of water was used at the product surface.

$$h \cdot (T_{air} - T) = \lambda \cdot h_m \cdot (P_{surface} - P_{air}) + k_T \cdot \frac{\partial T}{\partial x} |_{surface}$$
 [2.30]

The finite difference method was used to solve the heat transfer equation. No attempt was made to describe the transport of water within the product. A linear relationship was used for the value of P_{surface} (Equation [2.31]).

$$P_{\text{surface}} = a + b \cdot T$$
 [2.31]

Although a term for evaporation was used to improve the heat transfer model, this model is not suitable for predicting yield during cooking.

A different technique, was utilized by Mittal and Zhang (2000) to develop a model for convective thermal processing of frankfurters. This model was based upon an artificial neural network. Input variables for the ANN were fat-protein ratio, initial temperature, initial moisture content, frankfurter radius, ambient temperature, relative humidity, and process time. The artificial neural network was trained using data from validated mathematical models. The models were based upon one-dimensional heat and mass transfer equations. Moisture diffusivity and equilibrium moisture content as functions of temperature, fat protein ration, and relative humidity were used in the model following the work of Mittal and Blaisdell (1982):

$$D_{m} = Exp(-8.6787 + 0.08468 \cdot FP - 0.3614 \cdot RH \cdot FP - 4341.5 / T_{abs} + 8.55 \cdot C) \quad [2.32]$$

$$m_{\text{equilibrium}} = -0.102 \cdot \ln(-R_g \cdot FP \cdot (T + 5.665) \cdot \ln(RH) / 1.132 \cdot 10^7)$$
 [2.33]

The ANN was trained using 13,500 data points generated from the mathematical models. Fat-protein ratio was found not to be an important factor in predicting moisture content or temperature. As discussed earlier, artificial neural networks pose some advantages over purely numerical models, and may be effective for use in optimization experiments. The primary advantage of artificial neural networks is that they can be utilized to produce results much faster than models based upon the finite difference or finite element methods. As a result, ANN's have promise for optimization studies, real-time control, and other situations where fast calculations are essential. However, ANN's are still limited in that they must be "trained" with data either from experimental or model sources. The theoretical basis of numerical models means that they can be more easily adapted to changing processing conditions without the need for "training".

2.4.6 Other types of cooking

Models are available for several other types of cooking. Mallikarjunan et al.

(1996) developed a model for microwave cooking of shrimp. Heat transfer was modeled using a two-dimensional transport equation in axial coordinates.

$$\frac{\partial T}{\partial t} = \alpha \cdot \left[\frac{1}{r} \cdot \frac{\partial T}{\partial r} + \frac{\partial^2 T}{\partial r^2} + \frac{\partial^2 T}{\partial z^2} \right] + \frac{Q}{\rho \cdot c_p}$$
 [2.34]

where Q is the heat generated by the microwaves and is given

$$Q = Q_0 \cdot \left[exp \left[\frac{-(R-r)}{\delta_p} \right] + exp \left[\frac{-(Z-z)}{\delta_p} \right] \right]$$
 [2.35]

Moisture loss during cooking was calculated using the following equation:

$$-\frac{\partial m}{\partial t} = h_m \cdot A \cdot (P_{sat} - P_w) + \frac{\rho \cdot V \cdot c_p}{\lambda} \cdot \left(\frac{\partial T}{\partial t}\right)$$
 [2.36]

Heat transfer at the surface was modeled using a convective heat transfer equation with a term for water evaporation. Equation [2.36] is somewhat unusual in that the evaporation term is generally included in the heat transfer equation. The result is that Equation [2.36] does not account for internal resistance to moisture transport.

Equations were solved using the finite difference method. Constant thermal properties were used. The surface heat transfer coefficient was calculated using the equation for natural convection over a horizontal cylinder:

$$h_{T} = 1.3196 \cdot \left(\frac{\Delta T}{\Delta d}\right)^{0.25}$$
 [2.37]

Simulation results were validated by collecting transient temperature and mass data during cooking in a household microwave oven. The model temperature predictions were within 6°C of the experimental values. Mass losses were within 0.8% of the predicted values.

Another type of cooking uses far-infrared radiation for heating. Shilton et al. (2002) developed a model for far-infrared cooking of beef patties. The model accounted for heat transfer and evaporative mass losses during cooking. Heat transfer was modeled using a one-dimensional Fourier equation with a term for the latent heat associated with water evaporation. Mass transport was modeled by a diffusion equation. The boundary condition for heat transfer at the surface was given by:

$$k_T \cdot \frac{dT}{dx} = \sigma \cdot \left(T_{\text{heating element}}^4 - T_{\text{surface}}^4 \right)$$
 [2.38]

A convective boundary condition was used for the mass transfer equation.

$$D_{m} \cdot \frac{dC}{dx} = h_{m} \cdot (C_{air} - C_{surface})$$
 [2.39]

The mass diffusion coefficient was calculated using an equation by Maroulis et al. (1998).

$$D_{m} = a \cdot \exp(b/T) \cdot \exp(c/C)$$
 [2.40]

Thermal conductivity and density were modeled as a function of temperature using equations by Choi and Okos (1985).

$$k = a + b \cdot T - c \cdot T^2$$
 [2.41]

$$\rho = a - b \cdot T - c \cdot T^2$$
 [2.42]

The authors noted that the heat transfer model was not accurate for patties containing high levels of fat. To more accurately model heat transfer in high-fat patties, an effective thermal conductivity was calculated.

$$k = (a + b \cdot T - c \cdot T^2) + (h_{eff_1} + h_{eff_2} T)$$
 [2.43]

This technique allowed more accurate modeling of heat transfer for meat containing high levels of fat. However, it did not actually relate heat transfer to fat content or describe the transfer of fat out of the product. Addition of a more detailed fat transfer component would increase the utility of the model.

2.5 Thermal and physical properties required for modeling

Before it is possible to create cooking models based on heat and mass transfer principles, accurate values for the thermal and physical properties of meat products must be known. Since these values may vary widely with temperature and composition, it is necessary to quantify these effects. Thermal and physical properties of a wide range of food products are available from food engineering textbooks and handbooks, such as those published by ASHRAE (Stroshine and Hamann, 1996; ASHRAE, 1998). Although

the properties of interest can often be obtained, care must be taken to scrutinize the conditions for which they are accurate.

Numerous articles have been published on the thermal properties of meat products. These properties were reviewed extensively by Sanz et al. (1987). Experimental values for thermal conductivity, enthalpy, apparent heat capacity, and density of beef, pork, mutton, poultry, and fish were reported. Most of the property values listed were in the -30 to 30°C temperature range. Other articles related to thermal properties of meat and meat products have been written by McProud and Lund (1983), Perez and Calvelo (1984), Dincer (1996), and Tsai et al. (1998). Moisture diffusivity data for a wide range of foods were compiled by Zogzas et al. (1996). Enthalpy data for meat products have been published by Levy (1979), Skala et al. (1989), and Tocci and Mascheroni (1998).

The rate of moisture transport in meat products is considerably lower than the rate of heat transfer. Zanoni et al. (1997) reported that moisture diffusion affected only a 3 mm deep layer of the product surface. Chen et al. (1999) reported similar results. These results give insight into the development of element meshes for future cooking models. The region of highest activity for moisture transfer is confined to a layer close to the surface of the patty, and thus a fine mesh should be used in that area.

Accurate values for thermal and physical properties are critical to development of cooking models based on transport equations. Small deviations in property values often result in large differences in model performance. Thus, care must be used when selecting property data from published sources. The product composition can often have a dramatic effect on physical properties. Thus, composition-dependent property equations, such as those developed by Choi and Okos (1986), are often utilized.

2.6 Microbial models

Mathematical microbial models can provide important tools for predicting the growth or reduction of microorganisms in foods. When properly utilized, models can provide an initial estimate of microbial behavior without the investment in time and materials required for microbial challenge studies. The use of models is also less expensive. Although microbial challenge studies may still be required to verify model results, the model may be used to more efficiently design such studies by selecting the conditions to be tested. Models can be used to quickly determine the effects of process changes on microbial food safety. These capabilities are invaluable for the planning of hazard analysis critical control programs. Graphical depictions of changes in microbial counts can serve as educational tools. This is especially valuable for showing non-microbiologists the effects of processing on microbial safety. However, the limitations of the model must be considered whenever a model is used to predict microbial activity in food products (FSIS, 2002).

Mathematical modeling of microbial activity in food products has been extensively reviewed in the literature (Whiting and Buchanan, 1994; Whiting, 1995; Roberts, 1997). Whiting (1995) classified microbial models based upon a three-level scheme-as primary, secondary, or tertiary. Primary models describe the changes in a microbial population as a function of time. Secondary models describe the primary model parameters as functions of environmental parameters. Tertiary models combine primary and secondary models with a user interface to produce a complete simulation tool.

2.6.1 Primary models

Primary models describe the number of bacteria in a population as a function of time. Mathematical equations are used to describe the growth or inactivation curve using a set of parameter values. Ideally, these parameters relate to descriptive terms such as lag time or generation time. Examples of primary models are linear models, exponential models, and models based on the Gompertz function (Whiting, 1995). A log-linear inactivation model is given by Equation [2.44].

$$\log N = \log N_0 + \frac{1}{D} \cdot (t - t_0)$$
 [2.44]

Equation [2.45] is an inactivation model based on first-order kinetics.

$$\frac{N}{N_0} = e^{-k \cdot t}$$
 [2.45]

A primary model for microbial inactivation based on a Gompertz equation was parameterized by Van Impe et al. (1995).

$$y = a \cdot \exp \left[-\exp \left(\frac{\mu_{\text{max}} \cdot e}{b} \cdot (\lambda - t) + 1 \right) \right]$$
 [2.46]

Peleg and Cole (1998) suggested a primary inactivation model based on a Weibull distribution (Equation [2.47]).

$$\log_{10} S(t) = -b(T) \cdot t^{n(T)}$$
 [2.47]

Each type of primary model has its own merits and inherent weaknesses. The log-linear model is the most commonly used inactivation model in both industry and academia. Large quantities of data have been amassed using the model parameters for numerous microorganisms and processing conditions. This makes implementation of the log-linear model the easiest of any of the primary models. Additionally, log-linear models have become ingrained as the "standard" for microbial inactivation and are thus widely accepted in industry. However, microbial inactivation does not always follow log-linear kinetics (Peleg, 1997). Other types of inactivation models may be more suitable for modeling inactivation in these cases. Unfortunately, these equations are often more cumbersome to use, and suitable experimental data for model constants are not as widely available as for log-linear models. To develop modeling software that is both flexible and as widely acceptable as possible in nature, log-linear inactivation kinetics should be utilized. However, to develop the most accurate model for specific cases, other types of primary models may be superior.

2.6.2 Secondary models

Secondary models describe the changes in primary model parameters as a function of environmental conditions. These models can show the effects of variables

such as temperature, pH, water activity, and substrate composition. Examples of secondary models are Arrhenius relationship models, response surface models, and square root models (Whiting, 1995).

An Arrhenius relationship for the inactivation constant, k, was given by Geankoplis (1993).

$$k = a \cdot e^{-E_a/R \cdot T}$$
 [2.48]

Equation [2.49] is a square-root relationship for k (Whiting, 1995).

$$\sqrt{k} = a(T - T_0)$$
 [2.49]

Mattick et al. (2001) parameterized the following log-logistic secondary models for *Salmonella*. The models are designed to be used with the primary model in Equation [2.47].

$$b(T) = 6.841/\{1 + \exp[(76.14 - T)/4.204]\}$$
 [2.50]

$$n(T) = 0.670/\{1 + \exp[(T - 80.14)/3.785]\}$$
 [2.51]

Juneja and Eblen (1999) developed a response surface model for inactivation of Listeria monocytogenes (Equation [2.52]). The model described decimal reduction time as a function of temperature, pH, salt content, and sodium pyrophosphate content.

$$\begin{split} \ln(D) &= c_1 + c_2 \cdot (T) + c_3 \cdot (pH) + c_4 \cdot (salt) + c_5 \cdot (phos) + c_6 \cdot (T) \cdot (pH) \\ &+ c_7 \cdot (T) \cdot (salt) + c_8 \cdot (T) \cdot (phos) + c_9 \cdot (pH) \cdot (salt) + c_{10} \cdot (pH) \cdot (phos) \\ &+ c_{11} \cdot (salt) \cdot (phos) + c_{12} \cdot (T)^2 + c_{13} \cdot (pH)^2 + c_{14} \cdot (salt)^2 + c_{15} \cdot (phos)^2 \end{split}$$

2.6.3 Tertiary models

Tertiary models combine primary and secondary models with a user-interface to to produce a complete simulation tool. Two widely used tertiary models in the United States are the American Meat Institute Process Lethality Determination Spreadsheet (AMI, 2003) and the United States Department of Agriculture's Pathogen Modeling Program (USDA, 2004).

The AMI model is based upon a Microsoft Excel spreadsheet (AMI, 2003). The spreadsheet uses a log-linear thermal death time model to calculate process lethality based on time/temperature data inputted by the user. The user must also input z and T_{ref} values for the thermal death time models. A table of z and T_{ref} values for common meat microorganisms is supplied to aid the user in choosing input values. Unfortunately, z values may be influenced by numerous conditions that are not accounted for by the chart of suggested values. Thus many users will likely choose z and T_{ref} values that are

inappropriate for the cooking process of interest and therefore generate lethality data that are highly suspect.

The Pathogen Modeling Program (version 7.0) is a menu-based program that is based upon a suite of models (USDA, 2004). The program provides tools for assessing microbial inactivation of *Clostridium botulinum*, *Escherichia coli* O157:H7, and *Listeria monocytogenes*, but not *Salmonella*. The models for microbial inactivation and survival are based upon a logistic inactivation model (Equation [2.53]).

$$\log \frac{N}{N_0} = \log \left[\frac{a(1 + e^{-b_1 + t_1})}{(1 + e^{b_1(t - t_1)})} + \frac{(1 - a)(1 + e^{-b_2 \cdot t_1})}{(1 + e^{b_2(t - t_1)})} \right]$$
 [2.53]

2.7 Combined models

Several authors have attempted to combine cooking models with microbial inactivation models. Zanoni et al. (1997) linked inactivation models for *Enterococcus* faecium to a cooking model for Bologna sausage. Two different inactivation models were utilized. The first was a simple first order inactivation model.

$$\frac{dN}{dt} = -k \cdot N$$
 [2.54]

The second was a model developed by Whiting and Buchanan (1994).

$$\log N = \log N_0 + \log \left[\frac{a \cdot (1 + \exp(-b_1 \cdot t_1))}{(1 + \exp(b_2 \cdot (t - t_1)))} + \frac{(1 - a) \cdot (1 + \exp(-b_2 \cdot t_1))}{(1 + \exp(b_2 \cdot (t - t_1)))} \right]$$
 [2.55]

The model was validated by inoculated challenge studies. At log reductions below 6, both the first-order inactivation model and the Whiting and Buchanan model predicted reductions within 1- log of the experimental values. At reductions above 6-log, the first order model greatly overestimated inactivation. However, at log reductions above 6, the Whiting and Buchanan model was within 1-log of the experimental data. Unlike the first-order model, the Whiting and Buchanan model incorporates a tailing effect at high levels of inactivation, which provided a better fit to the experimental data. This clearly illustrates how certain inactivation models may be more accurate than others under some conditions.

The contact-cooking model developed by Pan et al. (2000) included a first-order inactivation model for *E. coli* O157:H7.

$$\frac{dN}{dt} = \frac{-2.303}{D_{ref} \cdot 10^{(T_{ref} - T(t))/z}} \cdot N$$
 [2.56]

Temperature data from each time step were utilized to obtain the number of microbes at each nodal location. The total surviving population at each time step was then determined. However, the inactivation model was not validated using experimental data.

Mallikarjunan et al. (1996) included an inactivation model for *Listeria* monocytogenes with a model for microwave cooking of cocktail shrimp. The inactivation model assumed first-order reaction kinetics.

$$-\frac{dN}{dt} = a \cdot e^{-\frac{E_a}{R_g \cdot T}} \cdot N$$
 [2.57]

The inactivation model was validated by injecting a liquid inoculum into the geometric center of each shrimp. After cooking, the shrimp were tested for surviving bacteria. This methodology made it impossible to track the actual numbers of surviving Listeria as a function of time. Although useful for predicting the worst-case scenario, this technique probably overestimates the cooking required for most products where microorganisms are present either at the surface or dispersed throughout the product.

2.8 Limitations of models

Although microbial models can be valuable tools, there are limitations inherent in any model. A model is generally only accurate for the range of conditions under which it was developed. Extrapolating outside of the ranges used for the model development may give misleading results. Models are generally microbe specific, and a model for one microorganism cannot be expected to produce accurate results for another microorganism, or even for a different product.

2.9 Summary

The models contained in the previous sections describe cooking processes with varying degrees of complexity. Although each of the models discussed has its own merits, none of the published models provide a "complete" description of the cooking process. Ideally, a cooking model should be based entirely upon engineering first-principles, be flexible for a wide range of products and product conditions, and describe the interrelationships between all of the components of the cooking process including heat transfer, moisture transfer, and the transfer of fat. The goal of the following sections was to develop such a model.

3 MATERIALS AND EXPERIMENTAL METHODS

3.1 Overview

The study was broken up into three major groups of experiments. In the first group of experiments, ground beef, ground pork, and ground turkey patties were cooked in a laboratory convection oven. The results of these experiments were used to illustrate and quantify the differences in cooking characteristics between species and fat content. In the second group of experiments, laboratory studies were conducted to determine the fat holding capacity of ground beef. The data generated in these experiments were later used to develop the fat transfer portion of the cooking model (Chapter 4). The third set of experiments involved cooking ground beef patties in an industrial moist-air impingement oven. These data were then analyzed to determine the effects of processing conditions on yield and temperature profiles. In addition, results from this group of experiments were utilized to validate the computer-cooking model that is described in Chapter 4.

3.2 Laboratory oven cooking tests

3.2.1 Experimental procedure

A series of laboratory experiments was conducted to investigate the effect of meat species and initial fat content on cooking characteristics during convection cooking of ground beef, ground pork, and ground turkey patties. All cooking tests were conducted using a custom built, laboratory convection oven.

The laboratory convection oven consisted of three chambers (Figure 3.1). These included a large conditioning chamber (Figure 3.2), a steam generator, and the cooking chamber itself.

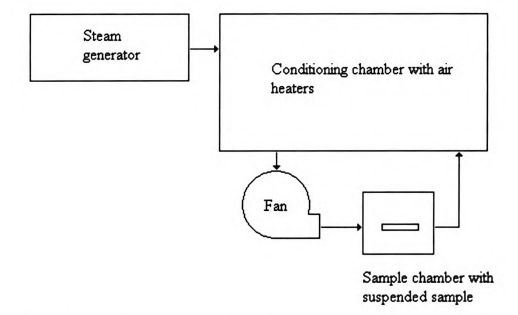


Figure 3.1 – General arrangement of the laboratory convection oven showing directions of steam and airflow.



Figure 3.2 - Interior of laboratory oven conditioning chamber.

The conditioning chamber was the largest portion of the oven and was used to heat and condition the cooking air to the desired temperature and moisture content. The dimensions of the conditioning chamber were approximately 83 cm in length by 56 cm in width by 51 cm in height. The conditioning chamber contained four 350-watt strip heaters (McMaster-Carr: Cleveland, OH). Steam was injected into the conditioning chamber from the steam generation unit. The steam generation unit contained water heated by a 750-watt immersion heater (Tempco: Wood Dale, IL). An electronically activated solenoid valve was utilized to inject steam into the conditioning chamber. The sample chamber was a small container located at the edge of the conditioning chamber. The dimensions of the cooking chamber were approximately 10 cm by 10 cm by 10 cm. Cooking air was drawn from the conditioning chamber by a 6-watt centrifugal fan (Dayton model 4C440: Niles, IL) and passed through the sample chamber by means of tubular ducts (Figure 3.3).

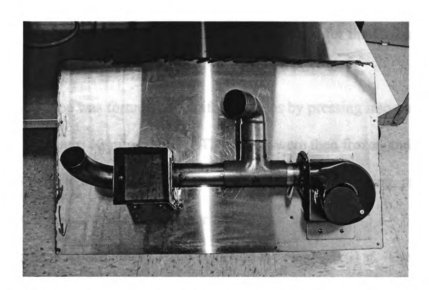


Figure 3.3 - Interior of laboratory oven showing fan, ducts, and sample chamber (located at left).

The oven was connected to a computer interface that continuously monitored and controlled oven temperature and moisture content. During cooking, oven dry bulb and wet bulb temperature were controlled within \pm 0.2°C. Dry bulb and wet bulb temperature within the conditioning chamber was monitored using a high temperature dry bulb/wet bulb humidity probe (Viasala model DMP 246: Viasala, Woburn, MA). The airflow in the cooking chamber was 1.3 m/s.

Ground turkey, ground beef, and ground pork were purchased from a local grocery store. Additional ground pork was provided from the Michigan State University Meat Laboratory. Two fat contents of each meat species were utilized: 1.4 and 8.6% for ground turkey, 7.2 and 17.5% for ground beef, and 15.7 and 41.9% for ground pork. Fat contents were determined in triplicate by solvent extraction (AOAC method 991.36: AOAC, 2000). The moisture content of each species was determined in triplicate by oven drying (AOAC method 950.46: AOAC, 2000). Moisture contents were 74.8 and 73.0% wet basis for the 1.4 and 8.6% fat ground turkey, 71.5 and 63.3% wet basis for the 7.2 and 17.5% fat ground beef, and 64.1 and 43.6% wet basis for the 15.7 and 41.9% fat ground pork.

Each meat type was formed into uniform patties by pressing into plastic petri dishes (52 mm diameter; 13 mm height). The patties were then frozen and removed from the dishes prior to use in the cooking experiments. Before cooking, patties were tempered to 4°C by placing in a refrigerator for 2-3 h.

Prior to heating, each patty was weighed to the nearest 0.01 g. The radius and thickness of each patty were then measured, to the nearest 0.1 mm, using a digital caliper.

A 24-gauge type-K thermocouple (Omega: Stamford, CT) was then inserted into the geometric center of each patty using a placement jig (Figure 3.4).

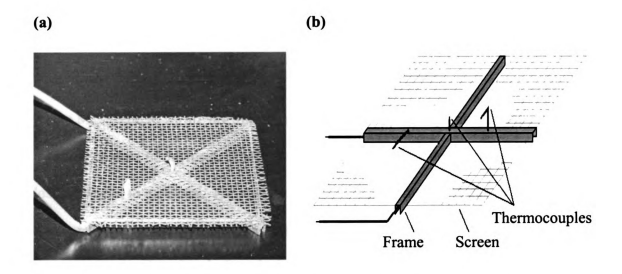


Figure 3.4 – (a) Picture and (b) schematic of jig used to place thermocouples into meat patties during cooking experiments.

Patties were then placed into the cooking chamber of the oven, where they were supported on a wire mesh screen. This allowed for airflow on all sides of the product. The patties were cooked one at a time in the convection oven to center temperatures of 45, 55, 65, 75, and 85°C at an oven temperature of 177°C and a wet bulb temperature of 82°C. Five patties were cooked at each condition. After cooking, the patties were removed from the oven and weighed to the nearest 0.01 g. The new thickness and diameter of each patty were measured using the caliper, and the patties were frozen at 5°C pending further analysis. After 24 h, the patties were removed from the freezer, and the moisture content was measured by oven drying (AOAC Method 950.46: AOAC, 2000).

The amount of water lost during cooking was calculated for each patty using the initial and final moisture contents (Equation [3.1]).

$$\Delta M_{\text{moisture}} = M_{\text{initial}} \cdot X_{\text{w,initial}} - M_{\text{final}} \cdot X_{\text{w,final}}$$
 [3.1]

where $M_{initial}$ and M_{final} are the initial and final mass of the patty and X_w is the wet basis moisture content of the meat. These data were used to calculate the component of yield loss attributed to moisture. For many of the samples, the mass lost due to moisture loss was considerably less than the total mass loss. The mass loss not accounted for by moisture was attributed to fat loss during cooking. These losses were calculated using Equation [3.2].

$$\Delta M_{fat} = \Delta M_{total} - \Delta M_{moisture}$$
 [3.2]

3.2.2 Statistical analysis

Analysis of variance (ANOVA) was used to evaluate the effects (α=0.05) of initial fat content, cooking time, and time-fat interaction on center temperature, cooking yield, fat loss, and volume change within each meat species. ANOVA was conducted using the Microsoft Excel Data Analysis Package (Microsoft Excel Version 2000:Redmond, WA).

3.3 Measurement of fat holding capacity

3.3.1 Experimental procedure

Laboratory experiments were conducted in an isothermal water bath to determine the fat holding capacity of ground beef. The fat holding capacity of the meat is the maximum amount of fat bound in the meat after a given heat treatment. The fat holding capacity of the meat was determined as a function of temperature and time using a so-called "net test" (Barbut, 1996).

Two lots of ground beef were acquired from the Michigan State University Meat Laboratory. The fat contents of the two lots were 5.6 and 15.0% fat by mass, determined in triplicate using solvent extraction (AOAC method 991.36: AOAC, 2000).

Brass tubes were used to contain the meat samples during cooking and were chosen due to their high thermal conductivity. The tubes were cut from 0.36 mm thick brass tube stock (K&S Engineering: Chicago, IL). The tubes had an inside diameter of 7.9 mm and a length of approximately 122 mm.

Prior to each heating test, a silicone stopper was placed in one end of each heating tube. Teflon tape (13 mm width) was then wrapped around the silicone stopper to ensure that the closed end of the tube was watertight. The weight of the combined tube, stopper, and tape was then measured to the nearest 0.1 mg using an electronic balance.

Approximately 3.5g of meat was then loaded into each tube by hand. During loading, the meat was packed into the closed end of the brass tube by firmly tapping the tube on the bench top. After loading, the total weight of the tube and meat was measured to the nearest 0.1 mg.

A 30 μm nylon mesh (Spectrum Labs: Rancho Dominguez, CA) was then attached over the open end of each tube using laboratory tape. A type-T thermocouple probe (Cole Parmer: Vernon Hills, IL) was inserted through the silicone stopper and into the approximate center of the meat sample within the tube. Tubes were then placed into an isothermal water bath (Neslab: Newington, NH) for one of four holding times. The open end of each tube was held above the surface of the water by a test tube rack. The entire meat sample was located in the submerged portion of the brass tube. The time measurement was started when the temperature of the center of the sample was within 1.0°C of the water bath temperature. Samples were heated at water temperatures of 30, 35, 40, 45, 50, 55, 60, 65, 70, 75, 80, 85, and 90°C and heating times of 2, 5, 10, and 15 minutes. Five tubes were heated simultaneously for each time-temperature combination.

After heating, the tubes were removed from the water bath, and the surface moisture was removed with a paper towel. The tubes were then placed, mesh-side down in centrifuge tubes (length: 102 mm, diameter: 14.7 mm: Fisher: Pittsburgh, PA). A brass spacer fabricated from the same stock used to produce the heating tubes was placed in the bottom of each centrifuge tube (Figure 3.5). The length of the brace spacers was approximately 27 mm. Prior to centrifuging, the silicone stoppers and Teflon tape were removed from each tube. The tubes were centrifuged at 25°C and 1000g for 15 minutes.

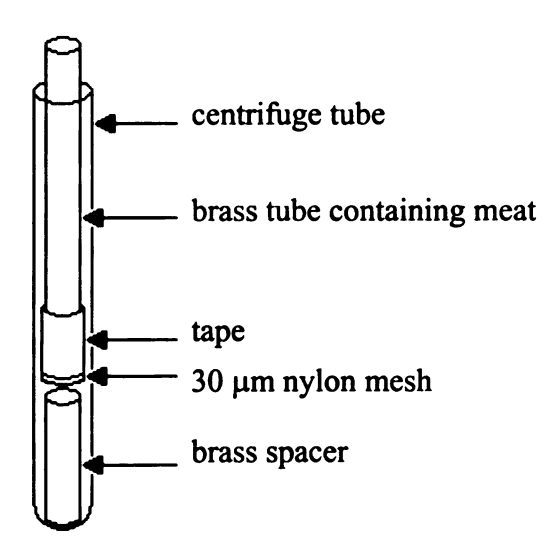


Figure 3.5 – Schematic of tube setup used for centrifuging.

After centrifuging, two distinct layers were observed in each tube. A solid layer of extracted fat was located above a liquid layer (Figure 3.6). For the purposes of this study, only the fat located in the solid layer was of interest, as this is the component most often overlooked by cooking models. To separate the solid fat from the liquid layer, the brass tube containing the meat sample was first removed from each tube. A syringe with an 18-gauge needle (BD: Franklin Lakes, NJ) was then used to withdraw the liquid layer from beneath the solid fat layer. The centrifuge tube containing the spacer and the fat layer was then heated in a 102°C convection oven for 24 hours to drive off any remaining water. After heating, the tube was removed from the oven and allowed to cool in a dessicator for one hour. The tube was then weighed to the nearest 0.1 mg, and the weight of fat in the tube determined by subtracting the weight of the empty tube and spacer from the weight of the tube containing the spacer and extracted fat.

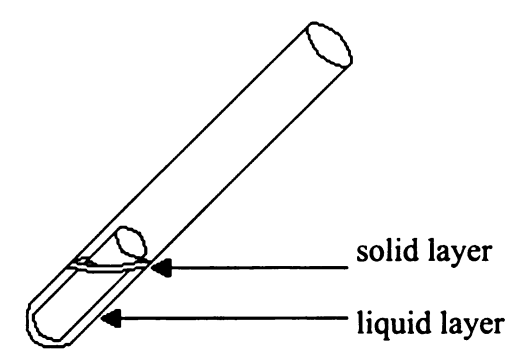


Figure 3.6 – Schematic of the centrifuge tube after centrifuging showing the two distinct layers that formed within the tube. In this schematic the heating tube has been removed. The liquid layer contains water and soluble proteins. The solid layer is composed of fat.

The fat content remaining in each sample after centrifuging was determined by subtracting the mass of the extracted fat from the initial mass of fat in the sample prior to heating. It was assumed that no protein was present in the extracted fat. The fat content was expressed in terms of dry basis fat content by dividing the mass of fat remaining in the sample by the mass of non-fat dry matter in the sample. This fat content was considered the fat holding capacity of the meat under the specific conditions of temperature and time.

3.3.2 Statistical analysis

Quadratic response-surface models were used to describe the fat holding capacity of each batch of meat as functions of time and temperature (Equation 3.3).

$$F = \beta_0 + \beta_1 \cdot T + \beta_2 \cdot T^2 + \beta_3 \cdot t + \beta_4 \cdot t^2 + \beta_5 \cdot t \cdot T + \varepsilon$$
 [3.3]

The statistical significance (α =0.05) of each regression parameter was determined using t-statistics. The models were then adjusted accordingly to eliminate non-significant terms. A regression model was also fit to the combined FHC results of the low and high fat ground beef (Equation [3.4]).

$$F = \beta_0 + \beta_1 \cdot T + \beta_2 \cdot T^2 + \beta_3 \cdot t + \beta_4 \cdot t^2 + \beta_5 \cdot F + \beta_6 \cdot t \cdot T + \beta_7 \cdot T \cdot F_0 + \beta_8 \cdot t \cdot F_0 \quad [3.4]$$

The statistical significance (α =0.05) of each regression parameter was determined using t-statistics, and the model was again adjusted to eliminate non-significant terms.

3.4 Industrial oven cooking tests

3.4.1 Experimental procedure

A series of cooking tests were conducted using a commercial continuous-feed moist-air impingement oven (Stein model JSO-IV:FMC FoodTech, Sandusky, OH) located at the FMC FoodTech Technical Center (Sandusky, OH). The JSO-IV oven consisted of two 3.65 m long cooking sections with a 0.8 m intermediate section. The belt width of the oven was 1.02 m. The oven was equipped with 1.07 m long in-feed and discharge sections, which were not utilized during this study.



Figure 3.7 - Stein model JSO-IV moist-air impingement oven.

Commercially produced, pre-formed, frozen hamburger patties (Gordon Foods, Grand Rapids, MI) were used for the cooking tests. The patties had a thickness of 1 cm and average diameters of ~12 cm. The average uncooked patty weight was 105 g. The labeled fat content was 10%. This fat content was confirmed using solvent extraction (AOAC method 991.36: AOAC, 2000).

Tests were conducted using a 1/3 partial factorial design (Table 3.1) comprised of three cooking temperatures (121, 177, and 232°C), three oven steam contents (50, 70, and 90% steam by volume), and three oven fan speeds (50, 75, and 100% of full). For each cooking condition, three oven belt speeds were chosen to produce varying degrees of doneness (undercooked, fully cooked, and over cooked). Belt speeds were chosen based upon the experience of a trained operator and adjusted as required to achieve the desired patty temperatures. Two hamburger patties were cooked at each belt speed, for a total of 54 patties.

Table 3.1. Treatment conditions utilized for model validation experiments.

Experiment	Temp. (°C)	Steam by Volume	Air Flow	Time (Min.)
_	• ` ` `		m/s	
1	121	50 %	11.4	5
6	121	50 %	16.8	11
8	121	50 %	21.8	8
11	121	70 %	11.4	8
13	121	70 %	16.8	5
18	121	70 %	21.8	11
21	121	88 %	11.4	11
23	121	78 %	16.8	. 8
25	121	78 %	21.8	5
30	177	50 %	11.4	8
32	177	50 %	16.8	6
34	177	50 %	21.8	3
37	177	70 %	11.4	3
47	177	83 %	11.4	6
49	177	84 %	16.8	3
50	177	86 %	16.8	6
54	177	86 %	21.8	8
56	232	50 %	11.4	5
58	232	50 %	16.8	2
63	232	50 %	21.8	7
66	232	70 %	11.4	7
68	232	70 %	16.8	5
70	232	70 %	21.8	2
73	232	82 %	11.4	2
75	232	82 %	11.4	7
78	232	82 %	16.8	7
80	232	82 %	21.8	5

Prior to cooking, the frozen patties were tempered in a -3°C cooler (> 3 h) to provide a uniform initial temperature distribution. Before each cooking run, the patties were weighed to the nearest 0.1 g. The radius and diameter of each patty were measured to the nearest 0.1 mm using a digital caliper. A 24-gauge type-K thermocouple (Omega: Stamford, CT) was then placed and held at the center of each patty using a placement jig

(Figure 3.4). Additional thermocouples were positioned at the top and bottom surfaces of the patties and held in place by the placement jig. The thermocouples were attached to an oven data logger (Datapaq model 9000: Datapaq, Wilmington, MA). that was able to pass through the oven with the patties during cooking. During the cooking process, patty and air temperatures were recorded every 1 second.

Patties were placed on the center of the oven belt and allowed to cook for the designated time. The patties were then removed from the oven and immediately weighed to the nearest 0.1 g to determine post-cooking weight. The thickness and diameter of each patty was then re-measured to the nearest 0.1 mm. After weighing and measuring, the patties were frozen (-20°C) using an impingement freezer and placed into sealed plastic bags pending further analysis. Dwell time in the impingement freezer was 2 minutes.

After each cooking run, the data were uploaded to a personal computer, and temperature versus time curves were constructed. The bulk moisture content of each patty was determined using oven drying (AOAC Method 950.46: AOAC, 2000). The cooking yield was calculated for each patty by dividing the mass of the cooked patty by the mass of the patty prior to cooking. Using the moisture content of the raw and cooked meat, the mass of water that exited the patty during cooking was calculated (Equation [3.1]).

3.4.2 Statistical analysis

Multiple linear regression was conducted to quantify the effects of the cooking variables on the center temperature achieved in the patties during cooking. Equation [3.5] was used as the basis for the regression.

$$T_{center} = \beta_0 + \beta_1 \cdot T_{oven} + \beta_2 \cdot X_{steam} + \beta_3 \cdot time + \beta_4 \cdot Airflow + \varepsilon$$
 [3.5]

A second regression was performed in an attempt to quantify the effects of cooking parameters on cooking yield. Regression was performed using Equation [3.6] as a basis.

Yield =
$$\beta_0 + \beta_1 \cdot T_{oven} + \beta_2 \cdot X_{Steam} + \beta_3 \cdot time + \beta_4 \cdot Airflow + \epsilon$$
 [3.6]

3.5 Cooking model validation

3.5.1 Cooking model

A computer model was developed to simulate moist-air impingement cooking of ground-and-formed meat and poultry patties. Development of this model is detailed in Chapter 4. The model was based upon heat and mass transfer principles and did not require experimental data for its development, with the exception of the relationships utilized for the fat holding capacity. However, it was necessary to validate the model using experimental data to validate its performance. This was conducted using data generated in the industrial cooking tests (Section 3.4) and additional published data from a pilot-scale impingement oven.

3.5.2 Experimental data

The finished computer model was validated using the data generated in the industrial impingement cooking tests described in Section 3.4. The computer model requires user input of oven temperature, steam fraction, air velocity, and cooking time. Additional inputs required are product initial temperature, product moisture content, product fat content, and meat species. The computer model was executed using the 27 sets of process conditions listed in Table 3.1. The input conditions for the ground beef were an initial temperature of -2 to 0°C, initial moisture content of 66% wet basis, and initial fat content of 10% wet basis. The element mesh was set up for a patty diameter of 12 cm and thickness of 1 cm (see Chapter 4 for element mesh).

Output data were generated for the transient patty center and surface temperatures, final bulk moisture content, and final cooking yield. The output were compared to the temperature profiles generated during the cooking experiments as well as to the final yield and moisture values measured after the cooking tests. A standard error of prediction (SEP) between the transient model and experimental temperature profiles was calculated for each run (Equation [3.7]).

$$SEP = \sqrt{\frac{\sum (T_{predicted} - T_{measured})^2}{n-1}}$$
 [3.7]

The differences between the predicted and measured yield, moisture content, and fat loss were determined for each model run. The aggregate standard error of prediction

was also calculated for the endpoint yield, moisture content, and fat loss for all of the model runs.

3.5.3 Comparisons with literature data

In addition to the model validation using experimental data from the industrial cooking tests, the cooking model was compared to published data for ground chicken breast patties (Murphy et al, 2001a and b). The purpose of this comparison was to demonstrate the versatility of the model. The published data were collected using a pilot-scale moist-air impingement oven (Stein model 102: Stein, Sandusky, OH). Murphy et al. (2001a) developed a regression model for cooking time as a function of center temperature, oven air velocity, and oven wet bulb temperature (Equation [3.8]).

$$\ln(t) = 8.8678 + 0.0278 \cdot T - 2.0410 \cdot \ln(T_{wb}) - 0.2306 \cdot V_{air} + 0.0481 \cdot \ln(T_{wb} \cdot V_{air})$$
[3.8]

The regression for cooking time had an R^2 of 0.95. Murphy et al. (2001b) developed a second regression model for yield of ground chicken patties as a function of patty center temperature, oven air velocity, and oven air wet bulb temperature (Equation [3.9]). The regression model for yield had an R^2 of 0.89.

Yield =
$$75.4031 + 0.9309 \cdot T - 1.2443 \cdot V_{air} + 0.1047 \cdot V_{air}^2 - 0.0121 \cdot T^2 - 0.0102 \cdot T_{wb} \cdot V_{air} + 0.0027 \cdot T_{wb} \cdot T$$
 [3.9]

The geometry of the Stein 102 oven used by Murphy et al. (2001a and b) was different from the geometry of the Stein JSO-IV. The Stein 102 oven used an array of round nozzles rather than the slot nozzles utilized in the JSO-IV oven (Chapter 4). Therefore, it was necessary to modify the cooking model with an equation for an array of round nozzles as discussed in Chapter 4.

Model simulations were conducted using the process conditions of Murphy et al. (2001a and b). These conditions were a dry bulb cooking temperature of 149°C, wet bulb air temperatures of 40, 70, 85, and 95°C, and air velocities of 1.53, 2.13 and 2.73 m/s. The product settings for the model were chicken at an initial moisture content of 80% wet basis, initial fat content of 0.2% dry basis, and initial temperature of 4°C. The element mesh was adjusted for a patty diameter of 127 mm and a thickness of 12.7 mm. Cooking model tests were run using each combination of dry bulb temperature, wet bulb temperature, and airflow giving a total of 12 cooking conditions. The cooking time of each simulation was adjusted to give a final patty temperature of 80°C.

For each model run, the temperature profile from the model was compared to the temperature profile generated by the regression model at 1 second intervals for the temperature range between 55 and 80°C (the calibration range of the regression model). Transient standard error of prediction was calculated for each run using Equation [3.7]. The same procedure was used to calculate the SEP for transient yield value for each run.

3.6 Salmonella inactivation model validation

The location of the impingement oven utilized for our experiments did not allow for inoculated challenge studies. Therefore, simulated Salmonella Senftenberg

inactivation results were compared to literature values for ground meat patties cooked in a pilot-scale moist-air impingement oven (Murphy et al., 2002). Simulated results for *Listeria innocua* were also compared to literature values (Murphy et al., 2002) to demonstrate the flexibility of the model.

The model was run using the equations for the geometry of the Stein 102 oven (array of round nozzles). The cooking air conditions utilized for the model runs were an oven air temperature of 288°C, a steam content of 25% by volume, and an air velocity of 4 m/s. Although the patties used by Murphy et al. (2002) were composed of a mixture of ground beef and ground turkey, the ground beef setting was utilized for the model runs. This setting was chosen based upon the fairly high (20% wet basis) fat content of the meat. The product properties were an initial moisture content of 58% wet basis, initial fat content of 20% wet basis, and initial temperature of -2°C.

The model was run once for inactivation of *S*. Senftenberg and once for inactivation of *L. innocua*. The D and z-values for the model runs were set to 312 seconds and 6.23°C for *S*. Senftenberg and 1,508 seconds and 4.90°C for *L. innocua*, at a reference temperature of 60°C (Murphy et al., 2003). The reference temperature for both sets of D and z values was 60°C. The experiments of Murphy et al. (2002) utilized ground meat with an initial inoculum of 10⁷ CFU/g. Therefore, the model was set to run with a limit of 7-log total reduction. Transient inactivation curves generated by the model for each organism were plotted on the same graphs as data from the published study and SEP's calculated between the model and experimental data.

4 MODEL DEVELOPMENT

4.1 Introduction

A computer model was developed for moist-air impingement cooking of ground and formed meat and poultry products. The computer model is composed of a coupled heat and mass transfer model combined with a model for *Salmonella* inactivation. The finite element method (FEM) was used to numerically solve the differential equations associated with the heat and mass transfer model. The model was programmed using Microsoft Visual Basic (Version 6.0 professional edition: Microsoft, Redmond, WA).

A typical impingement oven has impinging jets located above and below the product (Figure 4.1). The cooking air enters the ductwork and is forced through slots normal to the product. Not shown in Figure 4.1 is the perforated belt that the product travels on through the oven. A typical impingement oven would contain many pairs of impingement jets arranged in series along the length of the belt.

The computer model was developed for an oven with the following controllable variables: airflow, air temperature, steam content by volume, and cooking time. The distance between the impinging jets and the product surface must also be specified. For the purpose of modeling, it was assumed that the upper and lower impinging jets were located an identical distance from the product surface.

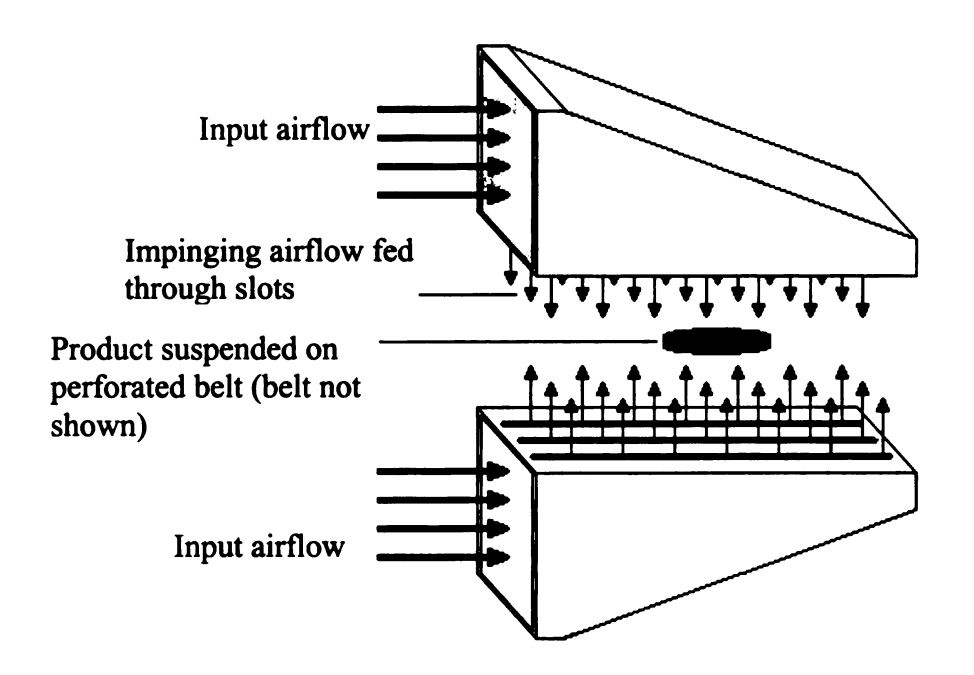


Figure 4.1 - Illustration of the airflow within an impingement oven in relation to the product.

The coupled heat and mass transfer model was based upon three transport components. The three components were heat transfer, moisture transfer, and fat transfer. Incorporation of the fat transfer component represents one of the unique aspects of the cooking model as compared to most previous models that have been published. The three transport solutions were coupled through the boundary conditions and interdependent thermo-physical properties.

The boundary conditions associated with moist-air impingement ovens are somewhat different than those in conventional convection ovens. One of the unique aspects of moist-air impingement ovens is the very high oven air moisture content that is often used for meat product cooking. The high fraction of water in the air results in a condensing boundary condition during the period in which the surface of the patty is below the dew point of the cooking air. This condensing condition increases the rate of

heat transfer and reduces the rate of moisture loss from the product. Inclusion of the condensing boundary condition is another unique aspect of this cooking model.

Two different sets of boundary conditions were used to model the cooking process – one for the impinging flows on the horizontal surface of the patties and one for the vertical edges of the patties. The first set of boundary conditions was used to describe the impinging flow that is the predominant mechanism for heat and mass transfer in moist-air impingement ovens. The boundary conditions used to model impinging flow were based on an expansion of the technique of Millsap and Marks (2002) and depended on transport correlations published by Martin (1977). The second set of boundary conditions was used to describe the convection that occurs along the vertical surfaces (edges) of the patty. These conditions were based upon transport correlations for turbulent flow past a flat plate (Bejan, 1995).

The following set of basic assumptions was utilized when developing the heat and mass transfer model.

- 1. Heat transfer occurs by conduction within the patty and by a combination of convection, condensation, and evaporation at the patty surface.
- 2. Moisture and fat transfer within the patty occur primarily by diffusion and capillary flow, respectively.
- When the temperature of the patty is below the dew point, moisture condenses at the patty surface, and the moisture content of the patty surface does not change.
 When the surface temperature of the patty is above the dew point, water evaporates at the surface.

- 4. The phase change from solid to liquid water occurs at a single temperature. A phase change from solid to liquid fat occurs at a single fat melting point.
- 5. Mass transport of water within the patty does not occur at temperatures below the freezing temperature. Mass transport of fat does not occur below the melting point of the fat.
- 6. Fat transport within the patty is driven by the gradient between the local fat content and the value at the surface. Surface fat content is a function of time, temperature, and initial fat content.
- 7. The size and shape of the patty does not change during cooking.
- 8. Boundary conditions were assumed to be the same for the top and bottom of each patty.

4.2 Heat and mass transfer model

4.2.1 Heat transfer solution

The heat transfer simulation was formulated using the Fourier equation written in terms of enthalpy. The enthalpy formulation was utilized to produce a model free from discontinuities caused by the phase changes of fat and water. Similar techniques for modeling heat transfer have been utilized by Volner and Cross (1981), Pan (1998), and Pan et al. (2000).

Most ground beef and poultry patties are shaped like short cylinders (Figure 4.2). This geometry allows heat and mass transfer in formed patties to be modeled using two-dimensional axisymmetric solutions. Heat transfer by conduction within the patties was modeled using Equation [4.1].

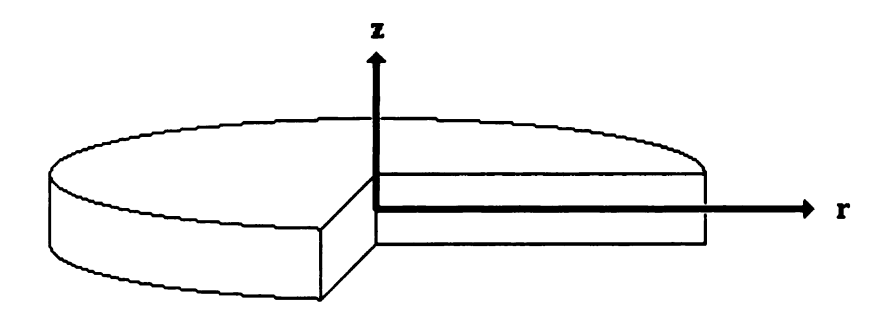


Figure 4.2 – Geometry of a patty illustrating radial coordinate system.

$$\frac{\partial H}{\partial t} = \frac{1}{r} \cdot \frac{\partial}{\partial r} \left(r \cdot \frac{k_T}{c_p \cdot \rho} \frac{\partial H}{\partial r} \right) + \frac{\partial}{\partial z} \left(\frac{k_T}{c_p \cdot \rho} \frac{\partial H}{\partial z} \right)$$
[4.1]

Heat capacity (c_p) , thermal conductivity (k_T) , and density (p) were modeled using transient values based on product composition and temperature (Section 9.3). Patties were assumed to be at a uniform internal temperature prior to cooking. The initial product temperature was converted to enthalpy using an equation based on the technique of Voller and Cross (1981): (Equation [4.2]).

$$H = \begin{cases} c_{p,frozen} \cdot T & T < T_{freezing} \\ c_{p,frozen} \cdot T_{freezing} & T = T_{freezing} \\ c_{p,frozen} \cdot T_{freezing} + \lambda_w + c_p \cdot \left(T - T_{freezing}\right) & T_{freezing} < T <= T_{melting,fat} \\ c_{p,frozen} \cdot T_{freezing} + \lambda_w + c_p \cdot \left(T - T_{freezing}\right) + \lambda_f & T > T_{melting,fat} \end{cases}$$

$$[4.2]$$

Equation [4.2] converts temperature values into enthalpy based upon an absolute zero reference temperature. Provision was made for two phase changes within the product during cooking. The first was the phase change between ice and liquid water, and the second was the phase change between solid and liquid fat. An initial temperature equal to the freezing temperature of the meat was assumed to imply a completely frozen sample.

A similar technique was used to convert enthalpy values back to temperature for display purposes (Equation [4.3]). The variables $c_{p,f}$ and $c_{p,t}$ in Equation [4.3] are the heat capacities of the frozen and thawed meat, T_f and T_m are the freezing temperature of water and the melting temperature of fat, and $\lambda_{f,w}$ and $\lambda_{f,f}$ are the latent heats of fusion for water and fat respectively. Based on the results of the fat holding capacity experiments described in Section 3.3, a value of 45°C was used for the fat melting temperature.

$$T = \begin{cases} H/c_{p,f} \\ T_{f} \end{cases}$$

$$T = \begin{cases} (H - \lambda_{w} - 273 \cdot c_{p,f})/c_{p,t} \\ T_{m} \\ \left(H - \lambda_{w} - 273 \cdot c_{p,f} - \lambda_{w}\right)/c_{p,t} \end{cases}$$

$$\begin{split} H &\leq c_{p,f} \cdot T_f \\ c_{p,f} \cdot T_f &\leq H \\ &\leq c_{p,f} \cdot T_f + \lambda_w \\ c_{p,f} \cdot T_f + \lambda_w &< H \\ &\leq c_{p,f} \cdot T_f + \lambda_f + T_f \cdot c_{p,t} \\ c_{p,f} \cdot T_f + \lambda_f + T_f \cdot c_{p,t} &< H \\ &\leq c_{p,f} \cdot T_f + \lambda_f + T_f \cdot c_{p,t} + \lambda_f \\ H &> c_{p,f} \cdot T_f + \lambda_f + T_m \cdot c_{p,t} + \lambda_f \end{split}$$

[4.3]

The boundary conditions for heat transfer were composed of a convection term and a moisture transport term (Equation [4.4]).

$$k_T \cdot \frac{\partial T}{\partial n} = h_T \cdot (T_{air} - T_{surface}) + h_{m,water} \cdot \lambda_{vaporization} \cdot (C_{air} - C_{surface})$$
 [4.4]

During the period in which the surface temperature of the meat is below the dew point temperature of the cooking air, heat transfer due to condensation occurs, causing additional heat transfer into the patty. When the surface temperature of the meat exceeds the dew point temperature, evaporation occurs at the patty surface, limiting sensible temperature increases in the product. This has the effect of limiting the maximum surface temperature reached at the product surface as a function of oven conditions and surface moisture content. Until the surface of the patty reaches low moisture contents due to drying, the surface temperature never exceeds the wet bulb temperature.

At the vertical and radial centerlines of the product, heat transfer was assumed to be zero due to product symmetry (Equations [4.5] and [4.6]).

$$\frac{\partial T}{\partial r} = 0 \qquad r = 0 \qquad [4.5]$$

$$\frac{\partial \Gamma}{\partial z} = 0 \qquad z = 0 \qquad [4.6]$$

4.2.2 Moisture transfer solution

Moisture transfer within the product was modeled using a two-dimensional equation for diffusion in radial coordinates (Equation [4.7]).

$$\frac{\partial m}{\partial t} = \left(\frac{1}{r} \cdot \frac{\partial}{\partial r} \left(r \cdot \frac{k_{m,water}}{c_{m,water} \cdot \rho} \cdot \frac{\partial m}{\partial r} \right) + \frac{\partial}{\partial z} \left(\frac{k_{m,water}}{c_{m,water} \cdot \rho} \cdot \frac{\partial m}{\partial z} \right) \right)$$
[4.7]

The units for m_{water} are decimal dry basis moisture content. Mass transfer at the product surface was modeled using a convective boundary condition (Equation [4.8]).

$$k_{m,water} \frac{\partial m}{\partial n} = h_{m,water} \cdot (C_{air} - C_{surface})$$
 [4.8]

The concentration of moisture in the cooking air was calculated using Equation [4.9].

$$C_{air} = \rho_{steam} \cdot X_{air}$$
 [4.9]

 X_{air} is the molar fraction of steam in the cooking air. This is equal to the percentage of steam by volume. The density of steam (ρ_{steam}) was calculated using an equation derived from tabular data (see Section 9.2).

$$\rho_{\text{steam}} = -0.0002 \cdot \log(T) + 0.0015$$
 [4.10]

The concentration of moisture at the patty surface was calculated using Equation [4.11].

$$C_{\text{surface}} = \text{ERH} \cdot C_{\text{sat}}$$
 [4.11]

Equilibrium relative humidity (ERH) was calculated using an equation by Huang and Mittal (1995).

ERH =
$$\exp\left(\frac{-5222.47 \cdot \text{m}^{-1.0983}}{1.9818 \cdot \text{T}}\right)$$
 [4.12]

In Equation [4.12], m is dry basis moisture content, T is absolute temperature, and ERH is decimal equilibrium relative humidity. The saturation concentration (C_{sat}) was calculated using Equation [4.13]. Equation [4.13] was developed using regression of steam table data as shown in Section 9.2.

$$C_{\text{sat}} = 8.121 \cdot 10^{-10} \cdot \text{T}^3 - 3.520 \cdot 10^{-8} \cdot \text{T}^2 + 1.320 \cdot 10^{-6} \cdot \text{T} + 6.215 \cdot 10^{-7}$$
 [4.13]

At the radial and vertical centerlines of the patty, mass transfer was assumed to be zero due to product symmetry (Equations [4.14] and [4.15]).

$$\frac{\partial m}{\partial r} = 0 r = 0 [4.14]$$

$$\frac{\partial m}{\partial z} = 0 z = 0 [4.15]$$

4.2.3 Fat transfer solution

Fat transfer was modeled using a two-dimensional formulation of Darcy's law for diffusion of liquids through porous media (Datta, 2002).

$$\frac{\partial F}{\partial t} = \left(\frac{1}{r} \cdot \frac{\partial}{\partial r} \left(r \cdot D_{cap,fat} \cdot \frac{\partial F}{\partial r}\right) + \frac{\partial}{\partial z} \left(D_{cap,fat} \cdot \frac{\partial F}{\partial z}\right)\right)$$
[4.16]

Fat content was written in terms of dry basis fat content. $D_{cap.fat}$ is the capillary diffusivity of fat in the product.

The fat content at the surface of the patty was modeled using an equation generated from experimental values as detailed in Section 3. Equation [4.17] was utilized to set the values of the fat content at each boundary node as a function of temperature and product composition. This equation was derived from experimental data (Section 5.3.)

$$F = 0.7062 - 0.0193 \cdot T + 0.0001 \cdot T^{2} + 0.0069 \cdot F_{initial} + 0.0002 \cdot T \cdot F_{initial}$$
 [4.17]

At the radial and vertical centerlines of the patty, fat transfer was assumed to be zero due to product symmetry (Equations [4.18] and [4.19]).

$$\frac{\partial F}{\partial r} = 0 \qquad r = 0 \qquad [4.18]$$

$$\frac{\partial F}{\partial z} = 0 z = 0 [4.19]$$

4.2.4 Heat and mass transfer coefficients – Array of slot nozzles

Heat and mass transfer coefficients utilized in Equations 4.4 through 4.8 were modeled as functions of instantaneous process conditions using the technique of Millsap and Marks (2002). For the surfaces of the patty subject to impingement conditions (the top and bottom), correlations developed by Martin (1977) for an array of slot nozzles were used to determine heat and mass transfer coefficients. Prandtl number, Schmidt number, and Reynolds number were first calculated using Equations [4.20], [4.21], and [4.22] respectively.

$$Pr = \frac{c_{p,mix} \cdot \mu_{mix}}{k_{mix}}$$
 [4.20]

$$Sc = \frac{\mu_{mix}}{\rho_{mix} \cdot D_{AB}}$$
 [4.21]

$$Re = \frac{v_{jet} \cdot \rho_{mix} \cdot W}{\mu_{mix}}$$
 [4.22]

Values for the heat capacity $(c_{p,mix})$, viscosity (μ_{mix}) , thermal conductivity (k_{mix}) , density (ρ_{mix}) , and diffusivity (D_{sa}) of the air-steam mixture were calculated using the relationships in Section 9.2. The (W) term in Equation [4.22] is the slot width of the impinging jets. The term, v, in Equation [4.22] is the jet exit velocity.

Nusselt and Sherwood numbers were calculated using Equations [4.23] and [4.24], respectively (Martin, 1977).

Nu =
$$\frac{2}{3} \cdot \Pr^{0.42} \cdot f_0 \frac{3}{4} \cdot \left(\frac{2 \cdot \text{Re}}{\frac{f_0}{f_0} + \frac{f_0}{f}} \right)^{\frac{2}{3}}$$
 [4.23]

$$Sh = \frac{2}{3} \cdot Sc^{0.42} \cdot f_0 \frac{3}{4} \cdot \left(\frac{2 \cdot Re}{\frac{f}{f_0} + \frac{f_0}{f}} \right)^{\frac{2}{3}}$$
 [4.24]

where f_0 is a function of the slot geometry, and is given by Equation [4.25].

$$f_0 = \left(60 + 4 \cdot \left(\frac{H}{W} - 2\right)^2\right)^{-1/2}$$
 [4.25]

In Equation [4.25], H represents the spacing between the impinging jets and the product surface, and W represents the slot width of the jets. Heat and mass transfer coefficients were calculated from the Nusselt and Sherwood numbers using Equations [4.26] and [4.27], respectively.

$$h_{T} = \frac{Nu \cdot k_{mix}}{W}$$
 [4.26]

$$h_{m,water} = \frac{Sh \cdot D_{sa}}{W}$$
 [4.27]

For the vertical surfaces of the patty (the patty edges), correlations for turbulent flow past a flat plate (Bejan, 1995) were used to calculate heat and mass transfer coefficients. Turbulent flow was assumed due to the flow regime created by configuration of the oven ductwork and turbulent air coming off of the top and bottom surfaces of the patty. Reynolds number was calculated using Equation [4.28] where (E) is the edge height of the patty.

$$Re = \frac{\mathbf{v} \cdot \rho_{\text{mix}} \cdot \mathbf{E}}{\mu_{\text{mix}}}$$
 [4.28]

Prandtl and Schmidt numbers were calculated using Equations [4.20] and [4.21], respectively. Nusselt and Sherwood numbers were calculated using Equations [4.29] and [4.30].

$$Nu = 0.037 \cdot Re^{\frac{4}{5}} \cdot Pr^{\frac{1}{3}}$$
 [4.29]

$$Sh = 0.037 \cdot Re^{\frac{4}{5}} \cdot Sc^{\frac{1}{3}}$$
 [4.30]

Heat and mass transfer coefficients were then calculated using Equations [4.31] and [4.32], respectively.

$$h_{T} = \frac{Nu \cdot k_{mix}}{E}$$
 [4.31]

$$h_{m,water} = \frac{Sh \cdot D_{sa}}{E}$$
 [4.32]

4.2.5 Heat and mass transfer coefficients – array of round nozzles

In addition to the correlations for an array of slot nozzles, additional correlations were utilized to predict the heat and mass transfer coefficients for an array of round nozzles (Martin, 1977). Nusselt and Sherwood numbers were calculated using equations [4.33] and [4.34], respectively.

$$Nu = Pr^{0.42} \cdot K_A (H_{slot}/D, f) \cdot G(H_{slot}/D, f) \cdot F(Re)$$
 [4.33]

$$Sh = Sc^{0.42} \cdot K_A (H_{slot}/D, f) \cdot G(H_{slot}/D, f) \cdot F(Re)$$
 [4.34]

 $K_A(H_{slot}/D, f)$ is the array correction function and is given by Equation [4.35].

$$K_A(H_{slot}/D, f) = \left[1 + \left(\frac{H_{slot}/D}{0.6/\sqrt{f}}\right)^6\right]^{-0.05}$$
 [4.35]

where:

$$f = 0.785 \cdot (D/L)^2$$
 [4.36]

In the above equations, D and L represent the nozzle diameter and nozzle spacing, respectively. G(f, H/D) is a geometric function (Equation [4.37]), and F(Re) is a function of the Reynolds number (Equation [4.38]).

$$G(f, H_{slot}/D) = 2 \cdot \sqrt{f} \cdot \frac{1 - 2.2 \cdot \sqrt{f}}{1 + 0.2 \cdot (H_{slot}/D - 6) \cdot \sqrt{f}}$$
 [4.37]

$$F(Re) = 0.5 \cdot Re^{2/3}$$
 [4.38]

From the values of Nusselt and Sherwood numbers, values for heat and mass transfer coefficients were calculated using Equations [4.26] and [4.27] respectively.

4.3 Microbial inactivation model

A simple first-order inactivation model (Equation [4.39]) was combined with the heat and mass transfer model.

$$\log_{10}\left(\frac{N_0}{N}\right) = \frac{\Delta t}{D}$$
 [4.39]

where:

$$D = D_{ref} \cdot 10^{(T_{ref} - T)/z}$$
 [4.40]

The reduction in the number of Salmonella at each node was determined by calculating the fraction of survivors after each time step. The number of survivors after each time step was calculated by inserting the temperature data generated by the cooking model into Equation [4.41]. The overall reduction at the center of the patty was then

determined for the entire cooking process. The aggregate microbial reduction for the entire patty was calculated by calculating the volume average of all the nodes.

$$N = N_0 / 10^{\frac{\Delta t}{D}}$$
 [4.41]

4.4 Finite element formulation

4.4.1 Introduction

The finite element method (FEM) was utilized to solve the cooking model equations. The finite element is a common numerical method for solving differential equations that are difficult to solve using analytical techniques. The finite element method has several advantages over other numerical techniques that make it very suitable for formulating cooking models. FEM is readily adaptable to irregular geometries, it can be applied to systems containing more that one set of physical properties, and it is readily applied using computers.

The following sections briefly describe the finite element method and the techniques used to convert the model equations into computerized form. A much more detailed description of the finite element method was given by Segerlind (1984).

4.4.2 Finite element basics

To apply the finite element method, the geometry of the system must first be broken down into a finite number of discrete regions referred to as elements. Elements are typically triangular or quadrilateral, although other geometries can also be utilized.

The corners of each element are referred to as nodes. Adjacent elements share the nodes at the corners they have in common. When the finite element method is performed, a numerical solution is generated for each node in the element mesh. Increasing or decreasing the number of nodes controls the resolution of the model. Models with a large number of nodes produce finer resolution at the expense of increased computing time.

Figure 4.3 shows the geometry of the system used for the computer model as well as the element mesh. Figure 4.4 is a view of the element mesh with the coordinate axis indicated.

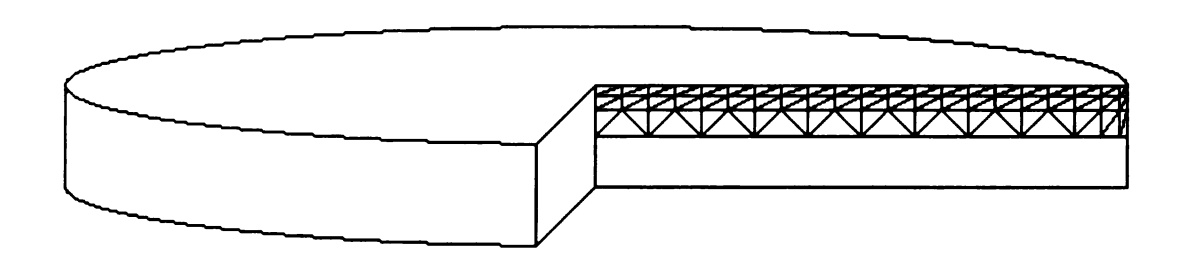


Figure 4.3 - Geometry of a ground meat patty with the modeled region and element mesh indicated.

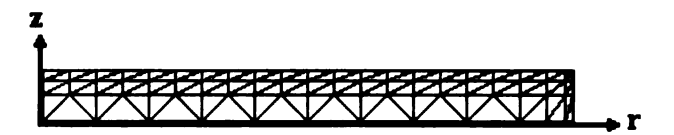


Figure 4.4 - Illustration of the finite element mesh utilized for the model.

The radial symmetry of ground meat and poultry patties allowed patties to be modeled as two-dimensional axisymmetric bodies. For the purpose of the cooking model, the modeled region was broken down into 117 triangular elements. This resulted in 82 nodes. The density of the element grid was higher at the patty surface to better

model the larger moisture, fat, and temperature gradients present near the product surface. The 117-node element mesh was chosen to balance solution accuracy with computing time (see Section 5.5.1).

4.4.3 Governing equations

As discussed in the previous sections, the cooking model was formulated using three sets of differential equations. The basic solution of the heat transfer, moisture transfer, and fat transfer equations using the finite element method is very similar.

Therefore, solution of a generic transport equation will be shown with emphasis given to the differences between the three solutions.

The basis for each transport solution was the time-dependent two-dimensional field equation expressed in radial coordinates (Equation [4.42]).

$$\lambda \frac{\partial \phi}{\partial t} = \frac{1}{r} \left[D_r \frac{\partial}{\partial r} \left(r \frac{\partial \phi}{\partial r} \right) \right] + D_z \frac{\partial^2 \phi}{\partial z^2}$$
 [4.42]

Equation [4.41] is a generic form of the governing equations given by Equations [4.1], [4.7], and [4.16]. In Equation [4.42], the term (ϕ) is the unknown variable and corresponds to the enthalpy, moisture content, and fat-protein ratio in Equations [4.1], [4.7], and [4.16], respectively. The terms (λ) and (D) are combinations of thermophysical property values. For the heat transfer solution, the term D is equal to the thermal conductivity, and the term λ is equal to the product of the heat capacity and the density of the meat. For the moisture transfer solution, the term D is equal to the moisture conductivity, and the term λ is equal to the product of the specific moisture holding

capacity and the density of the meat. For the fat transfer solution, the D term is equal to the capillary diffusivity, and the λ term is not utilized.

The finite element method is a weighted residual technique. An approximate solution is substituted into the governing equations, and the error term calculated. The product of this term and a weighting function is then reduced to zero to produce a numerical solution. The weighting function may take many forms. The method chosen was Galerkin's method. In this method, the weighting function uses the same functions that were used for the approximate solution (Segerlind, 1984).

Using Galerkin's method for the axisymmetric field problem, the weighted residual equation is Equation [4.43].

$$\left\{ R^{(e)} \right\} = - \int_{V} \left[N \right]^{T} \left(\frac{D_{r}}{r} \frac{\partial}{\partial r} \left(r \frac{\partial \phi}{\partial r} \right) + D_{z} \frac{\partial^{2} \phi}{\partial z^{2}} + \lambda \frac{\partial \phi}{\partial t} \right) dV$$
 [4.43]

The term [N], is a vector of shape functions. Triangular elements were used for the cooking model. This allowed the density of the element mesh to be increased near the boundaries without dramatic change in the aspect ratio of the elements. Proper aspect ratio is desirable, as elements with greatly uneven lengths and widths can contribute to loss of solution accuracy (Segerlind, 1984). Figure 4.5 is an illustration of a typical triangular element. The element contains three nodes that are labeled as nodes i, j, and k.

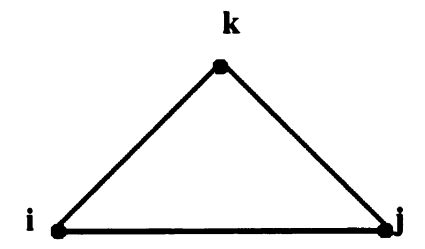


Figure 4.5 – Illustration of a triangular element showing counterclockwise node numbering.

The shape functions for a triangular element are given by Equations [4.44] through [4.46].

$$N_{i} = \frac{1}{2A} (a_{i} + b_{i}r + c_{i}z)$$
 [4.44]

$$N_{j} = \frac{1}{2A} (a_{j} + b_{j}r + c_{j}z)$$
 [4.45]

$$N_{k} = \frac{1}{2A} (a_{k} + b_{k}r + c_{k}z)$$
 [4.46]

where:

$$a_i = R_j Z_k - R_k Z_j$$
 $b_i = Z_j - Z_k$ $c_i = R_k - R_j$

$$a_j = R_k Z_i - R_i Z_k$$
 $b_j = Z_k - Z_i$ $c_j = R_i - R_k$

$$a_k = R_i Z_j - R_i Z_i$$
 $b_k = Z_i - Z_j$ $c_k = R_j - R_i$

The terms R_n and Z_n are the r and z coordinates of the nth node, respectively. After applying the product rule for differentiation and considerable manipulation (Segerlind, 1984), Equation [4.43] can be converted to the form of Equation [4.47].

$$\begin{aligned} \left\{ R^{(e)} \right\} &= \left(\int_{V} \left(D_{r} \frac{\partial [N]^{T}}{\partial r} \frac{\partial [N]}{\partial r} + D_{z} \frac{\partial [N]^{T}}{\partial z} \frac{\partial [N]}{\partial z} \right) dV \right) \left\{ \Phi^{(e)} \right\} \\ &= \int_{\Gamma} \left([N]^{T} D_{r} \frac{\partial \phi}{\partial r} \cos \theta + D_{z} \frac{\partial \phi}{\partial z} \sin \theta \right) d\Gamma + \int_{V} [N]^{T} \left(\lambda \frac{\partial \phi}{\partial t} \right) dV \end{aligned}$$
[4.47]

The first integral of Equation [4.47] is related to transport within the product and can be written as Equation [4.48], where $[k^{(e)}]$ is the element stiffness matrix.

$$\left[k^{(e)}\right] = \int_{V} \left(D_{r} \frac{\partial [N]^{T}}{\partial r} \frac{\partial [N]}{\partial r} + D_{z} \frac{\partial [N]^{T}}{\partial z} \frac{\partial [N]}{\partial z}\right) dV$$
 [4.48]

The second integral in Equation [4.47] is related to the derivative boundary condition and can be written as Equation [4.49], where $\{I^{(e)}\}$ is the inter-element vector.

$$\left\{ I^{(e)} \right\} = \int_{\Gamma} [N]^{T} \left(D_{r} \frac{\partial \phi}{\partial r} \cos \theta + D_{z} \frac{\partial \phi}{\partial z} \sin \theta \right) d\Gamma$$
 [4.49]

The third integral in Equation [4.47] is a time-dependent capacitance term.

Using Equations [4.48] and [4.49], Equation [4.47] can be re-written in the form:

$$\left\{ R^{(e)} \right\} = \left\{ I^{(e)} \right\} + \left[k^{(e)} \right] \left\{ \Phi^{(e)} \right\} + \left[C^{(e)} \right] \left\{ \dot{\Phi}^{(e)} \right\}$$
 [4.50]

where $[C^{(e)}]$ is called the capacitance matrix and is given by Equation [4.51], and $\{\dot{\Phi}\}$ represents the nodal values of $\partial\Phi/\partial t$.

$$\left[C^{(e)}\right] = \int_{V} \lambda[N]^{T} [N] dV$$
 [4.51]

Inserting the shape functions into the element stiffness matrix and integrating gives the form of the stiffness matrix shown in Equation [4.52].

$$[k^{(e)}] = \frac{2\pi \overline{r} D_r}{4A} \begin{bmatrix} b_i^2 & b_i b_j & b_i b_k \\ b_i b_j & b_j^2 & b_j b_k \\ b_i b_k & b_j b_k & b_k^2 \end{bmatrix} + \frac{2\pi \overline{r} D_z}{4A} \begin{bmatrix} c_i^2 & c_i c_j & c_i c_k \\ c_i c_j & c_j^2 & c_j c_k \\ c_i c_k & c_j c_k & c_k^2 \end{bmatrix}$$
 [4.52]

Expanding the capacitance matrix using a lumped solution gives the form of the capacitance matrix given by Equation [4.53]. The lumped solution assumes that the variation $\partial \phi / \partial t$ is constant across each element. This is the solution that provides for the maximum operating range of the final model.

$$\left[C^{(e)} \right] = \frac{\lambda A}{3} \begin{bmatrix} 1 & 0 & 0 \\ 0 & 1 & 0 \\ 0 & 0 & 1 \end{bmatrix}$$
 [4.53]

Treatment of the inter-element vector is somewhat more involved. A derivative boundary condition over a boundary Γ can be specified using Equation [4.54].

$$D_{r} \frac{\partial \phi}{\partial r} \cos \theta + D_{z} \frac{\partial \phi}{\partial z} \sin \theta = -M\phi_{b} + S$$
 [4.54]

The right hand side of Equation [4.54] can be substituted into Equation [4.49] yielding Equation [4.55].

$$\left\{I^{(e)}\right\} = \int_{\Gamma} [N]^{T} \left(M[N] \left(\Phi^{(e)}\right) - S\right) d\Gamma$$
[4.55]

Upon expansion, Equation [4.55] produces two terms given by Equations [4.56] and [4.57].

$$\left[k_{M}^{(e)}\right] = \int_{\Gamma_{BC}} M[N]^{T}[N] d\Gamma$$
 [4.56]

$$\left\{ f_{S}^{(e)} \right\} = \int_{\Gamma_{BC}} S[N]^{T} d\Gamma$$
 [4.57]

Equations [4.56] and [4.57] can be expanded into the form of Equation [4.58] and [4.59].

$$\left[k_{M}^{(e)}\right] = \frac{2\pi ML}{12} \begin{bmatrix} (3R_{i} + R_{j}) & (R_{i} + R_{j}) & 0\\ (R_{i} + R_{j}) & (R_{i} + 3R_{j}) & 0\\ 0 & 0 & 0 \end{bmatrix}$$
 [4.58]

$$\left\{ f_{S}^{(e)} \right\} = \frac{2\pi SL}{6} \begin{cases} 2R_{i} + R_{j} \\ R_{i} + 2R_{j} \\ 0 \end{cases}$$
 [4.59]

For the convective heat transfer boundary condition, the term M is equal to the heat transfer coefficient h. The term S is equal to the heat transfer coefficient multiplied by the temperature of the bulk fluid. Since the heat transfer solution was formulated in terms of enthalpy, the equilibrium enthalpy related to the oven air temperature was calculated using Equation [4.2] and substituted in place of the oven air temperature in calculating S.

For the convective moisture transfer boundary condition, the term M is equal to the convective mass transfer coefficient h_m. The S term is equal to the convective mass transfer coefficient multiplied by the equilibrium moisture content for the meat under the given oven air temperature and moisture conditions. Equilibrium moisture content was calculated using Equation [4.60] derived from the work of Huang and Mittal (1995).

EMC =
$$\left(\frac{1.9818 \cdot T_{\text{surface}} \cdot \ln(RH)}{-5222.47}\right)^{-1/1.0983}$$
 [4.60]

where:

$$RH = 100 \cdot \left(C_{\text{oven}} / C_{\text{sat}} \right)$$
 [4.61]

4.4.4 Finite difference time solution

A finite difference time-solution was used to provide a FEM solution over a number of time steps. This resulted in an equation with a time-step term (Equation [4.62]).

$$([C] + \theta \Delta t[k]) \{\Phi\}_b = ([C] - (1 - \theta) \Delta t[K]) \{\Phi\}_a + \Delta t((1 - \theta)\{F\}_b + \theta\{F\}_a)$$
[4.62]

Setting the value of θ equal to $\frac{1}{2}$ (central difference method), results in Equation [4.63].

$$\left([C] + \frac{\Delta t}{2} [k] \right) \left\{ \Phi \right\}_{b} = \left([C] - \frac{\Delta t}{2} [K] \right) \left\{ \Phi \right\}_{a} + \frac{\Delta t}{2} \left(\left\{ F \right\}_{b} + \left\{ F \right\}_{a} \right)$$
[4.63]

Equation [4.63] can be reduced to Equation [4.64].

$$[A]{\Phi}_{b} = [P]{\Phi}_{a} + {F*}$$
[4.64]

where:

$$[A] = \left([C] + \frac{\Delta t}{2} [k] \right)$$
 [4.65]

$$[P] = \left([C] - \frac{\Delta t}{2} [k] \right)$$
 [4.66]

and

$$\{F^*\} = \frac{\Delta t}{2} (\{F\}_a + \{F\}_b)$$
 [4.67]

4.4.5 Application of FEM solution

Equation [4.64] has a form that can be readily programmed into a personal computer. For the cooking model, three sets of element solutions were constructed. The first set of equations was related to the heat transfer portion of the model (Equation [4.1]). The second set of equations was related to mass transport due to moisture migration (Equation [4.7]). The third set of equations was related to fat transfer (Equation [4.16]). The finite element solution was programmed using Microsoft Visual Basic (Version 6.0 professional edition: Microsoft, Redmond, WA); (Section 9.5).

4.4.6 User interface

A Windows-based user interface for the model was developed using Microsoft Visual Basic. The user interface consisted of two primary window screens controlled by a menu toolbar. Illustrations of each interface screen are shown in Section 9.4.

The first of the windows is the input screen. On this screen, the user inputs the oven air temperature, the oven steam content or wet bulb temperature, the air velocity, and the cooking time. The user also has the option of inputing a set of transient oven conditions using a file input. The input screen also requires the user to specify the initial temperature, fat content, and moisture content of the meat. Buttons are available for selecting between beef, pork, and turkey. The final component of the interface screen is the microbial inactivation input section. Default D, z, and reference temperature values for a seven-strain *Salmonella* cocktail in beef (Smith et al., 2001) are incorporated into the model. However, these defaults may be replaced with values specified by the user.

The second screen of the user interface is the output screen. On this screen, the output temperature, moisture, yield, and microbial inactivation are displayed in graphical form. The final temperature, moisture, yield, and lethality values are also given in digital form. A message is displayed in the inactivation output section indicating whether or not the required level of lethality was achieved for the product selected.

5 RESULTS AND DISCUSSION

5.1 Overview

The experimental results for this study are grouped into three main sections. The first section (Section 5.2) describes the results of a set of experiments conducted using a laboratory convection oven. Patties of ground turkey, ground beef, and ground pork were cooked to various endpoint temperatures to determine the effects of meat species and initial fat content on cooking yield, heating rate, and shrinkage. These experiments were intended to provide insight on differences in cooking behavior between meat species and fat content and to evaluate the need for including fat transfer in meat cooking models.

Section 5.3 describes the results of a series of experiments conducted to determine the fat holding capacity of ground beef as affected by isothermal heating. These data were used to develop an expression for fat holding capacity as a function of initial fat content and temperature. This expression was then included as a portion of the cooking model (Section 4.2.3).

Section 5.4 describes the results of experiments conducted using an industrial moist-air impingement cooking system (Stein model JSO-IV). Ground beef patties were cooked in the oven using various cooking conditions. The effects of oven conditions on cooking time, yield, and volume change were determined. Additionally, data from this set of experiments were used to validate the heat and mass transfer components of the cooking model.



5.2 Laboratory oven cooking tests

In these tests, small meat patties were cooked in a laboratory convection oven to determine the effect of species and initial fat content on fat loss for ground turkey, ground beef, and ground pork (Section 3.2). The effects of species and fat content on cooking time, yield, and volume change were also determined.

5.2.1 Cooking time

For each cooking test, the time required to reach the target endpoint center temperature was measured. Using this information, temperature versus time plots were constructed for each species and fat content (Figures 5.1-5.3)

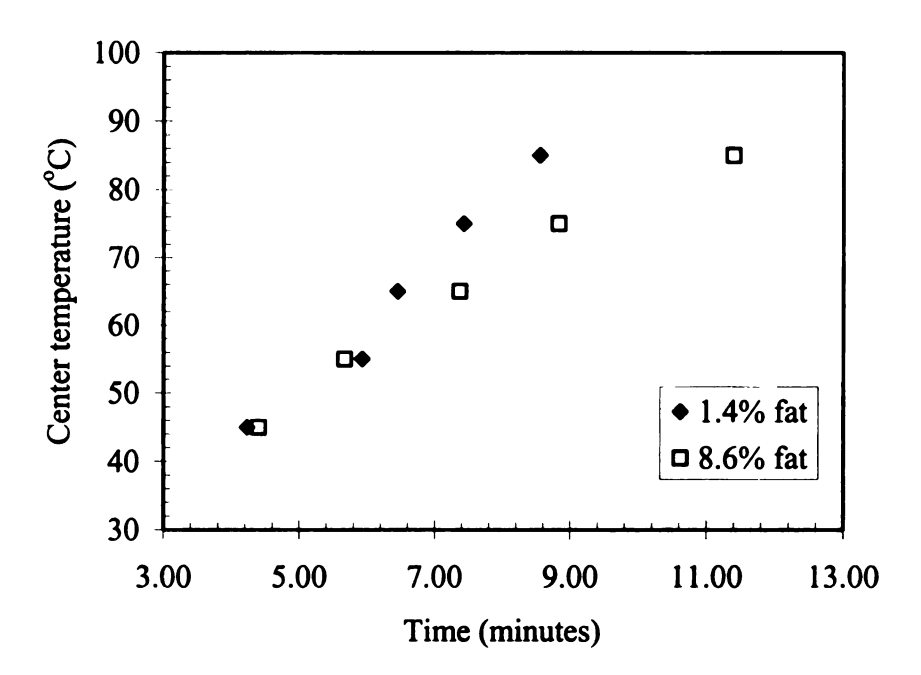


Figure 5.1 – Center temperature as a function of cooking time for ground turkey patties cooked in a laboratory convection oven: means of 5 replicates.

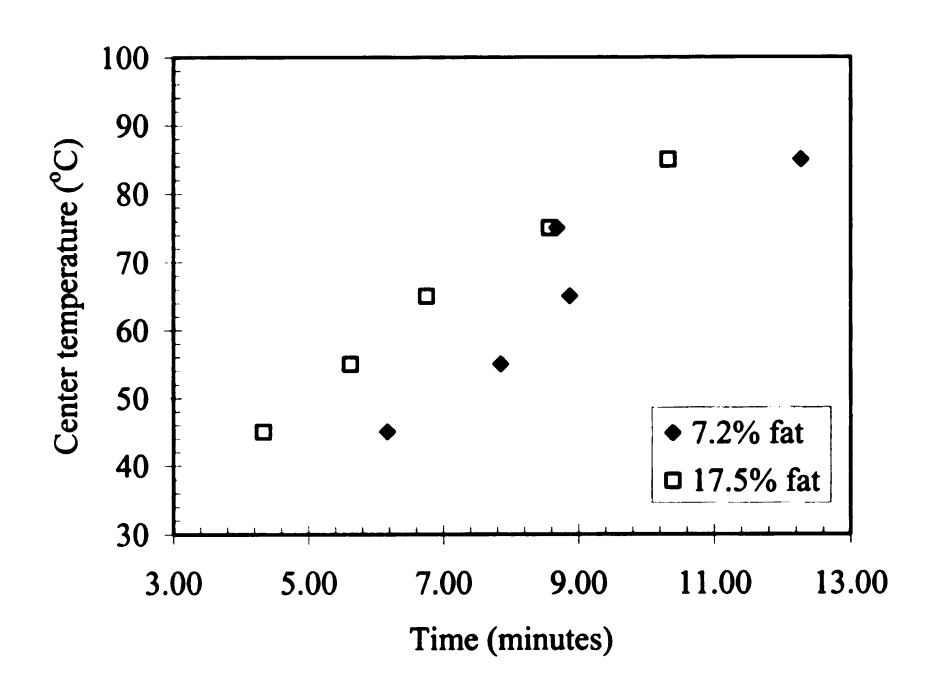


Figure 5.2 – Center temperature as a function of cooking time for ground beef patties cooked in a laboratory convection oven: means of 5 replicates.

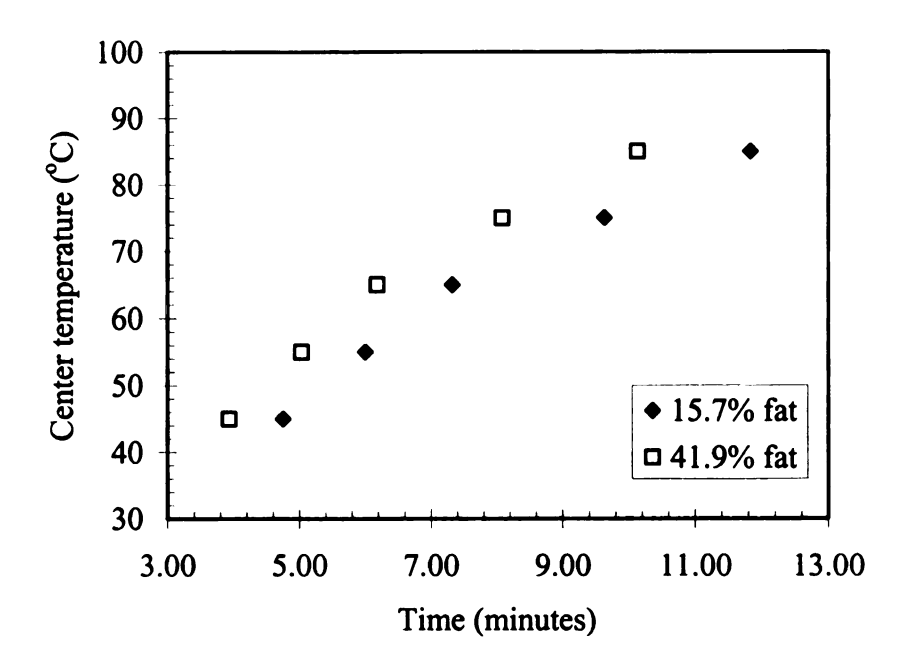


Figure 5.3 – Center temperature as a function of cooking time for ground pork patties cooked in a laboratory convection oven: means of 5 replicates.

The cooking rates of turkey differed between the 1.4% and 8.6% fat samples (Figure 5.1). The temperature of both the low and high fat patties increased as a function of time. However, the heating rate of the 1.4% fat samples was slightly higher. The 1.4% fat patties took 254 seconds to reach 45°C compared to 264 seconds for the 8.6% fat patties. The difference in heating time increased as the patties reached higher temperatures. The 1.4% fat patties reached 85°C in 513 seconds compared to 684 seconds for the 8.6% fat patties, a difference of almost 3 minutes. Analysis of variance confirmed the statistical significance (P<0.05) of differences in heating times between the two fat contents (Table 5.1).

Table 5.1 - Analysis of variance for cooking time of ground turkey patties as affected by temperature and initial fat content.

Factor	Sum of Squares	Degrees of Freedom	Mean Square	F-Value	P-Value
Temperature	661821.3	4	165455.3	48.2258	< 0.001
Fat Content	59305.68	1	59305.68	17.2860	< 0.001
Interaction	57447.52	4	14361.88	4.1861	0.006

With ground beef, the heating rate was significantly higher for the 17.5% fat patties than for the 7.2% fat patties (Figure 5.2). The average time required to heat the 17.5% fat patties to 45°C was 260 seconds compared to 361 seconds for the 7.2% fat patties. The heating time increased with increasing patty temperature. The time required to reach 85°C was 619 seconds for the 17.5% fat patties compared to 836 seconds for the 7.2% fat patties. Analysis of variance showed both center point temperature and fat content to affect (P<0.05) heating time for ground beef patties (Table 5.2).

Table 5.2 - Analysis of variance for cooking time of ground beef patties as affected by temperature and initial fat content.

Factor	Sum of Squares	Degrees of Freedom	Mean Square	F-Value	P-Value
Temperature	742033.5	4	185508.4	19.7617	< 0.001
Fat Content	120835.3	1	120835.3	12.8723	< 0.001
Interaction	29187.52	4	7296.88	0.7773	0.547

As with the beef patties, the higher fat content pork patties took less time to heat than the lower fat patties (Figure 5.3). The average time required for the 41.9% fat patties to reach 45°C was 236 seconds compared to 285 seconds for the 15.7% fat patties. Heating temperature increased with increasing time. The time required for the 41.9% fat patties for each 85°C was 608 seconds compared to 710 seconds for the 15.7% fat patties. Analysis of variance showed temperature and fat content to be significant (P<0.05) with respect to heating time (Table 5.3).

Table 5.3 - Analysis of variance for cooking time of ground pork patties as affected by temperature and initial fat content.

Factor	Sum of Squares	Degrees of Freedom	Mean Square	F-Value	P-Value
Temperature	1036732	4	259182.9	59.6434	< 0.001
Fat Content	59512.5	1	59512.5	13.6951	< 0.001
Interaction	7689.6	4	1922.4	0.4424	0.777

In the case of the ground beef and ground pork patties, samples containing higher levels of fat achieved higher rates of heating. This was most likely due to the lower moisture content associated with the higher fat products. As water contributes the

greatest source of heat capacity in the meat matrix, lowering the water content would be expected to increase the heating rate. It has also been hypothesized that inclusion of high fat contents could result in convective heating within the meat, thereby increasing the heating rate (Shilton et al., 2002).

Unlike the ground pork and ground beef patties, the heating rate of the ground turkey patties was higher for the lower fat product. It should be noted that the compositions of the two ground turkey samples were more similar than those of the ground pork and ground beef samples. Specifically, the moisture content of the 8.6% fat ground turkey was only 1.8 w.b. moisture points lower than the moisture content of the 1.4% fat patties. This compares with differences in moisture content of 8.2 and 20.5 w.b. moisture points for the ground beef and ground pork, respectively. The smaller differences in moisture content for the ground turkey mean that the heat capacity of the two samples was nearly the same. Thus, moisture probably played a less significant role in differences in heating rate for the ground turkey patties.

The difference in heating rate between different fat levels of ground turkey patties was largest at temperatures above 55°C. Interaction between fat content and temperature was significant. This differs from ground beef and ground pork, which had consistent differences (i.e., no significant fat-temperature interaction). It is therefore likely that the different heating characteristics of the turkey were related to other compositional characteristics of the meat. The 8% initial fat ground turkey patties included ground skin as a method for increasing fat content. This may have contributed to the different heating characteristics of the ground turkey as compared to the ground beef and ground pork.

5.2.2 Cooking yield

For each test, the cooking yield was calculated at each endpoint temperature (Figures 5.4-5.6). Large differences in yield were evident between the 1.5% fat and 8.6% fat ground turkey patties (Figure 5.4). The yields of the 1.4% fat patties were consistently higher than the yields of the higher fat patties. The yield of the 1.4% fat patties ranged from 90% at 45°C down to 81% at 85°C compared to yields of about 83% to 63% for the 8.6% fat patties. The decrease in yield was approximately linear with respect to center temperature for both fat contents. Analysis of variance confirmed the significance (P<0.05) of both center temperature and fat content on cooking yield (Table 5.4). Higher yield losses for the 8.6% fat patties were presumably due to fat loss during cooking. However, the results presented in the next section do not support the conclusion that fat transport was solely responsible for yield differences between the two fat contents of turkey. It is possible that interaction between the fat and water within the patty resulted in lower water binding capacity for the higher fat patties, resulting in higher rates of moisture loss during cooking. Further experimentation is needed to determine the mechanisms for fat and water binding during cooking.

Table 5.4 – Analysis of variance of yield as a function of center temperature and initial fat content for ground turkey patties.

Factor	Sum of Squares	Degrees of Freedom	Mean Square	F-Value	P-Value
Temperature	1359.399	4	339.8498	10.5351	< 0.001
Fat Content	1751.823	1	1751.823	54.3051	< 0.001
Interaction	203.2676	4	50.8169	1.5753	0.200

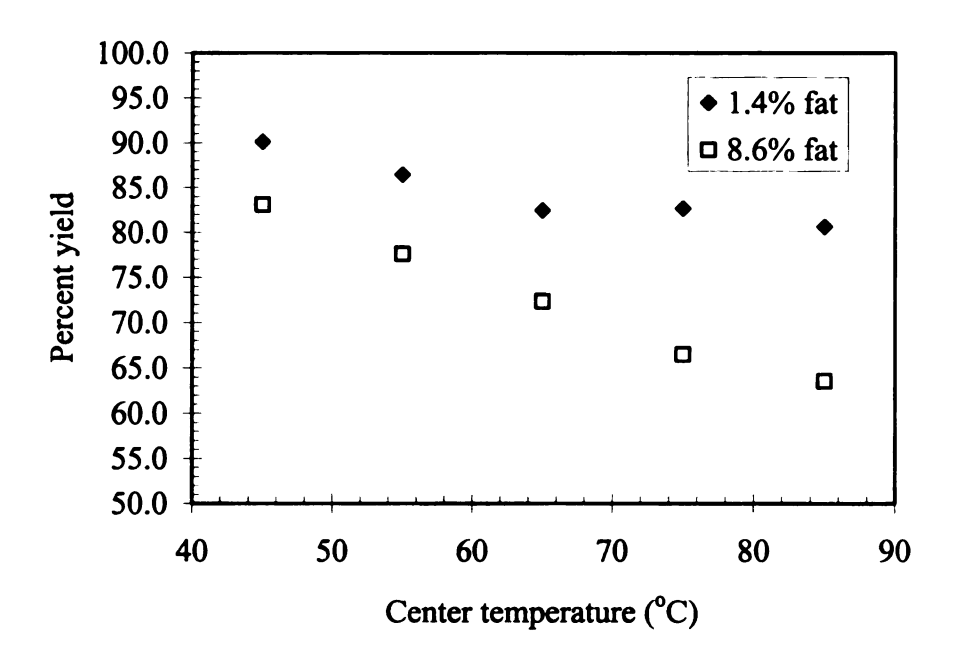


Figure 5.4 – Yield as a function of endpoint center temperature for ground turkey patties of two fat contents: means of 5 replicates.

For the ground beef, only minor differences in yield were detectable between the 7.2% and 17.5% fat samples at each cooking temperature (Figure 5.5). The yield of both products decreased from about 84% at 45°C to between 63 and 66% at 85°C. Analysis of variance indicated that yield was related (P<0.05) to center temperature but not to initial fat content for these data...

Table 5.5 - Analysis of variance of yield as a function of center temperature and initial fat content for ground beef patties.

Factor	Sum of Squares	Degrees of Freedom	Mean Square	F-Value	P-Value
Temperature	2135.567	4	533.8917	37.9595	< 0.001
Fat Content	9.6439	1	9.6439	0.6857	0.413
Interaction	21.9899	4	5.4975	0.3909	0.814

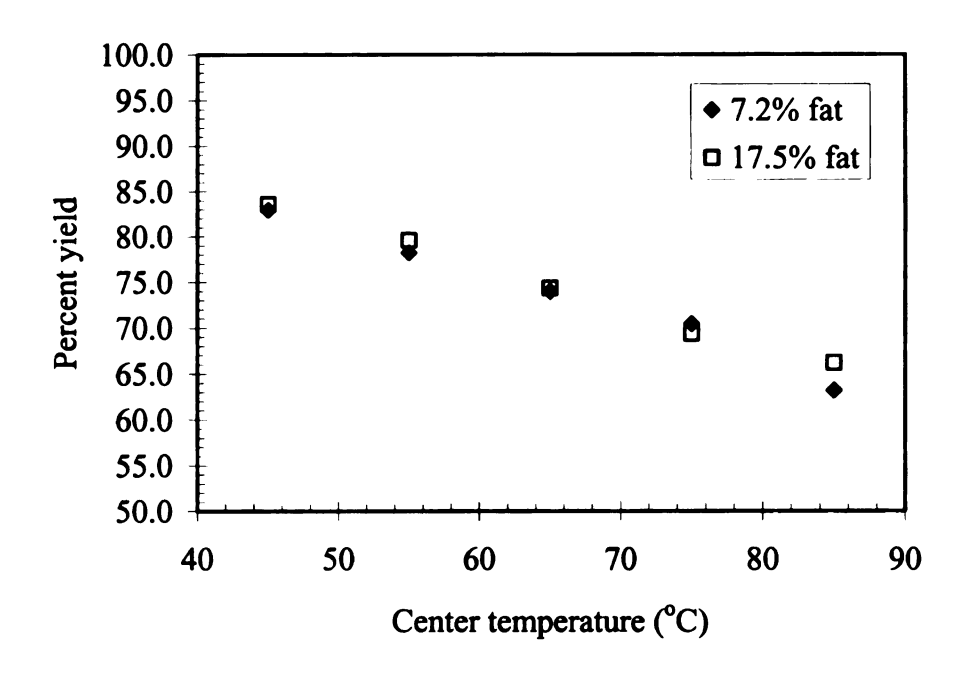


Figure 5.5 - Yield as a function of endpoint center temperature for ground beef patties of two fat contents: means of 5 replicates.

For ground pork, there were large differences in yield between the 15.7 and 41.9% fat patties (Figure 5.6). The yield of the lower fat patties was much higher at each center temperature. Cooking yield for the 15.7% fat patties ranged from about 90% at 45°C to about 71% at 85°C. Cooking yield for the 41.9% fat patties ranged from about 74% at 45°C to about 54% at 85°C. Cooking yield decreased linearly as a function of temperature for patties of both fat contents. Analysis of variance showed differences (P<0.05) in yield as a function of temperature, fat content, and temperature-fat interaction (Table 5.6).

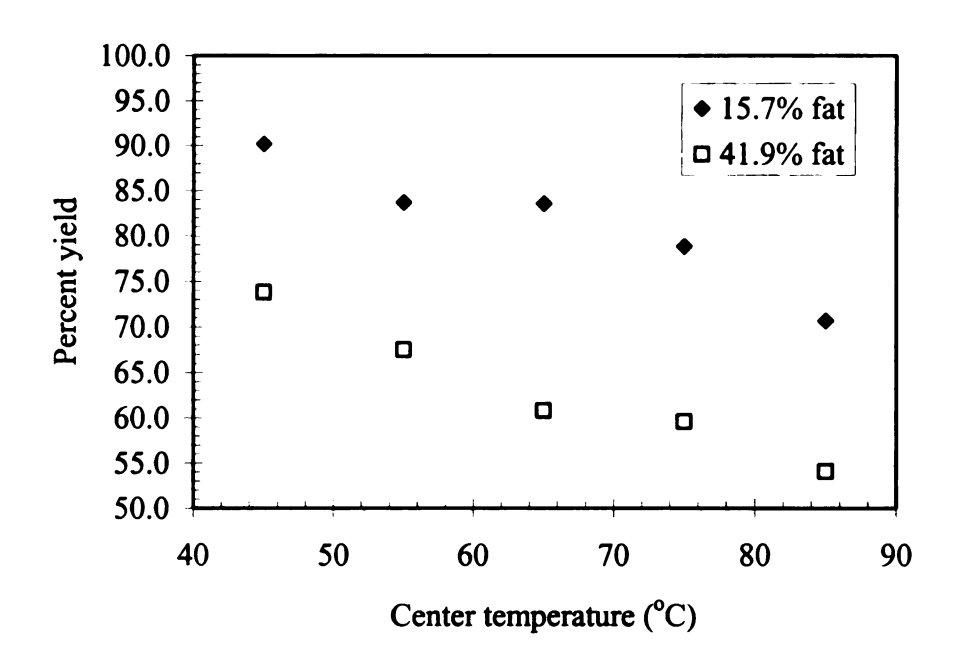


Figure 5.6 - Yield as a function of endpoint center temperature for ground pork patties of two fat contents: means of 5 replicates.

Table 5.6 - Analysis of variance of yield as a function of center temperature and initial fat content for ground pork patties.

Factor	Sum of Squares	Degrees of Freedom	Mean Square	F-Value	P-Value
Temperature	2132.37	4	533.0926	96.4285	< 0.001
Fat Content	4153.887	1	4153.887	751.376	< 0.001
Interaction	79.8724	4	19.9681	3.6119	0.013

The differences in cooking yield appear to be affected by both meat species and fat content. No significant correlation between initial fat content and cooking yield can be made across the three meat species. Although the yield at 85°C was lowest for the highest fat product (41.9% fat ground pork) and highest for the lowest fat product (1.4% fat ground turkey), the behavior of samples of in-between fat contents was not consistent. This could be caused by differences in protein conformation and fat composition of the

three meat species. It may also be due to differences in water and fat binding capacity of the meat proteins. Differences in particle size and porosity of the meat may also affect the cooking yields by changing the moisture and fat transport dynamics.

5.2.3 Fat loss

The amount of fat lost during cooking as a function of temperature for 1.4% and 8.6% fat ground turkey patties is shown in Figure 5.7. The amount of fat lost during cooking of ground turkey patties was below 2% for every temperature. Analysis of variance indicated that neither temperature nor initial fat content had a significant (P<0.05) effect on fat loss during cooking (Table 5.7).

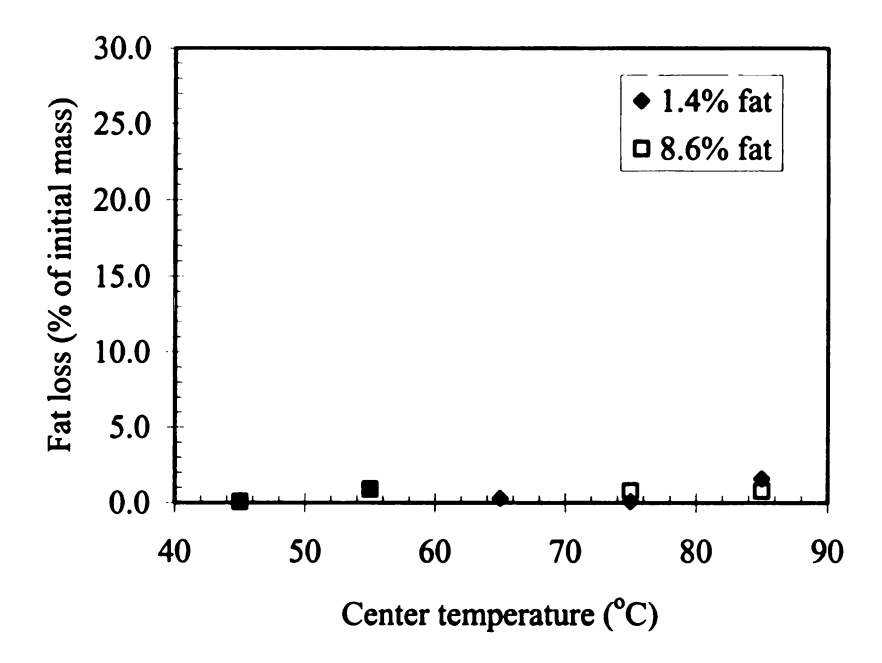


Figure 5.7 – Fat loss as a function of temperature for ground turkey patties of two fat contents: means of 5 replicates.

Table 5.7 – Analysis of variance for fat loss as functions of center temperature and initial fat content for ground turkey patties.

Factor	Sum of Squares	Degrees of Freedom	Mean Square	F-Value	P-value
Temperature	29.9082	4	7.4770	1.2317	0.3184
Fat Content	4.4131	1	4.4131	0.7270	0.4006
Interaction	17.8231	4	4.4558	0.7340	0.5760

The amount of fat lost during cooking of ground beef patties was much larger than the amounts lost during cooking of ground turkey (Figure 5.8). Fat losses were higher for the 17.5% fat patties, ranging up to 6% of the initial mass of the meat.

Analysis of variance showed that initial fat content had a significant (P<0.05) effect on the amount of fat lost during cooking (Table 5.8). A significant temperature effect on the amount of fat lost during cooking could not be shown.

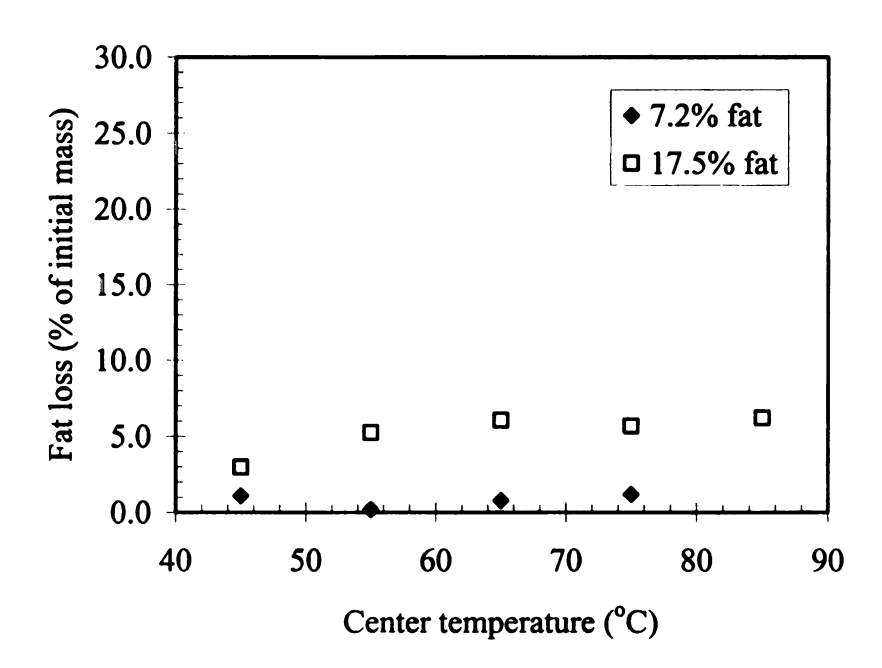


Figure 5.8 - Fat loss as a function of temperature for ground beef patties of two fat contents: means of 5 replicates.

Table 5.8 – Analysis of variance for fat loss as functions of center temperature and initial fat content for ground beef patties.

Factor	Sum of Squares	Degrees of Freedom	Mean Square	F-Value	P-value
Temperature	12.8007	4	3.2002	0.9060	0.4730
Fat Content	240.3399	1	240.3399	68.0423	< 0.001
Interaction	35.0635	4	8.7659	2.4817	0.065

Fat losses for ground pork were the highest of the three meat species tested (Figure 5.9). For the 15.7% fat pork patties, the amount of fat lost during cooking was low and never exceeded 2% of the initial patty mass. However, for the 41.9% fat patties, the amount of fat lost during cooking was much larger. The amount of fat lost during cooking was about 20.5% of the initial patty mass at 45°C. The amount of fat lost increased with increasing patty temperature up to about 28% at 85°C. Analysis of variance showed cooking temperature, fat content, and temperature-fat interaction to affect (P<0.05) fat loss (Table 5.9).

Table 5.9 – Analysis of variance for fat loss as functions of center temperature and initial fat content for ground pork patties.

Factor	Sum of Squares	Degrees of Freedom	Mean Square	F-Value	P-value
Temperature	68.6303	4	17.1576	14.3904	< 0.001
Fat Content	5660.502	1	5660.502	4747.583	< 0.001
Interaction	56.5569	4	14.1392	11.8589	< 0.001

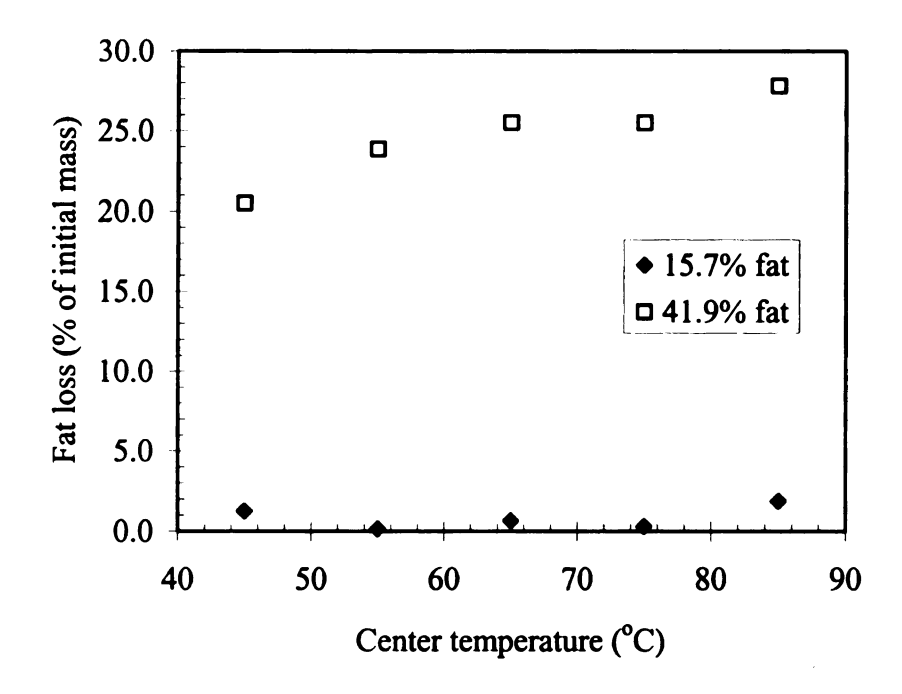


Figure 5.9 - Fat loss as a function of temperature for ground pork patties of two fat contents: means of 5 replicates.

The quantities of fat lost by the 17.5% fat ground beef patties and 41.9% fat ground pork patties during cooking are of great significance for modeling. Cooking models that do not take fat loss into account will likely over predict cooking yields. For high fat products such a sausage, these errors in yield prediction could exceed 25%. Many models may account for fat losses indirectly by over predicting mass transfer coefficients. However, this method may restrict the utility of the models to products of similar composition. To produce robust cooking models, transport of both moisture and fat components should be considered.

5.2.4 Volume change

Plots of volume change as a function of product temperature were plotted for each meat species (Figures 5.10-5.12). The volume of ground turkey patties as a function of temperature is shown in Figure 5.10. Volume of the 1.4% fat patties ranged between 74 and 70% of the initial volume at center temperatures between 45 and 85°C. Volume of the 8.6% fat patties decreased more dramatically as a function of center temperature and ranged from 62% to 56% of the original volume at center temperatures of 45 and 85°C respectively. Analysis of variance showed that initial fat content had a significant effect on volume change during cooking (P<0.05) (Table 5.10). However, the relationship between center temperature and volume change was not statistically significant.

Although the change in volume was significantly different over the measured temperature range, both products exhibited major decreases in volume between the raw state and 45°C. This shows that major volume changes occur during the initial stages of cooking, and thus may be impossible to avoid during convection cooking.

Table 5.10 – Analysis of variance for effects of temperature and initial fat content on volume change for ground turkey patties cooked in a laboratory convection oven.

Factor	Sum of Squares	Degrees of Freedom	Mean Square	F-Value	P-Value
Temperature	253.4806	4	63.3702	1.0724	0.383
Fat Content	2910.062	1	2910.062	49.2471	< 0.001
Interaction	122.8181	4	30.7045	0.5196	0.722

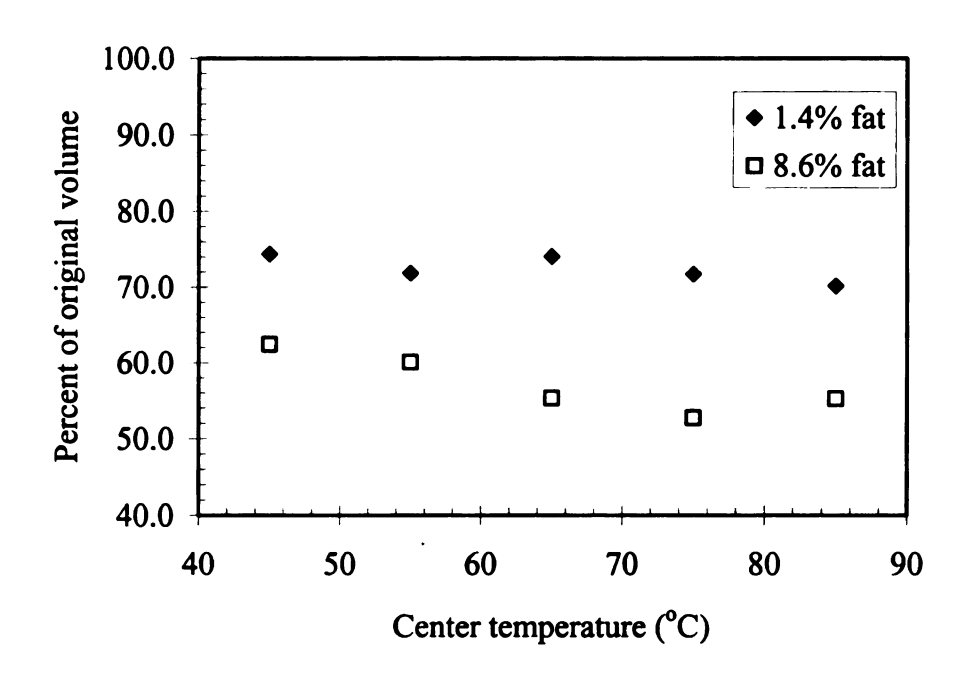


Figure 5.10 – Relationship between product temperature and volume change for ground turkey patties cooked in a laboratory convection oven: means of 5 replicates.

The ground beef patties exhibited a similar decrease in volume during cooking (Figure 5.11). Analysis of variance showed both center temperature and fat content to significantly affect volume (Table 5.11). Unlike the ground turkey and pork patties, the higher fat beef patties had less shrinkage during cooking than did the lower fat patties.

Table 5.11 – Analysis of variance for effects of temperature and initial fat content on volume change for ground beef patties cooked in a laboratory convection oven.

Factor	Sum of Squares	Degrees of Freedom	Mean Square	F-Value	P-Value
Temperature	1424.392	4	356.0981	11.5257	< 0.001
Fat Content	631.248	1	631.248	20.4314	< 0.001
Interaction	133.973	4	33.4933	1.0847	0.377

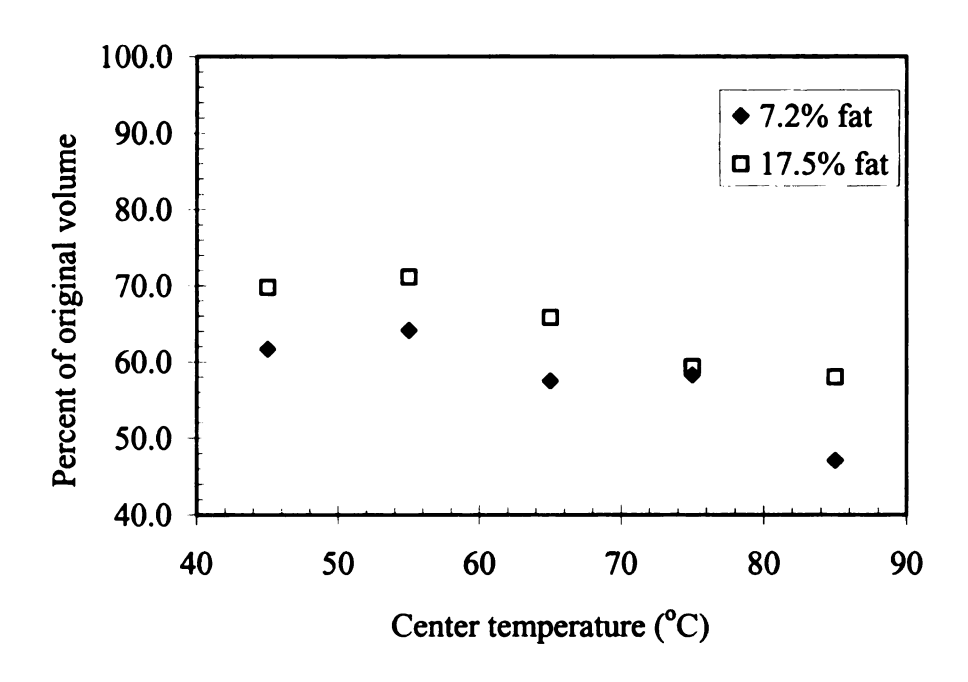


Figure 5.11 – Relationship between product temperature and volume change for ground beef patties cooked in a laboratory convection oven: means of 5 replicates.

The largest changes in volume during cooking occurred for ground pork patties (Figure 5.12). Volume decreased as a function of cooking temperature for both the 15.7% and 41.9% fat patties. The 15.7% fat patties ranged from about 74% to 60% of their original volumes at 45°C and 85°C, respectively. The 41.9% fat patties ranged from 70% to 42% of their original volumes at 45°C and 85°C, respectively. The large volume changes correlate with high yield losses during cooking. Analysis of variance indicated that both center temperature and fat content significantly (P<0.05) affected volume change (Table 5.12).

Table 5.12 – Analysis of variance for effects of temperature and initial fat content on volume change for ground pork patties cooked in a laboratory convection oven.

Factor	Sum of Squares	Degrees of Freedom	Mean Square	F-Value	P-Value
Temperature	2125.544	4	531.386	16.7989	< 0.001
Fat Content	1506.957	1	1506.957	47.6400	< 0.001
Interaction	451.4145	4	112.8536	3.5677	0.014

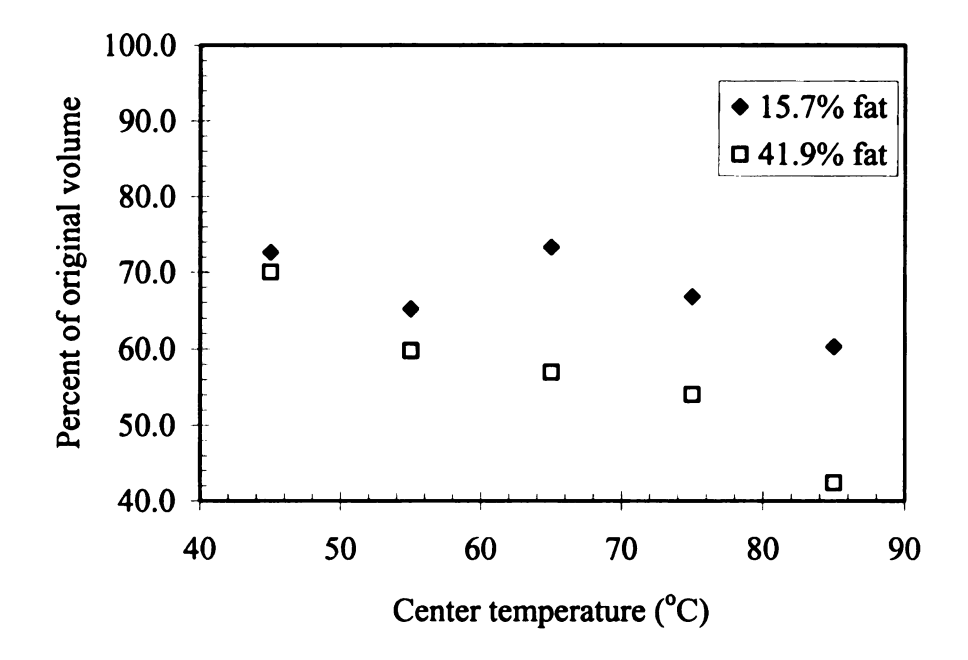


Figure 5.12 – Relationship between product temperature and volume change for ground pork patties cooked in a laboratory convection oven: means of 5 replicates.

Changes in volume are a major concern in the development of cooking models.

Slight changes in thickness greatly affect predictions of center temperature and may also have large effects on yield predictions. Due to the geometry of the products tested, most heat and mass transfer occurs in the axial direction. Therefore, changes in product thickness are of greater concern than changes in product radius.

Although the volume of all samples decreased with increasing product temperature, the same was not true for patty thickness. Most of the reduction in patty volume was caused by a reduction in patty diameter. The thicknesses of the 1.4 and 8.6% fat ground turkey patties, when cooked to a temperature of 85°C, were 120 and 110% of the initial values, respectively. The final thicknesses of the 7.2 and 17.5% fat ground beef patties were 97 and 120% of their initial values, respectively. The thicknesses of the 15.7 and 41.9% fat ground pork patties were 120 and 110% of their initial values, respectively. Therefore, in all but one case, patty thickness actually increased, while the radius decreased.

These results indicate that changes in volume cannot be modeled by simply reducing the size of the element mesh in proportion to the reduction in product mass. Further information is needed to determine the mechanisms for patty shrinkage. This would be an excellent area for further study.

5.3 Fat holding capacity experiments

Fat holding capacity (FHC) was determined as a function of temperature and initial fat content for two lots of ground beef with initial fat contents of 5.6 and 15% by mass (Section 3.3). The fat holding capacity of the meat was defined as the amount of fat remaining in the meat after heating and centrifuging for 15 minutes at 1000 g. The fat content of the centrifuged meat was expressed in terms of dry basis fat content using Equation [5.1].

$$F = M_{fat} / M_{dry matter}$$
 [5.1]

where M dry matter refers to the mass of meat that is neither water nor fat.

The mass of dry matter in each sample was calculated using Equation [5.2].

$$M_{dry matter} = M_{total} - (M_{fat} + M_{water})$$
 [5.2]

M_{fat} and M_{water} were calculated from the initial wet basis moisture and fat contents of the meat. The amount of dry matter was assumed to be constant during heating and centrifugation. During cooking, small quantities of dry matter are released in the forms of soluble proteins. Future studies should be conducted to describe the relationships between meat proteins and moisture and fat holding capacities in a more fundamental manner. However, inclusion of such relationships was beyond the scope of this study.

The fat content, F, was plotted as a function of heating temperature for each heating time (Figures 5.13-5.16, 5.18-5.21).

5.3.1 Low fat samples (5.6% initial fat wet basis)

The relationship between fat holding capacity and temperature for heating times of 2, 5, 10, and 15 minutes can be seen in Figures 5.13-5.16. The initial fat content of the ground beef was 0.14 g fat/g dry matter. For each heating time, the fat holding capacity was markedly lower at 55°C. The fat holding capacity of samples heated to 90°C ranged from 0.03 to 0.05 g fat/g dry matter.

Linear regression was used to fit a model for fat/dry matter ratio as a function of heating temperature and holding time for the 5.6% fat (wet basis) ground beef samples.

A quadratic response surface was chosen for the initial regression model (Equation [5.3]).

$$F = \beta_0 + \beta_1 \cdot T + \beta_2 \cdot T^2 + \beta_3 \cdot t + \beta_4 \cdot t^2 + \beta_5 \cdot t \cdot T + \varepsilon$$
 [5.3]

Regression coefficients for the response surface model are given in Table 5.13.

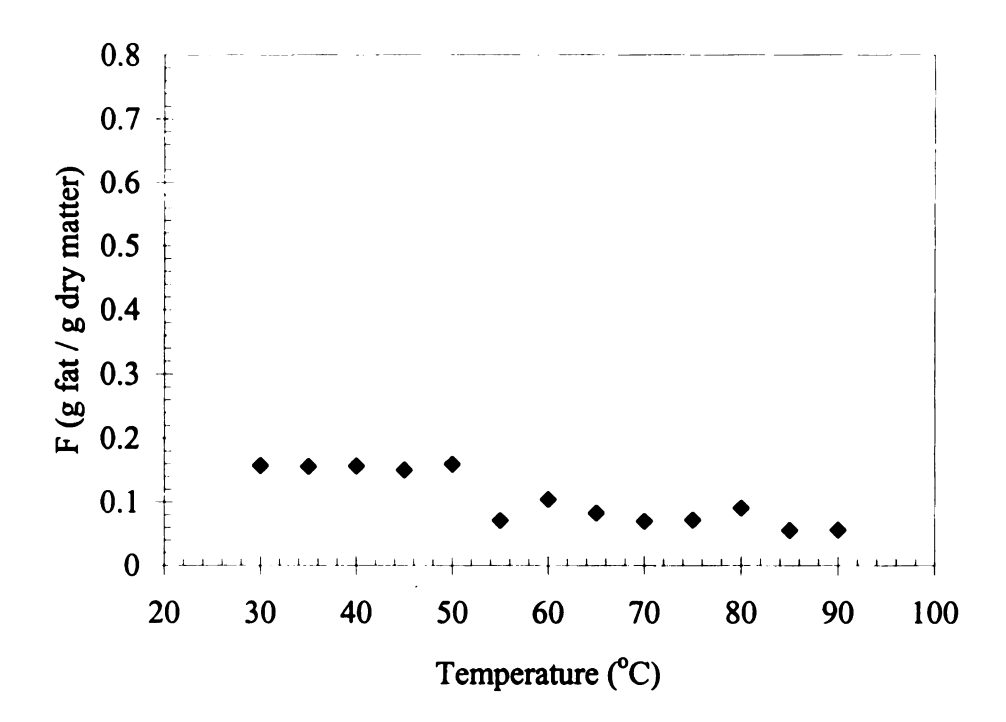


Figure 5.13 – Fat holding capacity as a function of temperature for 5.6% fat ground beef heated for 2 minutes at temperatures from 30 to 90°C: means of 5 replicates.

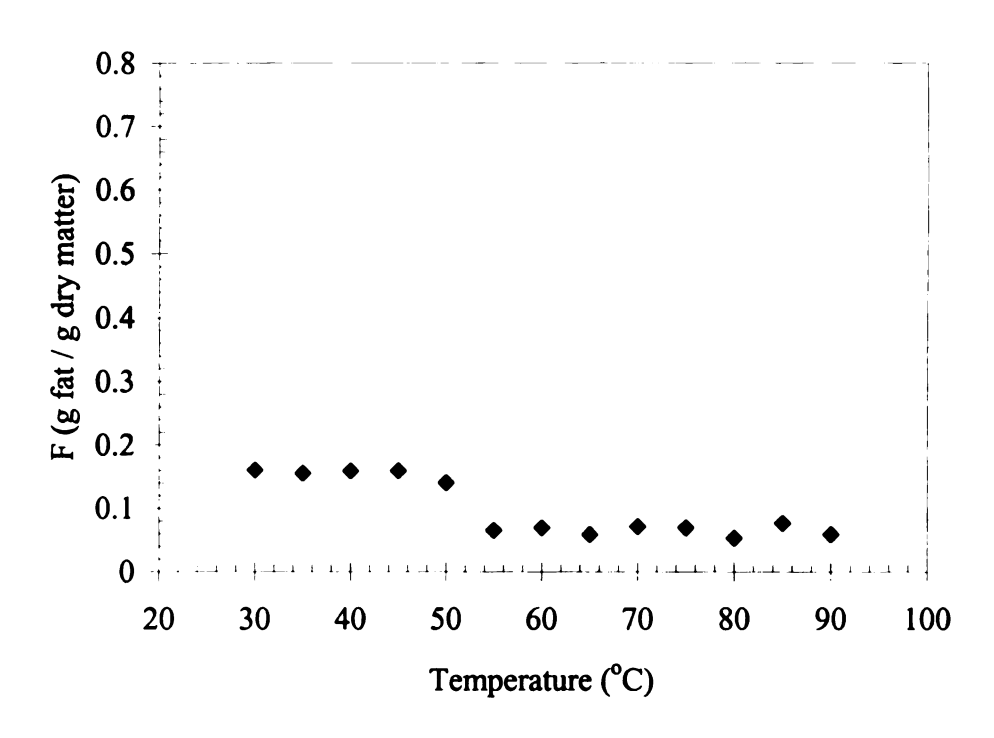


Figure 5.14 – Fat holding capacity as a function of temperature for 5.6% fat ground beef heated for 5 minutes at temperatures from 30 to 90°C: means of 5 replicates.

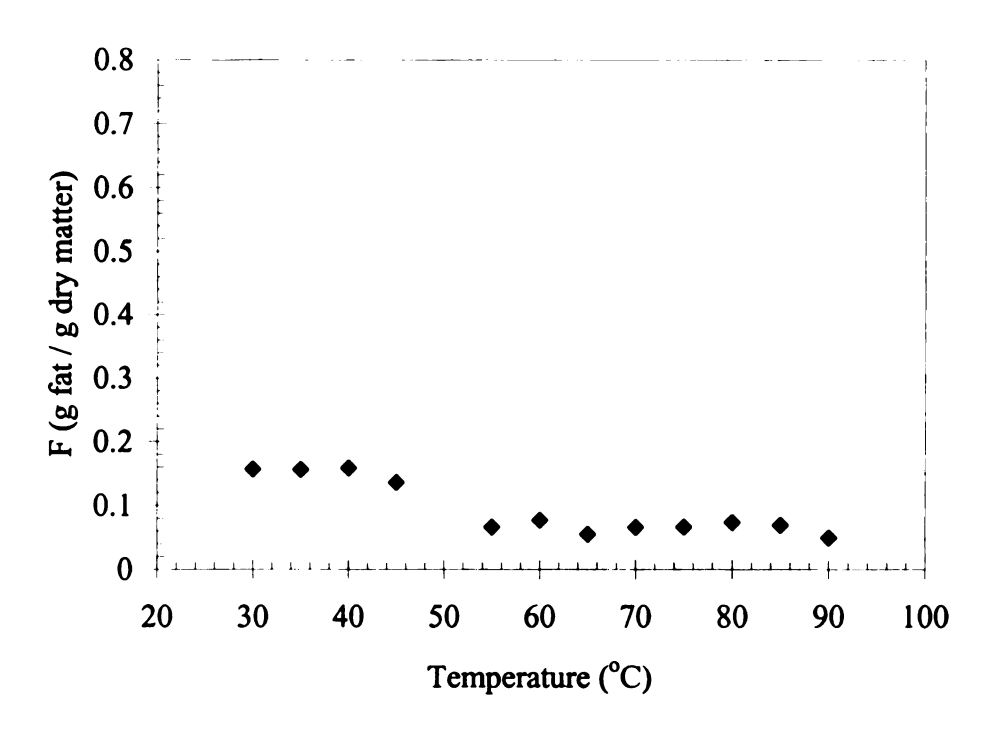


Figure 5.15 – Fat holding capacity as a function of temperature for 5.6% fat ground beef heated for 10 minutes at temperatures from 30 to 90°C: means of 5 replicates.

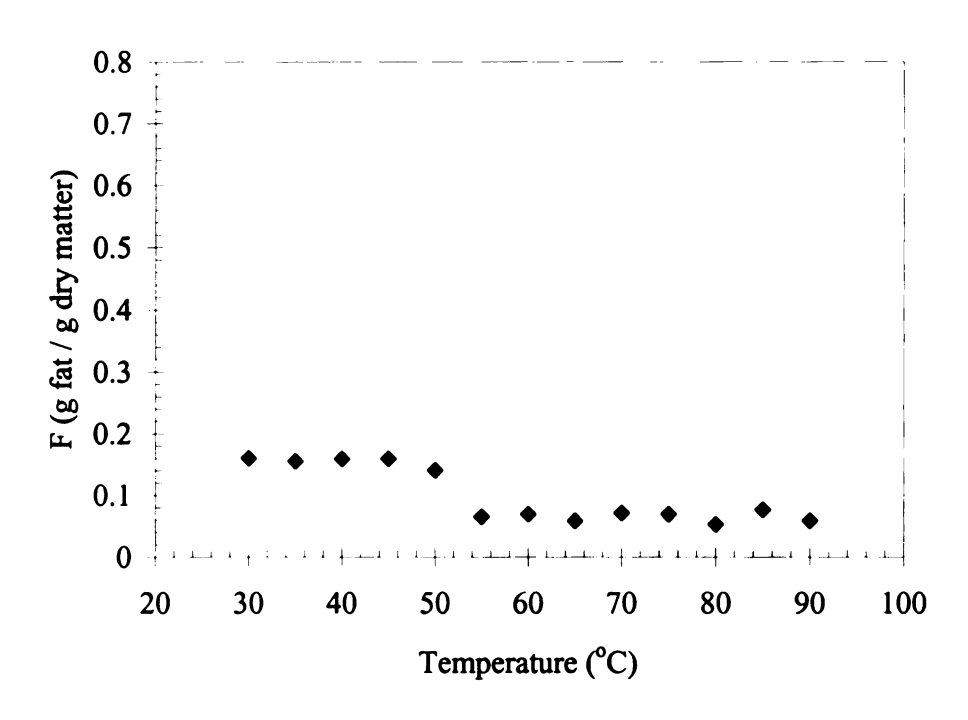


Figure 5.14 – Fat holding capacity as a function of temperature for 5.6% fat ground beef heated for 5 minutes at temperatures from 30 to 90°C: means of 5 replicates.

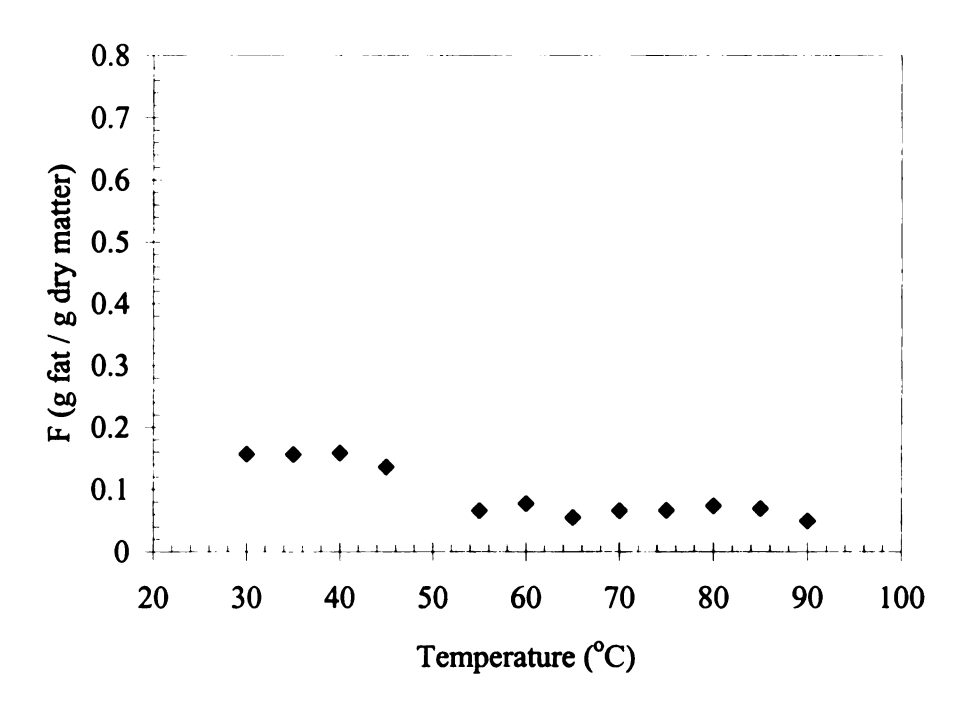


Figure 5.15 – Fat holding capacity as a function of temperature for 5.6% fat ground beef heated for 10 minutes at temperatures from 30 to 90°C: means of 5 replicates.

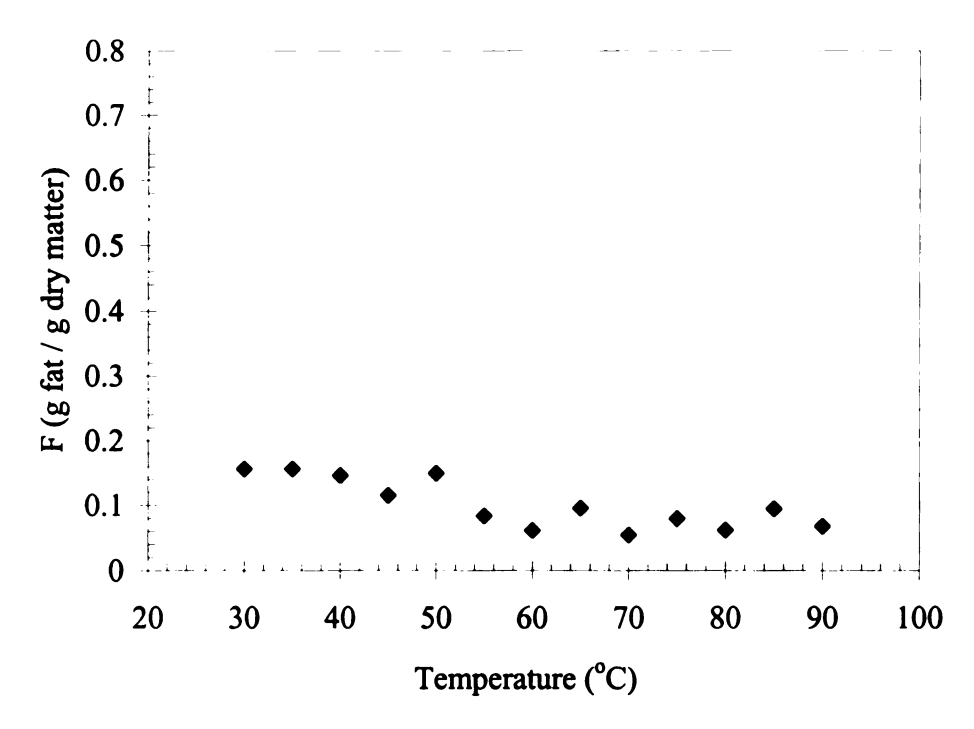


Figure 5.16 – Fat holding capacity as a function of temperature for 5.6% fat ground beef heated for 15 minutes at temperatures from 30 to 90°C: means of 5 replicates.

Table 5.13 – Results from regression of fat holding capacity as functions of time and holding temperature for 5.6% fat ground beef.

$$(\mathbf{F} = \boldsymbol{\beta}_0 + \boldsymbol{\beta}_1 \cdot \mathbf{T} + \boldsymbol{\beta}_2 \cdot \mathbf{T}^2 + \boldsymbol{\beta}_3 \cdot \mathbf{t} + \boldsymbol{\beta}_4 \cdot \mathbf{t}^2 + \boldsymbol{\beta}_5 \cdot \mathbf{t} \cdot \mathbf{T} + \boldsymbol{\varepsilon})$$

	Degrees of Freedom	Sum of Squares	Mean Square	F-Value P-Value
Regression	5	0.0703	0.0141	37.8124 < 0.001
Residual	46	0.0171	0.0004	
Total	51	0.0875		

Factor	Coefficient	Standard	t-Statistic	P-Value
		Error		
β_0 (g fat/g dry matter)	0.3459	0.0339	10.2141	< 0.001
β_1 (g fat/g dry matter).°C ⁻¹	-0.0060	0.0011	-5.6101	< 0.001
β_2 (g fat/g dry matter).°C ⁻²	3.28E-05	8.67E-06	3.7842	< 0.001
β_3 (g fat/g dry matter)·s ⁻¹	-0.0057	0.0032	-1.8057	0.078
β_4 (g fat/g dry matter)·s ⁻²	0.0002	0.0002	1.3904	0.171
β_5 (g fat/g dry matter)·°C ⁻¹ ·s ⁻¹	2.96E-05	2.86E-05	1.0368	0.305

Heating temperature was found to affect the fat holding capacity of the meat (P<0.05). The heating time and time-temperature interaction terms of the response surface model were not significant. A second regression was performed, neglecting the time and time-temperature interaction terms (Equation [5.4]).

$$F = \beta_0 + \beta_1 \cdot T + \beta_2 \cdot T^2 + \varepsilon$$
 [5.4]

The regression coefficients of the modified response surface model are given in Table 5.14.

Table 5.14 – Results from linear regression of fat holding capacity versus holding temperature for 5.6% fat ground beef.

$$(\mathbf{F} = \boldsymbol{\beta}_0 + \boldsymbol{\beta}_1 \cdot \mathbf{T} + \boldsymbol{\beta}_2 \cdot \mathbf{T}^2 + \boldsymbol{\epsilon})$$

	Degrees of Freedom	Sum of Squares	Mean Square	F-Value	P-Value
Regression	2	0.0691	0.0346	92.2654	2.43E-17
Residual	49	0.0184	0.0004		
Total	51	0.0875			

Factor	Coefficient	Standard Error	t-Statistic	P-value	
β_0 (g fat/g dry matter)	0.3178	0.0295	10.7649	<0.001	
β_1 (g fat/g dry matter) $^{\circ}$ C ⁻¹	-0.0057	0.0011	-5.4687	< 0.001	
β_2 (g fat/g dry matter) $^{\circ}$ C ⁻²	3.24E-05	8.69E-06	3.7254	< 0.001	

The regression model shows the fat holding capacity of the meat to be inversely proportional to the heating temperature. The drop off in fat holding capacity between 50 and 55°C is likely related to melting of fat globules within the meat matrix. The melting

temperatures of the most prevalent saturated fatty acids in ground beef occur near this range, with the melting temperatures of myristic, palmitic, and stearic acids being 54, 63, and 70°C, respectively (Bodwell and McClain, 1978). Ground beef with a fat content of only 5.6% contains only small quantities of extra-muscular fat and thus should be expected to contain lower percentages of saturated fatty acids. This could explain the lack of further losses in FHC at temperatures above 60°C.

The lack of time-significance seems to support the idea that fat holding capacity is largely related to the physical state of the fat itself. Since fat melting occurs over a short period, once the fat has melted, further heating should not affect the amount of liquid fat. If fat holding capacity changes were driven primarily by changes in protein conformation, denaturing, etc., longer heating times would be expected to produce increasingly lower levels of fat holding capacity.

A comparison of the fat holding capacity values predicted by the regression equation and the experimental data resulted in an R² of 0.79 (Figure 5.17). The root mean square error (RMSE) of the regression was 0.02 g fat/g dry matter.

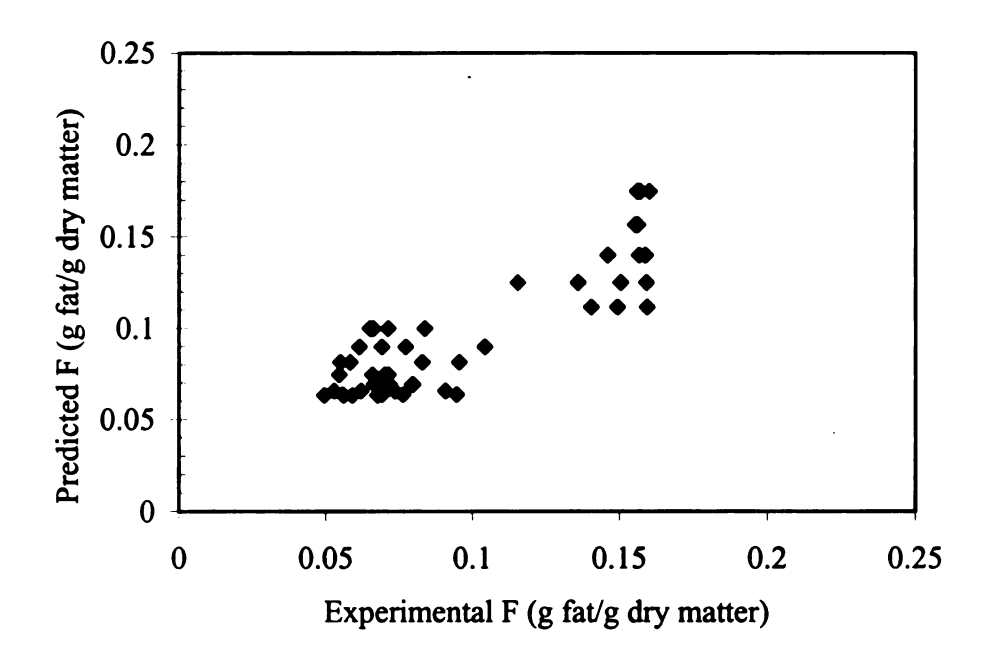


Figure 5.17 – Comparison of fat holding capacity calculated from regression model versus experimental values: means of 5 replicates.

5.3.2 High fat samples (15% initial fat wet basis)

The effect of temperature on fat holding capacity was much more pronounced for the 15% fat meat than for the 5.6% fat meat (Figures 5.18-5.21). The initial fat content of the 15% fat meat was 0.6 g fat/g dry matter. Fat holding capacity decreased with temperature and ranged between 0.07 and 0.17 g fat/g dry matter for samples heated to 90°C.

Multiple linear regression was again used to model fat content as functions of heating temperature and holding time, using a quadratic response surface equation (Equation [5.3]). The regression coefficients for the response surface equation are given in Table 5.15.

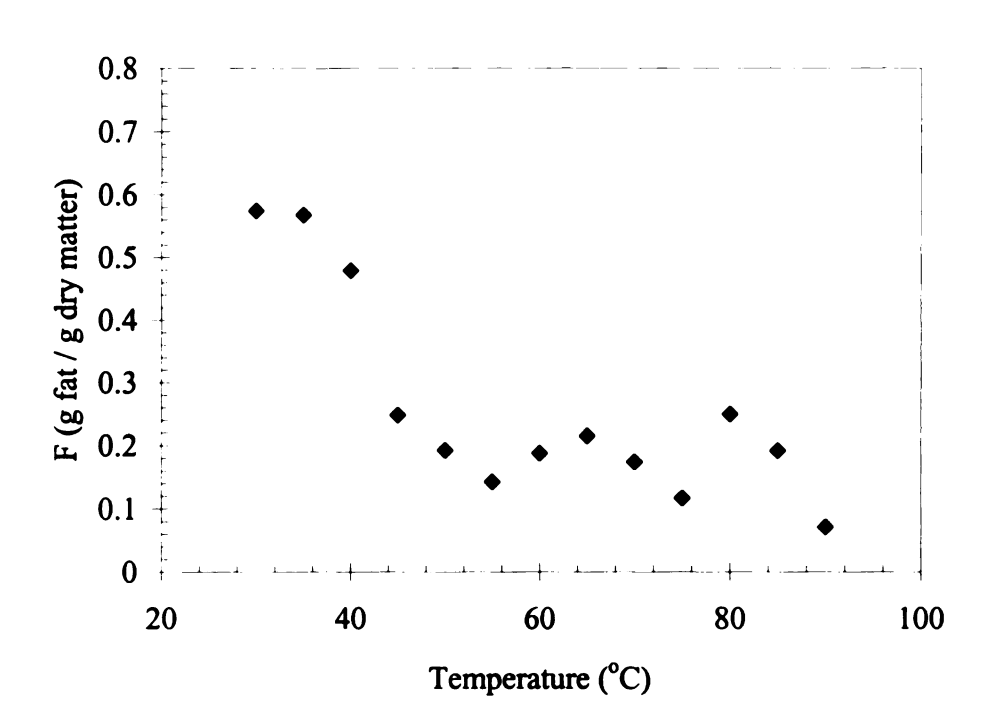


Figure 5.18 – Fat holding capacity as a function of temperature for 15% fat ground beef heated for 2 minutes at temperatures from 30 to 90°C: means of 5 replicates.

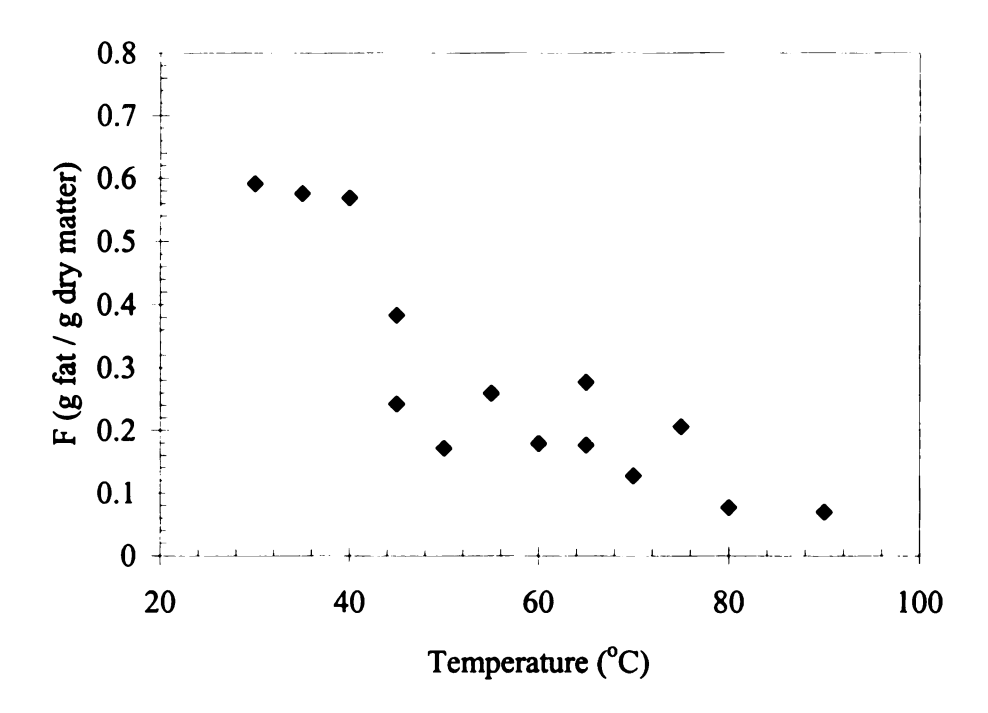


Figure 5.19 - Fat holding capacity as a function of temperature for 15% fat ground beef heated for 5 minutes at temperatures from 30 to 90°C: means of 5 replicates.

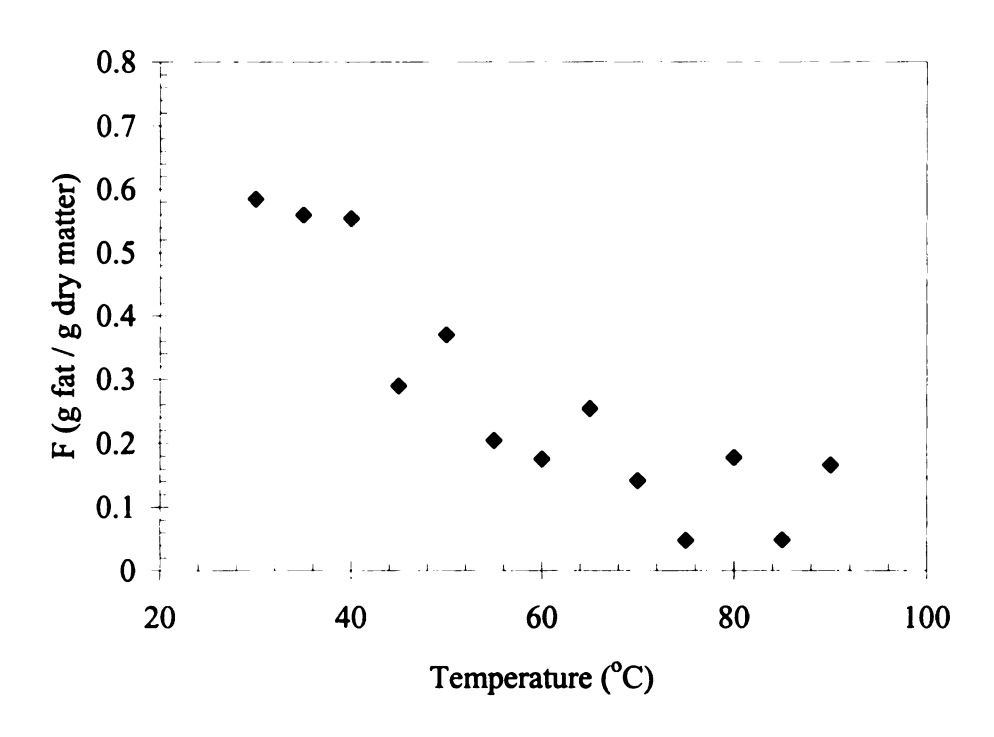


Figure 5.20 – Fat holding capacity as a function of temperature for 15% fat ground beef heated for 10 minutes at temperatures from 30 to 90°C: means of 5 replicates.

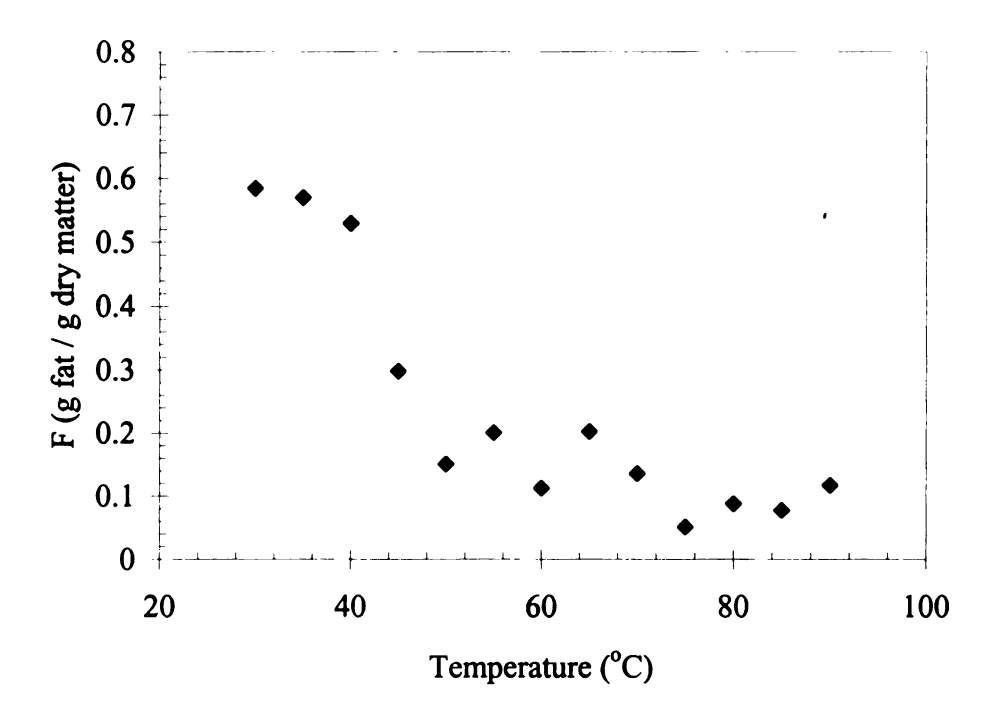


Figure 5.21 – Fat holding capacity as a function of temperature for 15% fat ground beef heated for 15 minutes at temperatures from 30 to 90°C: means of 5 replicates.

Table 5.15 – Results from regression of fat holding capacity versus time and holding temperature for 15% fat ground beef.

$$(\mathbf{F} = \boldsymbol{\beta}_0 + \boldsymbol{\beta}_1 \cdot \mathbf{T} + \boldsymbol{\beta}_2 \cdot \mathbf{T}^2 + \boldsymbol{\beta}_3 \cdot \mathbf{t} + \boldsymbol{\beta}_4 \cdot \mathbf{t}^2 + \boldsymbol{\beta}_5 \cdot \mathbf{t} \cdot \mathbf{T} + \boldsymbol{\varepsilon})$$

	Degrees of Freedom	Sum of Squares	Mean Square	F-Value P-Value
Regression	5	1.4071	0.2814	54.8295 < 0.001
Residual	47	0.2412	0.0051	
Total	52	1.6483		

Factor	Coefficient	Standard	t-Statistic	P-value
		Error		
β_0 (g fat/g dry matter)	1.3497	0.1237	10.9131	< 0.001
β_1 (g fat/g dry matter) ${}^{\circ}$ C ⁻¹	-0.0322	0.0039	-8.1558	< 0.001
β_2 (g fat/g dry matter) ${}^{\circ}$ C ⁻²	0.0002	3.19E-05	6.5391	< 0.001
β_3 (g fat/g dry matter)·s ⁻¹	0.0155	0.0117	1.3221	0.193
β_4 (g fat/g dry matter)·s ⁻²	-0.0006	0.0006	-1.0612	0.294
β_5 (g fat/g dry matter) ${}^{\circ}$ C ⁻¹ ·s ⁻¹	-0.0001	0.0001	-1.0881	0.282

Heating temperature again affected fat holding capacity (P<0.05). However, as with the lower fat beef, holding time and time-temperature interaction were not statistically significant. A modified regression was performed omitting the terms for holding time and time-temperature interaction (Equation [5.5]).

$$F = \beta_0 + \beta_1 \cdot T + \beta_2 \cdot T^2 + \varepsilon$$
 [5.5]

The regression coefficients of the modified regression are shown in Table 5.16.

Table 5.16 – Results of regression of fat holding capacity versus holding temperature for 15% fat ground beef.

$$(\mathbf{F} = \boldsymbol{\beta}_0 + \boldsymbol{\beta}_1 \cdot \mathbf{T} + \boldsymbol{\beta}_2 \cdot \mathbf{T}^2 + \boldsymbol{\varepsilon})$$

	Degrees of Freedom			F-Value	P-Value
Regression	2	1.3922	0.6961	135.9025	<0.001
Residual	50	0.2561	0.0051		
Total	52	1.6483			

Factor	Coefficien	t Standar	t-Statistic	P-Value
		d Error		
β_0 (g fat/g dry matter)	1.4163	0.1085	13.0474	< 0.001
β_1 (g fat/g dry matter).°C ⁻¹	-0.0329	0.0039	-8.5302	< 0.001
β_2 (g fat/g dry matter) ${}^{\circ}$ C ⁻²	0.0002	3.19E-05	6.4820	< 0.001

The fat holding capacity of the 15% fat ground beef was inversely proportional to the heating temperature. The effect of heating temperature was much more pronounced for the 15% fat ground beef than for the 5.6% fat product. The coefficient for the linear temperature term in the regression equation was -0.0329 (g fat/g dry matter)/°C for 15% fat ground beef, compared to -0.0057 (g fat/g dry matter)/°C for 5.6% fat ground beef.

Like the low fat samples, the largest change in fat holding capacity for the 15% fat samples occurred between 40 and 55°C. However, unlike the lower fat samples, fat holding capacity of the 15% fat samples continued to decrease at temperatures above 55°C. This was likely due to the inclusion of higher quantities of long chain saturated fatty acids.

The lack of time-dependence of the fat holding capacity was similar to that exhibited by the lower fat samples. This further supports the idea that fat holding

capacity, as measured in this study, is governed primarily by the physical state of the fat globules within the meat matrix. This is of special interest when formulating models for mass transfer, as the physical state of the fat must be considered. Clearly, solid fat does not have the transportability of liquid fat. However, it may be possible to develop highly advanced fat transport models based upon knowledge of the individual fat constituents of a given species and cut of meat. This would allow for maximum flexibility of advanced processing models.

A comparison of the fat holding capacity values predicted by the regression model (Equation [5.5]) to the experimental data resulted in an R² of 0.84 (Figure 5.22). The RMSE of the regression model was 0.071 g fat/g dry matter.

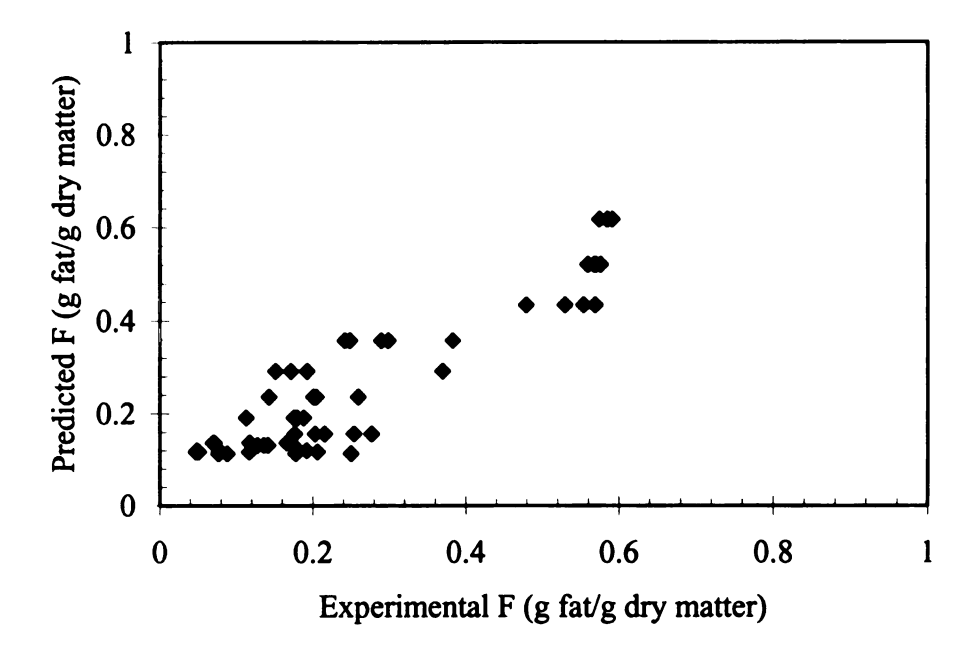


Figure 5.22 - Comparison of fat holding capacity calculated from regression model versus experimental values (15% fat): means of 5 replicates.

After completing separate regression analyses for the 5.6% and 15% fat ground beef samples, a combined regression was performed to create a model for fat holding capacity as a function of heating temperature, holding time, and initial fat content. A response surface model was chosen for the regression (Equation [5.6]). No second- order terms for fat content were utilized in the regression equation, because data were only available from two initial fat contents. The coefficients for the regression model are listed in Table 5.17.

$$F = \beta_0 + \beta_1 \cdot T + \beta_2 \cdot T^2 + \beta_3 \cdot t + \beta_4 \cdot t^2 \cdot \beta_5 \cdot F_0 + \beta_6 \cdot t \cdot T + \beta_7 \cdot T \cdot F_0 + \beta_8 \cdot t \cdot F + \varepsilon$$
[5.6]

Table 5.17 – Linear regression of fat holding capacity as functions of heating temperature, holding time, and initial fat content.

$$\begin{pmatrix} F = \beta_0 + \beta_1 \cdot T + \beta_2 \cdot T^2 + \beta_3 \cdot t + \beta_4 \cdot t^2 + \beta_5 \cdot F_0 + \beta_6 \cdot t \cdot T + \beta_7 \cdot T \cdot F_0 \\ + \beta_8 \cdot t \cdot F_0 + \epsilon \end{pmatrix}$$

	Degrees of Freedom	Sum of Squares	Mean Square	F-Value	P-Value
Regression	9	2.1005	0.2339	65.0322	< 0.001
Residual	95	0.3409	0.0036		
Total	104	2.4414			

Factor	Coefficient	Standard	t-Statistic	P-value
		Error		
β_0 (g fat/g dry matter)	0.3334	0.1104	3.0193	0.003
β_1 (g fat/g dry matter)°C ⁻¹	-0.0136	0.0027	-5.037	< 0.001
β_2 (g fat/g dry matter)°C ⁻²	0.0001	1.90E-05	6.3768	< 0.001
β_3 (g fat/g dry matter)·s ⁻¹	-0.0042	0.0111	-0.3804	0.704
β_4 (g fat/g dry matter)·s ⁻²	-0.0002	0.0003	-0.4541	0.651
β_5 (none)	0.0503	0.0080	6.3074	< 0.001
β ₆ (g fat/g dry matter)·°C ⁻¹ ·s ⁻¹	0.0001	0.0002	0.7967	0.428
β ₇ (°C ⁻¹)	-0.0005	0.0001	-4.2171	< 0.001
$\beta_8 \ (s^{-1})$	0.0008	0.0008	0.9458	0.347

None of the terms containing holding time were significant (P<0.05). A modified regression was performed excluding the time terms (Equation [5.7]).

$$F = \beta_0 + \beta_1 \cdot T + \beta_2 \cdot T^2 + \beta_3 \cdot F_0 + \beta_4 \cdot T \cdot F_0 + \varepsilon$$
 [5.7]

The coefficients of the modified regression are shown in Table 5.18.

Table 5.18 - Linear regression of fat holding capacity as a function of holding temperature and fat content.

$$(\mathbf{F} = \boldsymbol{\beta_0} + \boldsymbol{\beta_1} \cdot \mathbf{T} + \boldsymbol{\beta_2} \cdot \mathbf{T}^2 + \boldsymbol{\beta_3} \cdot \mathbf{F_0} + \boldsymbol{\beta_4} \cdot \mathbf{T} \cdot \mathbf{F_0} + \boldsymbol{\epsilon})$$

	Degrees of Freedom	Sum of Squares	Mean Square	F-Value	P-Value
Regression	4	1.9767	0.4942	106.330	< 0.001
Residual	100	0.4647	0.0046		
Total	104	2.4414			

Factor	Coefficient	Standard Error	t-Statistic	P-value
β_0 (g fat/g dry matter)	0.7062	0.0746	9.4719	0.006
β_1 (g fat/g dry matter)·°C ⁻¹	-0.0193	0.0026	-7.3996	< 0.001
β_2 (g fat/g dry matter)·°C ⁻²	0.0001	2.16E-05	5.0990	< 0.001
β_3 (none)	0.0069	0.0020	3.4355	< 0.001
β ₄ (°C ⁻¹)	0.0002	3.41E-05	7.1495	< 0.001

A comparison of the fat holding capacity values predicted by the regression and the experimental data produced an R^2 of 0.81 (Figure 5.23). The RMSE for the regression was 0.068 g fat/g dry matter.

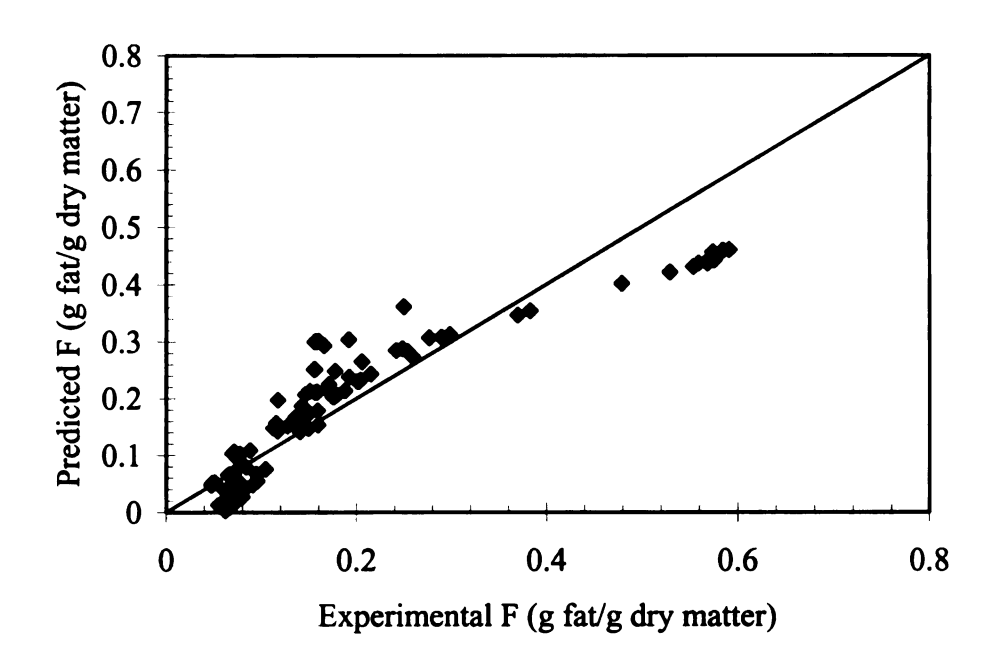


Figure 5.23 – Comparison of fat holding capacity calculated from regression model versus experimental values: means of 5 repetitions.

5.3.3 Summary

The regression models presented for fat holding capacity provide a tool that can be utilized as a component of the cooking model. However, it should be noted that this results in an empirical fat transfer model. The equations developed for fat holding capacity are specific for ground beef. Further studies should be conducted to measure the FHC of other meat species. In addition, mechanisms of fat transport should be further studied to produce a theoretical model for FHC.

The methods used to determine fat holding capacity were considered adequate for the purposes of this study. However, several factors should be taken into consideration for further experiments. The most probable source of error for the FHC experiments was in the centrifugation procedure. The centrifuge utilized for the study was held at 25°C. Although the centrifuge tubes were insulated from the rotor by plastic inserts, some re-

solidification of fat took place during centrifugation. To eliminate this potential source of error, a method of separating the free fat while maintaining the sample temperature should be determined. It may also be desirable to measure the fat content of the meat directly using a method such as solvent extraction rather than the method of mass balances utilized in this study.

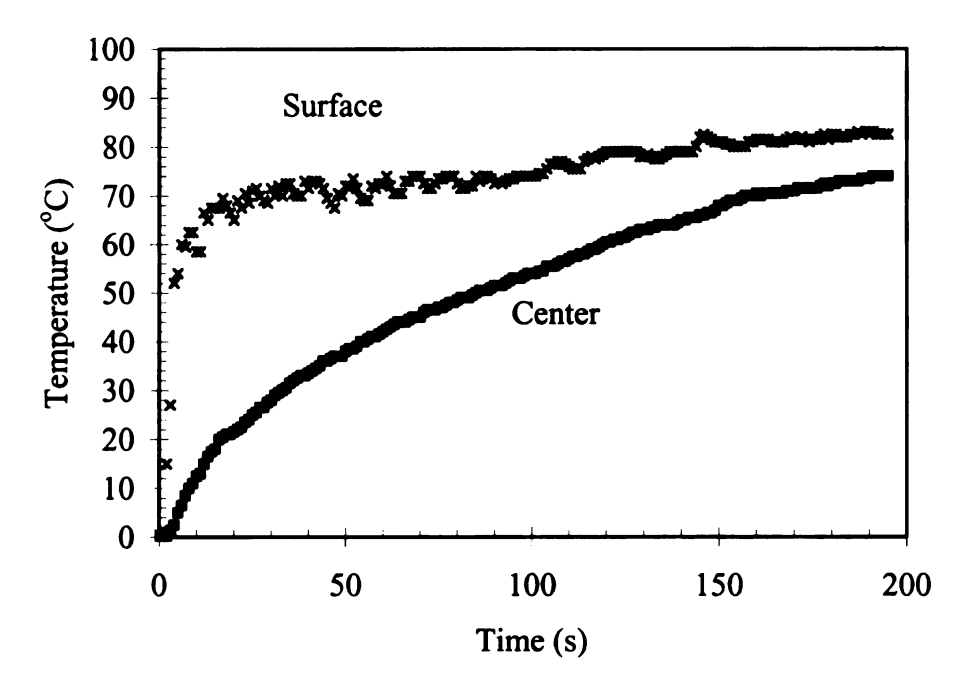
5.4 Industrial cooking tests

A set of cooking experiments was conducted using an industrial moist-air impingement oven (Stein Model JSO-IV:FMC Foodtech, Sandusky, OH). Ground beef patties were cooked under different cooking conditions to quantify the effects of process conditions on heating rate and cooking yield. The results of this set of experiments were also used to validate the computer-cooking model.

5.4.1 Cooking time

For each cooking experiment, temperature versus time was plotted for both the center and surface temperatures of the patty (Figure 5.24). The complete collection of temperature-time plots can be found in Chapter 9. The general form of each time-temperature plot was similar. After entering the oven, the surface temperature of the patty quickly rose to a semi-equilibrium level. Calculations showed that this level was equal to the wet bulb temperature of the meat surface (Section 4). The temperature at the meat surface was limited by a number of factors, including oven temperature, oven steam content, and the surface moisture content of the meat.

(a)



(b) Surface Temperature (°C) Center

Figure 5.24 – Example surface and center temperature versus time for ground beef patties cooked at (a) oven temperature: 121°C, oven steam content: 50% by volume, oven airflow: 11.4 m/s and (b) oven temperature: 232°C, oven steam content: 50% by volume, oven airflow: 16.8 m/s.

Time (s)

The center temperature of the meat increased at a much slower rate than the surface and approached the surface temperature asymptotically. For most cooking experiments, the center temperature of the patty was at least 10°C below the surface temperature at the end cooking.

Several revelations about the cooking process can be inferred from the experimental data. The first is that increasing the oven temperature does not proportionally increase the heating rate of the patties. The wet bulb temperature always limits the surface temperature of the patty. With the exception of extremely low surface moisture contents, the temperature of the patty surface cannot exceed the wet bulb temperature of the cooking air. The moisture content at which surface temperature will exceed the wet bulb temperature is a function of the equilibrium relative humidity of the meat. Under the conditions tested, this moisture content was between 5 and 7% wet basis. No observations of surface temperature exceeding 100°C were made for any of the 54 experimental cooking trials.

-		

Because the heating rate at the center of the patty is controlled by the thermal gradients between the center of the patty and the patty surface, the patty surface temperature is the limiting factor for cooking time. Multiple linear regression was used to describe center temperature as a function of oven temperature, steam content, cooking time, and airflow. Table 5.19 shows the results of the regression. As expected, steam content, and cooking time were significant (P<0.05). A positive correlation existed between center temperature and steam content and cooking time. Not-surprisingly, cooking time had the largest effect on center temperature. More interesting however, is that oven steam content had a much more pronounced effect on center temperature than did oven temperature. The effect of steam content resulted in a potential temperature difference of up to 9.8°C over the range of steam contents tested, as compared to a nonsignificant effect of oven temperature. This compares to a difference of only 3.4°C related to oven temperature, indicating that oven steam content has a much greater effect on the surface wet bulb temperature of the patty than oven temperature. This observation should be taken into account when working to optimize oven settings.

Table 5.19 – Linear regression of patty center temperature as functions of oven temperature, steam content, cooking time, and oven airflow.

$$(T = \beta_0 + \beta_1 \cdot T_{ovea} + \beta_2 \cdot M + \beta_3 \cdot t + \beta_4 \cdot V_{air})$$

	Degrees of Freedom	Sum of Squares	Mean Square	F-Value P-Value
Regression	4	6548.757	1637.189	35.6310 < 0.001
Residual	50	2297.425	45.9485	
Total	54	8846.182		

	Factor	Coefficient	Standard	t-Statistic	P-value
			Error		
$\overline{\beta_0}$	°C	30.3786	8.0882	3.7559	< 0.001
β_1	°C/°C	0.0306	0.0228	1.3391	0.187
β_2	°C·%Steam ⁻¹	0.2583	0.0641	4.0275	< 0.001
β_3	°C·s ⁻¹	4.1720	0.4146	10.0639	< 0.001
β4	°C·s·m ⁻¹	-0.0218	0.2194	-0.0993	0.921

Oven air velocity did not significantly affect the patty center temperature. The temperature gradients that drive conduction within the patty result from increases in the patty surface temperature. Although increasing the airflow has the effect of increasing the heat transfer coefficient at the patty surface, corresponding increases in the mass transfer coefficient result in increased evaporative cooling in the later stages of cooling. The result was a zero net gain in the heating rate of the patty for the conditions tested.

During the early stages of cooking, increases in airflow may increase the rate of condensation at the patty surface, thereby temporarily increasing the heating rate.

However, as illustrated in the heating curves, the surface temperature reaches equilibrium within about 10 seconds for the range of oven conditions tested. The marginal gains in

surface temperature heating rate caused by increasing airflow did not significantly increase the rate of heating at the patty center.

5.4.2 Cooking yield

Figure 5.25 shows the relationship between patty center temperature and cooking yield for ground beef patties cooked in the JSO-IV impingement oven. Cooking yields decreased as a function of patty center temperature.

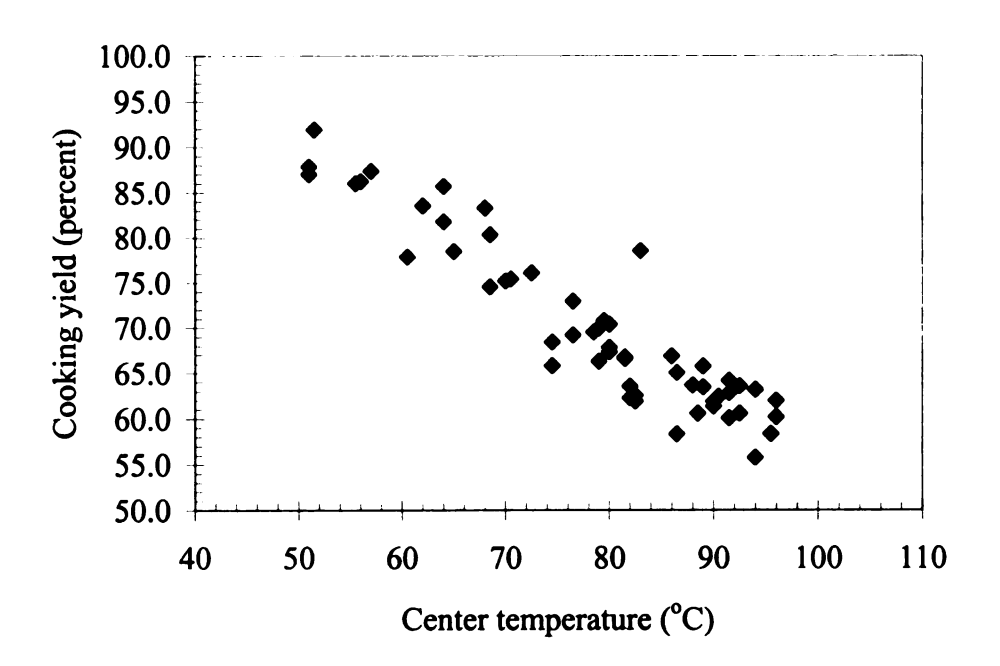


Figure 5.25 - Cooking yield as a function of endpoint center temperature for ground beef patties cooked in a Stein JSO-IV industrial moist air impingement oven.

The results of linear regression are shown in Table 5.20. Oven temperature, cooking time, and oven steam content were each found to significantly affect patty yield (P<0.05). Cooking time, oven temperature, and oven steam content each had a negative effect on cooking yield. Cooking time had the strongest effect on yield. Oven

temperature and steam content each had an effect approximately one order of magnitude below the effect of cooking time. Oven temperature created a potential difference in cooking yield of up to 5.6% over the range of temperatures used. Steam content had an effect equal to 4.8% yield over the range of steam contents tested.

Table 5.20 – Regression parameters for cooking yield as a function of oven temperature, steam content, cooking time, and airflow.

$$\left(Y = \beta_0 + \beta_1 \cdot T_{oven} + \beta_2 \cdot M + \beta_3 \cdot t + \beta_4 \cdot V_{air}\right)$$

	Degrees of Freedom	Sum of Squares	Mean Square	F-Value	P-Value
Regression	4	3836.668	959.1669	50.0733	< 0.001
Residual	50	957.7628	19.1553		
Total	54	4794.43			

Factor	Coefficient	Standard	t-Statistic	P-value
		Error		
β_0	109.6251	5.2223	20.9917	< 0.001
β_0 β_1 °C ⁻¹	-0.0503	0.0147	-3.4133	0.001
β_2 % Steam ⁻¹	-0.1259	0.0414	-3.0397	0.004
$\beta_3 \text{ s}^{-2}$	-3.4932	0.2677	-13.0507	< 0.001
β ₄ s·m ⁻¹	-0.0453	0.1416	-0.3201	0.750

5.4.3 Fat loss

For each patty, the cooking loss not accounted for by moisture loss was calculated and assumed to be entirely due to fat loss. The amount of fat lost increased with center temperature (Figure 5.26) and ranged from less than 1% of the initial mass at 50°C up to almost 10% of the initial mass at 95°C. This accounts for nearly all of the fat initially present in the patty. The results of linear regression for fat loss as a function of oven

parameters are shown in Table 5.21. Only cooking time significantly affected the yield lost due to fat. Clearly, the effects of fat loss must be taken into account to accurately model yield losses during cooking.

Table 5.21 - Regression parameters for fat loss as a function of oven temperature, steam content, cooking time, and airflow.

$$\left(\Delta Y_{fat} = \beta_0 + \beta_1 \cdot T_{oven} + \beta_2 \cdot M + \beta_3 \cdot t + \beta_4 \cdot V_{air}\right)$$

	Degrees of Freedom	Sum of Squares	Mean Square	F-Value	P-Value
Regression	4	88.1928	22.0482	7.7278	< 0.001
Residual	22	62.7679	2.8531		
Total	26	150.9607			

Factor	Coefficient	Standard Error	t-Statistic	P-value
$\overline{\mathrm{B}_{\mathrm{0}}}$	-3.0612	2.9207	-1.0481	0.306
B_1 (°C ⁻¹)	0.0070	0.0081	0.8722	0.393
B ₂ (% Steam ⁻¹)	0.0464	0.0230	2.0188	0.056
$B_3 (s^{-1})$	0.0118	0.0025	4.7997	< 0.001
$B_4 (s \cdot m^{-1})$	-0.0161	0.0771	-0.2085	0.837

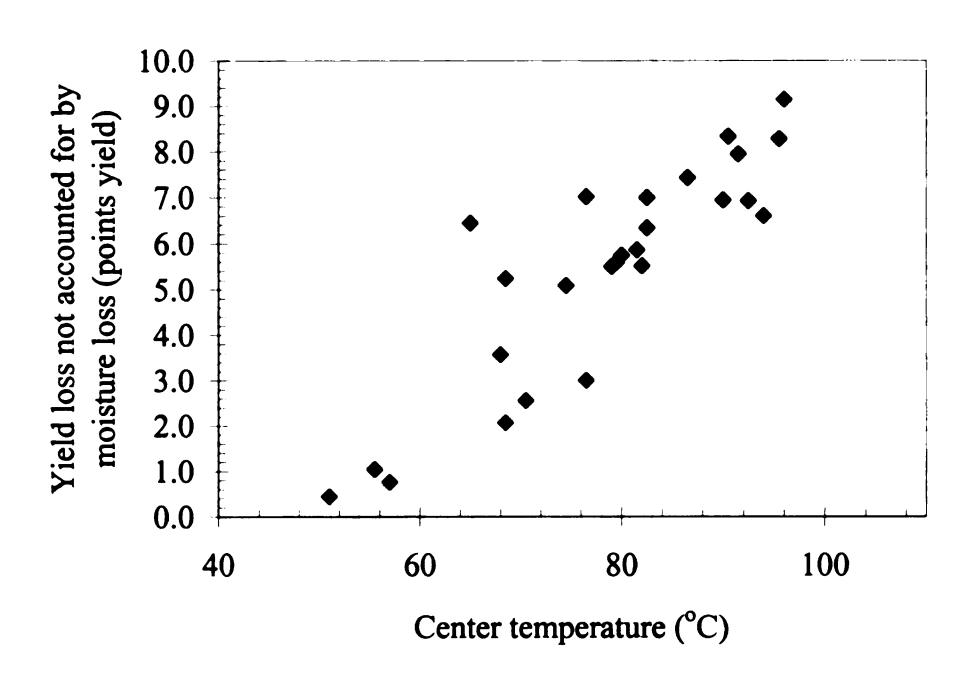


Figure 5.26 - Yield loss not accounted for by moisture loss as a function of endpoint temperature for ground beef patties cooked in a Stein JSO-IV industrial moist-air impingement oven.

5.4.4 Volume change

Patties exhibited a reduction in volume during cooking. The volume change was primarily due to dramatic reductions in the diameter of the patties during cooking. The diameter reduction as a function of endpoint center temperature is shown in Figure 5.27. The diameter of the patties decreased linearly as a function of center temperature. The thickness of the patties did not exhibit the same behavior. The thickness of the patties remained relatively unchanged during cooking, with approximately half of the patties undergoing slight decreases in thickness, and the other half undergoing slight increases. The average absolute change in thickness was 0.76 mm. The mean change in thickness was -0.14 mm.

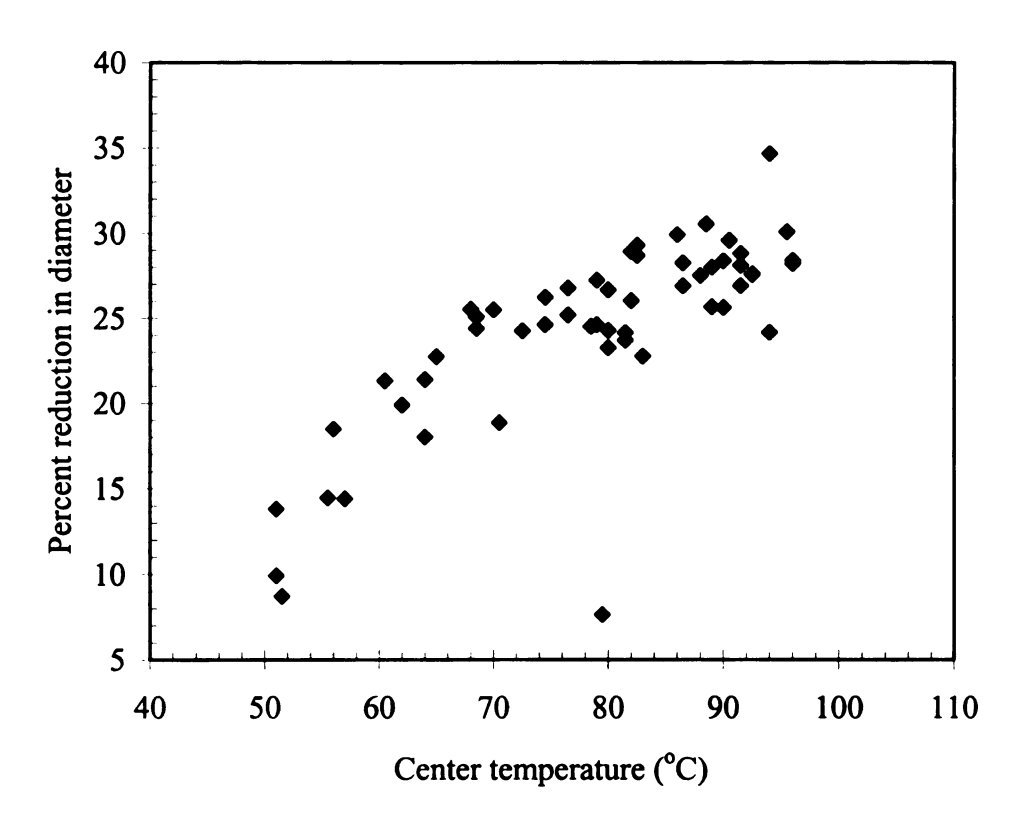


Figure 5.27 - Reduction in diameter during cooking as a function of cooking yield for ground beef patties cooked in a stein JSO-IV industrial moist-air impingement oven.

The fact that the diameter of the patties changes so drastically during cooking, while the thickness stays relatively unchanged, presents a challenge for modeling cooking. To model cooking as completely as possible, volume changes should be incorporated into the model. However, for patties such as those utilized in these experiments, heat and mass transfer occur primarily in the axial direction, due to the height/diameter ratio of the patties. Since patty thickness remains relatively unchanged, changes in volume do not affect heat and mass transfer dramatically from the standpoint of modeling. However, further research in this area could shed light on the changing physical conditions that occur within meat during cooking.

5.5 Cooking model validation

Validation of the cooking model was conducted using the data collected from cooking experiments with a Stein JSO-IV moist-air impingement oven (Sections 3.4 and 5.4). Validation was conducted for temperature, moisture, and yield. Additional comparisons were made using yield and temperature data from published sources (Murphy et al., 2001a and b).

5.5.1 Finite element mesh

The finite element mesh utilized for cooking model validation consisted of 116 triangular elements with a total of 78 nodes. The element mesh was shown graphically in Chapter 4. A total of 28 nodes were located along the convective boundaries of the patty geometry. Mesh density was lowest at the center of the patty and increased near the surface where the temperature and moisture gradients were expected to be highest.

The element mesh utilized was chosen to balance solution accuracy with computing time. Increasing the number of elements from 48 to 116 lowered the transient standard error of prediction for the center temperature of a test experiment from 11.6°C to 5.5°C. This increase in accuracy came at the cost of computing time. The 48 element model only took 17 seconds to complete, compared to 75 seconds for the 116 element model. Increasing the number of elements from 116 to 234 did not improve the accuracy of the temperature prediction. However, the computing time required to run each test was increased to 295 seconds. This clearly illustrates that increasing the mesh density comes at a major cost in computing time. This is of importance to users utilizing the

model to simulate large numbers of conditions for applications such as process optimization.

The value of the time step selected for the model was 1 second. This value was utilized to aid in comparisons with experimental data, which was recorded at one-second intervals. Unfortunately in certain cases, the one-second value for the time step may result in numerical oscillations if a constant element mesh size is utilized. Automatic routines for mesh generation and time step optimization could eliminate this potential problem.

5.5.2 Temperature profile-experimental data

Validation of temperature profiles was conducted by comparing transient center temperature data collected during the experimental tests to corresponding predictions generated by the model. Example center temperature profiles are shown in Figures 5.28-5.30. All experimental and predicted temperature results are graphed in Chapter 9.

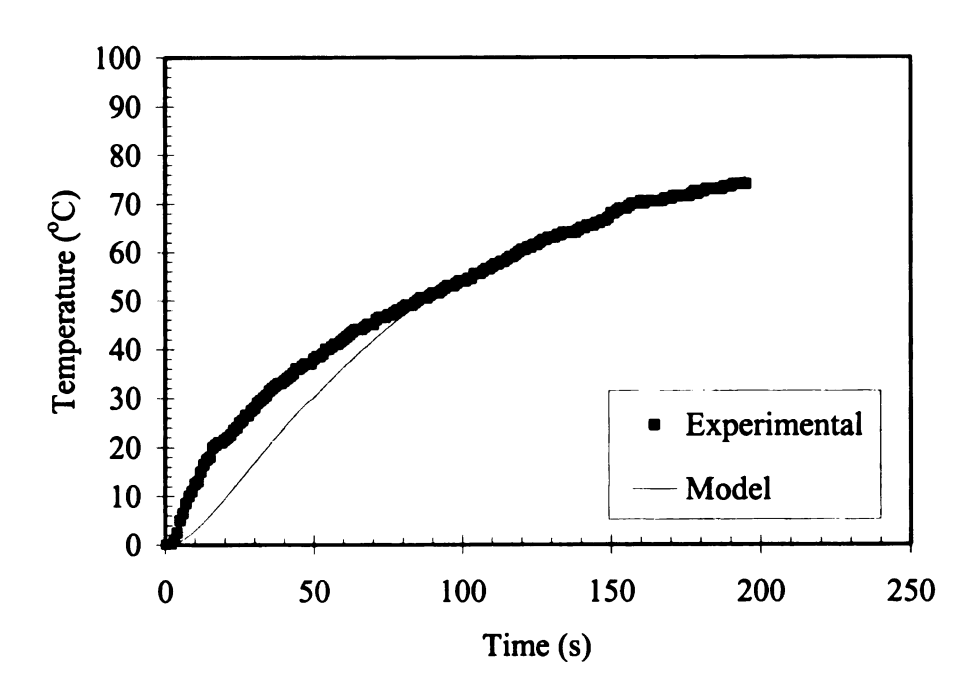


Figure 5.28 – Example comparison of experimental temperature data with data generated by the cooking model (oven temperature=121°C, steam content=50%, air velocity=11.4 m/s).

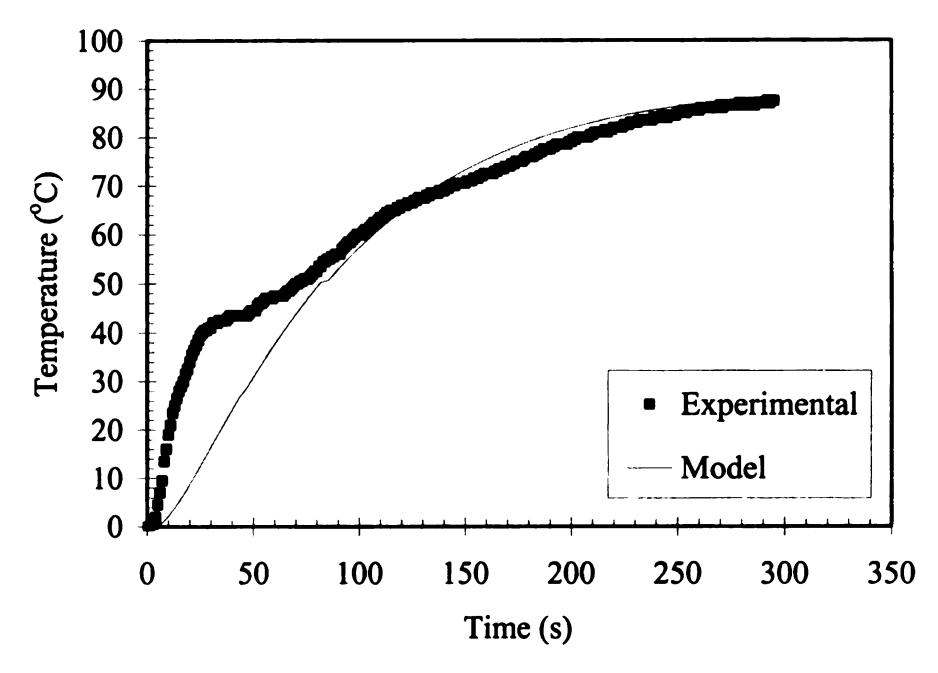


Figure 5.29 – Example comparison of experimental temperature data with data generated by the cooking model (oven temperature=121°C, steam content=70%, air velocity=11.4 m/s).

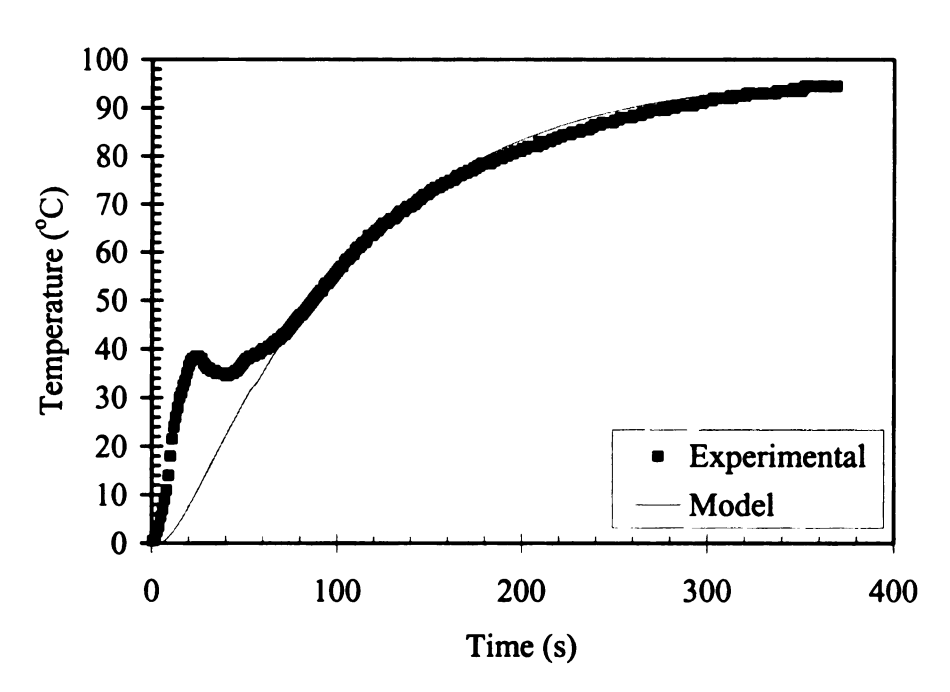


Figure 5.30 – Example comparison of experimental temperature data with data generated by the cooking model (oven temperature=121°C, steam content=88%, air velocity=11.4 m/s).

Figure 5.28 is typical of most comparisons in several respects. Noticeable deviation between the model and experimental data occurred during the early stages of cooking. During the later stages of cooking, profiles for the model and experimental data were very close. Although the level of agreement between the model and experimental data varied between cooking runs, the phenomenon of the predicted center temperature lagging behind the measured temperature during the early stages of cooking was common to all cooking experiments. These results were similar to those reported by Pan et al. (2000) who found that temperature values lagged below predicted values for contact cooking of hamburger patties. These deviations were largest between 0 and 40°C. Disparities in the sample cooking curve provided by Pan et al. (2000) were very similar to the predicted error shown in Figure 5.28.

Based on Figure 5.28, several conclusions can be made. First, it is possible that the deviation between the temperature profile predicted by the model and the experimental data was caused by inaccurate predictions of thermo-physical properties in the model. The thermal conductivity may have been underestimated at low temperatures. The model also may have overestimated the heat capacity of the product at low temperatures.

A second possibility for the deviation between the model and the experimental temperature profiles is the effect of volume change. The model did not take into account volume change during cooking. If the thickness of the patty changed significantly during cooking, the rate of heat transfer to the center of the patty may have changed, even under conditions of constant thermal properties. However, as discussed in Section 5.4.4, the thickness of the patties remained constant during cooking, with significant shrinkage occurring only in the radial direction. Because heat transfer occurred primarily in the vertical direction, it is unlikely that shape changes contributed significantly to error in the model for the product tested.

Figures 5.29 and 5.30 illustrate a more pronounced deviation between the model and experimental temperatures during the first minute of cooking. This type of deviation was seen in about half of the 54 cooking trials. Typically, the deviation consisted of an increase in measured temperature above the predicted value followed by a drop in temperature to a level consistent with the predicted value. This deviation typically occurred over a temperature range of 0 to 40°C. At temperatures above 40°C, the experimental temperature profiles then closely matched the values predicted by the cooking model.

One possibility for the disparity between the model and experimental data in the early stages of cooking is that the thermocouple measuring center temperature may have moved as the meat began to cook. Changes in product texture, along with diameter changes occurring during cooking, would explain why the thermocouple could move during the early portion of cooking. However, this explanation does not account for the resolution between the measured and predicted temperature values at higher temperatures.

The possibility that the author considers most likely is that fat-related effects were the cause of these deviations. From the fat holding capacity experiments in Section 3.3, large changes in fat holding capacitywere seen in the temperature range between 40 and 50°C. The laboratory experiments in Section 3.2 also show that yield loss is roughly linear at temperatures above 45°C. Most fat is in a form that is available for transport at temperatures above 45°C.

Prior to heating, ground beef consists of a mixture of ground fat and muscle particles. Unlike whole muscle products, the fat particles are dispersed throughout the meat, rather than in their naturally occurring structures. In this sense, the fat particles exist as a dispersed phase within a matrix of lean meat. When the fat particles are in solid form, physical forces serve to keep them in suspension within the meat. However, upon melting, the fat is free to exit the meat through capillary mechanisms.

It is proposed that during the initial phases of cooking, changes in the meat structure occurred that resulted in the thermocouple not giving an accurate representation of the average temperature in the center of the patty. Due to the near-frozen condition of the meat before cooking, the meat had a very firm initial texture. As a result, when the

thermocouple was inserted into the patty, a minute void space may have been created around the thermocouple, which would have provided a channel for condensing water to penetrate to the center of the patty, and thereby increase the thermocouple temperature above that of the meat. At temperatures above 40-50°C, constriction of the meat and filling of internal voids by melting fat would result in more intimate contact between the thermocouple and the meat matrix, thereby resulting in more accurate temperature readings. The vertical orientation of the thermocouple may have contributed to this type of effect by providing an uninterrupted vertical channel between the bottom and center of the patty.

This theory would explain the deviations seen in Figures 5.29 and 5.30. It is also highly likely that the deviation in Figure 5.28, although less pronounced than the others, was caused by a similar effect. In the temperature curves where significant deviations occur between the measured and predicted center temperature values, the measured center temperature value appears to temporarily move in the direction of the surface temperature of the patty, before dropping back down to a level more consistent with the predicted value. This seems to support the hypothesis that condensing water at the surface temperature may be penetrating the patty along the thermocouple "channel".

Unfortunately, accurate surface temperature values were not available for many of the cooking trials due to the difficulty in maintaining uninterrupted contact between the thermocouples and the patty surface during cooking. The high airflow of the oven, combined with changes in patty geometry, often separated the thermocouples from the patty surface. For this reason, surface temperature data are missing from many of the figures in Section 9.1. Due to inconsistentcies in the surface temperature data, it was not

considered meaningful to calculate transient SEP for the surface temperature of each model run. Instead, general observations of the predicted and measured surface temperatures were made.

For each simulated cooking run, the surface temperature of the meat quickly rose to a semi-equilibrium value. This temperature reflects the wet bulb temperature of the oven air. This temperature never exceeded the boiling point of water for any of the patties tested. For patties in which accurate surface temperatures are available, the predicted surface temperatures corresponded closely with the experimental values. In many cases, the measured surface temperature values were considerably different from the predicted values. However, it is the opinion of the author that these cases represent situations in which the thermocouple was not in contact with the actual surface of the patty. In some cases the thermocouple may have been lodged slightly below the surface of the patty. These cases illustrate the difficulty inherent in measuring the surface temperature of meat patties within commercial convection ovens.

Standard error of prediction was calculated for the center temperature data of each cooking trial, using temperature data collected at 1 second intervals from both the model and experiments. The SEP of the transient center temperatures for individual trials ranged from 2.1 to 13.9°C (Table 5.21). The overall SEP for all of the cooking trials was 8.0°C. The SEP for the final center temperature of all of the patties was also 8.0°C. The error in the temperature curves was generally concentrated in the early portion of the curves. The cooking experiments that were run for short times had the largest errors. As the patty center reached high temperatures, the differences between the model and experimental data became small. A second set of SEP data was generated for the portion of each

cooking run above 45°C (Table 5.22). These SEP's ranged from 0.5 to 10.8°C, a large improvement from the values taken over the entire temperature range. The overall SEP for all data points above 45°C was 5.8°C. The trials with large SEP values for temperature were generally the experiments with the shortest cooking times. In these trials, deviations between the model and experimental data at low temperatures affected a larger percentage of the total cooking time, thus resulting in larger SEP between experimental and predicted data.

Table 5.22 – Standard error of prediction for the entire trial (SEP) and for data above 45° C (SEP_{T>45°}C) for center temperature of beef paties.

Exp.	SEP (°C)	SEP _{T>45°C} (°C)	Exp.	SEP (°C)	SEP _{T>45°C} (°C)
#	(data points)	(data points)	#	(data points)	(data points)
la	5.5 (193)	1.2 (128)	1b	4.7 (157)	5.1 (63)
6a	3.9 (416)	4.1 (330)	6b	3.3 (418)	3.1 (324)
8a	2.4 (300)	1.2 (214)	8b	6.9 (303)	3.4 (247)
11a	6.9 (294)	2.8 (220)	11b	8.9 (295)	3.6 (244)
13a	4.0 (187)	3.1 (115)	13b	12.5 (189)	9.6 (152)
18a	4.1 (396)	3.6 (340)	18b	7.6 (396)	1.9 (341)
21a	5.5 (368)	2.4 (298)	21b	7.1 (369)	1.3 (294)
23a	3.0 (320)	3.1 (229)	23b	5.1 (301)	4.3 (214)
25a	5.1 (141)	4.1 (60)	25b	8.6 (117)	6.3 (60)
30a	3.2 (276)	2.1 (177)	30b	6.8 (280)	3.3 (206)
32a	4.2 (224)	1.7 (126)	32b	14.7 (224)	12.3 (196)
34a	5.3 (125)	2.5 (29)	34b	12.5 (116)	9.1 (68)
37a	7.1 (105)	0.5 (25)	37b	23.8 (108)	21.5 (69)
47a	2.1 (264)	1.7 (187)	47b	9.7 (273)	5.9 (206)
49a	8.0 (114)	9.5 (26)	49b	16.5 (120)	8.0 (27)
50a	9.5 (240)	7.7 (125)	50b	3.6 (240)	2.5 (129)
54a	13.5 (304)	10.8 (198)	54b	7.3 (313)	6.9 (254)
56a	6.3 (188)	5.5 (112)	56b	17.8 (186)	12.4 (119)
58a	13.1 (118)	7.1 (21)	58b	5.5 (116)	8.0 (23)
63a	7.2 (259)	5.1 (190)	63b	4.5 (262)	2.1 (169)
66a	4.0 (256)	1.8 (177)	66b	5.4 (260)	5.7 (161)
68a	2.8 (186)	0.8 (112)	68b	7.5 (190)	8.1 (83)
70a	7.1 (75)	*	70b	12.0 (70)	9.9 (11)
73a	10.7 (77)	*	73b	8.8 (73)	2.4 (5)
75a	8.0 (259)	2.3 (195)	75b	13.2 (259)	12.4 (235)
78a	2.2 (191)	0.9 (98)	78b	2.7 (192)	2.2 (109)
80a	8.3 (191)	2.5 (114)	80b	11.4 (192)	8.9 (161)

^{*} Center temperatures did not exceed 45°C

5.5.3 Temperature profile-published data

A total of 12 model runs were conducted to simulate the conditions utilized in the experiments of Murphy et al. (2001a). The center temperature profiles of each model run were compared to temperature predictions from the regression equation developed by Murphy et al. (see Section 3.5.3). Transient comparisons were made between the center

temperatures predicted by the model and the Murphy et al. regression equation for the temperature range between 55 and 80°C. The model and regression transient temperature data were compared at 1 second intervals. Standard error of prediction for transient center temperature was calculated for each model run (Table 5.23).

Table 5.23. Standard error of prediction for transient center temperature of ground chicken breast patties predicted by the model and by the regression equation of Murphy et al. (2001a).

Dry Bulb	Steam by	Airflow	SEP Center
Temperature (°C)	Volume	(m/s)	Temperature (°C)
149	6	1.53	10.3
149	6	2.13	12.4
149	6	2.73	13.5
149	25	1.53	1.4
149	25	2.13	1.6
149	25	2.73	2.4
149	60	1.53	2.6
149	60	2.13	1.6
149	60	2.73	1.8
149	91	1.53	3.7
149	91	2.13	2.8
149	91	2.73	3.2

For the wet bulb temperatures of 70 to 95°C, the SEP ranged from 1.1 to 6.1°C. This was comparable to the SEP of the experimental data collected from the Stein JSO-IV oven. However, for the driest cooking air condition (T_{wb}=40°C), the SEP ranged from 13.3 to 15.7°C. This indicates that the cooking model may not be reliable for extremely dry air conditions. This was probably due to the equation for equilibrium relative humidity. However, the cooking model was designed for high moisture impingement

ovens, so deviations at extremely dry conditions are not critical for the intended use of the model.

5.5.4 Moisture content- experimental data

For each experimental cooking run in the Stein JSO-IV oven, the endpoint moisture content predicted by the model was compared with the experimental values (Section 5.4.2). The deviations between the model and experimental moisture contents ranged from -5.2% to 3.6% wet basis moisture, with an average deviation of -0.04% wet basis (Table 5.24). This indicates that the model moisture predictions are centered around the measured values with little bias. Standard error of prediction for the complete set of final moisture contents was 2.3% moisture w.b.

Table 5.24 – Difference between measured and predicted moisture content for each oven condition. Experiment numbers correspond to the conditions listed in Table 3.1.

Experiment	
Number	predicted moisture content (% wet basis)
1	1.6
6	-4.7
8	-2.5
11	0.8
13	2.4
18	-1.2
21	-0.5
23	1.7
25	3.6
30	-5.2
32	-3.7
34	-0.3
37	0.0
47	0.0
49	-1.2
50	1.5
54	1.2
56	2.0
58	-0.8
63	-1.7
66	-1.3
68	0.6
70	0.0
73	1.8
75	1.2
78	3.5
80	4.0

5.5.5 Cooking yield – experimental data

For each cooking run in the Stein JSO-IV oven, the cooking yield predicted by the model was compared to the experimental value. Standard error of prediction for the complete set of cooking yields was 5.9%. The deviation in predicted yield ranged from –

10.2 to 10.5% with an average deviation of -1.2% (Table 5.25), indicating that the model had a slight bias towards overpredicting yield loss.

Table 5.25 – Difference between measured and predicted cooking yields for each oven condition. Experiment numbers correspond to the conditions in Table 3.1.

Experiment	Difference between predicted and
Number	measured cooking yield (% yield)
1	3.7
6	10.5
8	6.3
11	-3.4
13	-6.5
18	4.1
21	-2.3
23	-2.6
25	-5.7
30	9.3
32	0.9
34	4.1
37	-5.3
47	-3.6
49	-7.6
50	-10.2
54	-6.0
56	8.9
58	-4.7
63	-1.1
66	2.1
68	-0.4
70	2.4
73	-1.4
75	-4.3
78	-10.2
80	-8.4

5.5.6 Cooking yield – published data

Yield predictions of the model were also compared to yield predictions from the literature (Murphy et al., 2001b). The published paper presented a regression model for the yield of ground chicken patties cooked in a Stein model 102 impingement oven.

The model and published yield equation were compared using the same procedures described in Section 5.4.1.1. Like the temperature predictions, the yield data was a much closer fit for wet bulb temperatures between 70 and 95°C. The SEP in that temperature range varied from 1.1 to 6.1% yield. At a wet bulb temperature of 40°C, the SEP ranged from 13.3 to 15.7% yield.

5.6 Lethality model validation

For each run of the computer model, two sets of Salmonella lethality data were generated. The first set of data was the inactivation profile at the center point of the patty, generated using a log-linear equation. For the second data set, total inactivation of Salmonella within the patty was determined. A volume averaging procedure was used to determine total inactivation from inactivation at all of the nodal points. This overall reduction in Salmonella is the value that would be determined experimentally when counting the number of surviving organisms in a whole ground beef patty.

Due to facility constraints, it was not possible to perform inoculated challenge studies for *Salmonella* in the moist-air impingement oven used in this study. However, data exist in the literature for tests that were conducted in a pilot-scale impingement oven (Murphy et al., 2002).

In order to minimally validate the combined cooking/ inactivation model, simulations were conducted to compare values of microbial inactivation predicted by the model with those from the literature. The cooking model was run using the cooking conditions used by Murphy et al. (2002), as described in Section 3.6. The resulting inactivation profiles were plotted on the same graphs as data points reported in the published study (Figures 5.31 and 5.32).

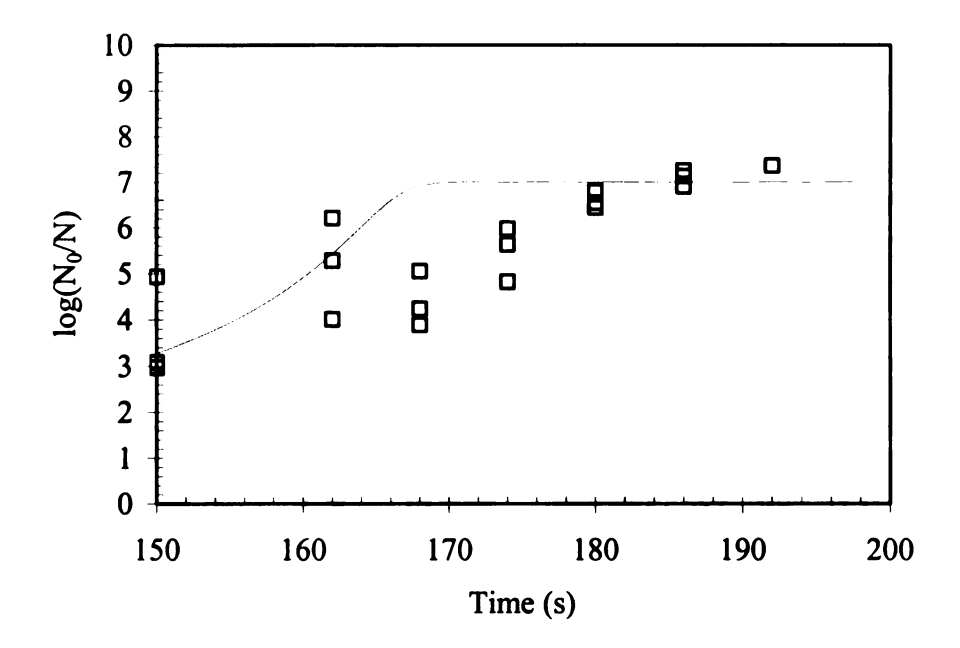


Figure 5.31 - Comparison between model *Salmonella* Senftenberg lethality predictions and data points published by Murphy et al. (2002).

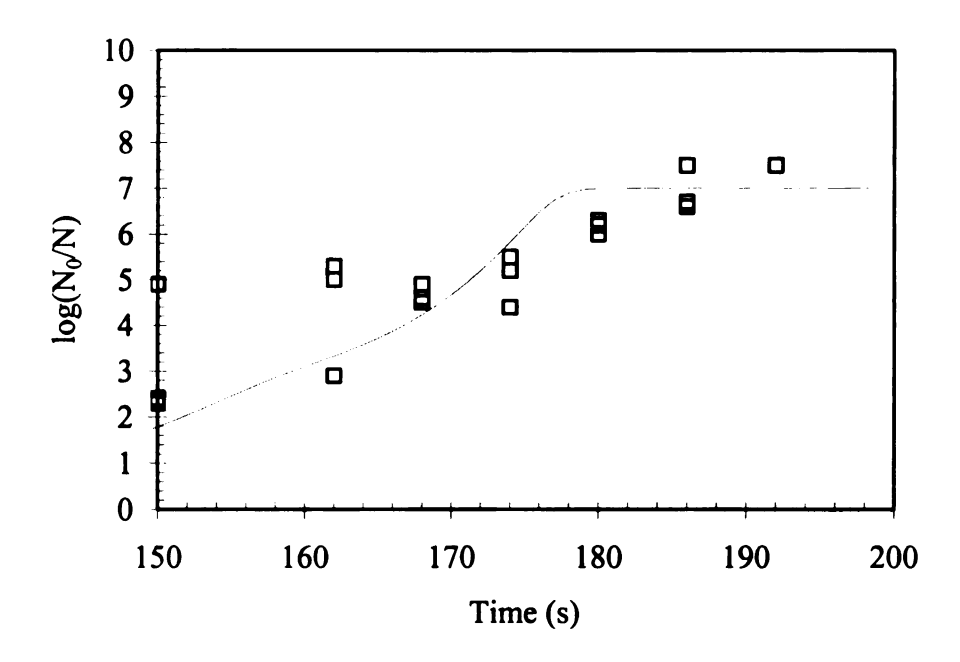


Figure 5.32 – Comparison between model *Listeria innocua* lethality predictions and data points published by Murphy et al. (2002).

The Salmonella Senftenberg inactivation curve predicted by the model was based on D and z-values for Salmonella Senftenberg heated in turkey (Murphy et al., 2003). For heating times of 150 and 160 seconds, the inactivation curve predicted by the model is within the bounds of the experimental data reported by Murphy et al. (2002). However, the model reaches a maximum reduction of 7-log (set by the initial inoculum level) approximately 15 seconds before the experimental data. At times above 180 seconds, both the model and experimental data indicate a reduction of 7-logs. Standard error of prediction for the Salmonella inactivation curve was 1.3 logs (n=21).

A comparison of the *Listeria* inactivation curve predicted by the model and the experimental data of Murphy et al. (2002) indicated a close fit between the experimental

and predicted inactivation's. The model inactivation curve was generated using D and z-values for *Listeria innocua* in ground turkey (Murphy et al., 2003). At a heating time of 150 seconds, the model slightly underestimated the level of lethality, although the model predictions were within 1-log of the lower end of the experimental data range. As heating time increased, the inactivation curve predicted by the model closely estimated the experimental data. Standard error of prediction for the *L. innocua* inactivation curve was 1.1 logs (n=21).

These comparisons only give a rough verification of the ability of the cooking model to predict microbial inactivation. However, the temperature prediction capability of the model has been verified much more extensively. Combining the temperature prediction capabilities of the model with experimentally derived kinetic parameters for microbial estimation (D and z-values) should enable the cooking model to produce an acceptable first estimate of microbial lethality during cooking. In addition, due to the design of the cooking model, the effects of process changes on corresponding changes in microbial lethality are readily visible. This makes the combined cooking and *Salmonella* inactivation model a valuable tool for predicting the effects of processing parameters on microbial safety.

5.7 Illustration of model utility

The utility of a combined cooking and inactivation model is several-fold. Some examples are listed below.

1. A processor uses a moist-air impingement oven to produce ready-to-eat ground beef patties. The oven is currently operated at a dry bulb temperature of 177°C, a steam content of 75% by volume, and an air velocity of 18 m/s. The dwell time in the oven is 3 minutes. The processor wishes to increase the throughput of the oven by adjusting the moisture content of the cooking air from 75 to 85% moisture by volume. The processor wants to know what the new oven dwell time will be to reach the same patty center temperature that was achieved by the previous process.

In this case, determining the new dwell time in the oven could be determined by running the cooking model under the new set of process conditions. Running the model under the original cooking conditions, the processor finds that the original final center temperature was 78.7°C. The processor then runs the model under the new conditions and sees that the dwell time that will achieve 78.7°C is 170 seconds, a ten second improvement over the original conditions, which would translate into a 5.8% increase in throughput.

2. In the situation above, the processor is concerned that the faster cooking time will not be adequate to achieve the desired level of microbial inactivation.

In this case, the processor can use the lethality prediction function of the computer model. Running the cooking model, the processor sees that the cooking process greatly exceeds the required lethality in both cases. However, based on a 6.5-log target

reduction, the higher steam content cooking air achieves the desired lethality 14 seconds earlier than the original condition.

3. The processor is not convinced that the current operating conditions are making the most efficient use of the oven system. Experience indicates that increasing the steam content of the oven will decrease cooking time. However, quantitative data are not available. The processor would like to develop a set of experiments to optimize the oven settings.

Taking the oven system offline to perform optimization experiments is time consuming and expensive. In addition to the time and manpower spent conducting the experiments, the oven must be taken out of production for the time period of the experiment. To determine the effects of changing process conditions, the processor runs simulations using the cooking model. Examples 1 and 2 show how the model can be used to illustrate changes in process conditions. By running the model under many more sets of conditions, the processor can determine the ideal settings for the desired cooking results.

4. Product output from oven systems sometimes falls behind due to problems with equipment and backups during previous unit operations. Operators might try to catch up with production quotas by increasing the oven belt speed. The manager is concerned that the desired level of microbial lethality is not being achieved due

to increases in belt speed. It is difficult for the manager to illustrate to the operators that their actions may result in food that is potentially unsafe.

This instance illustrates the benefit of the graphical temperature and lethality outputs of the model. The graphical outputs can be used to illustrate the effects of process changes to personnel with no knowledge of heat transfer or microbial inactivation kinetics. If the oven conditions utilized in Example 2 were in use, the oven would achieve a 6.5-log reduction in *Salmonella* in 129 seconds. Decreasing the dwell time by ten seconds (119 seconds cooking time) would decrease the predicted lethality to only 0.8-log. In this case, a very small adjustment in cooking time would result in a product that is potentially unsafe.

6 CONCLUSIONS

The main conclusions of this study were:

- 1. Fat content had a significant effect on the cooking time for ground turkey, ground beef, and ground pork. Differences in the time required to reach 85°C between different fat contents of each meat species were 171, 217, and 102 seconds for ground turkey, ground beef, and ground pork patties, respectively. Higher fat samples of ground beef and ground pork cooked faster than the lower fat samples. The opposite was true for ground turkey. Fat content significantly affected the yields of ground turkey with initial fat contents of 1.4% and 8.6%, and ground pork of initial fat contents of 15.7% and 41.9% fat. Differences in yield between fat contents of ground turkey and ground pork were 18 and 17%, respectively, when cooked to 85°C. No significant differences in yield were measured between ground beef with initial fat contents of 7.2 and 17.5%. Fat transfer contributed up to 6% of the yield loss of ground beef and up to 28% of the yield loss of ground pork patties.
- 2. Fat holding capacity of ground beef was modeled as a function of initial fat content and heating time using multiple linear regression. Holding time did not significantly affect fat holding capacity. The regression equation for fat holding capacity had a coefficient of variation of 0.81 and a standard error of prediction of 0.068 g fat/g dry matter. This equation was an important step towards developing

a model for heat and mass transfer of ground beef products that includes the effects of fat transport.

- 3. The effects of oven temperature, steam content, and airflow on heating time, yield, fat loss, and volume change of ground beef patties cooked in an industrial moist-air impingement oven were quantified. Multiple linear regression showed that oven steam content had the largest effect on both heating rate and cooking yield. Neither oven temperature nor air velocity had a significant effect on patty center temperature. Oven temperature, steam content, and cooking time all had significant affects on cooking yield. Fat loss increased roughly linearly, and patty diameter decreased roughly linearly with patty temperature. Patty thickness remained fairly constant during cooking.
- 4. A finite-element method-based cooking and *Salmonella* inactivation model was developed. The model was an improvement over previously published models for the following reasons:
 - a) The heat and moisture transport portions of the model were based completely on heat and mass transfer principles. Empirical correlations were only used for thermal property relationships. This allowed for maximum flexibility of the model over different cooking conditions.
 - b) Fat transport was incorporated in the model. The incorporation of fat transport created a model that could predict yield losses for products containing a wide range of fat levels.

- c) The model incorporated the transient effects of heat and mass transfer related to moist-air impingement, including the effects of condensation as a surface mass transfer process (rather than as an "effective heat transfer" effect).
- d) The model was validated with experimental data from an industrial moistair impingement oven.
- 5. The cooking model was validated using data collected from an industrial moist-air impingement oven. The transient standard error of prediction for temperature was 8°C. The model more accurately predicted temperatures above 45°C. At temperatures above 45°C, the SEP was reduced to 5.7°C. Predictions of moisture content had errors ranging from 0 to 5.2% wet basis. Predictions of cooking yield had errors ranging from 0.1 to 15.4% with an average deviation of 5.9%. Comparisons with temperature and yield data compiled by other researchers were also favorable. Standard error of prediction for center temperature of chicken patties at cooking air wet bulb temperatures between 70 and 95°C ranged from 1.4 to 3.7°C. Higher errors occurred at an air wet bulb temperature of 40°C. Standard errors of prediction for yield ranged from 1.1 to 15.7%.
- 6. The microbial lethality prediction of the model was compared to published data.

 Standard error of prediction for inactivation of *Salmonella* Senftenberg in ground beef patties was 1.3 logs (CFU/g). Standard error of prediction for *Listeria innocua* was 1.1 logs (CFU/g).

7 FUTURE WORK

There are a number of studies that should be conducted in order to further develop our understanding of the dynamics of meat and poultry cooking. The results of these studies could be utilized for the development of more precise and more robust cooking models. In addition, further understanding of the mechanics of cooking could improve our general understanding of the effects of processing on meat and poultry quality attributes. Recommendations for further studies include:

- 1. Experiments designed to determine the effects of protein and fat chemistry on fat and moisture transport should be conducted. Specifically, the effects of fat composition on transport properties should be investigated. Models for fat viscosity as functions of lipid composition and temperature could contribute greatly to understanding of fat transport mechanisms. Understanding of these mechanisms is needed to maximize the effectiveness of cooking models for a wide range of product compositions.
- 2. An analysis of the changes in meat microstructure during cooking should be performed. Such studies should include analysis of the changes in porosity during cooking as well as the relationships between meat microstructure and volume change. The dynamics of volume change during cooking should be investigated.

- 3. Studies should be designed to determine the driving forces for fat transport and moisture transport via drip loss. These phenomena are generally attributed to changes in water and fat holding capacities, but there is little understanding of the physical mechanisms behind such changes. Further knowledge of these driving forces is needed for the development of mechanistic models for water and fat holding capacities and transport.
- 4. Extensive validation of microbial inactivation kinetics during impingement cooking of meat and poultry products should be performed. This should be done utilizing inoculated challenge studies with an actual moist-air impingement oven.
- 5. Automatic mesh generation subroutines should be added to the cooking model.

 This would allow for much easier modeling of cooking for various product geometries. It would also allow for the cooking model to account for volume change during cooking.
- 6. The model should be used for optimization of impingment cooking processes, in terms of safety, cooking yield, and oven throughput.
- 7. The model should be adapted in the future to simulate cooking of whole-muscle products.

8 APPENDICES

8.1 Model and experimental temperature versus time curves for moist-air impingement cooking of ground beef patties.

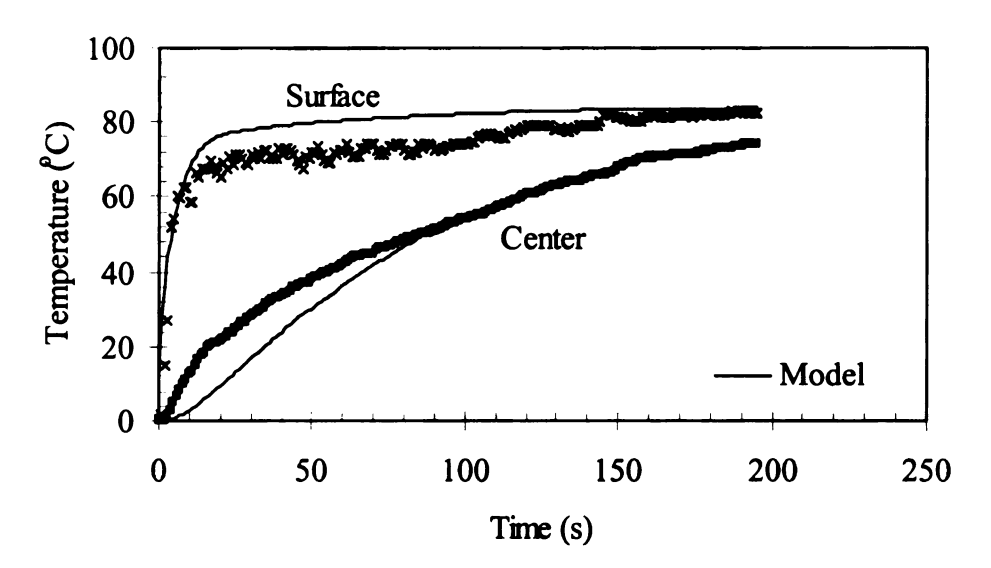


Figure 8.1 – Oven temperature: 121°C, oven steam content: 50% by volume, oven airflow: 11.4 m/s (Experiment 1a).

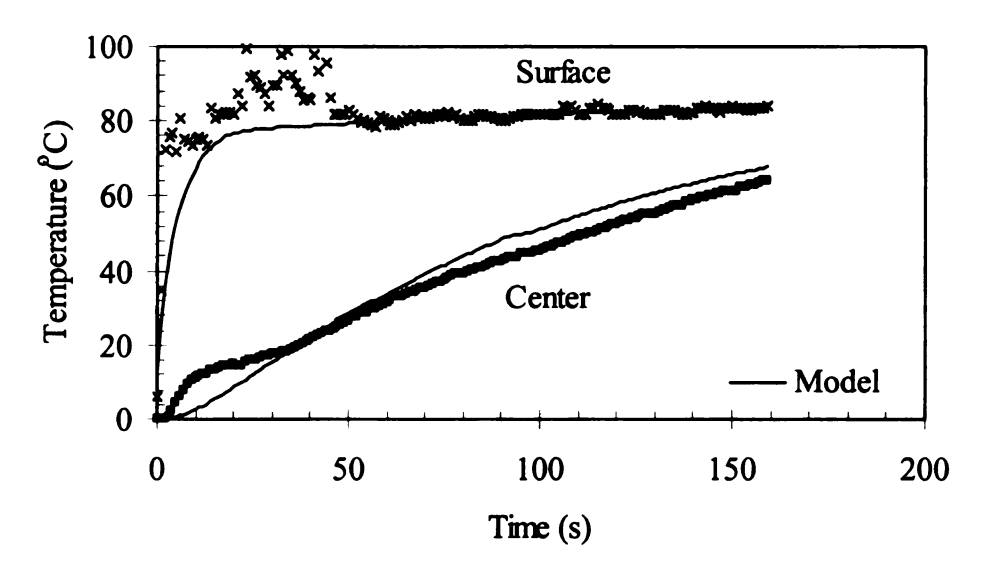


Figure 8.2 – Oven temperature: 121°C, oven steam content: 50% by volume, oven airflow: 11.4 m/s (Experiment 1b).

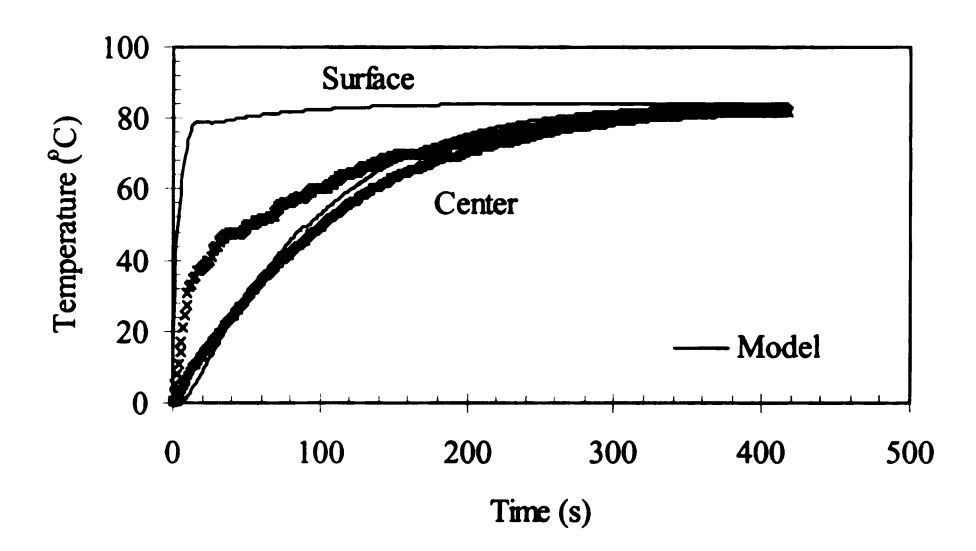


Figure 8.3 – Oven temperature: 121°C, oven steam content: 50% by volume, oven airflow: 16.8 m/s (Experiment 6a).

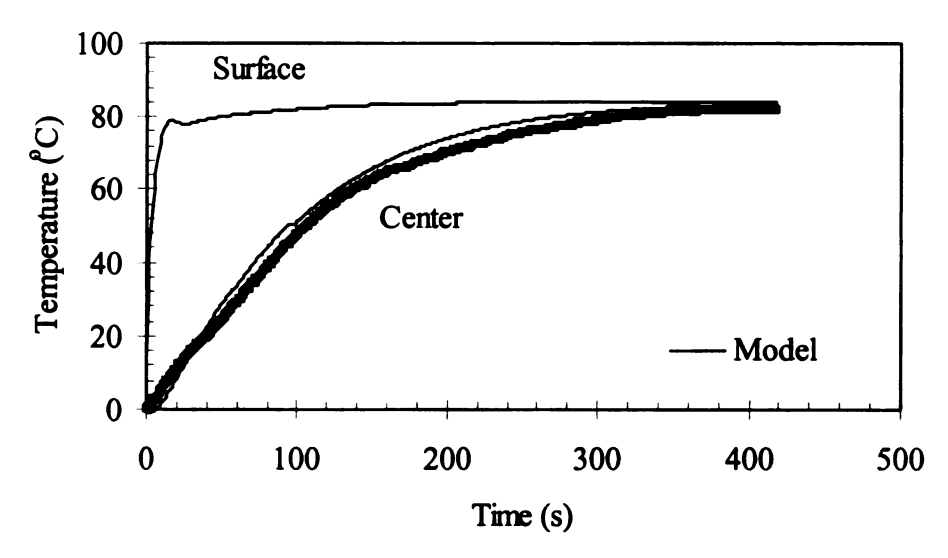


Figure 8.4 - Oven temperature: 121°C, oven steam content: 50% by volume, oven airflow: 16.8 m/s (Experiment 6b).

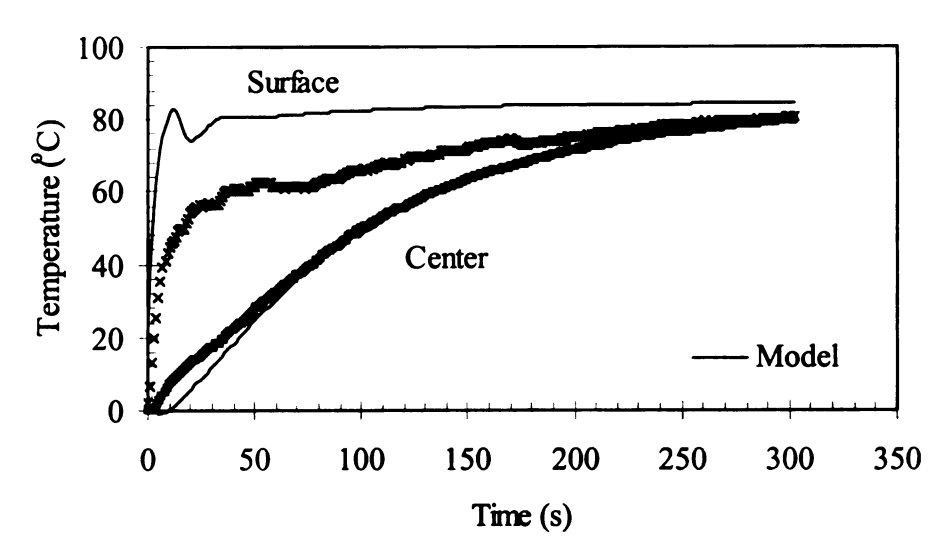


Figure 8.5 – Oven temperature: 121°C, oven steam content: 50% by volume, oven airflow: 21.8 m/s (Experiment 8a).

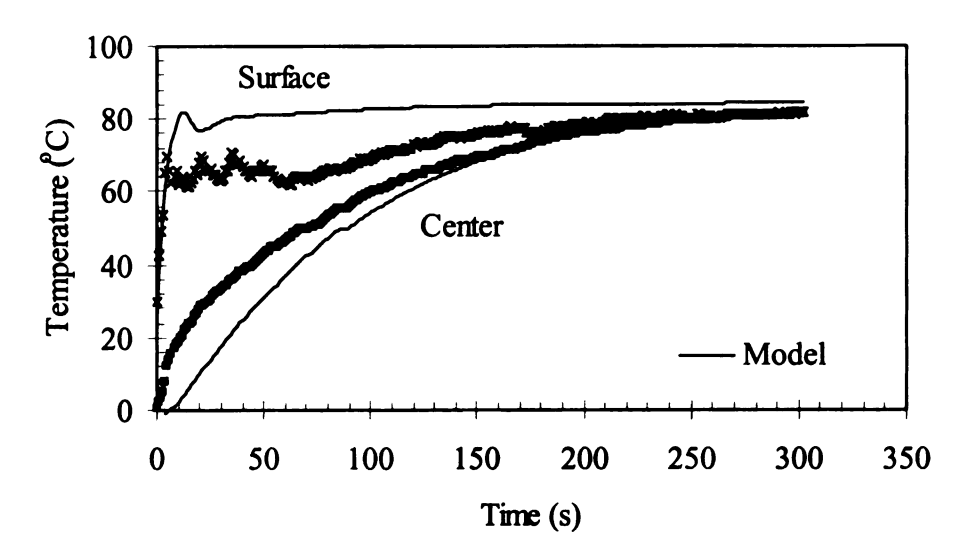


Figure 8.6 – Oven temperature: 121°C, oven steam content: 50% by volume, oven airflow: 21.8 m/s (Experiment 8b).

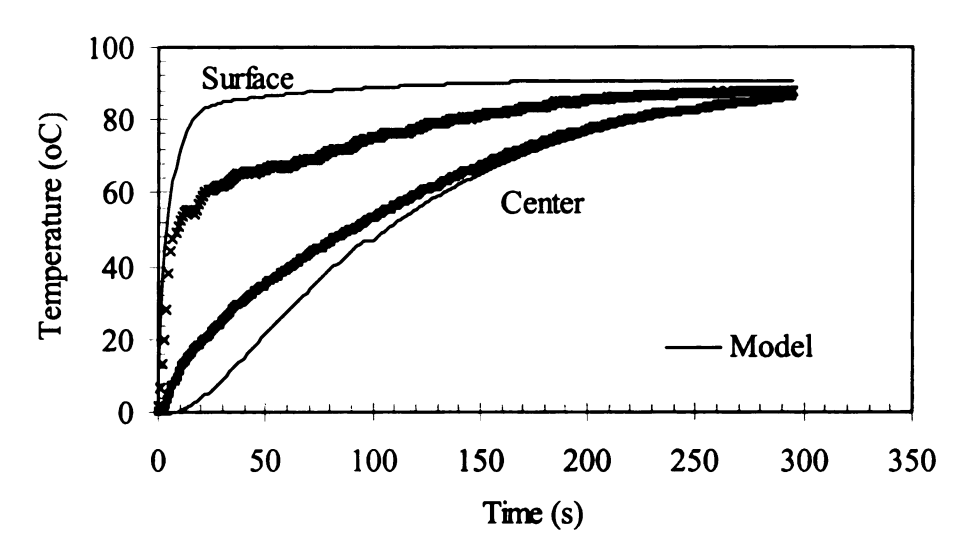


Figure 8.7 – Oven temperature: 121°C, oven steam content: 70% by volume, oven airflow: 11.4 m/s (Experiment 11a).

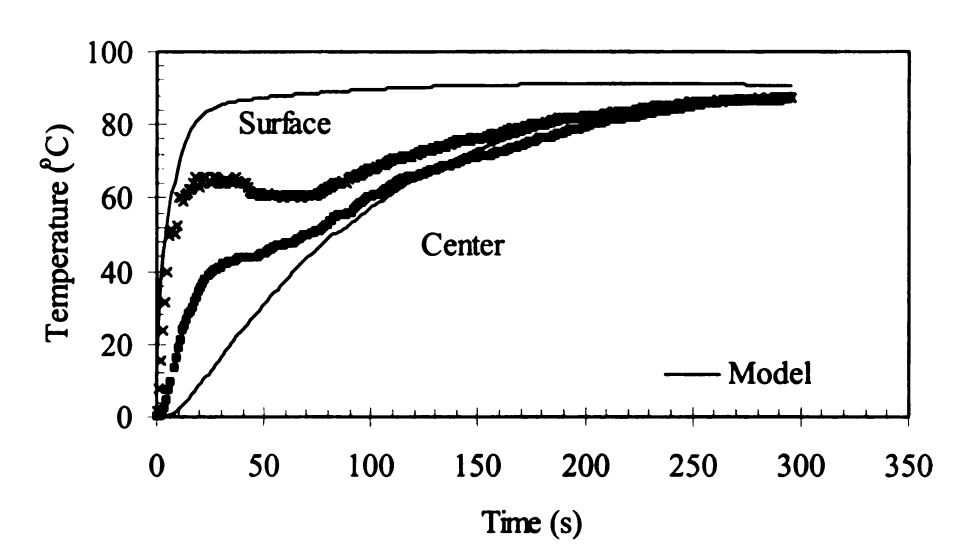


Figure 8.8 – Oven temperature: 121°C, oven steam content: 70% by volume, oven airflow: 11.4 m/s (Experiment 11b).

		ı
and the state of t		

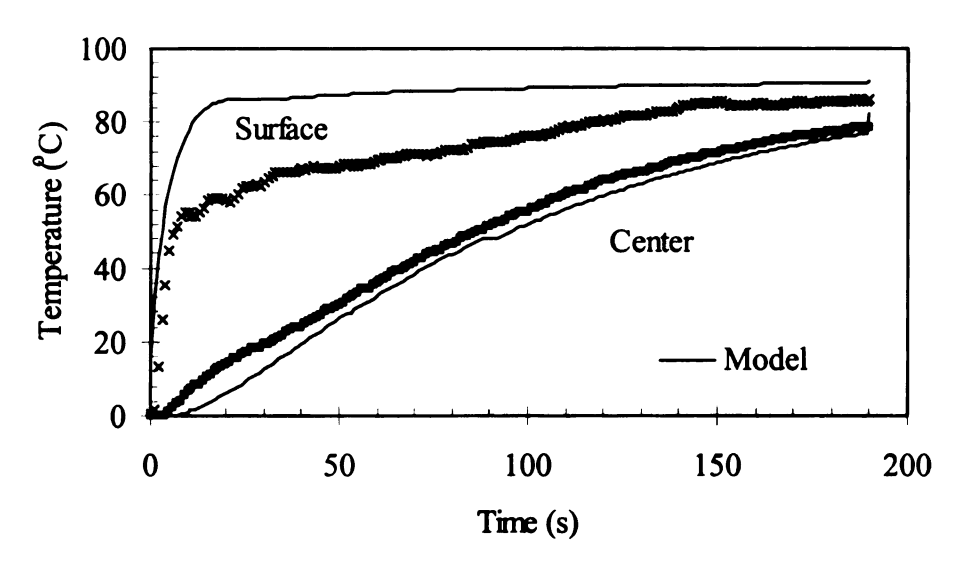


Figure 8.9 – Oven temperature: 121°C, oven steam content 70% by volume, oven airflow: 16.8 m/s (Experiment 13a).

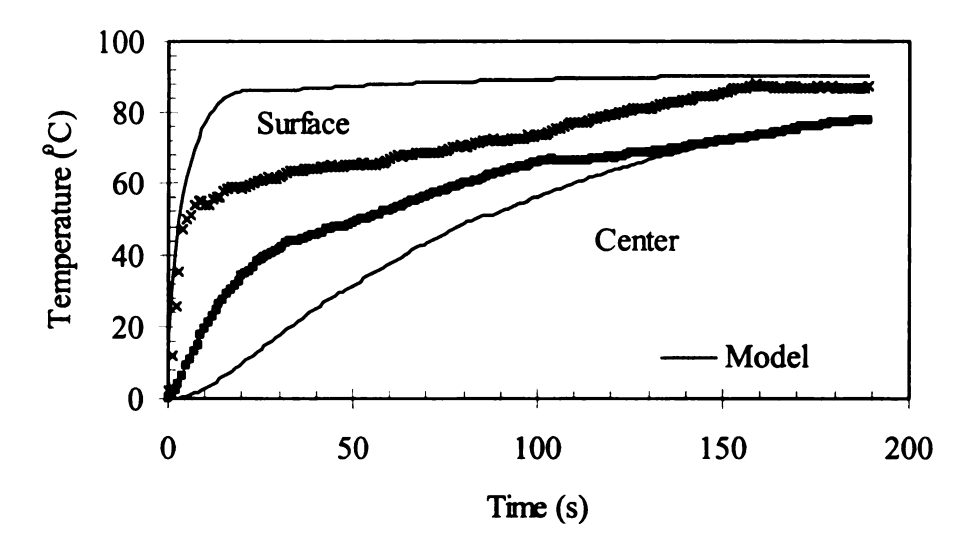


Figure 8.10 – Oven temperature: 121°C, oven steam content 70% by volume, oven airflow: 16.8 m/s (Experiment 13b).

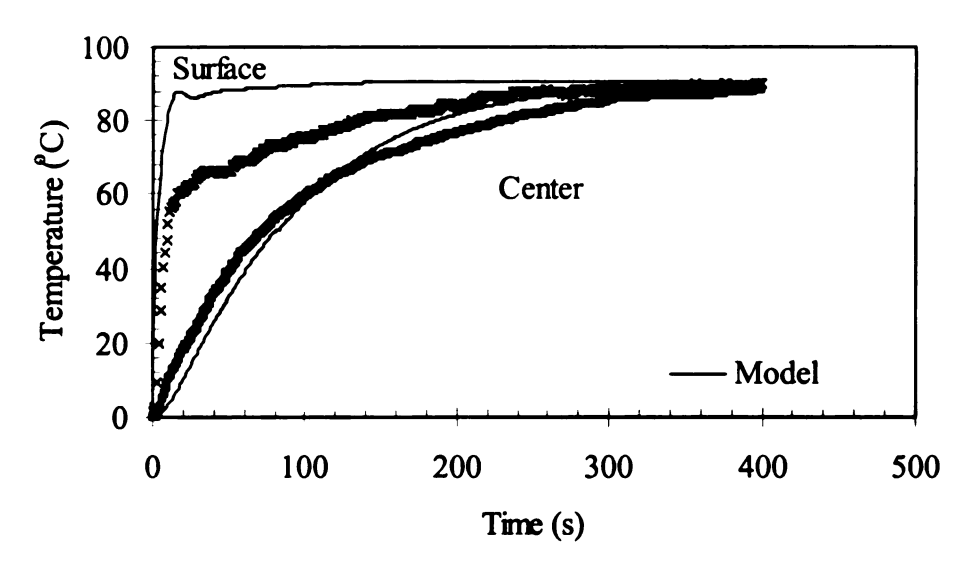


Figure 8.11 – Oven temperature: 121°C, oven steam content: 70% steam volume, oven airflow: 21.8 m/s (Experiment 18a).

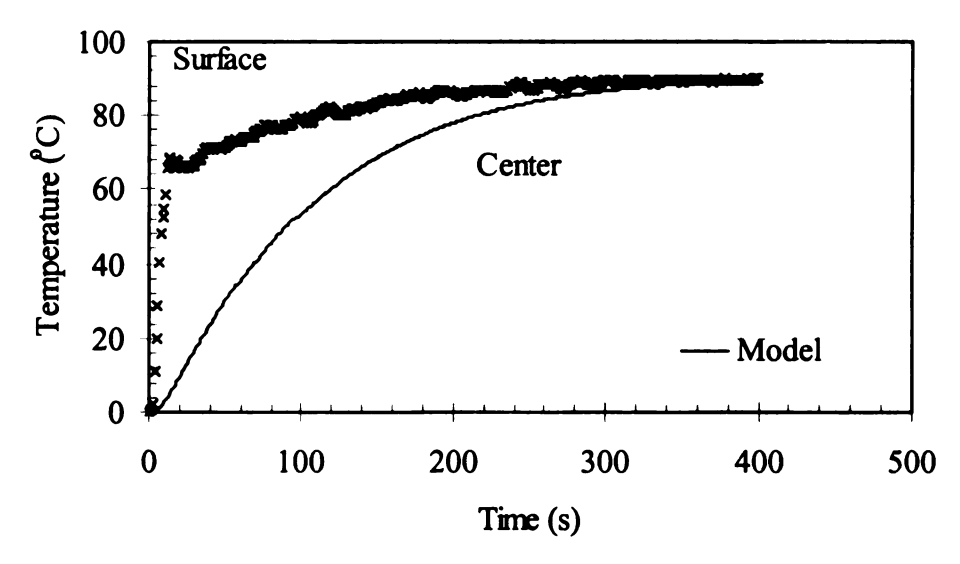


Figure 8.12 – Oven temperature: 121°C, oven steam content: 70% steam volume, oven airflow: 21.8 m/s (Experiment 18b).

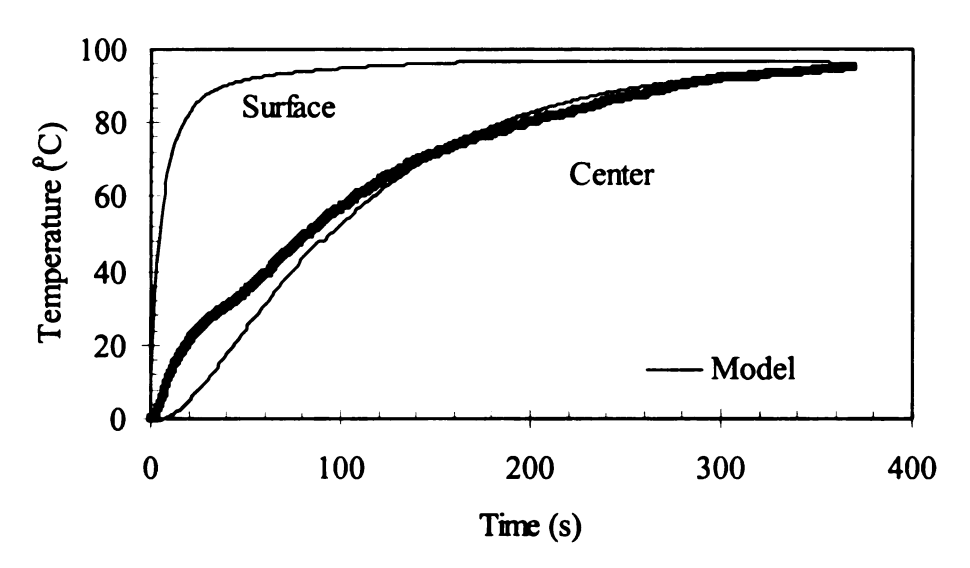


Figure 8.13 – Oven temperature: 121°C, oven steam content: 88% by volume, oven airflow: 11.4 m/s (Experiment 21a).

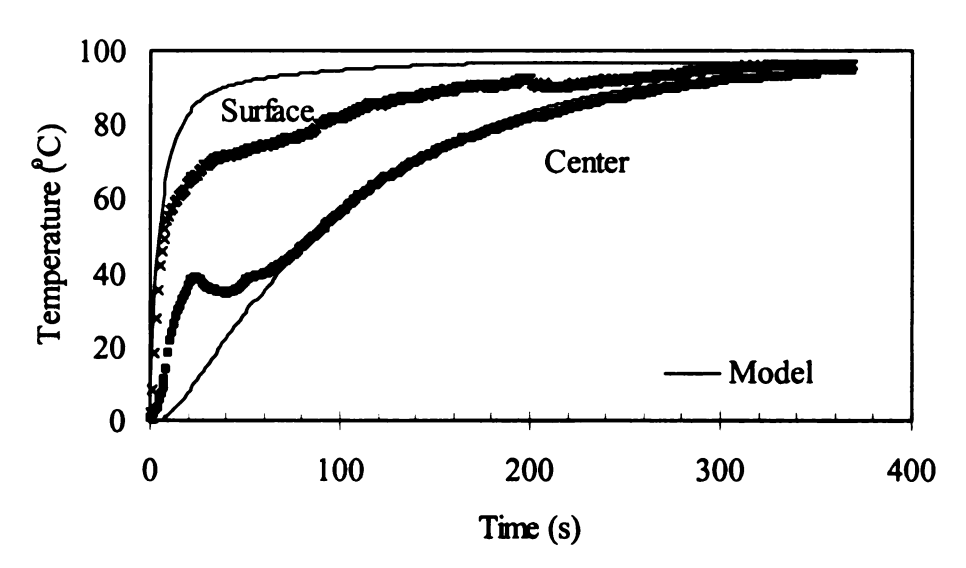


Figure 8.14 – Oven temperature: 121°C, oven steam content: 88% by volume, oven airflow: 11.4 m/s (Experiment 21b).

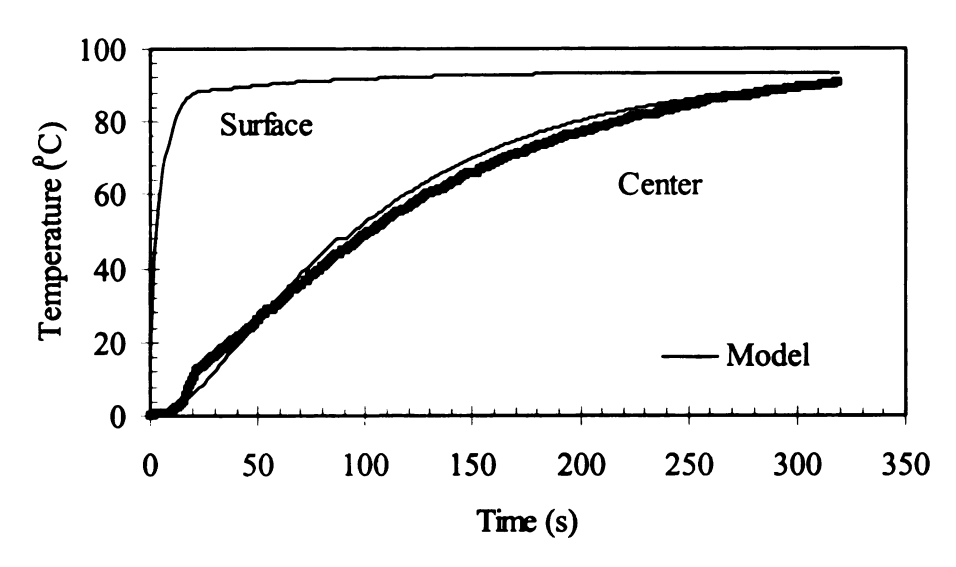


Figure 8.15 – Oven temperature: 121°C, oven steam content: 78% by volume, oven airflow: 16.8 m/s (Experiment 23a).

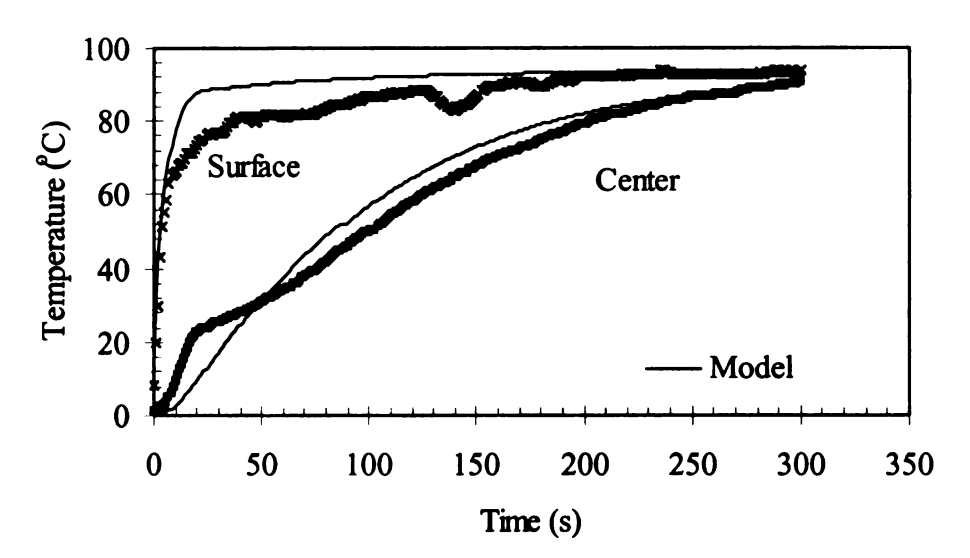


Figure 8.16 – Oven temperature: 121°C, oven steam content: 78% by volume, oven airflow: 16.8 m/s (Experiment 23b).

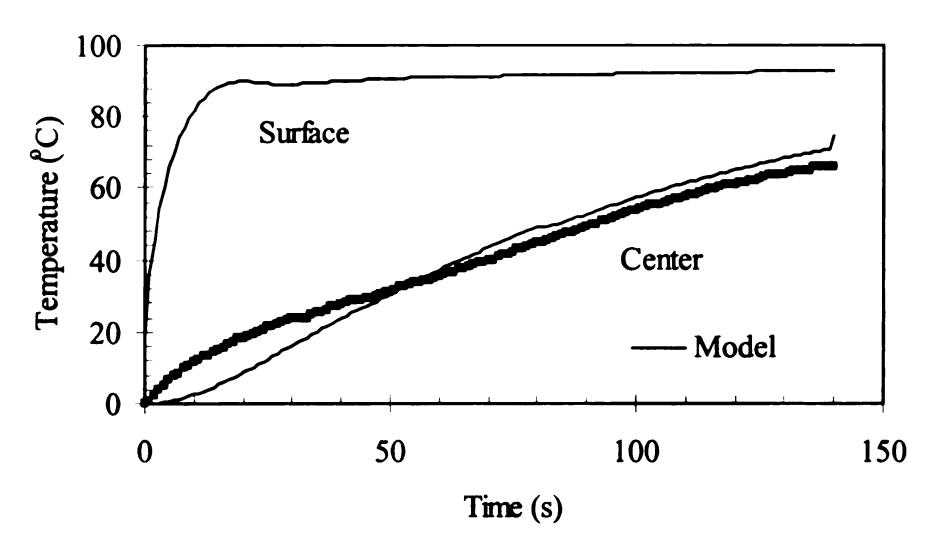


Figure 8.17 - Oven temperature: 121°C, oven steam content: 78% by volume, oven airflow: 21.8 m/s (Experiment 25a).

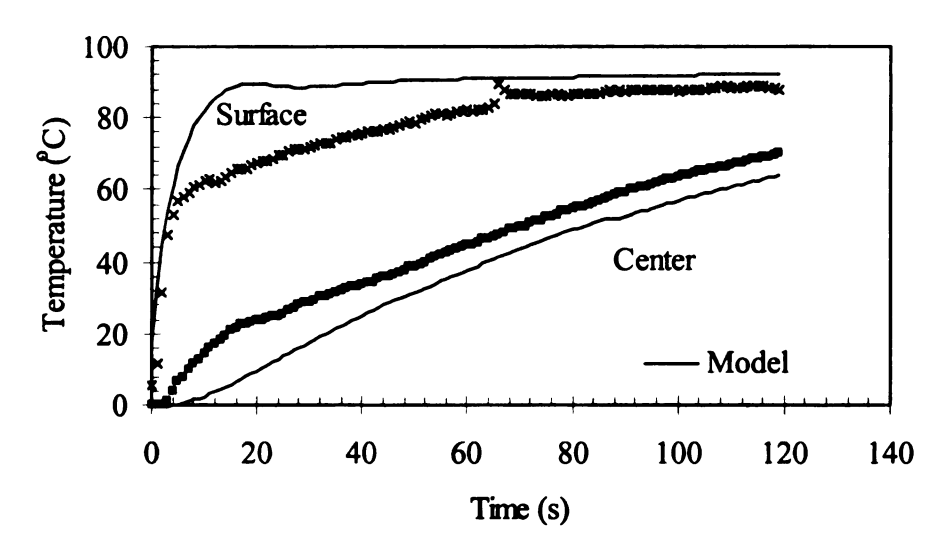


Figure 8.18 - Oven temperature: 121°C, oven steam content:78% by volume, oven airflow: 21.8 m/s (Experiment 25b).

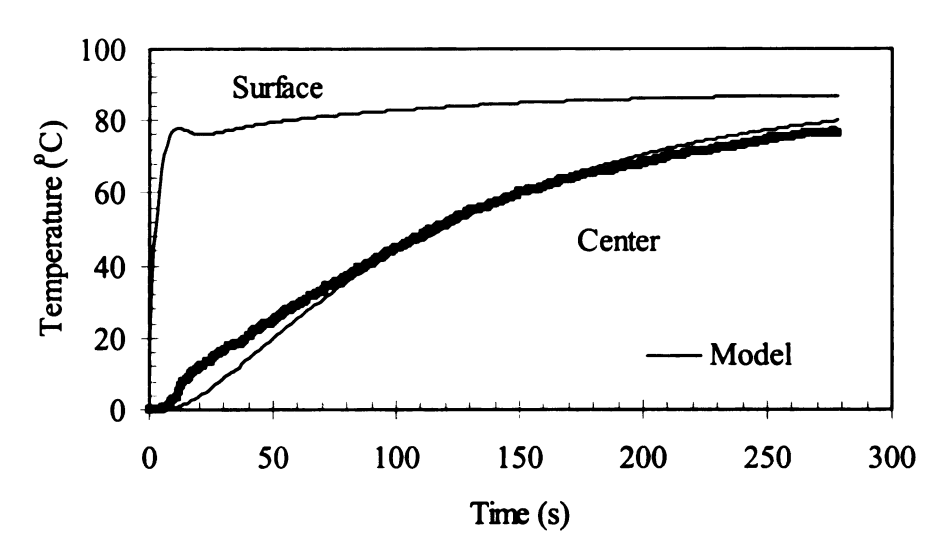


Figure 8.19 – Oven temperature: 177°C, oven steam content: 50% by volume, oven airflow: 11.43 m/s (Experiment 30a).

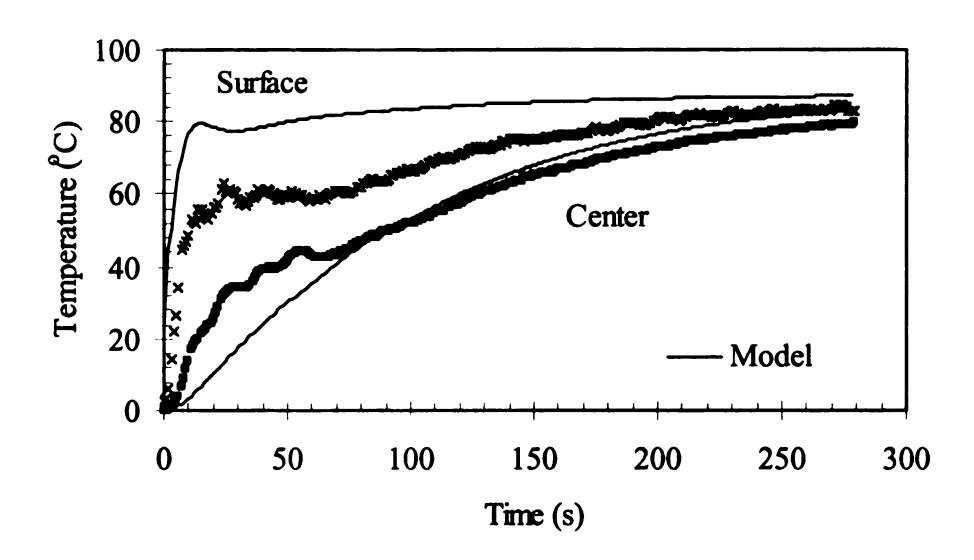


Figure 8.20 – Oven temperature: 177°C, oven steam content: 50% by volume, oven airflow: 11.43 m/s (Experimen 30b).

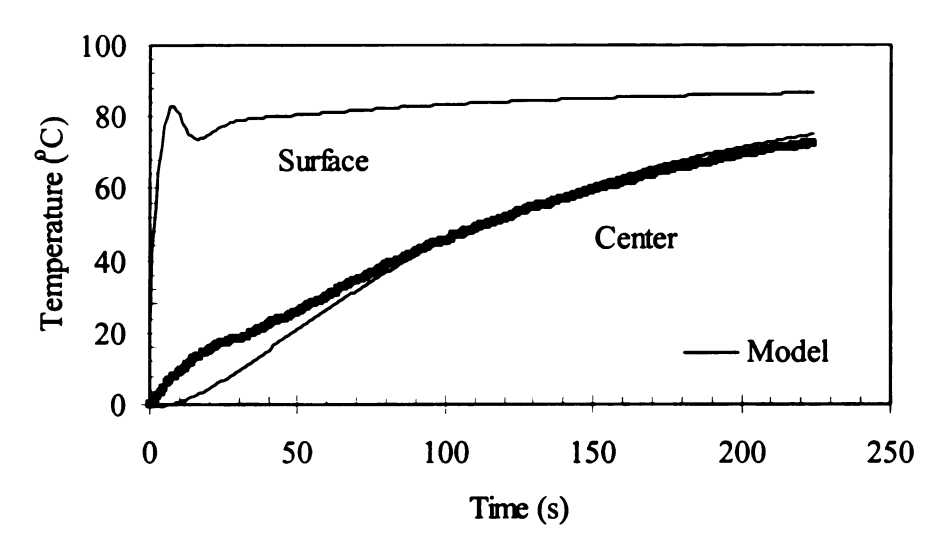


Figure 8.21 - Oven temperature: 177°C, oven steam content: 50% by volume, oven airflow: 16.8 m/s (Experiment 32a).

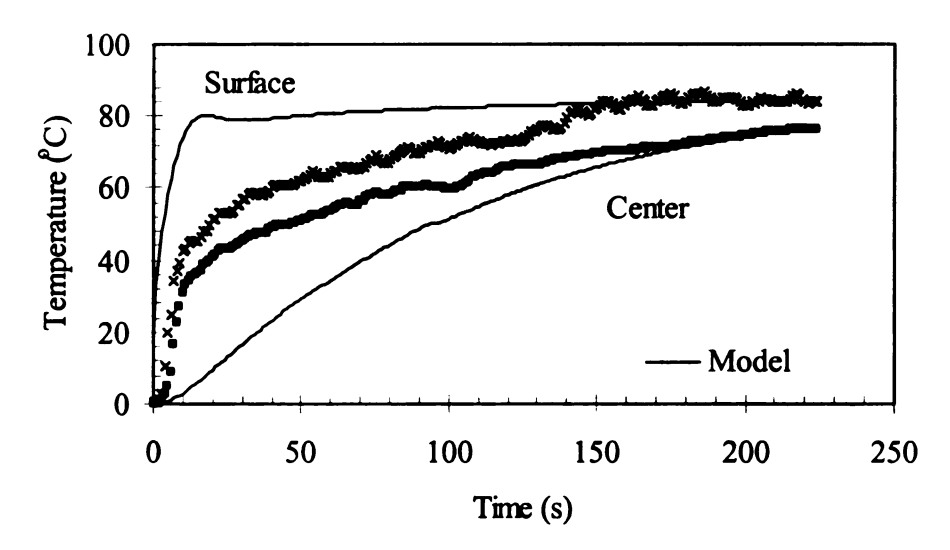


Figure 8.22 - Oven temperature: 177°C, oven steam content: 50% by volume, oven airflow: 16.8 m/s (Experiment 32b).

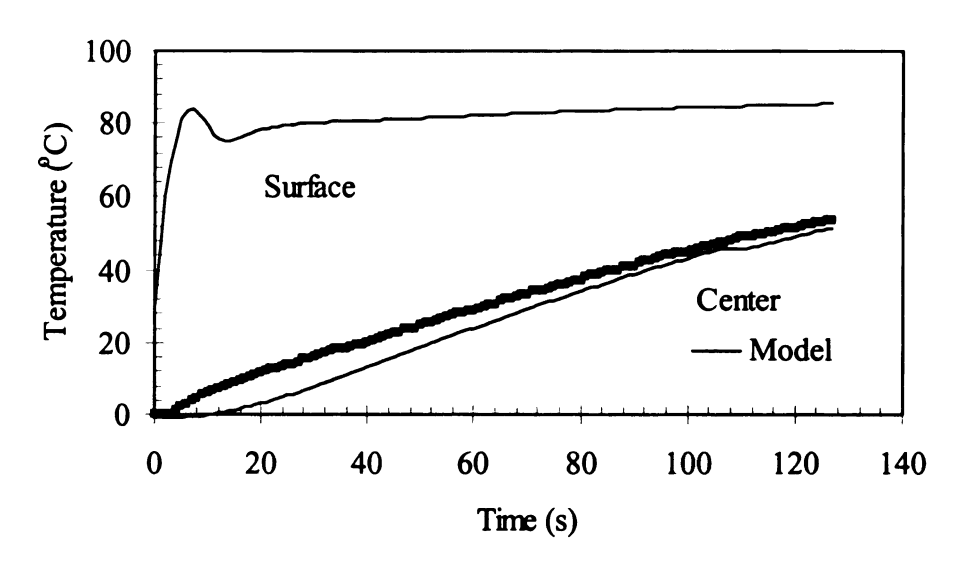


Figure 8.23 - Oven temperature: 177°C, oven steam content: 50% by volume, oven airflow: 21.8 m/s (Experiment 34a).

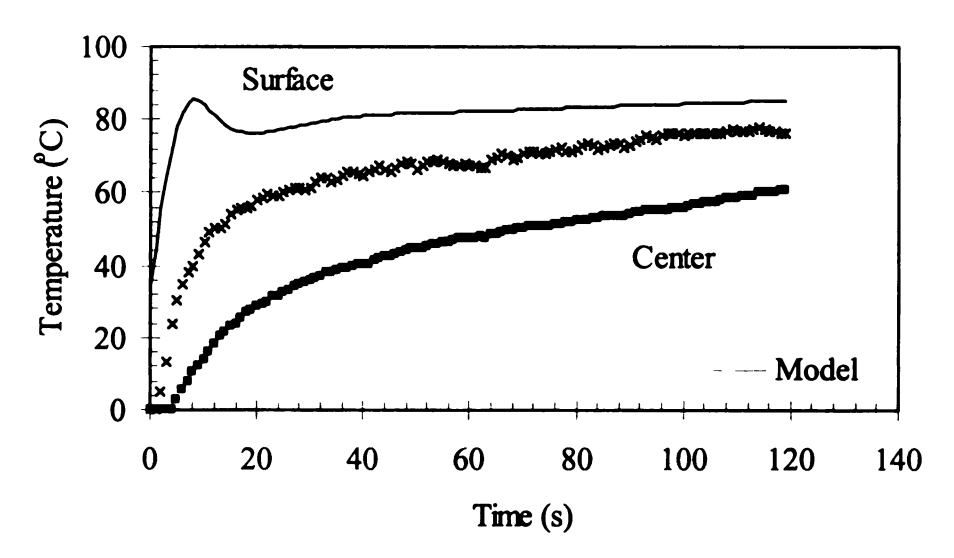


Figure 8.24 - Oven temperature: 177°C, oven steam content: 50% by volume, oven airflow: 21.8 m/s (Experiment 34b).

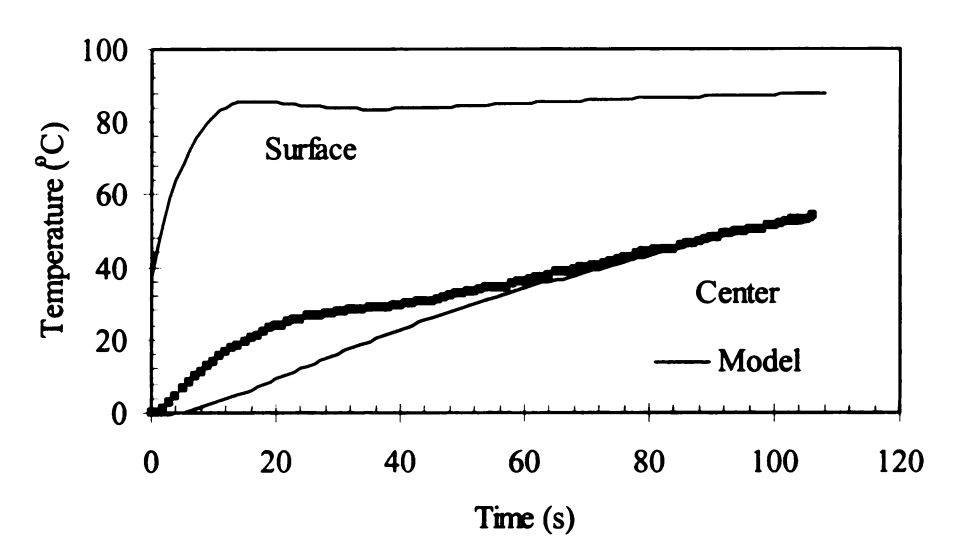


Figure 8.25 – Oven temperature: 177°C, oven steam content: 70% by volume, oven airflow: 11.4 m/s (Experiment 37a).

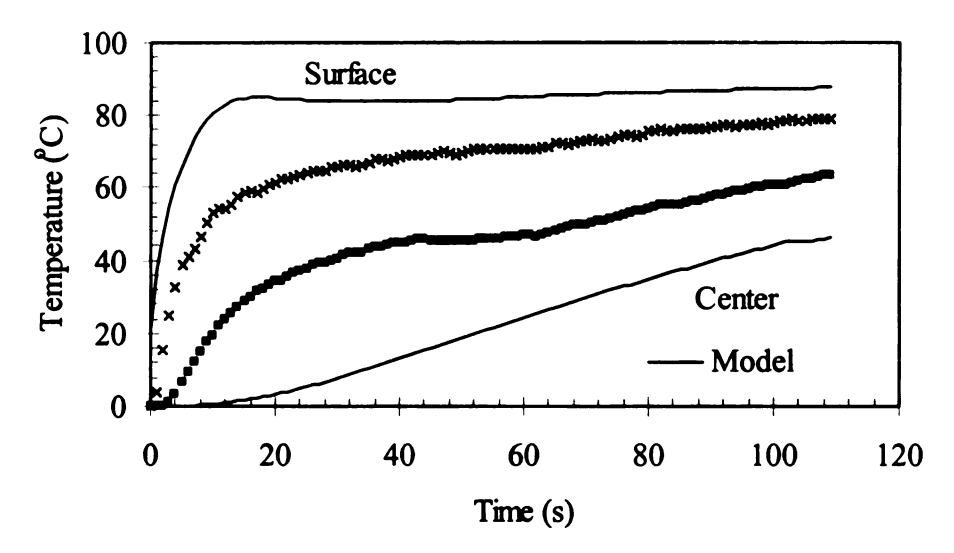


Figure 8.26 – Oven temperature: 177°C, oven steam content: 70% by volume, oven airflow: 11.4 m/s (Experiment 37b).

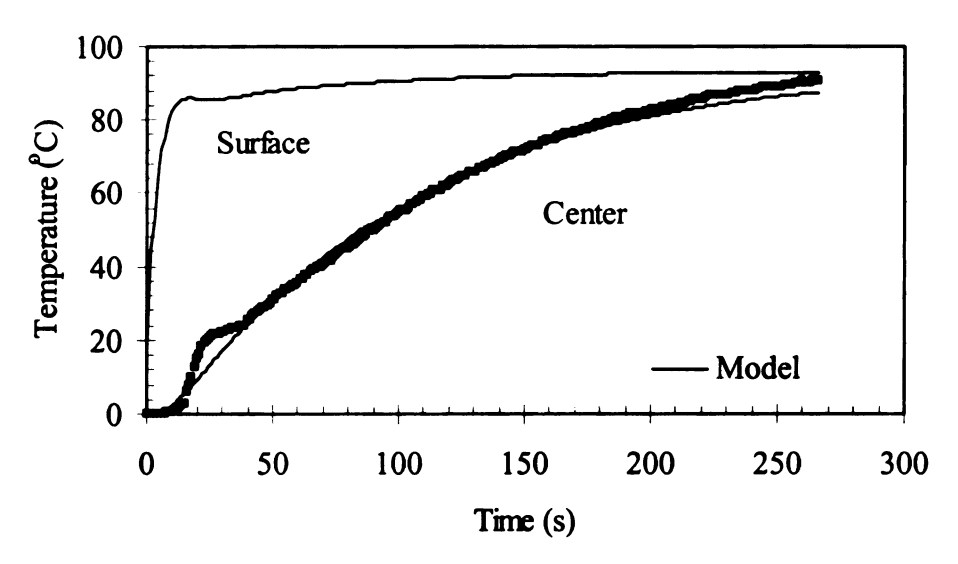


Figure 8.27 - Oven temperature: 177°C, oven moisture content: 83% by volume, oven airflow: 11.4 m/s (Experiment 47a).

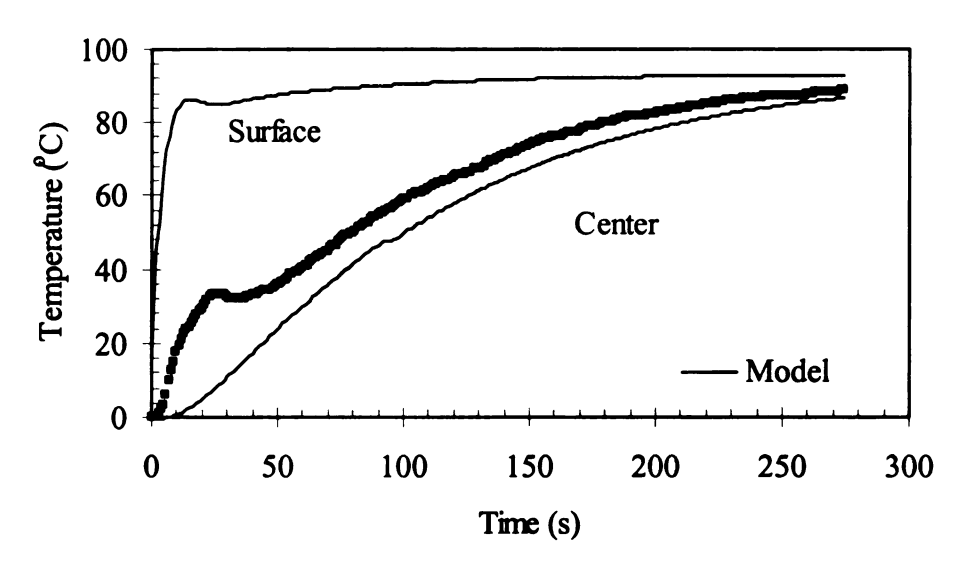


Figure 8.28 - Oven temperature: 177°C, oven moisture content: 83% by volume, oven airflow: 11.4 m/s (Experiment 47b).

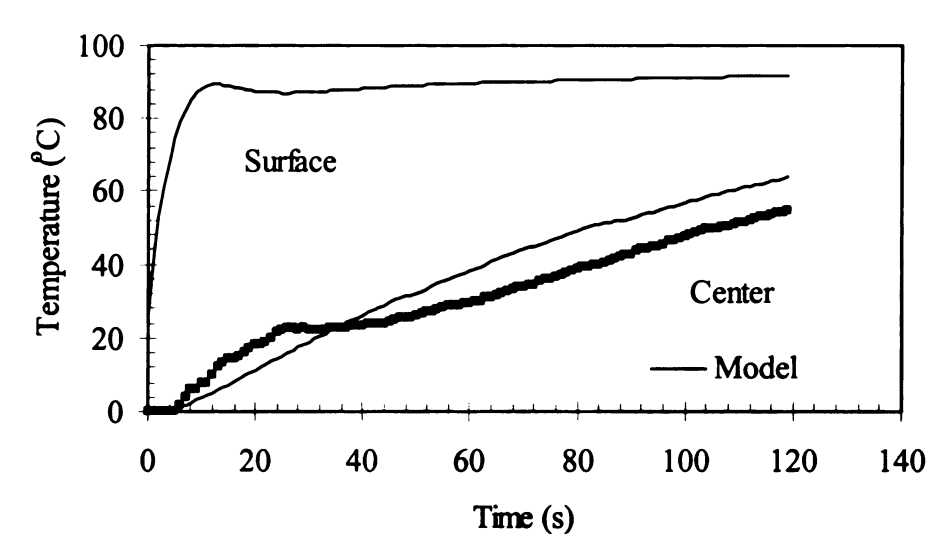


Figure 8.29 - Oven temperature: 177°C, oven steam content: 84% by volume, oven airflow: 16.8 m/s (Experiment 49a).

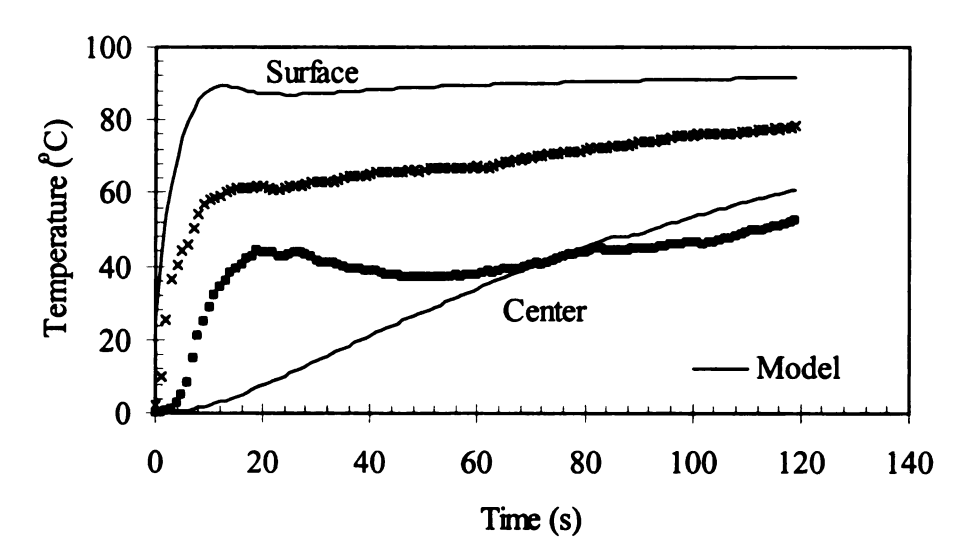


Figure 8.30 - Oven temperature: 177°C, oven steam content: 84% by volume, oven airflow: 16.8 m/s (Experiment 49b).

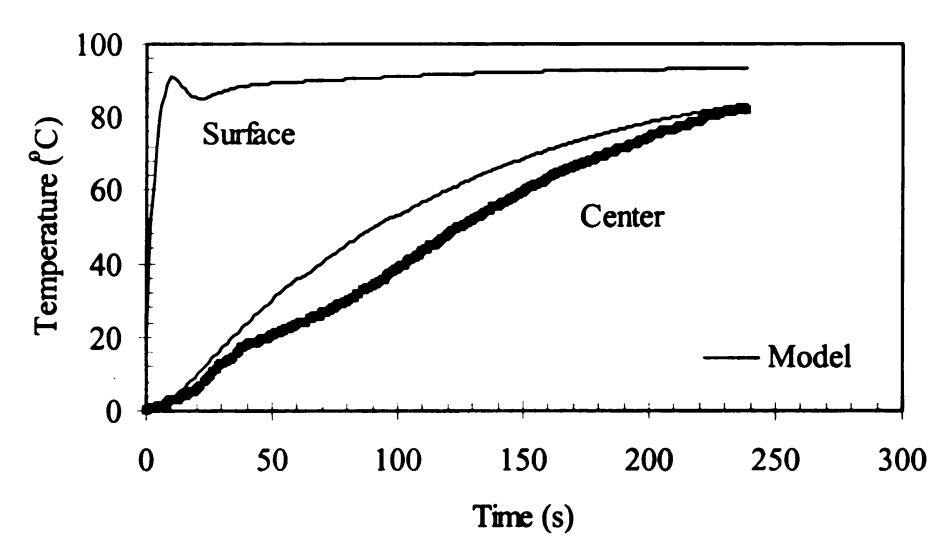


Figure 8.31 - Oven temperature: 177°C, oven steam content: 86% by volume, oven airflow: 16.8 m/s (Experiment 50a).

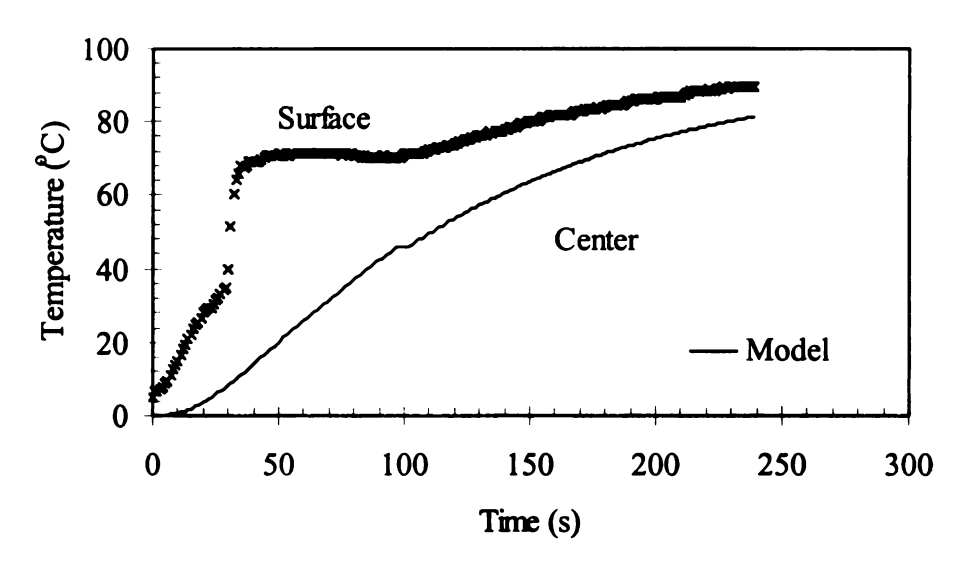


Figure 8.32 - Oven temperature: 177°C, oven steam content: 86% by volume, oven airflow: 16.8 m/s (Experiment 50b).

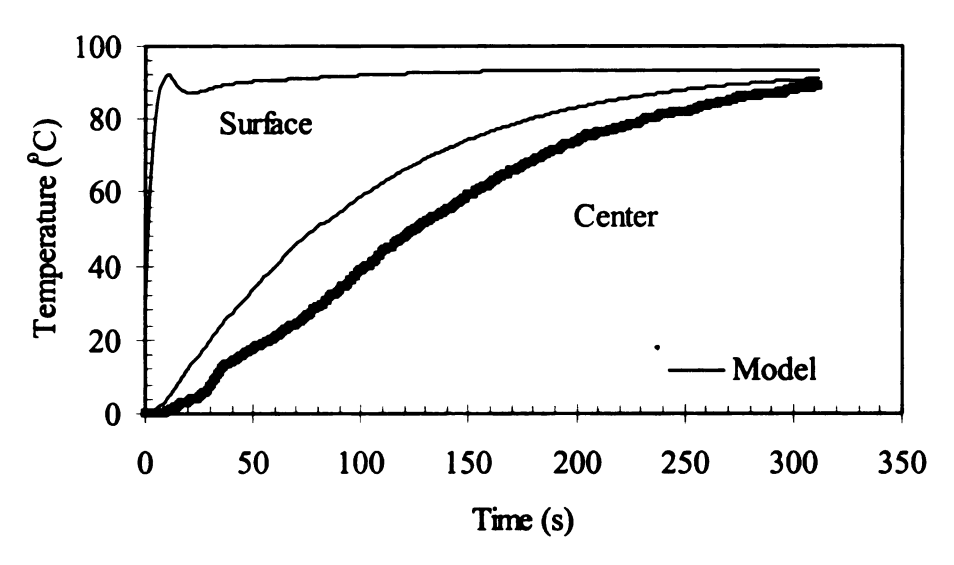


Figure 8.33 - Oven temperature: 177°C, oven steam content: 86% by volume, oven airflow: 21.8 m/s (Experiment 54a).

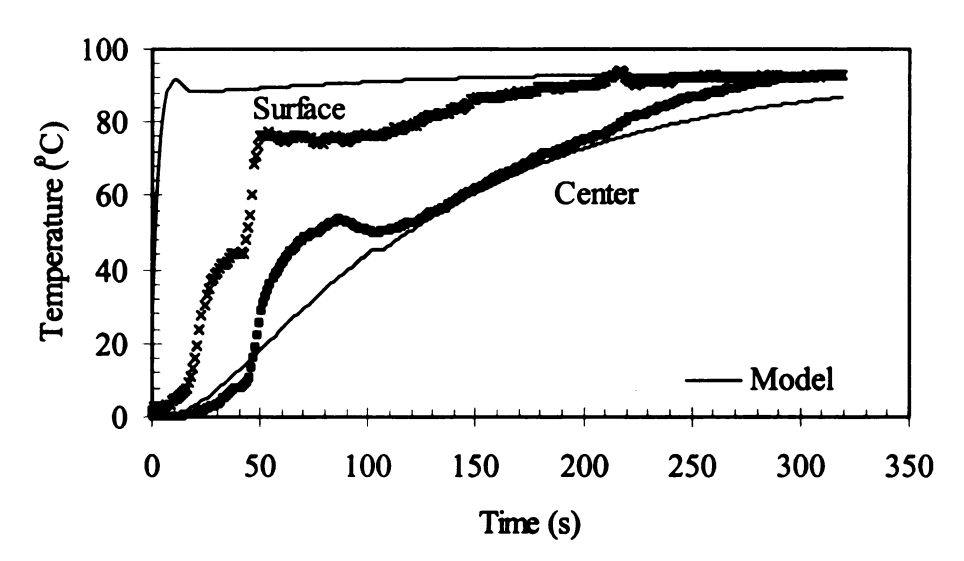


Figure 8.34 - Oven temperature: 177°C, oven steam content: 86% by volume, oven airflow: 21.8 m/s (Experiment 54b).

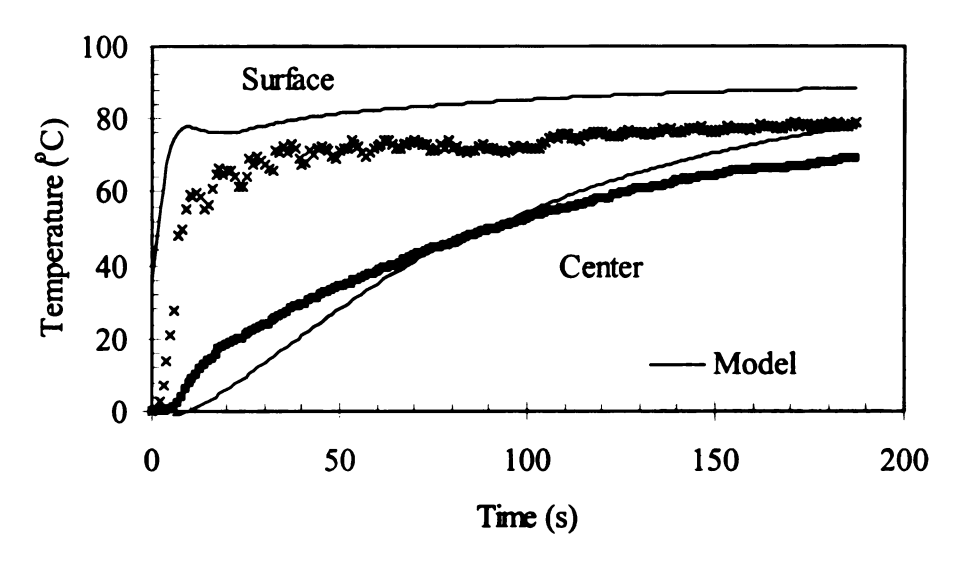


Figure 8.35 - Oven temperature: 232°C, oven steam content: 50% by volume, oven airflow: 11.4 m/s (Experiment 56a).

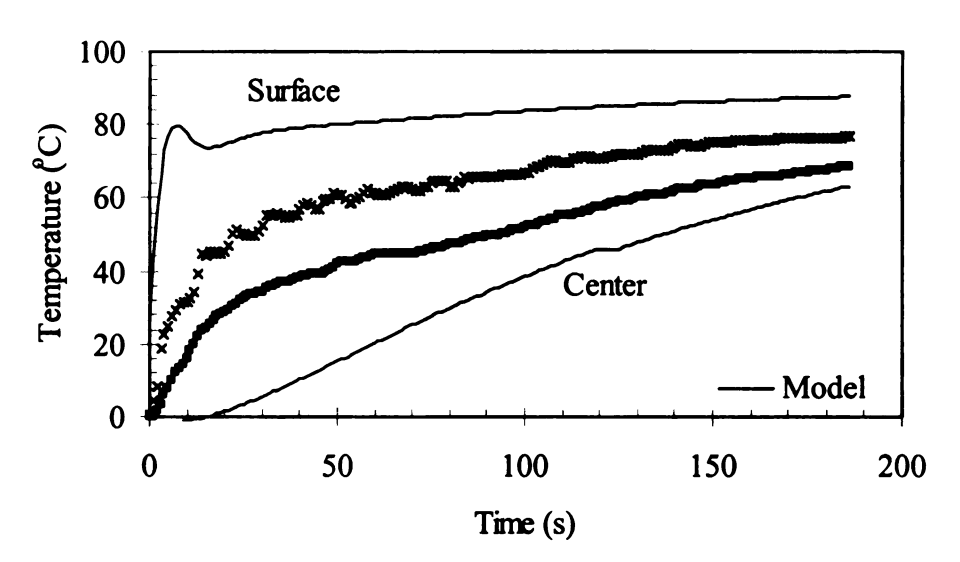


Figure 8.36 - Oven temperature: 232°C, oven steam content: 50% by volume, oven airflow: 11.4 m/s (Experiment 56b).

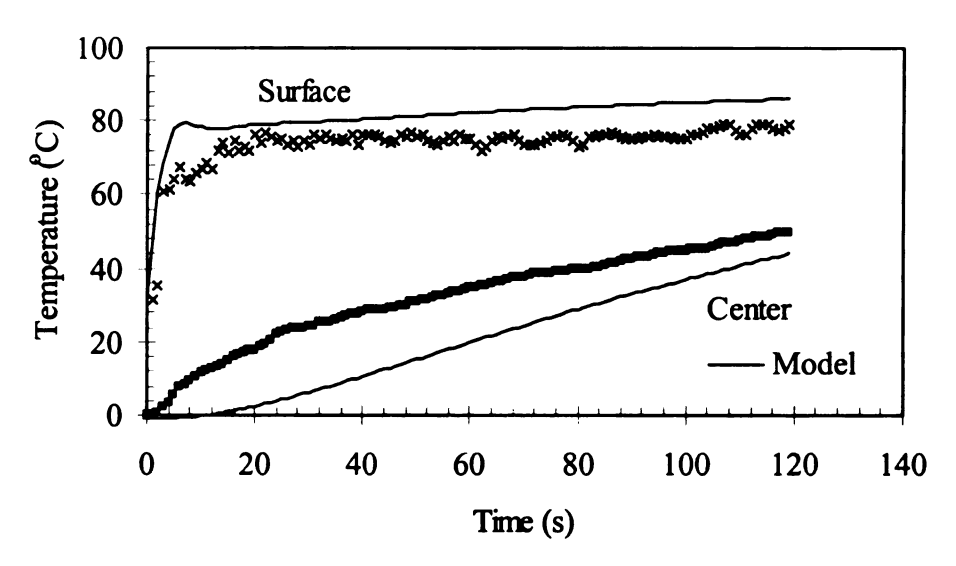


Figure 8.37 – Oven temperature: 232°C, oven steam content: 50% by volume, oven airflow: 16.8 m/s (Experiment 58a).

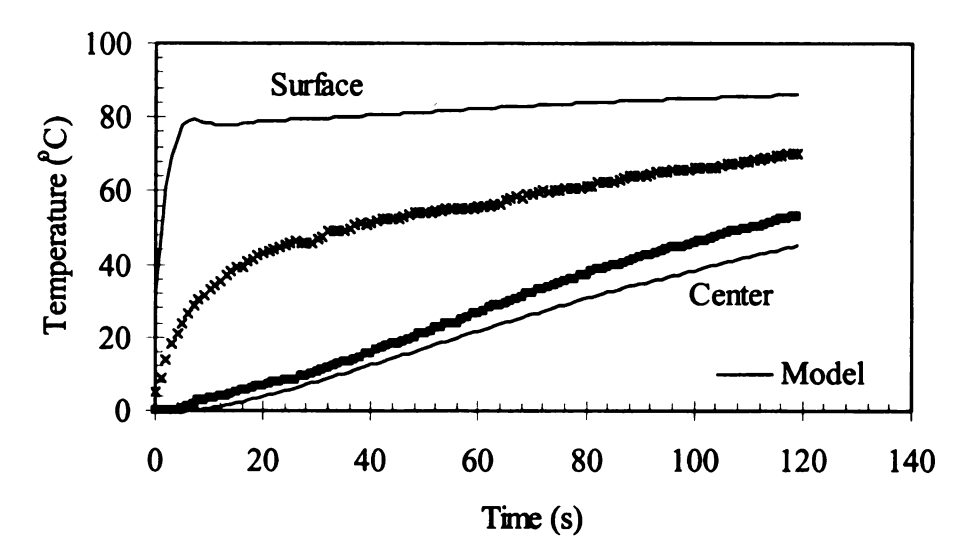


Figure 8.38 – Oven temperature: 232°C, oven steam content: 50% by volume, oven airflow: 16.8 m/s (Experiment 58b).

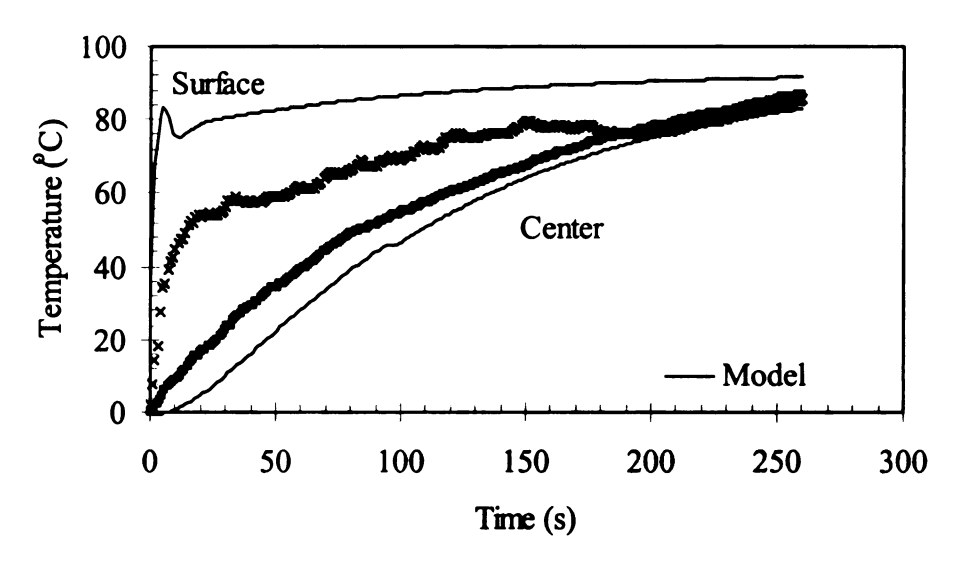


Figure 8.39 - Oven temperature: 232°C, oven steam content: 50% by volume, oven airflow: 21.8 m/s (Experiment 63a).

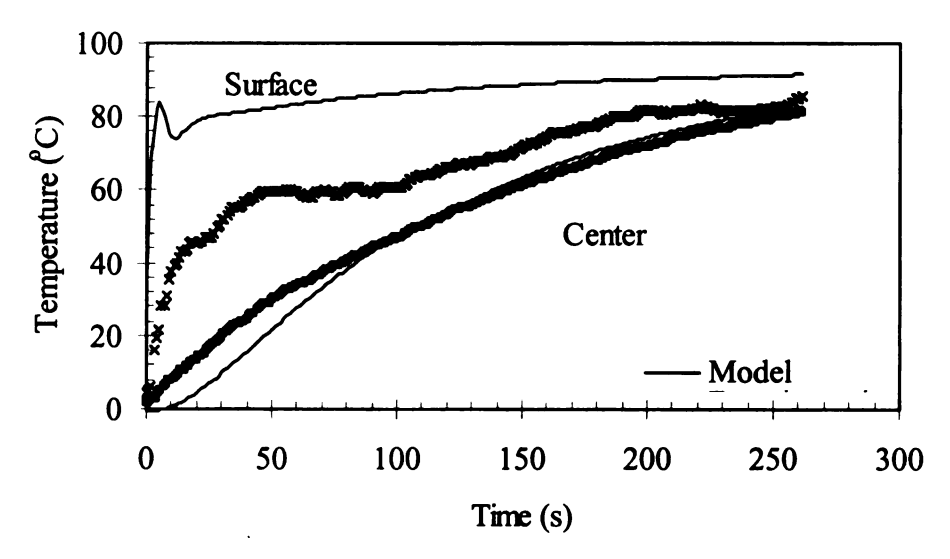


Figure 8.40 - Oven temperature: 232°C, oven steam content: 50% by volume, oven airflow: 21.8 m/s (Experiment 63b).

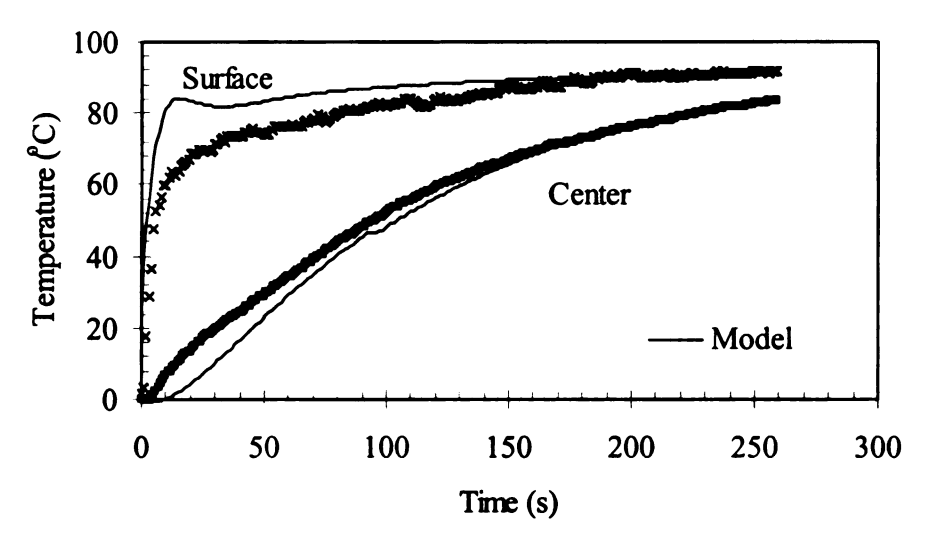


Figure 8.41 - Oven temperature: 232°C, oven steam content: 70% by volume, oven airflow: 11.4 m/s (Experiment 66a).

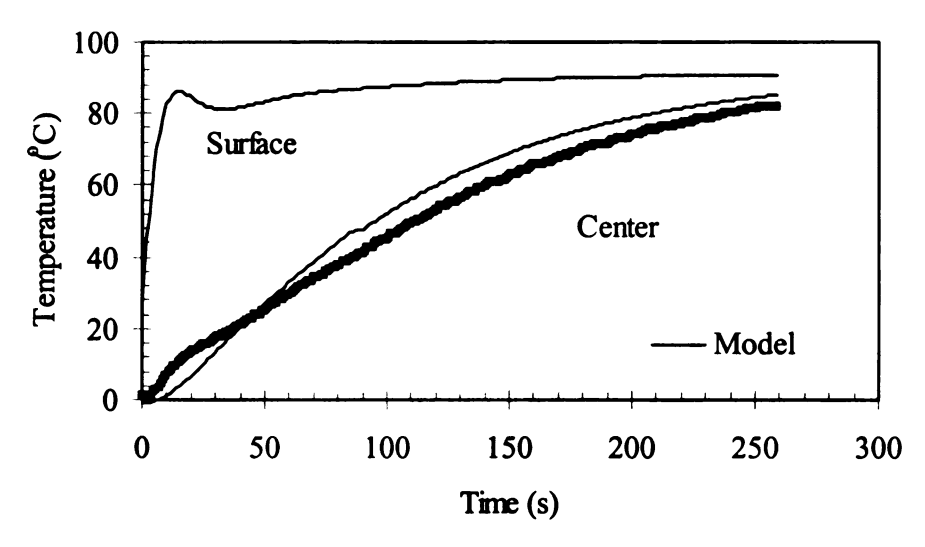


Figure 8.42 - Oven temperature: 232°C, oven steam content: 70% by volume, oven airflow: 11.4 m/s (Experiment 66b).

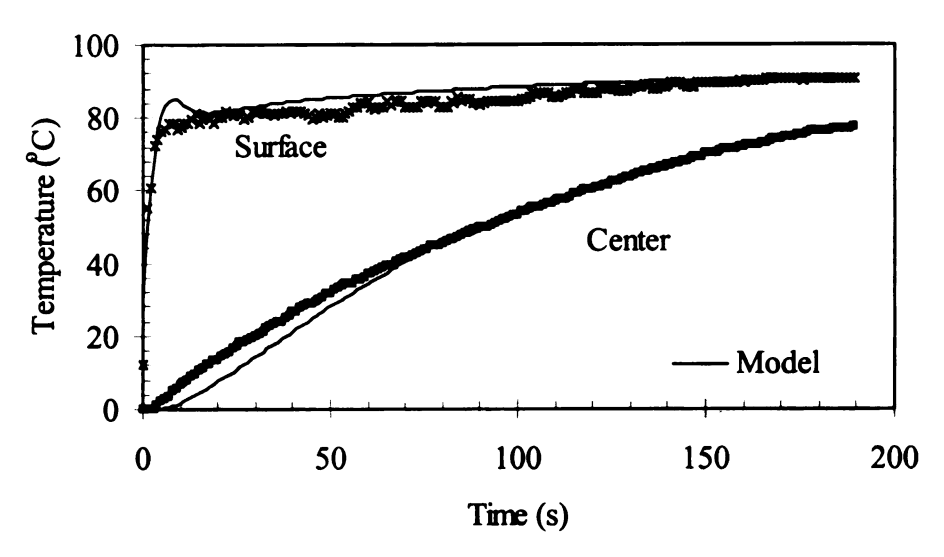


Figure 8.43 - Oven temperature: 232°C, oven steam content: 70% by volume, oven airflow: 16.8 m/s (Experiment 68a).

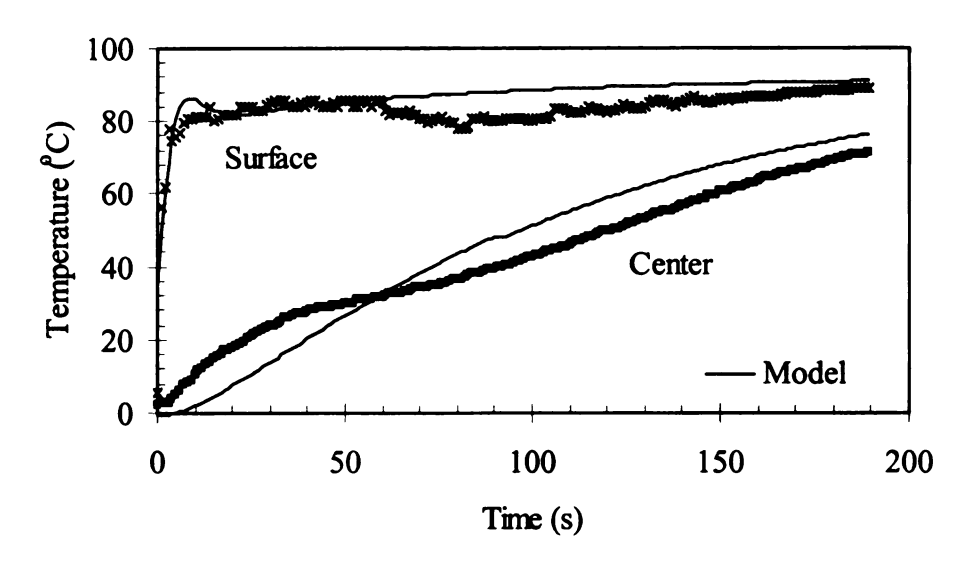


Figure 8.44 - Oven temperature: 232°C, oven steam content: 70% by volume, oven airflow: 16.8 m/s (Experiment 68b).

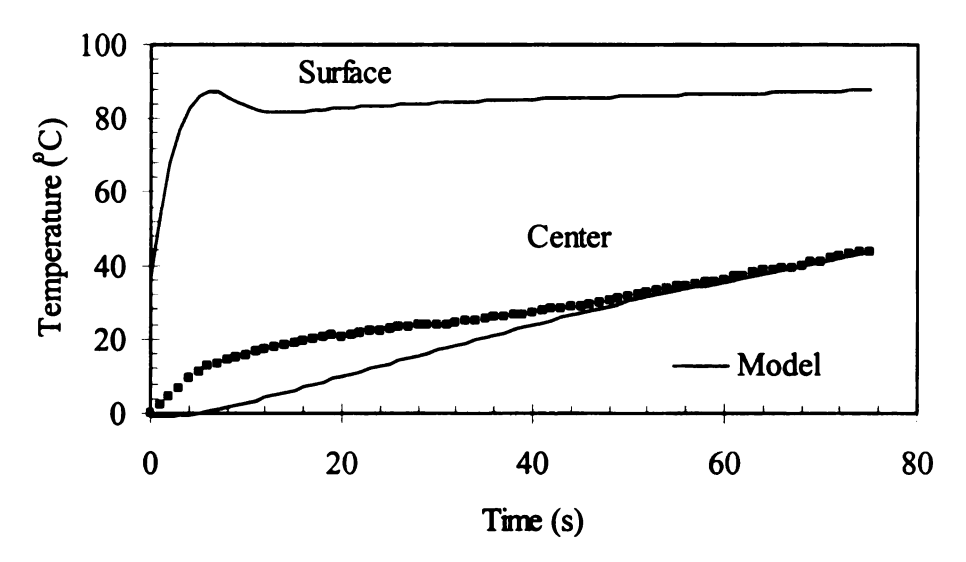


Figure 8.45 - Oven temperature: 232°C, oven steam content: 70% by volume, oven airflow: 21.8 m/s (Experiment 70a).

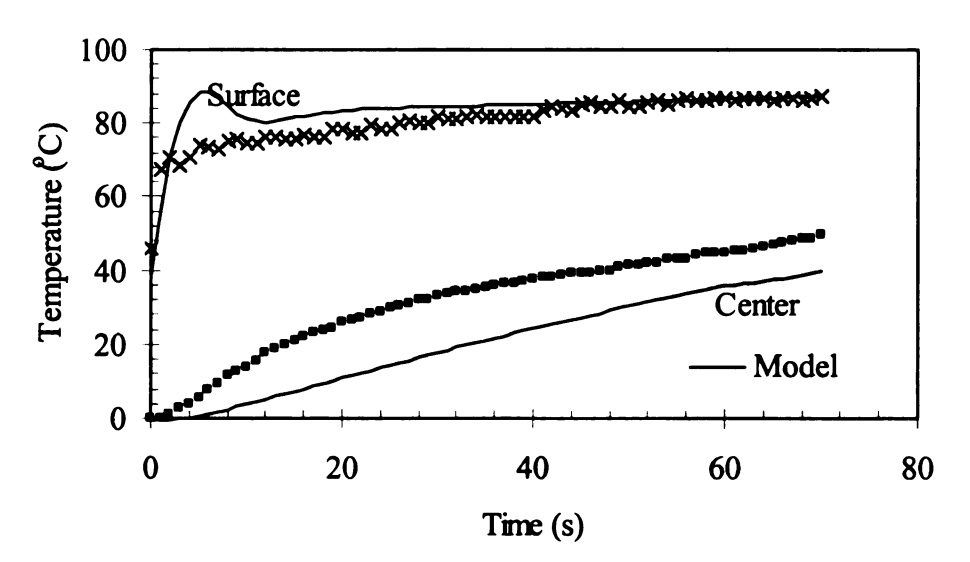


Figure 8.46 - Oven temperature: 232°C, oven steam content: 70% by volume, oven airflow: 21.8 m/s (Experiment 70b).

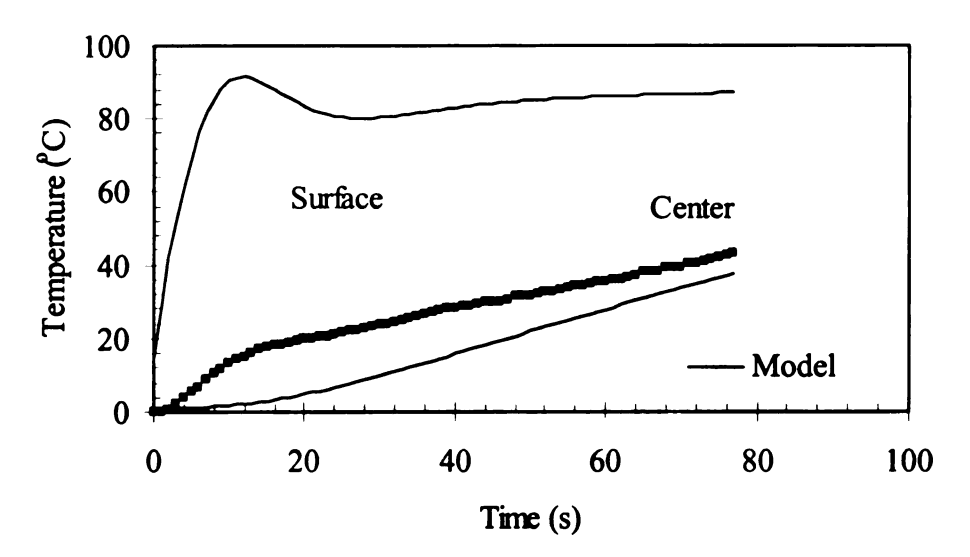


Figure 8.47 - Oven temperature: 232°C, oven steam content: 82% by volume, oven airflow: 11.4 m/s (Experiment 73a).

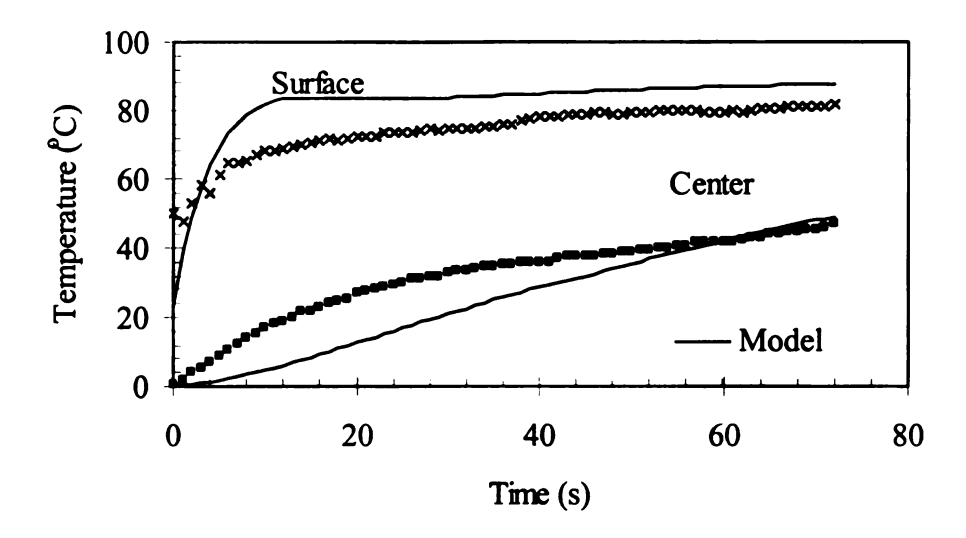


Figure 8.48 - Oven temperature: 232°C, oven steam content: 82% by volume, oven airflow: 11.4 m/s (Experiment 73b).

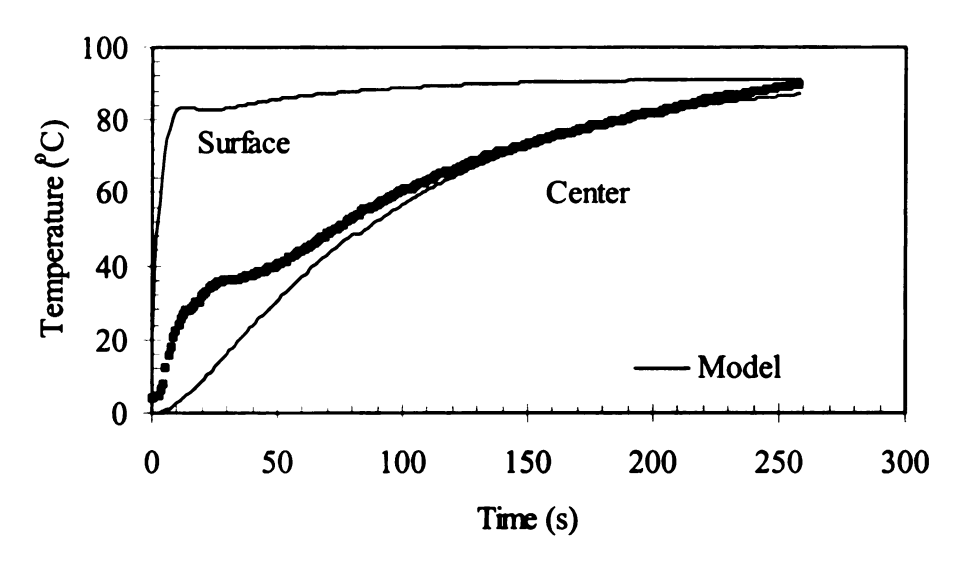


Figure 8.49 – Oven temperature: 232°C, oven steam content: 82% by volume, oven airflow: 11.4 m/s (Experiment 75a).

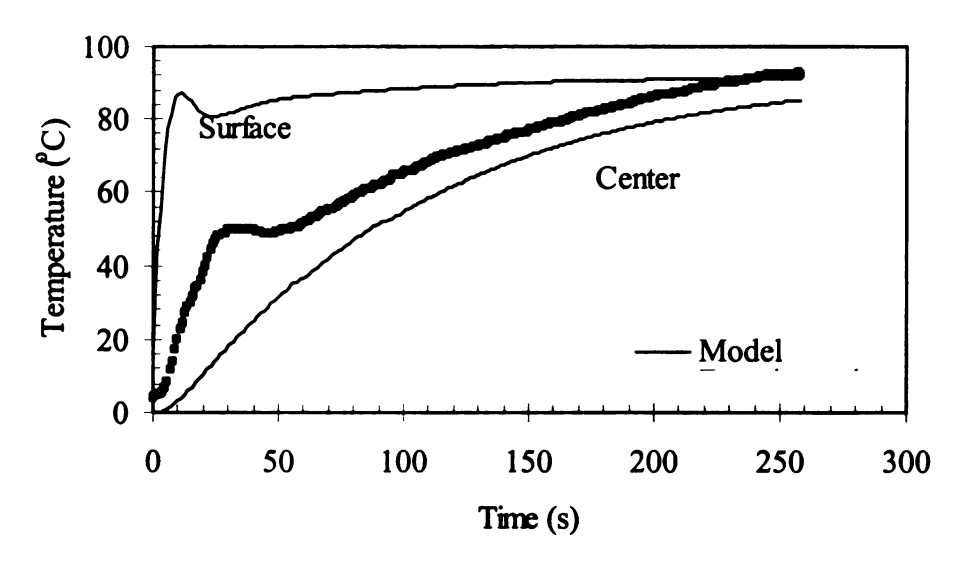


Figure 8.50 – Oven temperature: 232°C, oven steam content: 82% by volume, oven airflow: 11.4 m/s (Experiment 75b).

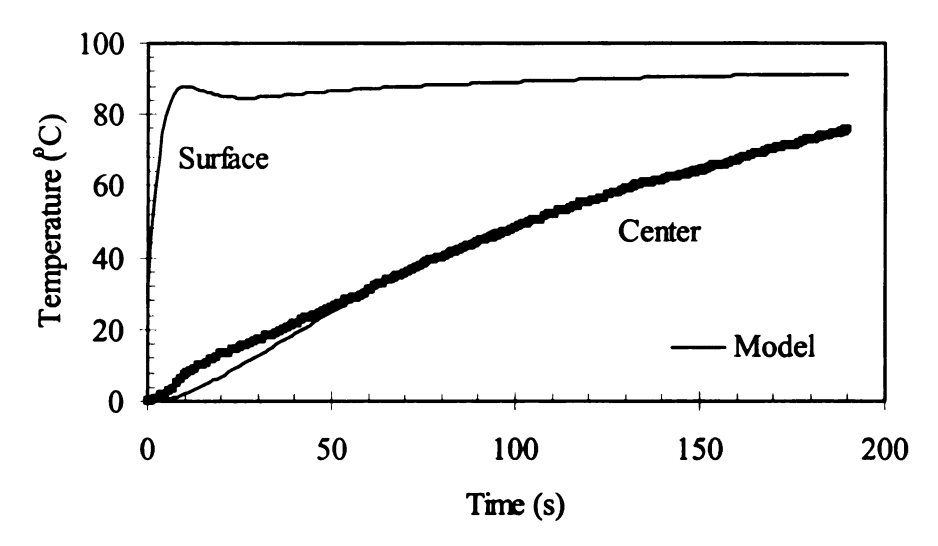


Figure 8.51 – Oven temperature: 232°C, oven steam content: 82% by volume, oven airflow: 16.8 m/s (Experiment 78a).

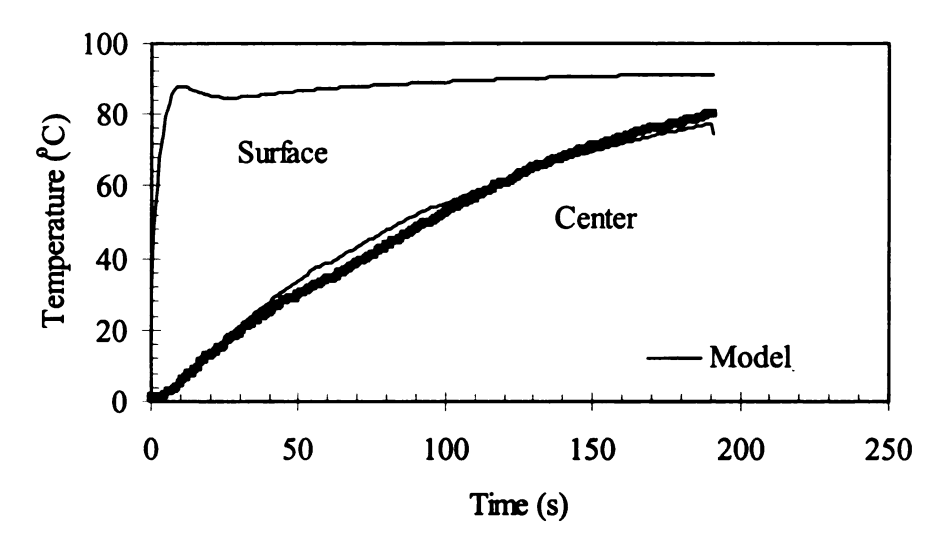


Figure 8.52 – Oven temperature: 232°C, oven steam content: 82% by volume, oven airflow: 16.8 m/s (Experiment 78b).

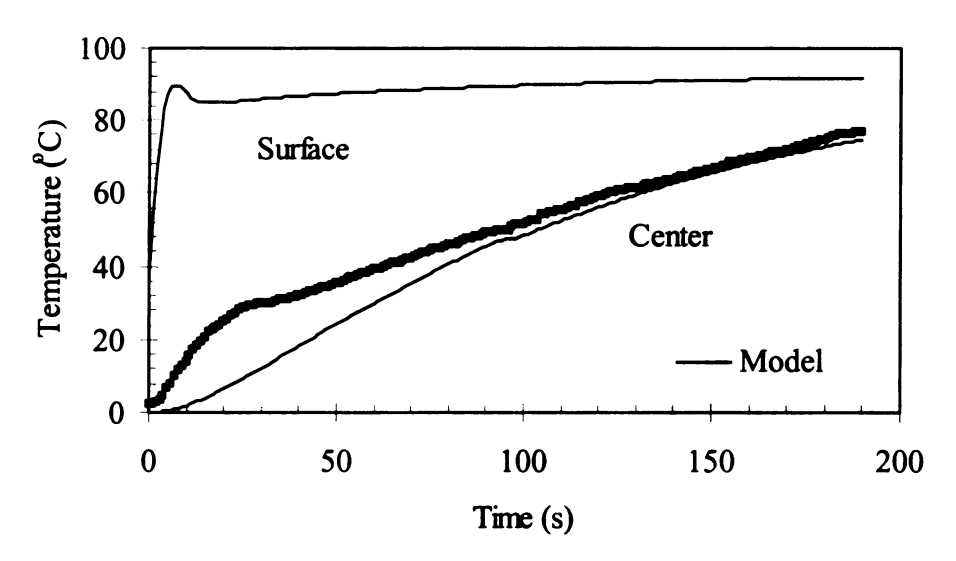


Figure 8.53 – Oven temperature: 232°C, oven steam content: 82% by volume, oven airflow: 21.8 m/s (Experiment 80a).

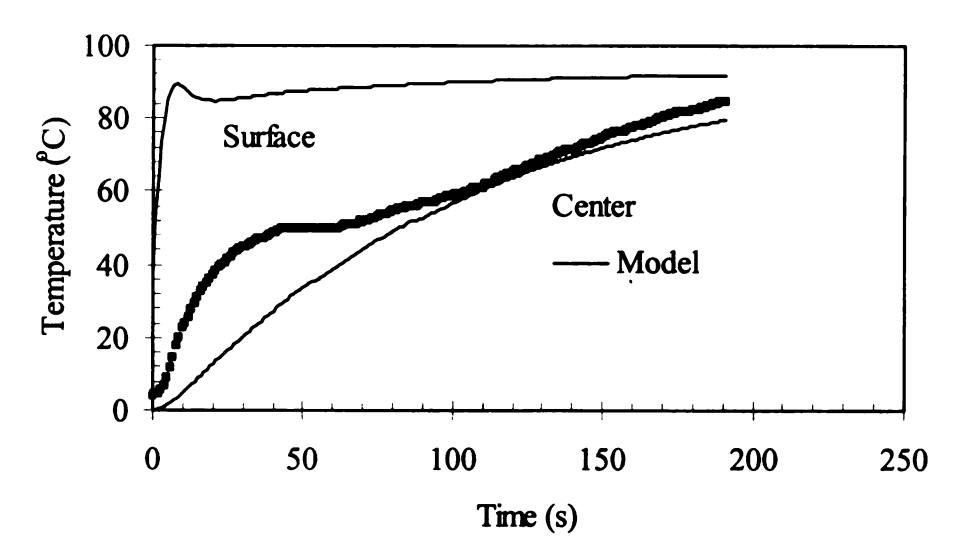


Figure 8.54 – Oven temperature: 232°C, oven steam content: 82% by volume, oven airflow: 21.8 m/s (Experiment 80b).

8.2 Derivation of cooking-air thermo-physical property equations

The oven-air thermo-physical properties used in the cooking model were modeled using non-steady-state relationships. The latent heat of vaporization for water as a function of temperature was modeled using linear regression of tabular data (Geankoplis, 1993); (Equation [8.1]).

$$\lambda = -2.429 \cdot T + 2502.8 \tag{8.1}$$

The resulting regression had an R² value of 0.998 (Figure 8.55).

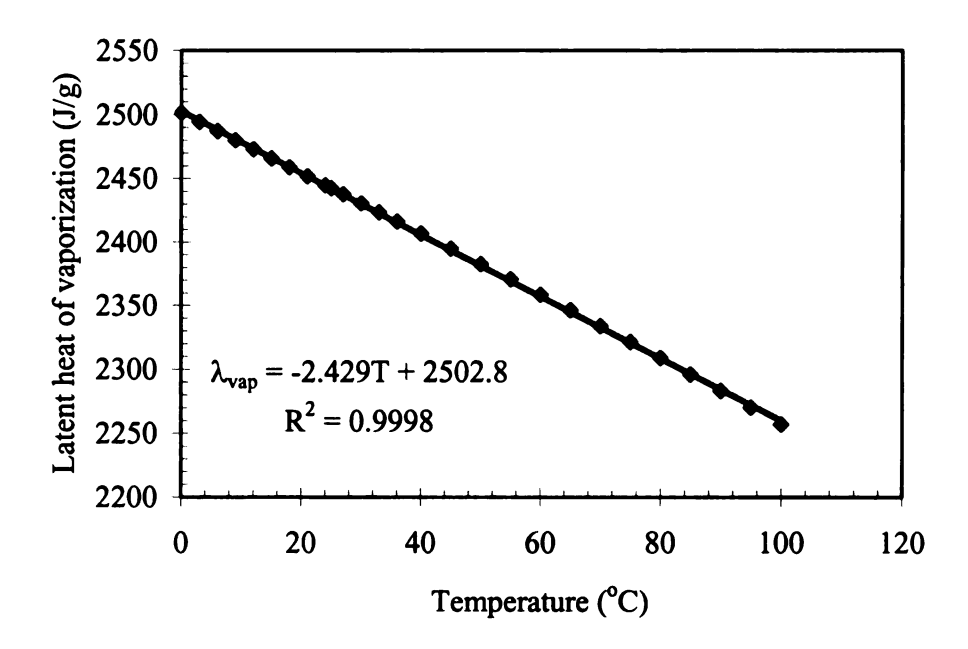


Figure 8.55 - Latent heat of vaporization for water as a function of temperature (From tabular data: Geankoplis, 1993).

The viscosity of air was modeled as a function of temperature using regression of tabular data (Geankoplis, 1993); (Equation [8.2]).

$$\mu_{\text{air}} = -0.0000000002 \cdot T^2 + 0.0000005 \cdot T + 0.0002 \qquad \qquad [~8.2~]$$

The resulting regression equation had an R² value of 0.9998 (Figure 8.56).

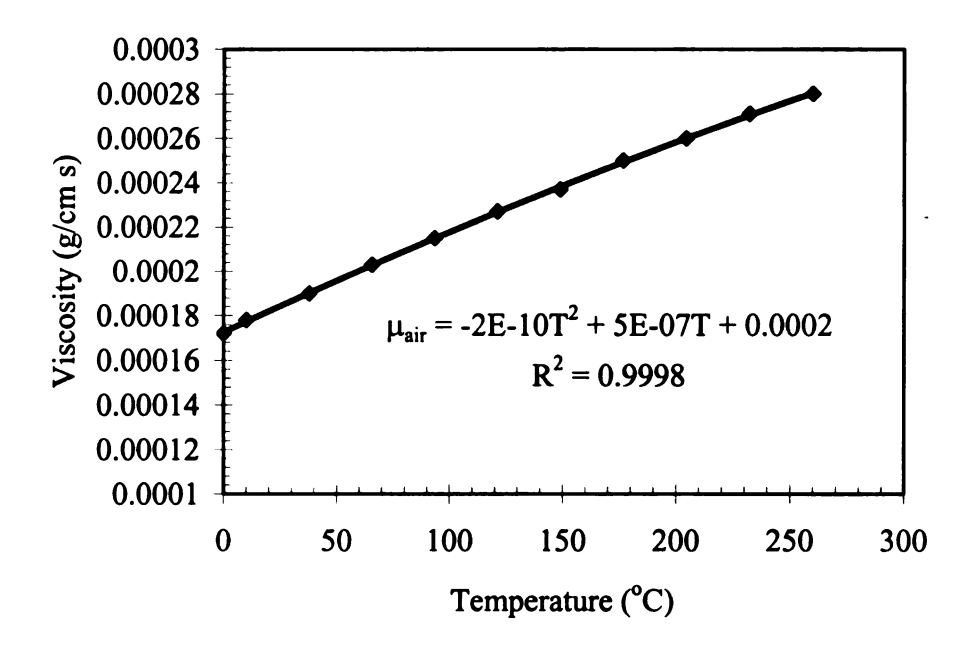


Figure 8.56 - Viscosity of air as a function of temperature (From tabular data: Geankoplis, 1993).

The viscosity of steam was modeled as a function of temperature using regression of tabular data (Geankoplis, 1993); (Equation [8.3]).

$$\mu_{\text{steam}} = -0.00000001 \cdot \text{T}^2 + 0.00004 \cdot \text{T} + 0.0089$$
 [8.3]

The resulting regression had an R² value of (Figure 8.57).

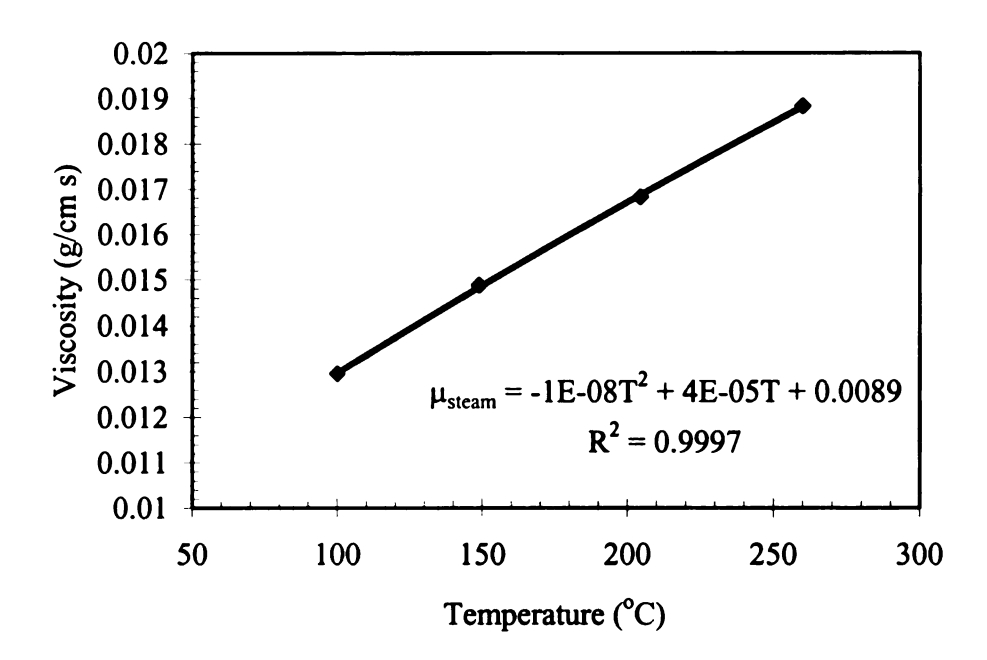


Figure 8.57 - Viscosity of steam as a function of temperature (From tabular data: Geankoplis, 1993).

A mixture equation developed by Burmeister (1983) was utilized to calculate the viscosity of the air-steam mixture (Equation [8.4]).

$$\mu_{\text{mix}} = \frac{\mu_{\text{air}}}{1 + \phi_{\text{as}} \cdot X_{\text{s}} / X_{\text{a}}} + \frac{\mu_{\text{steam}}}{1 + \phi_{\text{sa}} \cdot X_{\text{a}} / X_{\text{s}}}$$
 [8.4]

where:

$$\phi_{as} = \frac{1}{\sqrt{8}} \cdot \frac{\left[1 + \left(\frac{\mu_{air}}{\mu_{steam}}\right)^{0.5} \left(\frac{M_{steam}}{M_{air}}\right)^{0.25}\right]^{2}}{\left(1 + \frac{M_{air}}{M_{steam}}\right)}$$
[8.5]

and

$$\phi_{sa} = \frac{1}{\sqrt{8}} \cdot \frac{\left[1 + \left(\frac{\mu_{steam}}{\mu_{air}}\right)^{0.5} \left(\frac{M_{air}}{M_{steam}}\right)^{0.25}\right]^{2}}{\left(1 + \frac{M_{steam}}{M_{air}}\right)}$$
[8.6]

The density of air was modeled as a function temperature using regression of tabular data (Geankoplis, 1983); (Equation [8.7]).

$$\rho_{\text{air}} = -0.00000000002 \cdot T^3 + 0.00000001 \cdot T^2 - 0.0000004 \cdot T + 0.0013$$
 [8.7]

The regression equation had an R² value of 1 (Figure 8.58).

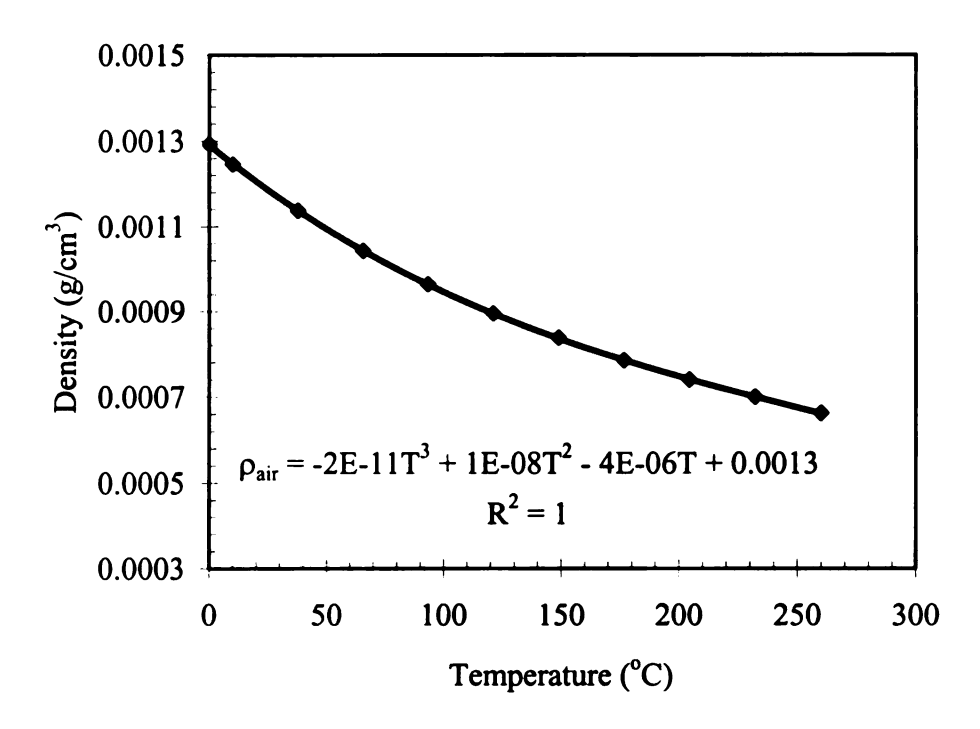


Figure 8.58 - Density of air as a function of temperature (from tabular data: Geankoplis, 1993).

The density of water vapor at temperatures below 100°C was modeled as a function of temperature using tabular data (Geankoplis, 1993); (Equation [8.8]).

$$\rho_{vapor} = 0.00000000003 \cdot T^4 + 0.00000000025 \cdot T^3 - 0.0000000039 \cdot T^2 + 0.000000085 \cdot T$$

[8.8]

The regression equation had an R² value of 1 (Figure 8.59).

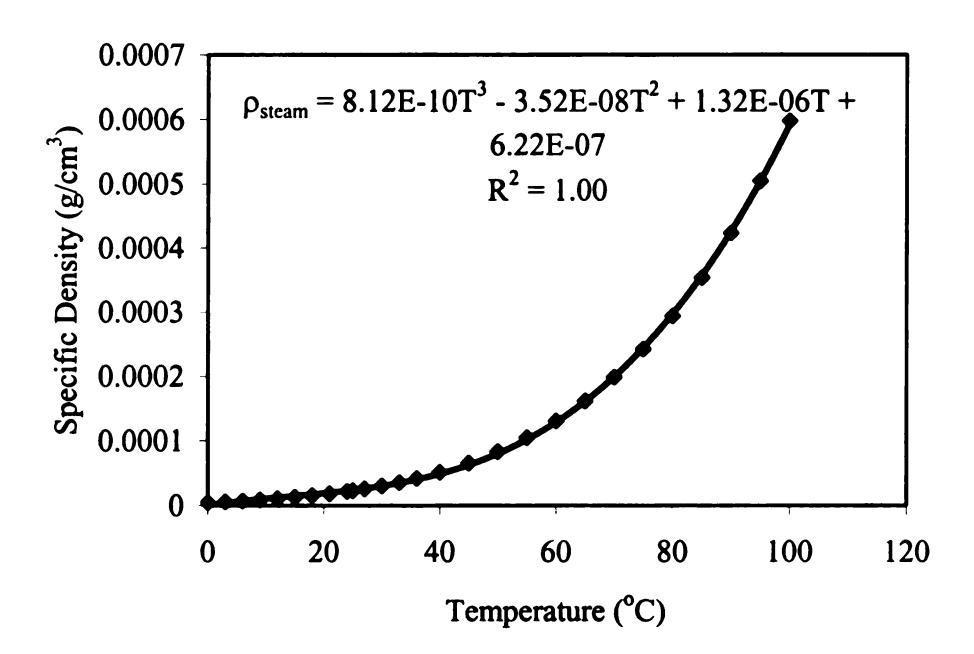


Figure 8.59 - Density of saturated steam as a function of temperature (From tabular data: Geankoplis, 1993).

The density of steam at atmospheric pressure and temperatures above 100°C was modeled as a function of temperature using regression of tabular data (Geankoplis, 1993); (Equation [8.9]).

$$\rho_{\text{steam}} = -0.0002 \cdot \log(T) + 0.0015$$
 [8.9]

The regression equation had an R² value of 0.999 (Figure 8.60).

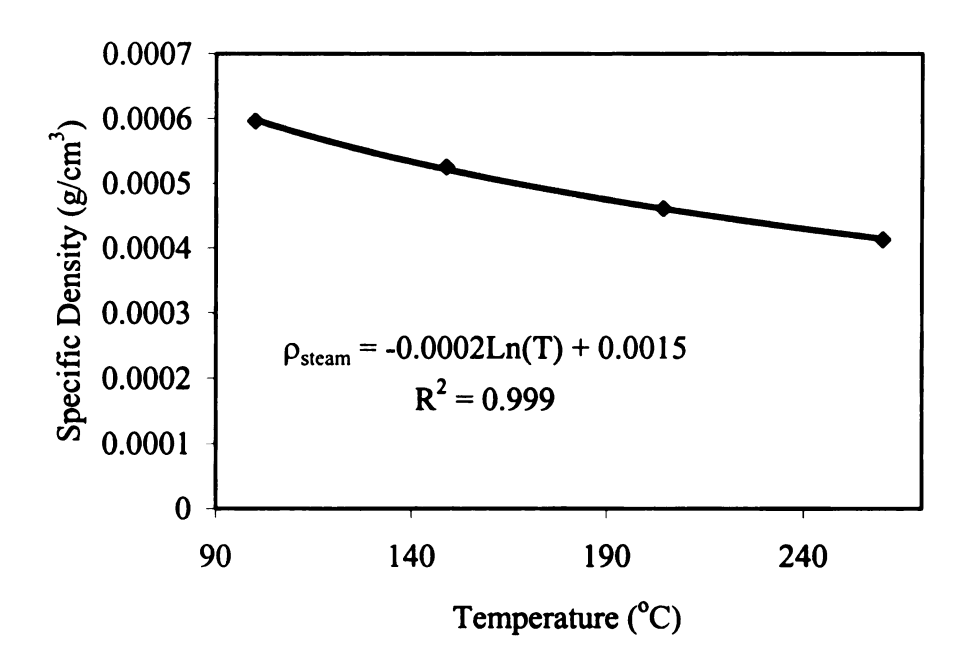


Figure 8.60 - Density of steam at 101.35 kPa as a function of temperature (From tabular data: Geankoplis, 1993).

The density of the air-steam mixture was assumed given by Equation [8.10] which assumes that the molar fraction of each component is equal to the volume fraction.

$$\rho_{\text{mix}} = \rho_{\text{air}} \cdot X_{\text{air}} + \rho_{\text{steam}} \cdot X_{\text{steam}}$$
 [8.10]

The heat capacity of the air-steam mixture was calculated as functions of temperature and composition using an equation given by Millsap (2002); (Equation [8.11]).

$$c_{p,mix} = \frac{\left(\rho_{air} \cdot X_{air} \cdot cp_{air} + \rho_{steam} \cdot X_{steam} \cdot cp_{steam}\right)}{\left(\rho_{air} \cdot X_{air} + \rho_{steam} \cdot X_{steam}\right)}$$
[8.11]

The thermal conductivity of air was modeled as a function of temperature using regression of tabular data (Geankoplis, 1993); (Equation [8.12]).

$$k_{air} = 0.000000003 \cdot T^2 + 0.0000008 \cdot T + 0.002$$
 [8.12]

The regression had an R² value of 0.9999 (Figure 8.61).

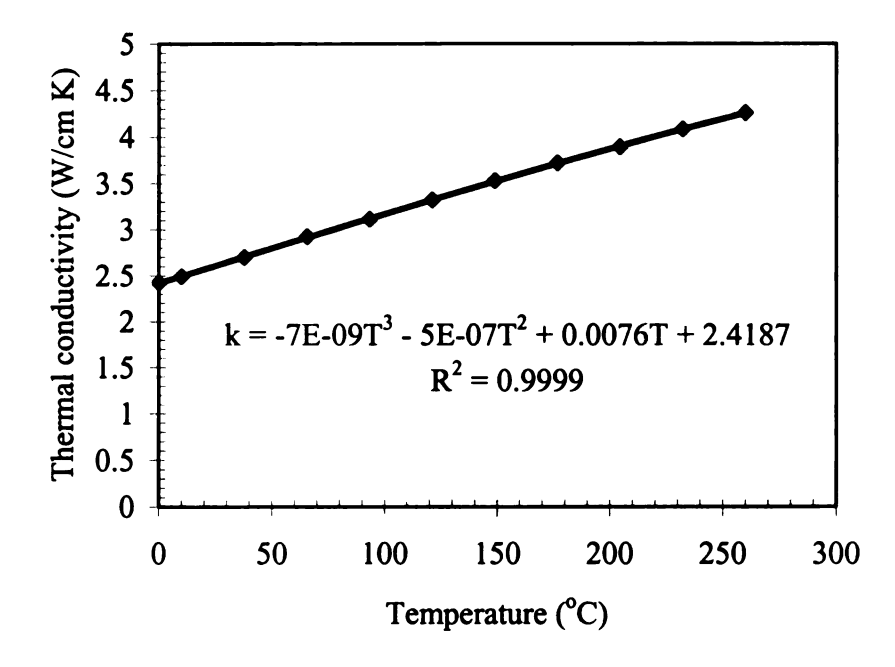


Figure 8.61 - Thermal conductivity of air as a function of temperature (From tabular data: Geankoplis, 1993).

The thermal conductivity of steam was modeled as a function of temperature using regression of tabular data (Geankoplis, 1993); (Equation [8.13]).

$$\mathbf{k}_{\text{steam}} = 0.0000009 \cdot \mathbf{T} + 0.0002$$
 [8.13]

The regression had an R² value of (Figure 8.62).

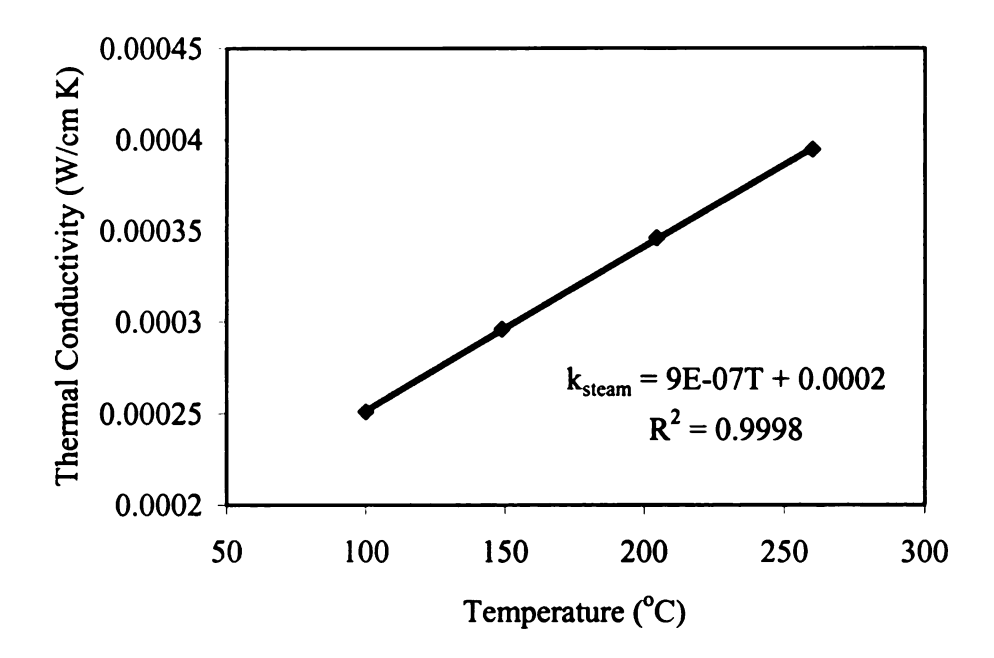


Figure 8.62 - Thermal conductivity of steam as a function of temperature (From tabular data: Geankoplis, 1993).

Thermal conductivity of the air-steam mix was modeled using an equation given by Burmeister (1983); (Equation [8.14]).

$$k_{\text{mix}} = \frac{k_{\text{air}}}{1 + A_{\text{as}} \cdot \begin{pmatrix} X_{\text{steam}} \\ X_{\text{air}} \end{pmatrix}} + \frac{k_{\text{steam}}}{1 + A_{\text{sa}} \cdot \begin{pmatrix} X_{\text{air}} \\ X_{\text{steam}} \end{pmatrix}}$$
[8.14]

where:

$$A_{as} = \frac{1}{4} \left\{ 1 + \left[\left(\frac{\mu_{air}}{\mu_{steam}} \right) \left(\frac{M_{steam}}{M_{air}} \right)^{0.75} \left(\frac{1 + \frac{S_{air}}{T_{air,K}}}{1 + \frac{S_{steam}}{T_{air,K}}} \right) \right]^{0.5} \right\}^{2} \cdot \left\{ \frac{1 + \left[0.733 \cdot \left(S_{air} \cdot S_{steam} \right)^{0.5} \right] / T_{air,K}}{1 + \frac{S_{air}}{T_{air,K}}} \right\}$$

[8.15]

and:

$$A_{sa} = \frac{1}{4} \left\{ 1 + \left[\left(\frac{\mu_{steam}}{\mu_{air}} \right) \left(\frac{M_{air}}{M_{steam}} \right)^{0.75} \left(\frac{1 + \frac{S_{steam}}{T_{air,K}}}{1 + \frac{S_{sair}}{T_{air,K}}} \right) \right]^{0.5} \right\}^{2} \cdot \left\{ \frac{1 + \left[0.733 \cdot \left(S_{steam} \cdot S_{air} \right)^{0.5} \right] / T_{air,K}}{1 + \frac{S_{steam}}{T_{air,K}}} \right\}$$
[8.16]

The diffusivity of steam in air was modeled using an equation from Vargaflik (1966); (Equation [8.17]).

$$D_{sa} = 0.216 \cdot \left(\frac{T_{air,K}}{273}\right)^{1.8}$$
 [8.17]

8.3 Product thermo-physical properties

Composition dependent values of product thermo-physical properties were used for the model calculations (Equations [8.18] and [8.19]). The heat capacity of meat was modeled as a function of the mass fractions of water, protein, and fat (Choi and Okos, 1986). Separate equations were utilized for the temperature ranges below (Equation [8.18]) and above (Equation [8.19]) freezing.

$$c_{p,\text{frozen}} = c_{p,\text{ice}} \cdot X_{W} + c_{p,\text{protein}} \cdot X_{P} + c_{p,\text{fat}} \cdot X_{F}$$
 [8.18]

$$c_{p} = c_{p,water} \cdot X_{W} + c_{p,protein} \cdot X_{P} + c_{p,fat} \cdot X_{F}$$
 [8.19]

Thermal conductivity of the meat was calculated using a series model based upon the volume fraction and thermal conductivity of the water, protein, and meat fractions of the meat (Choi and Okos, 1986); (Equation [8.20]).

$$k_{T} = k_{water} \cdot X_{water} + k_{protein} \cdot X_{protein} + k_{fat} \cdot X_{fat}$$
 [8.20]

The density of the meat was calculated using a parallel model based upon the density of the water, fat, and protein components of the meat (Choi and Okos, 1986); (Equation [8.21]).

$$\rho = \frac{1}{m_{\text{water}}/\rho_{\text{water}} + m_{\text{fat}}/\rho_{\text{fat}} + m_{\text{protein}}/\rho_{\text{protein}}}$$
 [8.21]

The moisture diffusivity of the meat was modeled as a function of fat-protein ratio and temperature using an equation developed by Mittal and Blaisdell (1984); (Equation [8.22]).

$$k_m = 0.003 \cdot \exp\left(-0.442 \cdot FP - \frac{4829.7}{T} + 11.55\right)$$
 [8.22]

A constant value of 64.4 J/g was utilized for the latent heat a fusion of fat (Skala et al., 1989). The latent heat of fusion for water was set at 337.8 J/g (Geankoplis, 1993). A value of 0.003 g/g was utilized for the value of moisture capacity, c_m (Chen et al., 1999). A constant value of 0.0008 g/s·cm² was utilized for the fat conductivity, k_f.

8.4 Screen shots from Visual Basic cooking model user interface

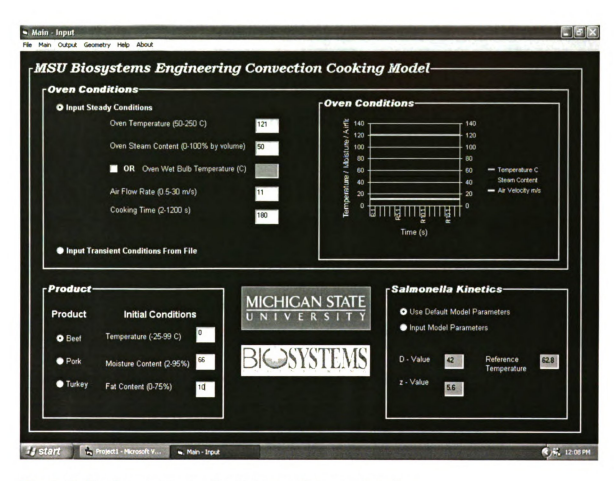


Figure 8.63 - Input screen of cooking model user interface.

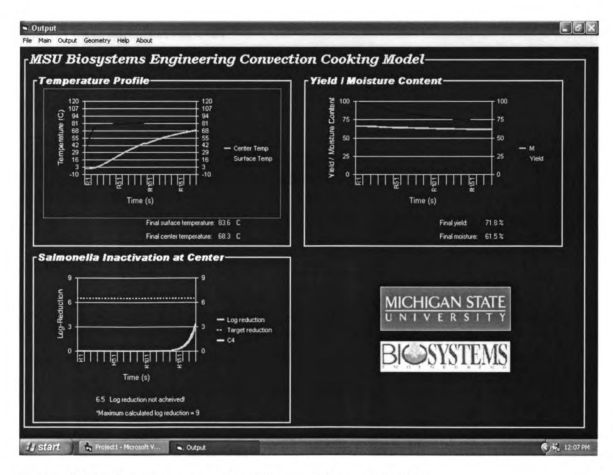


Figure 8.64 - Output screen of cooking model user interface.

8.5 Visual Basic model code

Module - Main

Version 1.0 – July 2004

By Adam E. Watkins and Dr. Bradley P. Marks

Department of Biosystems and Agricultural Engineering

Michigan State University

Sub Main()

'Open the main input file. Contains node data, element data, boundary nodes, etc.

Open "c:\TdmField47.txt" For Input As #1

'Open the main output file

Open "c:\modeloutput.txt" For Output As #3

'Input setup information

Input #1, NumNodes, NumEle, NumBdyNodes, NumMatlSets, NumDerivBdy

'Set solution timestep to 1 s

timestep = 1

'Format display

'Input oven conditions from a file or from the input screen

If Form1.Option2 = True Then

Open "c:\OvenConditions.txt" For Input As #2 'Open oven conditions input file
Input #2, NumTimeSteps 'Get cooking time from file
ReDim OvenConditions(NumTimeSteps, 3) 'Dimension oven conditions matrix
Call InputOvenConditions(OvenConditions(), NumTimeSteps) 'Get oven conditions from file
Form1.Frame3.Visible = True 'Show oven conditions graph

^{&#}x27;Many of the modules associated with the basic FEM architecture were provided by or modified

^{&#}x27; from modules provided by Dr. Larry Segerlind - Michigan State University. These modules

^{&#}x27;have been identified in the module comment statements.

^{&#}x27; FEM cooking and microbial inactivation model - Main Module

^{&#}x27; This module controls the calculations for a two-dimensional heat and mass transfer problem.

Form1.MSChart1.Visible = True 'Show oven conditions graph 'Labels on graph OvenConditions(0, 1) = "Temperature C" OvenConditions(0, 2) = "Steam Content" 'Labels on graph OvenConditions(0, 3) = "Air Velocity m/s" 'Labels on graph Form1.MSChart1.ChartData = OvenConditions 'Plot oven conditions on graph Close #2 'Close oven conditions file Else 'Oven conditions from form 'Input cooking time NumTimeSteps = Form1.Text4.Text 'Dimension oven conditions matrix ReDim OvenConditions(NumTimeSteps, 3) For I = 1 To NumTimeSteps OvenConditions(I, 1) = Form1.Text1.Text'Oven temperature C OvenConditions(I, 2) = Form1.Text2.Text 'Oven steam content % by volume If OvenConditions(I, 2) = 0 Then OvenConditions(I, 2) = 1 OvenConditions(I, 3) = Form1.Text3.Text'Oven air velocity cm/s Next I Form 1. Frame 3. Visible = True 'Show oven conditions graph Form1.MSChart1.Visible = True 'Show oven conditions graph OvenConditions(0, 1) = "Temperature C" 'Labels on graph OvenConditions(0, 2) = "Steam Content" 'Labels on graph OvenConditions(0, 3) = "Air Velocity m/s" 'Labels on graph Form1.MSChart1.ChartData = OvenConditions 'Plot oven conditions on graph End If 'Dimension matrix of coordinate data ReDim Coord(NumNodes, 2) ' Coord(,1) X coordinate ' Coord(,2) Y coordinate 'Dimension element material set ReDim EleMatlData(NumEle) ReDim EleNodeData(NumEle, 4) 'Dimension matrix of element node data EleNodeData%(,1) = Node I' EleNodeData%(,2) = Node J ' EleNodeData%(,3) = Node K ' EleNodeData%(,4) = Node M ReDim SubDerivBC(NumDerivBdy + 1, 2) 'Subscripts of the derivative ' boundary condition 'Convection or impingement at each ReDim BoundaryType(NumDerivBdy + 1) ' derivative boundary 'Vector of boundary nodes ReDim BdyNode(NumBdyNodes) 'Input node, element, and derivative boundary data Call InputBasicData(NumMatlSets, NumNodes, NumEle, Coord(), EleMatlData(), EleNodeData()) Call InputDerivBC(NumDerivBdy, NumBdyNodes, BdyNode(), SubDerivBC(), BoundaryType()) Close #1 'Close input data file 'Input type of product If Form1.Option3 = True Then Meat = 1'Beef Target reduction TR = 6.5'Label on Salmonella reduction graph Form2.Label2.Caption = "6.5" ElseIf Form1.Option4 = True Then

Meat = 2'Pork

TR = 6.5'Target reduction

'Label on Salmonella reduction graph Form2.Label2.Caption = "6.5"

ElseIf Form1.Option5 = True Then

Meat = 3Turkey

TR = 7'Target reduction

Form2.Label2.Caption = "7" 'Label on Salmonella reduction graph

End If

'Input meat temperature, moisture, and fat content

InitialT = Form1.Text5.Text'Initial meat temperature InitialM = Form1.Text6.Text 'Initial meat moisture content

If InitialM = 0 Then InitialM = 0.1'Avoid zero moisture condition not allowed

by model equations

'Initial meat fat content InitialF = Form 1.Text7.Text

'Input Salmonella reduction equation coefficients

Dvalue = Form1.Text9.Text

'D-value Salmonella Z = Form1.Text10.Text'z-value Salmonella

Tref = Form1.Text11.Text 'T-ref Salmonella

'Dimension vectors for calculation of inactivation

ReDim AverageN(NumTimeSteps) 'Volume average of microbial concentration

'Overall microbial reduction **Dim Reduction As Variant** 'Center microbial reduction ReDim logreduction(NumNodes)

Ninitial = 1000000000'Value used for log-reduction calculation

ReDim No(NumNodes) 'Used for log-reduction calculation 'Used for log-reduction calculation ReDim NW(NumNodes) ReDim Nnew(NumNodes) 'Used for log-reduction calculation 'Used for log-reduction calculation ReDim NnewW(NumNodes)

For X = 1 To NumNodes

No(X) = Ninitial'Create a nodal microbial concentration vector

NW(X) = Ninitial

Next X

'Dimension global solution vector

ReDim GSV(NumNodes) 'Enthalov ReDim GSV_M(NumNodes) 'Moisture ReDim GSV_F(NumNodes) 'Fat

'Vector of temperature values

ReDim temperature(NumNodes) Temperature vector

'Calculate solid content of the product

Solid = 100 - InitialM - InitialF 'Initial solid material in meat (NOT fat or water)

'Load vectors of moisture and FP values

```
For K = 1 To NumNodes
        GSV M(K) = InitialM
                                           'Load vector of nodal moisture values
        GSV F(K) = InitialF / Solid
                                           'Load vector of nodal fat values
        temperature(K) = InitialT
                                           'Load vector of initial temperature values
Next K
'Calculate the initial thermophysical properties of the product
Call CalculateInitialProperties(heat_capacity_f, Meat, Solid, InitialT, InitialM, InitialF, heat_capacity,
latentW, frozenH, latentF)
'Formulate enthalpy table for reconversion to temperature
LevelOne = frozenH
LevelTwo = frozenH + latentW
LevelFive = frozenH + latentW + (2 * 3.35)
LevelThree = frozenH + latentW + (45 * 3.35) + (2 * 3.35)
LevelFour = frozenH + latentW + (45 * 3.35) + latentF + (2 * 3.45)
'Percent of water thawed at the exact value of freezing temperature
PercentThawed = 1
'Convert product temperature to enthalpy
If InitialT < -2 Then
         For K = 1 To NumNodes
                 GSV(K) = (InitialT + 273) * heat_capacity_f
        Next K
ElseIf InitialT = -2 Then
        For K = 1 To NumNodes
                 GSV(K) = frozenH + PercentThawed * latentW
        Next K
ElseIf InitialT > -2 And InitialT <= 45 Then
        For K = 1 To NumNodes
                 GSV(K) = ((2 + InitialT) * 3.35) + (frozenH + latentW)
        Next K
ElseIf InitialT > 45 Then
        For K = 1 To NumNodes
                 GSV(K) = ((2 + InitialT) * 3.35) + (frozenH + latentW + latentF)
        Next K
End If
'Calculate oven air moisture content from wet bulb temperature if specified in that manner
If Form1.Check1.Value = 1 Then
        Twb = Form1.Text8.Text
        Tov = Form1.Text1.Text
        latent = (-2.429 * Form1.Text1.Text + 2502.8)
        Cwb = 8.12078904E-10 * Twb ^ 3 - 0.000000035203247 * Twb ^ 2 + 0.00000131977474 *
Twb
             + 0.000000621530732
        ConcOvenAir = Cwb - ((0.000731 / latent) * (Tov - Twb))
End If
```

'Dimension output matrices

ReDim Output(NumTimeSteps, 2) Temperature output

ReDim AverageOutput(NumTimeSteps, 2) 'Yield and moisture output ReDim AverageFat(NumTimeSteps) 'Element average fat content

'Dimension matrix of Element Physical Data

ReDim ElePhyData(NumMatlSets, 15) 'ElePhyData(,1) Equation coef, Dx

'ElePhyData(,2) Equation coef, Dy
'ElePhyData(,3) Equation coef, G
'ElePhyData(,4) Equation coef, Q
'ElePhyData(,5) Equation coef, lamda
'ElePhyData(,6) Equation coef, Dx_M
'ElePhyData(,7) Equation coef, Dy_M
'ElePhyData(,8) Equation coef, G_M
'ElePhyData(,9) Equation coef, Q_M
'ElePhyData(,10) Equation coef, lamda_M
'ElePhyData(,11) Equation coef, Dx_F
'ElePhyData(,12) Equation coef, Dy_F
'ElePhyData(,13) Equation coef, G_F
'ElePhyData(,14) Equation coef, Q_F
'ElePhyData(,15) Equation coef, lamda F

'Calculate Bandwidth

Call CalcBandwidth(NumEle, EleNodeData(), BandWidth)

'Dimension element matrices

'Element force vector

Dim EFQ(4) 'Enthalpy
Dim EFQ_M(4) 'Moisture
Dim EFQ_F(4) 'Fat

'Element force vector, derivative BC

Dim EFS(2) 'Enthalpy
Dim EFS_M(2) 'Moisture
Dim EFS F(2) 'Fat

'Element stiffness matrix

Dim ESM(4, 4) 'Enthalpy
Dim ESM_M(4, 4) 'Moisture
Dim ESM_F(4, 4) 'Fat

'Element stiffness matrix, derivative BC

Dim EKM(2, 2) 'Enthalpy
Dim EKM_M(2, 2) 'Moisture
Dim EKM_F(2, 2) 'Fat

'Element subscript values

Dim EleSub(4)

'Element Phi values (nodal unknown values)

Dim ElePhiVal(4) 'Enthalpy
Dim ElePhiVal_M(4) 'Moisture
Dim ElePhiVal_F(4) 'Fat

'Element capacitance matrix

Dim ECM(4, 4) 'Enthalpy
Dim ECM_M(4, 4) 'Moisture
Dim ECM_F(4, 4) 'Fat

'Element capacitance matrix, derivative BC

Dim ECQ(4, 4) 'Enthalpy
Dim ECQ_M(4, 4) 'Moisture
Dim ECQ F(4, 4) 'Fat

'Dimension the arrays for the global system of equations

NumEleSub = 4 NumEleNodes = 4

'Vectors used in finite difference time solution

Temporary solution vector

ReDim Temp(NumNodes) 'Enthalpy ReDim Temp_M(NumNodes) 'Moisture ReDim Temp F(NumNodes) 'Fat

'Global force vector

ReDim GFV(NumNodes) 'Enthalpy ReDim GFV_M(NumNodes) 'Moisture ReDim GFV_F(NumNodes) 'Fat

'Global stiffness matrix

ReDim GSM(NumNodes, BandWidth) 'Enthalpy ReDim GSM_M(NumNodes, BandWidth) 'Moisture ReDim GSM_F(NumNodes, BandWidth) 'Fat

'Global capacitance matrix

ReDim GCM(NumNodes, BandWidth) 'Enthalpy 'Moisture ReDim GCM M(NumNodes, BandWidth) 'Fat ReDim GCM F(NumNodes, BandWidth) 'Global A matrix used for FD time solution ReDim GAM(NumNodes, BandWidth) 'Enthalpy ReDim GAM M(NumNodes, BandWidth) 'Moisture 'Fat ReDim GAM F(NumNodes, BandWidth) 'Global P matrix used for FD time solution ReDim GPM(NumNodes, BandWidth) 'Enthalpy ReDim GPM_M(NumNodes, BandWidth) 'Moisture ReDim GPM F(NumNodes, BandWidth) 'Fat 'Vector used for volume averaging ReDim Volume(NumEle) FEM / Finite difference time solution 'Zero the global matrices Call ZeroGlobalMatrices(NumNodes, BandWidth, GFV(), GSM(), GFV_M(), GSM_M(), GFV_F(), $GSM_F(), GCM(), GCM_M(), GCM_F())$ 'Show message indicating program is running Form6.Show 'Initialize the global matrices for the first time step of the time solution T = 1'Build the banded system of equations For KK = 1 To NumEleCall CalculateProperties(Meat, Solid, NumEle, EleNodeData(), ElePhyData(), temperature(), GSV M(), GSV F(), moisture capacity, density) Call ESMatrix2DField(EleMatlData(), EleNodeData(), Coord(), ElePhyData(), EFQ(), ESM(), EFQ M(), ESM M(), EFQ F(), ESM F(), Volume(), KK) Call EleCapMatrix(ElePhyData(), EleNodeData(), ECM(), ECM_M(), ECM_F(), Coord(), KK) Call EleSubscriptValues(EleNodeData(), KK, NumEleSub, EleSub()) Call BuildBandedSystem(NumEleSub, EleSub(), EFQ(), ESM(), GFV(), GSM(), ECM(), GCM(), EFQ M(), ESM M(), GFV M(), GSM M(), ECM M(), GCM M(), EFQ F(), $ESM_F()$, GFV F(), GSM F(), ECM F(), GCM F()) Next KK

^{&#}x27;Add in the derivative boundary conditions when they occur - direct stiffness method

```
For I = 1 To NumDerivBdy
        Call CalDerivBC(heat capacity f, frozenH, latentW, latentF, I, Coord(), SubDerivBC(),
EleSub(),
                EKM(), EFS(), GSV(), EKM M(), EFS_M(), GSV_M(), EKM F(), EFS_F(),
        GSV_F(),
                OvenConditions(), T, BoundaryType(), InitialM, InitialF, moisture capacity, density,
                temperature(), ConcOvenAir)
        Call BuildBandedSystem(NumEleSub, EleSub(), EFS(), EKM(), GFV(), GSM(), ECQ(),
GCM(),
                EFS M(), EKM M(), GFV M(), GSM M(), ECQ M(), GCM M(), EFS F(),
        EKM_F(),
                GFV F(), GSM F(), ECQ F(), GCM F())
Next I
'Set force vector values for next time step
For X = 1 To NumNodes
        GFV A(X) = GFV(X)
        GFV M A(X) = GFV M(X)
        GFV F A(X) = GFV F(X)
Next X
'Begin time stepping solution
For T = 1 To NumTimeSteps
        'Construct global matrices using direct stiffness method
        For KK = 1 To NumEle
                Call CalculateProperties(Meat, Solid, NumEle, EleNodeData(), ElePhyData(),
                        temperature(), GSV M(), GSV F(), moisture capacity, density)
                Call ESMatrix2DField(EleMatlData(), EleNodeData(), Coord(), ElePhyData(),
EFQ(),
                        ESM(), EFQ M(), ESM M(), EFQ F(), ESM F(), Volume(), KK)
                Call EleCapMatrix(ElePhyData(), EleNodeData(), ECM(), ECM M(), ECM F(),
                        Coord(), KK)
                Call EleSubscriptValues(EleNodeData(), KK, NumEleSub, EleSub())
                Call BuildBandedSystem(NumEleSub, EleSub(), EFQ(), ESM(), GFV(), GSM(),
ECM(),
                        GCM(), EFQ_M(), ESM_M(), GFV_M(), GSM_M(), ECM_M(),
               GCM M(),
                        EFQ_F(), ESM_F(), GFV_F(), GSM_F(), ECM_F(), GCM_F())
       Next KK
        'Add in the derivative boundary conditions when they occur - direct stiffness method
       NumEleSub = 2
       For I = 1 To NumDerivBdy
               Call CalDerivBC(heat capacity f, frozenH, latentW, latentF, I, Coord(),
SubDerivBC(),
```

NumEleSub = 2

```
EleSub(), EKM(), EFS(), GSV(), EKM M(), EFS M(), GSV M(),
                       EKM F(), EFS F(), GSV F(), OvenConditions(), T, BoundaryType(),
                       InitialM, InitialF, moisture capacity, density, temperature(), ConcOvenAir)
               Call BuildBandedSystem(NumEleSub, EleSub(), EFS(), EKM(), GFV(), GSM(),
ECQ(),
                       GCM(), EFS M(), EKM M(), GFV M(), GSM M(), ECQ M(),
               GCM M(),
                       EFS F(), EKM F(), GFV F(), GSM F(), ECQ F(), GCM F()
       Next I
       'Build matrices for finite difference (time) solution
       Call BuildGAM(BandWidth, GAM(), GCM(), GSM(), GAM M(), GCM M(), GSM M(),
               GAM F(), GCM F(), GSM F(), timestep, NumNodes)
       Call BuildGPM(BandWidth, GPM(), GCM(), GSM(), GPM M(), GCM M(), GSM M(),
               GPM F(), GCM F(), GSM F(), timestep, NumNodes)
       Call ModifyGFV(GFV(), GFV_A(), GFV_Star(), GFV_M(), GFV_M_A(), GFV_M_Star(),
               GFV F A(), GFV F Star(), GFV F(), timestep, NumNodes)
       'Solution of equations
       Call MultpyBandMatrix(NumNodes, BandWidth, GPM(), GSV(), Temp())
       Call MultpyBandMatrix(NumNodes, BandWidth, GPM M(), GSV M(), Temp M())
       Call MultpyBandMatrix(NumNodes, BandWidth, GPM F(), GSV F(), Temp F())
       For I = 1 To NumNodes
               Temp(I) = Temp(I) + GFV_Star(I)
               Temp M(I) = Temp M(I) + GFV M Star(I)
               Temp F(I) = Temp F(I) + GFV F Star(I)
               GFV A(I) = GFV(I)
               GFV M A(I) = GFV M(I)
               GFV F A(I) = GFV F(I)
       Next I
       Call DecompBandMatrix(NumNodes, BandWidth, GAM())
       Call DecompBandMatrix(NumNodes, BandWidth, GAM M())
       Call DecompBandMatrix(NumNodes, BandWidth, GAM F())
       Call SolveBandMatrix(NumNodes, BandWidth, GSV(), Temp(), GAM())
       Call SolveBandMatrix(NumNodes, BandWidth, GSV_M(), Temp_M(), GAM_M())
       Call SolveBandMatrix(NumNodes, BandWidth, GSV F(), Temp F(), GAM F())
        'Convert enthalpy data back to temperature for display
       Call ConvertHtoTemp(heat capacity f, GSV(), GSV M, GSV F, temperature(), NumNodes,
               InitialM, Solid, frozenH, latentW, latentF, heat capacity, LevelOne, LevelTwo,
               LevelThree, LevelFour, LevelFive)
        'Calculate surface fat for next time step
       Call CalculateSurfaceFatContent(InitialF, T, GSV_F(), NumBdyNodes, BdyNode(),
       temperature(), T)
        'Calculate Salmonella reduction
```

Call CalculateSurvivors(NumNodes, timestep, temperature(), Ninitial, No(), NW(), Nnew(),

```
NnewW(), logreduction(), logreductionW, Dvalue, Tref, Z, TimeToLimit, TR)
```

```
'Volume averaging of Salmonella reduction
```

```
Call CalculateElementAverage(Volume(), NumEle, EleNodeData(), Nnew(), WeightedAverage)
```

AverageN(T) = WeightedAverage

Reduction = -Log(AverageN(T) / Ninitial) / Log(10)

'Calculate the average moisture and FP of each element for overall yield and bulk moisture determination

'Moisture

Call CalculateElementAverage(Volume(), NumEle, EleNodeData(), GSV_M(), WeightedAverage)

'Fat

Call CalculateElementAverage(Volume(), NumEle, EleNodeData(), GSV_F(), WeightedAverage)

AverageFat(T) = WeightedAverage

F = AverageFat(T)

'Calculate yield from moisture and fat percentages

Fat = F * Solid 'Mass fat based on 100 g initial
Water = M * (Fat + Solid) / (1 - M) 'Mass water based on 100 g initial

Total = Fat + Water + Solid 'Total mass

'_____

' OUTPUT SECTION

1

'Graph yield

AverageOutput(T, 2) = Total 'Yield AverageOutput(0, 2) = "Yield" 'Graph label

'Graph moisture

AverageOutput(T, 1) = WeightedAverage 'Moisture AverageOutput(0, 1) = "M" 'Graph label

M = AverageOutput(T, 1) / 100

'Graph temperature output

Output(0, 1) = "Center Temp" 'Graph labels
Output(0, 2) = "Surface Temp" 'Graph labels
Output(T, 1) = temperature(1) 'Center temperature
Output(T, 2) = temperature(4) 'Surface temperature

'Graph Salmonella reduction

Output S(0, 1) = "Log reduction" 'Graph label

```
'Graph label
        Output_S(0, 2) = "Target reduction"
        Output S(T, 1) = logreduction(1)
                                             'Graph Salmonella reduction from linear eqn.
                                             'Graph target reduction
        Output S(T, 2) = TR
                                             'Graph Salmonella reduction from logistic eqn.
        Output S(T, 3) = logreductionW
         'Write data to output file
        Write #3, temperature(1), temperature(2), temperature(4), Total, M, logreduction(1),
                 logreductionW, Reduction
        'Labels for Salmonella reduction graph
         If logreduction(1) < TR Then
                 Form2.Label3.Caption = "Log reduction not acheived!"
                 Form2.Label4.Visible = False
                 Form2.Label5.Visible = False
        Else
                 Form2.Label3.Caption = "Log reduction acheived at:"
                 Form2.Label4.Visible = True
                 Form2.Label5.Visible = True
                 Form2.Label4.Caption = TimeToLimit
                 Form2.Label5.Caption = "s"
        End If
Next T
          'End time stepping
'Digital display of endpoint data
Form2.Label8.Caption = Round(temperature(4), 1)
                                                   'Display surface temperature
Form2.Label9.Caption = Round(temperature(1), 1)
                                                   'Display center temperature
Form2.Label12.Caption = Round(Total, 1)
                                                    'Display yield
                                                   'Display moisture content
Form2.Label13.Caption = Round((M * 100), 1)
'Remove run message box
Form6.Hide
'Display graphs
                                                     Temperature graph
Form2.MSChart1.ChartData = Output
Form2.MSChart2.ChartData = AverageOutput
                                                     'Yield/Moisture graph
                                                     'Salmonella graph
Form2.MSChart3.ChartData = Output S
Close #3
```

End Sub

Module - CalcDerivBC

```
Sub CalDerivBC(heat capacity f, frozenH, latentW, latentF, I, Coord(), SubDerivBC(), EleSub(),
EKM(),
        EFS(), GSV(), EKM M(), EFS M(), GSV M(), EKM F(), EFS F(), GSV F(),
        OvenConditions(), T, BoundaryType(), InitialM, InitialF, moisture capacity, density,
        temperature(), ConcOvenAir)
This subroutine calculates the element contributions resulting from
'derivative boundary conditions
'Assign the node numbers of the side to the array EleSub()
EleSub(1) = SubDerivBC(I, 1)
EleSub(2) = SubDerivBC(I, 2)
'Grab oven conditions
OvenAirT = OvenConditions(T, 1)
OvenAirM = OvenConditions(T, 2)
OvenAirV = OvenConditions(T, 3) * 100
'Evaluate the coefficients in the element matrices
XLength = Coord(SubDerivBC(I, 1), 1) - Coord(SubDerivBC(I, 2), 1)
YLength = Coord(SubDerivBC(I, 1), 2) - Coord(SubDerivBC(I, 2), 2)
Ri = Coord(SubDerivBC(I, 1), 1)
R_i = Coord(SubDerivBC(I, 2), 1)
SideLength = Sqr(XLength ^ 2 + YLength ^ 2)
'Get temperature and moisture for each boundary
   T1 = temperature at node 1 of boundary
   T2 = temperature at node 2 of boundary
T1 = 1 * temperature(SubDerivBC(I, 1))
T2 = 1 * temperature(SubDerivBC(I, 2))
Tave = (T1 + T2) / 2
   M1 = moisture at node 1 of boundary (decimal)
   M2 = moisture at node 2 of boundary (decimal)
M1 = GSV M(SubDerivBC(I, 1))
M2 = GSV M(SubDerivBC(I, 2))
Mave = (M1 * 1 + M2 * 1) / 2
If Mave < 0 Then Mave = 0.01
'Convert moisture content to dry basis
MDB = (100 * Mave) / (100 - Mave)
```

```
'Oven geometry
Height = 6.35 'cm
 S = 4.6482 'cm
 E = 1.17
                                'cm
 W = 0.635
                                   'cm
 F = W / (2 * S)
                                                                                    'Martin Equation parameter
 fo = (60 + 4 * (Height / W - 2)^2)^--0.5 'Martin Equation parameter
 'Calculate air physical properties as functions of temperature and steam content
 'Steam concentration g/cm<sup>3</sup>
 If OvenAirT <= 100 Then
                      DensitySatSteam = 8.12078904E-10 * OvenAirT ^ 3 - 0.000000035203247 * OvenAirT ^ 2 +
                                          0.00000131977474 * OvenAirT + 0.000000621530732
 ElseIf OvenAirT > 100 Then
                      DensitySatSteam = -0.0002 * Log(OvenAirT) + 0.0015
                                                                                                                                                                           'g/cm^3
 End If
  If Form1.Check1.Value = 1 Then
                     OvenAirM = ConcOvenAir
                     density_air = -0.00000000002 * OvenAirT ^ 3 + 0.00000001 * OvenAirT ^ 2 - 0.000004 *
                                          OvenAirT + 0.0013
                                                                                                                          'g/cm^3
                     X_S = OvenAirM / (OvenAirM + density_air)
Else
                     X S = OvenAirM / 100
End If
'Mass fraction air
X A = 1 - X S
'Molar weight of steam and air
M steam = 18
M_air = 28
S a = 79
                                'K
S s = 559.5 'K
'Latent heat
latent = 1.2 * (-2.429 * Tave + 2502.8) 'J/g
'Air and steam viscosity
viscosity air = -0.0000000002 * OvenAirT ^ 2 + 0.0000005 * OvenAirT + 0.0002
                                                                                                                                                                                                                  'g/cm s
viscosity_steam = -0.00000001 * OvenAirT ^ 2 + 0.00004 * OvenAirT + 0.0089
                                                                                                                                                                                                                 'g/cm s
phi_as = 1 / 8 ^ 0.5 * ((1 + (viscosity_air / viscosity_steam) ^ 0.5 * (M_steam / M_air) ^ 0.25) ^ 2 / (1 + (viscosity_air / viscosity_steam) ^ 0.5 * (M_steam / M_air) ^ 0.25) ^ 2 / (1 + (viscosity_air / viscosity_steam) ^ 0.5 * (M_steam / M_air) ^ 0.25) ^ 2 / (1 + (viscosity_air / viscosity_steam) ^ 0.5 * (M_steam / M_air) ^ 0.25) ^ 2 / (1 + (viscosity_air / viscosity_steam) ^ 0.5 * (M_steam / M_air) ^ 0.25) ^ 2 / (1 + (viscosity_steam) ^ 0.5 * (M_steam / M_air) ^ 0.25) ^ 2 / (1 + (viscosity_steam) ^ 0.5 * (M_steam / M_air) ^ 0.25) ^ 2 / (1 + (viscosity_steam) ^ 0.5 * (M_steam / M_air) ^ 0.25) ^ 2 / (1 + (viscosity_steam) ^ 0.5 * (M_steam / M_air) ^ 0.25) ^ 2 / (1 + (viscosity_steam) ^ 0.5 * (M_steam / M_air) ^ 0.25) ^ 2 / (1 + (viscosity_steam) ^ 0.5 * (M_steam / M_air) ^ 0.25) ^ 2 / (1 + (viscosity_steam) ^ 0
                     (M_air / M_steam)) ^ 0.5)
```

```
phi_sa = 1 / 8 ^ 0.5 * ((1 + (viscosity_steam / viscosity_air) ^ 0.5 * (M_air / M_steam) ^ 0.25) ^ 2 / (1 + (viscosity_steam / viscosity_air) ^ 0.5 * (M_air / M_steam) ^ 0.25) ^ 2 / (1 + (viscosity_steam / viscosity_steam / viscosity_steam) ^ 0.5 * (M_air / M_steam) ^ 0.25) ^ 2 / (1 + (viscosity_steam / viscosity_steam / viscosity_s
                                                (M steam / M air)) ^ 0.5)
  'Mixture viscosity
viscosity mix = viscosity air / (1 + phi as * X S/X A) + viscosity steam / (1 + phi sa * X A/
X S
  'Air and mixture density
density air = -0.00000000002 * OvenAirT ^ 3 + 0.00000001 * OvenAirT ^ 2 - 0.000004 * OvenAirT
                                                                                                                                                                 'g/cm^3
density mix = density air * X A + DensitySatSteam * X S
                                                                                                                                                                                                                                                                                                                                                                                                            'g/cm^3
'Heat capacity
cpair = 1.01
                          cpsteam = 0.00000087429 * OvenAirT ^ 2 + 0.00018055 * OvenAirT + 1.8616 '1.888 '4.2
                          cpmix = (density air * X A * cpair + DensitySatSteam * X S * cpsteam) / (density air * X A +
DensitySatSteam * X S)
'Diffusivity
Dsa = (2.16 * 10 ^ -5 * ((OvenAirT + 273) / 273) ^ 1.8) * 10000
                                                                                                                                                                                                                                                                                                                                                                                                                                    'cm^2/s
A as = 0.25 * (1 + ((viscosity air * viscosity steam) * (M steam / M_air) ^ 0.75 + (1 + S_a / S_a) ^ 0.75 + (1 + S_a / 
(OvenAirT+
                                              273)) / (1 + S s / (OvenAirT + 273))) ^ 0.5) ^ 2 * (1 + 0.733 * (S a * S s) ^ 0.5 / (OvenAirT
                                               (1 + S a / (OvenAirT + 273))'
A sa = 0.25 * (1 + ((viscosity\_steam / viscosity\_air) * (M_air / M_steam) ^ 0.75 * (1 + S_s / M_steam
(OvenAirT+
                                               273)) / (1 + S a / (OvenAirT + 273))) ^ 0.5) ^ 2 * <math>(1 + 0.733 * (S a * S s) ^ 0.5 / (OvenAirT + 273))) ^ 0.5) ^ 2 * (1 + 0.733 * (S a * S s) ^ 0.5 / (OvenAirT + 273))) ^ 0.5) ^ 2 * (1 + 0.733 * (S a * S s) ^ 0.5 / (OvenAirT + 273))) ^ 0.5) ^ 2 * (1 + 0.733 * (S a * S s) ^ 0.5 / (OvenAirT + 273))) ^ 0.5) ^ 2 * (1 + 0.733 * (S a * S s) ^ 0.5 / (OvenAirT + 273))) ^ 0.5) ^ 2 * (1 + 0.733 * (S a * S s) ^ 0.5 / (OvenAirT + 273))) ^ 0.5) ^ 2 * (1 + 0.733 * (S a * S s) ^ 0.5 / (OvenAirT + 273))) ^ 0.5) ^ 2 * (1 + 0.733 * (S a * S s) ^ 0.5 / (OvenAirT + 273))) ^ 0.5) ^ 2 * (1 + 0.733 * (S a * S s) ^ 0.5 / (OvenAirT + 273))) ^ 0.5) ^ 2 * (1 + 0.733 * (S a * S s) ^ 0.5 / (OvenAirT + 273))) ^ 0.5) ^ 2 * (1 + 0.733 * (S a * S s) ^ 0.5 / (OvenAirT + 273))) ^ 0.5) ^ 2 * (1 + 0.733 * (S a * S s) ^ 0.5 / (OvenAirT + 273))) ^ 0.5) ^ 2 * (1 + 0.733 * (S a * S s) ^ 0.5 / (OvenAirT + 273))) ^ 0.5) ^ 2 * (1 + 0.733 * (S a * S s) ^ 0.5) ^ 2 * (S a * S s) ^ 0.5) ^ 2 * (S a * S s) ^ 0.5) ^ 2 * (S a * S s) ^ 0.5) ^ 2 * (S a * S s) ^ 0.5) ^ 2 * (S a * S s) ^ 0.5) ^ 2 * (S a * S s) ^ 0.5) ^ 2 * (S a * S s) ^ 0.5) ^ 2 * (S a * S s) ^ 0.5) ^ 2 * (S a * S s) ^ 0.5) ^ 2 * (S a * S s) ^ 0.5) ^ 2 * (S a * S s) ^ 0.5) ^ 2 * (S a * S s) ^ 0.5) ^ 2 * (S a * S s) ^ 0.5) ^ 2 * (S a * S s) ^ 0.5) ^ 2 * (S a * S s) ^ 0.5) ^ 2 * (S a * S s) ^ 0.5) ^ 2 * (S a * S s) ^ 0.5) ^ 2 * (S a * S s) ^ 0.5) ^ 2 * (S a * S s) ^ 0.5) ^ 2 * (S a * S s) ^ 0.5) ^ 2 * (S a * S s) ^ 0.5) ^ 2 * (S a * S s) ^ 0.5) ^ 2 * (S a * S s) ^ 0.5) ^ 2 * (S a * S s) ^ 0.5) ^ 2 * (S a * S s) ^ 0.5) ^ 2 * (S a * S s) ^ 
                                               (1 + S s / (OvenAirT + 273))'
'Thermal conductivity
k \text{ air} = -0.0000000003 * OvenAirT ^ 2 + 0.0000008 * OvenAirT + 0.002
                                                                                                                                                                                                                                                                                                                                                                                                                                                      'W/cm C
k steam = 0.000000009 * OvenAirT + 0.0002
k_{mix} = (k_{air} / (1 + A_{as} * (X_S / X_A)) + k_{steam} / (1 + A_{sa} * (X_A / X_S)))
                                                                                                                                                                                                                                                                                                                                                                                                                                                                                                                                        'W/cm
'Calculate Prandtl and Schmidt numbers
Pr mix = cpmix * viscosity mix / k mix
Sc mix = viscosity mix / (density_mix * Dsa)
'Calculate oven steam moisture concentration
If Form1.Check1.Value = 1 Then
                                               ConcOvenAir = ConcOvenAir
Else
```

```
ConcOvenAir = DensitySatSteam * OvenAirM / 100
                                                                      'g/cm^3
End If
'Calculate model parameters
'Convection condition
If BoundaryType(I) = 1 Then
         'Calculate transport coefficients
        Re = OvenAirV * density_mix * E / viscosity_mix
        Nu = 0.037 * Re^0.8 * Pr mix^(1/3)
        SH = 0.037 * Re ^ 0.8 * Sc_mix ^ (1/3)
        H M = SH * Dsa / E
        h = Nu * k_mix / E
        'Calculate surface moisture concentration
        If Tave < 0 Then
                Csat = 0.000000621530732
        Else
                Csat = 8.12078904E-10 * Tave ^ 3 - 0.000000035203247 * Tave ^ 2 +
                        0.00000131977474 * Tave + 0.000000621530732
        End If
        'Calculate effective relative humidity
        RH = 100 * (ConcOvenAir / Csat)
        MDB = (Mave * 100) / (100 - Mave)
        ERH = Exp((-5222.47 * (MDB ^ -1.0983)) / (1.9818 * (Tave + 273)))
        Cs = ERH * Csat
        'Calculate energy fluxes
        Q_{conv} = h * (OvenAirT - Tave)
        If ConcOvenAir > Csat Then
                Q_cond = H_M * latent * (ConcOvenAir - Cs)
                Q evap = 0
        Else
                Q_{cond} = 0
        End If
        If Cs > ConcOvenAir Then
                Q_evap = H_M * latent * (Cs - ConcOvenAir)
                Q_{cond} = 0
        Else
                Q_{evap} = 0
        End If
```

```
Q total = Q conv + Q cond - Q evap
         'Effective heat transfer coefficient based on total flux (convection, condensing, evaporation)
        heff = Q total / (OvenAirT - Tave)
         'Calculate equilibrium values under current conditions
        'Enthalpy
        Hequilibrium = OvenAirT * 3.35 + frozenH + latentW + latentF + (2 * 3.35)
        'Moisture
        If RH \ge 97 Then
                 EMCWB = InitialM
        Else
                 EMC = ((1.9818 * (Tave + 273) * Log(RH / 100)) / -5222.47) ^ (1 / -1.0983)
                 EMCWB = (100 * EMC) / (100 + EMC)
        End If
        X = 1 * InitialM
        If X \leq (EMCWB * 1) Then
                 EMCWB = X
        End If
        'FEM boundary coefficients
        'Heat transfer
        CoefM = heff * SideLength / 6
        CoefS = heff * Hequilibrium * SideLength / 2
        'Moisture transfer
        CoefM_M = H_M * density * moisture_capacity * SideLength / 6
                                                                                'Moisture transfer
        CoefS M = H M * density * moisture capacity * EMCWB * SideLength / 2
        'Stein JSO-IV impingement condition
ElseIf BoundaryType(I) = 2 Then
                                                           'Impingement
         'Calculate transport coefficients
        Re = OvenAirV * W * density_mix / viscosity_mix
        Nu = (2/3) * Pr mix ^ 0.42 * fo ^ 0.75 * ((2 * Re) / (F / fo + fo / F)) ^ (2/3)
        SH = (2/3) * Sc_mix ^0.42 * fo ^0.75 * ((2 * Re) / (F / fo + fo / F)) ^(2/3)
        H M = SH * Dsa / W
        h = Nu * k mix / W
         'Calculate surface moisture concentration
         If Tave < 0 Then
                Csat = 0.000000621530732
```

```
Else
        Csat = 8.12078904E-10 * Tave ^ 3 - 0.000000035203247 * Tave ^ 2 +
                 0.00000131977474 * Tave + 0.000000621530732
End If
 'Calculate effective relative humidity
RH = 100 * (ConcOvenAir / Csat)
MDB = (Mave * 100) / (100 - Mave)
ERH = Exp((-5222.47 * (MDB ^ -1.0983)) / (1.9818 * (Tave + 273)))
Cs = ERH * Csat
'Calculate energy fluxes
Q_{conv} = h * (OvenAirT - Tave)
If ConcOvenAir > Cs Then
        Q_cond = H_M * latent * (ConcOvenAir - Cs)
        Q evap = 0
Else
        Q_{cond} = 0
End If
If Cs > ConcOvenAir Then
        Q evap = H M * latent * (Cs - ConcOvenAir)
        Q cond = 0
Else
        Q_{evap} = 0
End If
Q_{total} = Q_{conv} + Q_{cond} - Q_{evap}
'Effective heat transfer coefficient based on total flux (convection, condensing, evaporation)
heff = Q_total / (OvenAirT - Tave)
'Calculate equilibrium values under current conditions
'Enthalpy
Hequilibrium = OvenAirT * 3.35 + frozenH + latentW + latentF + (2 * 3.35) '792.64 + 6.44
'Moisture
If RH >= 97 Then
        EMCWB = InitialM
Else
        EMC = ((1.9818 * (Tave + 273) * Log(RH / 100)) / -5222.47) ^ (1 / -1.0983)
        EMCWB = (100 * EMC) / (100 + EMC)
End If
X = 1 * InitialM
If X \leq (EMCWB * 1) Then
        EMCWB = X
```

```
'FEM boundary coefficients
      'Heat transfer
     CoefM = heff * SideLength / 6
     CoefS = heff * Hequilibrium * SideLength / 2
      'Moisture transfer
     CoefM_M = H_M * density * moisture_capacity * SideLength / 6
                                                                            'Moisture transfer
     CoefS_M = H_M * density * moisture_capacity * EMCWB * SideLength / 2
                                    'Small oven
ElseIf BoundaryType(I) = 3 Then
     W = 2.6
      'Calculate transport coefficients
     Re = OvenAirV * density_mix * W / viscosity_mix
     Nu = 0.037 * Re ^ 0.8 * Pr_mix ^ (1/3)
     SH = 0.037 * Re^0.8 * Sc_mix^0(1/3) + 0.037 * Re^0.8 * Sc_mix^0(1/3)
     H_M = SH * Dsa / W
     h = Nu * k mix / W
      'Calculate surface moisture concentration
      If Tave < 0 Then
              Csat = 0.000000621530732
     Else
              Csat = 8.12078904E-10 * Tave ^ 3 - 0.000000035203247 * Tave ^ 2 +
                      0.00000131977474 * Tave + 0.000000621530732
     End If
      'Calculate effective relative humidity
     RH = 100 * (ConcOvenAir / Csat)
     MDB = (Mave * 100) / (100 - Mave)
     ERH = Exp((-5222.47 * (MDB ^ -1.0983)) / (1.9818 * (Tave + 273)))
     Cs = ERH * Csat
      'Calculate energy fluxes
     Q_{conv} = h * (OvenAirT - Tave)
     If ConcOvenAir > Csat Then
              Q cond = H M * latent * (ConcOvenAir - Cs)
              Q_{evap} = 0
     Else
              Q_{cond} = 0
```

End If

```
If Cs > ConcOvenAir Then
                 Q_evap = H_M * latent * (Cs - ConcOvenAir)
                 Q cond = 0
        Else
                 Q_{evap} = 0
        End If
        Q total = Q conv + Q cond - Q evap
        'Effective heat transfer coefficient based on total flux (convection, condensing, evaporation)
        heff = Q total / (OvenAirT - Tave)
         'Calculate equilibrium values under current conditions
         'Enthalpy
         Hequilibrium = OvenAirT * 3.35 + frozenH + latentW + latentF + (2 * 3.35)
         'Moisture
        If RH \ge 97 Then
                 EMCWB = InitialM
        Else
                EMC = ((1.9818 * (Tave + 273) * Log(RH / 100)) / -5222.47) ^ (1 / -1.0983)
                EMCWB = (100 * EMC) / (100 + EMC)
        End If
        X = 1 * InitialM
        If X \leq (EMCWB * 1) Then
                EMCWB = X
        End If
         'FEM boundary coefficients
         'Heat transfer
        CoefM = heff * SideLength / 6
        CoefS = heff * Hequilibrium * SideLength / 2
         'Moisture transfer
        CoefM_M = H_M * density * moisture_capacity * SideLength / 6
                                                                               'Moisture transfer
        CoefS M = H M * density * moisture capacity * EMCWB * SideLength / 2
ElseIf BoundaryType(I) = 4 Then
                                    'Stein 102 oven
        h = 8
                   'height above belt
        d = 1.27
                    'nozzle diameter
                    'nozzle spacing
        L = 6
```

End If

```
F = 0.906 * (d/l)^2 offset rows configuration
                        ' 0 0 0 0
                            0 0 0
F = 0.785 * (d/L)^2 'even rows configuration
                         ' 0 0 0 0
                           0 0 0 0
'Calculate transport coefficients
Re = OvenAirV * d * density_mix / viscosity_mix
KHDF = (1 + ((h/d)/(0.6/Sqr(F)))^6)^-0.05
GFHD = ((1 - (2.2 * Sqr(F))) / (1 + 0.2 * (h / d - 6) * Sqr(F))) * 2 * Sqr(F)
FREARN = 0.5 * (Re ^ 0.66)
Nu = (Pr mix ^ 0.42) * KHDF * GFHD * FREARN
SH = (Sc\ mix ^0.42) * KHDF * GFHD * FREARN
H M = SH * Dsa / d
h = Nu * k mix / d
'Calculate surface moisture concentration
If Tave < 0 Then
        Csat = 0.000000621530732
Else
        Csat = 8.12078904E-10 * Tave ^ 3 - 0.000000035203247 * Tave ^ 2 +
                0.00000131977474 * Tave + 0.000000621530732
End If
'Calculate effective relative humidity
RH = 100 * (ConcOvenAir / Csat)
MDB = (Mave * 100) / (100 - Mave)
ERH = Exp((-5222.47 * (MDB ^ -1.0983)) / (1.9818 * (Tave + 273)))
Cs = ERH * Csat
'Calculate energy fluxes
Q conv = h * (OvenAirT - Tave)
If ConcOvenAir > Cs Then
        Q cond = H M * latent * (ConcOvenAir - Cs)
        Q evap = 0
Else
        Q_{cond} = 0
End If
If Cs > ConcOvenAir Then
        Q_evap = H_M * latent * (Cs - ConcOvenAir)
        Q cond = 0
Else
        Q_{evap} = 0
End If
```

```
Q \text{ total} = Q \text{ conv} + Q \text{ cond} - Q \text{ evap}
         'Effective heat transfer coefficient based on total flux (convection, condensing, evaporation)
        heff = Q total / (OvenAirT - Tave)
         'Calculate equilibrium values under current conditions
         'Enthalpy
         Hequilibrium = OvenAirT * 3.35 + frozenH + latentW + latentF '792.64 + 6.44
         'Moisture
        If RH \ge 97 Then
                 EMCWB = InitialM
        Else
                 EMC = ((1.9818 * (Tave + 273) * Log(RH / 100)) / -5222.47) ^ (1 / -1.0983)
                 EMCWB = (100 * EMC) / (100 + EMC)
        End If
        X = 1 * InitialM
        If X \leq (EMCWB * 1) Then
                 EMCWB = X
        End If
         'FEM boundary coefficients
         'Heat transfer
        CoefM = heff * SideLength / 6
        CoefS = heff * Hequilibrium * SideLength / 2
        'Moisture transfer
        CoefM_M = H_M * density * moisture_capacity * SideLength / 6
                                                                                  'Moisture transfer
        CoefS M = H M * density * moisture capacity * EMCWB * SideLength / 2
End If
'Evaluate the element matrices
EKM(1, 1) = 2 * 3.14 / 2 * CoefM * (3 * Ri + Ri)
EKM(1, 2) = 2 * 3.14 / 2 * CoefM * (Ri + Rj)
EKM(2, 1) = 2 * 3.14 / 2 * CoefM * (Ri + Rj)
EKM(2, 2) = 2 * 3.14 / 2 * CoefM * (Ri + 3 * Rj)
EKM_M(1, 1) = 2 * 3.14 / 2 * CoefM_M * (3 * Ri + Rj)
EKM M(1, 2) = 2 * 3.14 / 2 * CoefM M * (Ri + Rj)
EKM M(2, 1) = 2 * 3.14 / 2 * CoefM M * (Ri + Rj)
EKM_M(2, 2) = 2 * 3.14 / 2 * CoefM_M * (Ri + 3 * Rj)
```

```
EFS(1) = 2 * 3.14 / 3 * CoefS * (2 * Ri + Rj)

EFS(2) = 2 * 3.14 / 3 * CoefS * (Ri + 2 * Rj)

EFS_M(1) = 2 * 3.14 / 3 * CoefS_M * (2 * Ri + Rj)

EFS_M(2) = 2 * 3.14 / 3 * CoefS_M * (Ri + 2 * Rj)

End Sub
```

Module - MultplyBandMatrix

Sub MultpyBandMatrix(NumNodes, BandWidth, GSM(), GFV(), ProdVector())

'This module provided by Dr. Larry Segerlind - Michigan State University

This subprogram multiplies a symmetric banded matrix and a column vector

- ' The banded matrix is stored as a rectangular array and only the
- ' coefficients on and above the main diagonal are stored in the array.

End Sub

Module - EleSubscriptValues

Sub EleSubscriptValues(EleNodeData(), KK, NumEleSub, EleSub())

'This module provided by Dr. Larry Segerlind - Michigan State University

```
NumEleSub = 4
If (EleNodeData(KK, 4) = 0) Then NumEleSub = 3
EleSub(1) = EleNodeData(KK, 1)
EleSub(2) = EleNodeData(KK, 2)
EleSub(3) = EleNodeData(KK, 3)
EleSub(4) = EleNodeData(KK, 4)
```

End Sub

^{&#}x27;This subprogram calculates the subscripts associated with the

^{&#}x27; element. The subprogram allows the element to have one, two or

^{&#}x27; three unknown values at a node.

Module - ESMatrix2DField

Ak = XI * Yj - Xj * YI

Bi = Yj - Yk Bj = Yk - YIBk = YI - Yj

```
Sub ESMatrix2DField(EleMatlData(), EleNodeData(), Coord(), ElePhyData(), EFV(), ESM(),
EFV M(), ESM M(), EFV F(), ESM F(), Volume(), KK)
'This module heavily modified from a module by Dr. Larry Segerlind - Michigan State University
'This subprogram calculates the element stiffness matrix and element
' force vector for the three node triangular and the four node
' bilinear rectangular element
'Evaluation of the parameters in the element stiffness matrix
MatlSet = EleMatlData(KK)
Thermal properties
Dx = ElePhyData(MatlSet, 1)
Dy = ElePhyData(MatlSet, 2)
G = ElePhyData(MatlSet, 3)
Q = ElePhyData(MatlSet, 4)
'Moisture transfer properties
Dx M = ElePhyData(MatlSet, 6)
Dy M = ElePhyData(MatlSet, 7)
G M = ElePhyData(MatlSet, 8)
Q_M = ElePhyData(MatlSet, 9)
'Fat transfer properties
Dx F = ElePhyData(MatlSet, 11)
Dy F = ElePhyData(MatlSet, 12)
G F = ElePhyData(MatlSet, 13)
Q F = ElePhyData(MatlSet, 14)
'Evaluate the element stiffness matrix
If (EleNodeData(KK, 4) = 0) Then
                                       'Triangular Element
        XI = Coord(EleNodeData(KK, 1), 1)
        YI = Coord(EleNodeData(KK, 1), 2)
        X_j = Coord(EleNodeData(KK, 2), 1)
        Yj = Coord(EleNodeData(KK, 2), 2)
        Xk = Coord(EleNodeData(KK, 3), 1)
        Yk = Coord(EleNodeData(KK, 3), 2)
        Ai = Xj * Yk - Xk * Yj
        Aj = Xk * YI - XI * Yk
```

```
Ci = Xk - Xi
        Cj = XI - Xk
        Ck = Xj - XI
        TwiceArea = Ai + Aj + Ak
        Rbar = (XI + Xj + Xk) / 3
        Volume(KK) = TwiceArea * 3.14 * Rbar
        DxOver4A = Dx / (2 * TwiceArea)
        DyOver4A = Dy / (2 * TwiceArea)
        GAreaOver12 = G * TwiceArea / 24
        Dx MOver4A = Dx M/(2 * TwiceArea)
        Dy MOver4A = Dy M/(2 * TwiceArea)
        G MAreaOver12 = G M * TwiceArea / 24
        Dx FOver4A = Dx F/(2 * TwiceArea)
        Dy FOver4A = Dy F/(2 * TwiceArea)
        G FAreaOver12 = G F * TwiceArea / 24
        'Calculate the element stiffness matrix - enthalpy
        ESM(1, 1) = 2 * 3.14 * Rbar * (DxOver4A * Bi * Bi + DyOver4A * Ci * Ci) + 2 * 3.14 *
Rbar *
                GAreaOver12 * 2
        ESM(1, 2) = 2 * 3.14 * Rbar * (DxOver4A * Bi * Bj + DyOver4A * Ci * Cj) + 2 * 3.14 *
Rbar *
                GAreaOver12
        ESM(1, 3) = 2 * 3.14 * Rbar * (DxOver4A * Bi * Bk + DyOver4A * Ci * Ck) + 2 * 3.14 *
Rbar *
                GAreaOver12
        ESM(2, 1) = ESM(1, 2)
        ESM(2, 2) = 2 * 3.14 * Rbar * (DxOver4A * Bj * Bj + DyOver4A * Cj * Cj) + 2 * 3.14 *
Rbar *
                GAreaOver12 * 2
        ESM(2, 3) = 2 * 3.14 * Rbar * (DxOver4A * Bj * Bk + DyOver4A * Cj * Ck) + 2 * 3.14 *
Rbar *
                GAreaOver12
        ESM(3, 1) = ESM(1, 3)
        ESM(3, 2) = ESM(2, 3)
        ESM(3, 3) = 2 * 3.14 * Rbar * (DxOver4A * Bk * Bk + DyOver4A * Ck * Ck) + 2 * 3.14 *
Rbar
                * GAreaOver12 * 2
        'Calculate the element stiffness matrix - moisture
        ESM M(1, 1) = 2 * 3.14 * Rbar * (Dx MOver4A * Bi * Bi + Dy MOver4A * Ci * Ci) + 2 *
3.14
                * Rbar * G MAreaOver12 * 2
        ESM M(1, 2) = 2 * 3.14 * Rbar * (Dx MOver4A * Bi * Bj + Dy MOver4A * Ci * Cj) + 2 *
3.14
                * Rbar * G MAreaOver12
        ESM_M(1, 3) = 2 * 3.14 * Rbar * (Dx_MOver4A * Bi * Bk + Dy_MOver4A * Ci * Ck) + 2*
                3.14 * Rbar * G MAreaOver12
        ESM_M(2, 1) = ESM_M(1, 2)
```

```
ESM M(2, 2) = 2 * 3.14 * Rbar * (Dx MOver4A * Bj * Bj + Dy MOver4A * Cj * Cj) + 2 *
3.14
                * Rbar * G MAreaOver12 * 2
        ESM M(2, 3) = 2 * 3.14 * Rbar * (Dx MOver4A * Bj * Bk + Dy MOver4A * Cj * Ck) + 2
                 3.14 * Rbar * G MAreaOver12
        ESM M(3, 1) = ESM M(1, 3)
        ESM M(3, 2) = ESM M(2, 3)
        ESM_M(3, 3) = 2 * 3.14 * Rbar * (Dx_MOver4A * Bk * Bk + Dy MOver4A * Ck * Ck) + 2
                3.14 * Rbar * G MAreaOver12 * 2
        'Calculate the element stiffness matrix - fat
        ESM F(1, 1) = 2 * 3.14 * Rbar * (Dx FOver4A * Bi * Bi + Dy FOver4A * Ci * Ci) + 2 *
3.14 *
                Rbar * G FAreaOver12 * 2
        ESM F(1, 2) = 2 * 3.14 * Rbar * (Dx FOver4A * Bi * Bj + Dy FOver4A * Ci * Cj) + 2 *
3.14 *
                Rbar * G FAreaOver12
        ESM F(1, 3) = 2 * 3.14 * Rbar * (Dx FOver4A * Bi * Bk + Dy FOver4A * Ci * Ck) + 2 *
3.14 *
                Rbar * G FAreaOver12
        ESM F(2, 1) = ESM F(1, 2)
        ESM F(2, 2) = 2 * 3.14 * Rbar * (Dx FOver4A * Bj * Bj + Dy FOver4A * Cj * Cj) + 2 *
3.14 *
                Rbar * G FAreaOver12 * 2
        ESM F(2, 3) = 2 * 3.14 * Rbar * (Dx FOver4A * Bj * Bk + Dy FOver4A * Cj * Ck) + 2 *
3.14 *
                Rbar * G FAreaOver12
        ESM F(3, 1) = ESM F(1, 3)
        ESM F(3, 2) = ESM F(2, 3)
        ESM_F(3, 3) = 2 * 3.14 * Rbar * (Dx_FOver4A * Bk * Bk + Dy FOver4A * Ck * Ck) + 2 *
3.14
                * Rbar * G FAreaOver12 * 2
        'Calculate the element force vector - enthalpy
        EFV(1) = (2 * 3.14 / 4) * (Q * TwiceArea / 6) * (2 * XI + Xj + Xk)
        EFV(2) = (2 * 3.14 / 4) * (Q * TwiceArea / 6) * (XI + 2 * Xj + Xk)
        EFV(3) = (2 * 3.14 / 4) * (Q * TwiceArea / 6) * (XI + Xj + 2 * Xk)
        'Calculate the element force vector - moisture
        EFV M(1) = (2 * 3.14 / 4) * (Q_M * TwiceArea / 6) * (2 * XI + Xj + Xk)
        EFV M(2) = (2 * 3.14 / 4) * (Q M * TwiceArea / 6) * (XI + 2 * Xj + Xk)
        EFV M(3) = (2 * 3.14 / 4) * (Q M * TwiceArea / 6) * (XI + Xj + 2 * Xk)
        'Calculate the element force vector - fat
        EFV F(1) = (2 * 3.14 / 4) * (O F * TwiceArea / 6) * (2 * XI + Xj + Xk)
        EFV F(2) = (2 * 3.14 / 4) * (Q F * TwiceArea / 6) * (XI + 2 * Xj + Xk)
        EFV F(3) = (2 * 3.14 / 4) * (Q_F * TwiceArea / 6) * (XI + Xj + 2 * Xk)
```

'Rectangular element

Else

```
XLength = Coord(EleNodeData(KK, 2), 1) - Coord(EleNodeData(KK, 1), 1)
YLength = Coord(EleNodeData(KK, 4), 2) - Coord(EleNodeData(KK, 1), 2)
Area = XLength * YLength
Rbar = (Coord(EleNodeData(KK, 1), 1) + Coord(EleNodeData(KK, 2), 1) +
       Coord(EleNodeData(KK, 3), 1) + Coord(EleNodeData(KK, 4), 1)) / 4
Volume(KK) = Area * 2 * Rbar * 3.14
DxAover6B = Dx * YLength / (6 * XLength)
DyBover6A = Dy * XLength / (6 * YLength)
GAreaover36 = G * Area / 36
Dx MAover6B = Dx M * YLength / (6 * XLength)
Dy MBover6A = Dy M * XLength / (6 * YLength)
G MAreaover36 = G M * Area / 36
Dx FAover6B = Dx F * YLength / (6 * XLength)
Dy FBover6A = Dy F * XLength / (6 * YLength)
G FAreaover36 = G F * Area / 36
'Calculate element stiffness matrix - enthalpy
ESM(1, 1) = 2 * DxAover6B + 2 * DyBover6A + 4 * GAreaover36
ESM(1, 2) = -2 * DxAover6B + DyBover6A + 2 * GAreaover36
ESM(1, 3) = -DxAover6B - DyBover6A + GAreaover36
ESM(1, 4) = DxAover6B - 2 * DyBover6A + 2 * GAreaover36
ESM(2, 1) = ESM(1, 2)
ESM(2, 2) = ESM(1, 1)
ESM(2, 3) = ESM(1, 4)
ESM(2, 4) = ESM(1, 3)
ESM(3, 1) = ESM(1, 3)
ESM(3, 2) = ESM(2, 3)
ESM(3, 3) = ESM(1, 1)
ESM(3, 4) = ESM(1, 2)
ESM(4, 1) = ESM(1, 4)
ESM(4, 2) = ESM(2, 4)
ESM(4, 3) = ESM(3, 4)
ESM(4, 4) = ESM(1, 1)
'Calculate element stiffness matrix - moisture
ESM M(1, 1) = 2 * Dx MAover6B + 2 * Dy MBover6A + 4 * G MAreaover36
ESM M(1, 2) = -2 * Dx MAover6B + Dy MBover6A + 2 * G MAreaover36
ESM M(1, 3) = -Dx MAover6B - Dy MBover6A + G MAreaover36
ESM M(1, 4) = Dx MAover6B - 2 * Dy MBover6A + 2 * G MAreaover36
ESM M(2, 1) = ESM M(1, 2)
ESM M(2, 2) = ESM M(1, 1)
ESM M(2, 3) = ESM M(1, 4)
ESM M(2, 4) = ESM M(1, 3)
ESM M(3, 1) = ESM M(1, 3)
ESM M(3, 2) = ESM M(2, 3)
ESM M(3, 3) = ESM M(1, 1)
ESM M(3, 4) = ESM M(1, 2)
ESM M(4, 1) = ESM M(1, 4)
ESM_M(4, 2) = ESM_M(2, 4)
ESM M(4, 3) = ESM M(3, 4)
ESM M(4, 4) = ESM M(1, 1)
```

'Calculate element stiffness matrix - fat

```
ESM_F(1, 1) = 2 * Dx_FAover6B + 2 * Dy_FBover6A + 4 * G_FAreaover36
ESM F(1, 2) = -2 * Dx FAover6B + Dy_FBover6A + 2 * G_FAreaover36
ESM F(1, 3) = -Dx FAover6B - Dy FBover6A + G FAreaover36
ESM_F(1, 4) = Dx_FAover6B - 2 * Dy_FBover6A + 2 * G FAreaover36
ESM_F(2, 1) = ESM_F(1, 2)
ESM F(2, 2) = ESM F(1, 1)
ESM_F(2, 3) = ESM_F(1, 4)
ESM_F(2, 4) = ESM_F(1, 3)
ESM F(3, 1) = ESM F(1, 3)
ESM_F(3, 2) = ESM_F(2, 3)
ESM F(3, 3) = ESM F(1, 1)
ESM_F(3, 4) = ESM_F(1, 2)
ESM F(4, 1) = ESM F(1, 4)
ESM_F(4, 2) = ESM_F(2, 4)
ESM_F(4, 3) = ESM_F(3, 4)
ESM_F(4, 4) = ESM_F(1, 1)
'Calculate element force vector - enthalpy
EFV(1) = Q * Area / 4
EFV(2) = EFV(1)
EFV(3) = EFV(1)
EFV(4) = EFV(1)
'Calculate element force vector - moisture
EFV M(1) = Q M * Area / 4
EFV_M(2) = EFV_M(1)
EFV M(3) = EFV M(1)
EFV_M(4) = EFV_M(1)
'Calculate element force vector - fat
EFV_F(1) = Q_F * Area / 4
EFV F(2) = EFV F(1)
EFV F(3) = EFV F(1)
EFV_F(4) = EFV_F(1)
```

End If

Module - InputBasicData

Sub InputBasicData(NumMatlSets, NumNodes, NumEle, Coord(), EleMatlData(), EleNodeData())

This module slightly modified from a module by Dr. Larry Segerlind - Michigan State University

```
This subprogram inputs the nodal coordinates, the element material
```

```
For I = 1 To NumNodes
Input #1, Coord(I, 1), Coord(I, 2)
```

Next I

For I = 1 To NumEle
Input #1, EleMatlData(I), EleNodeData(I, 1), EleNodeData(I, 2), EleNodeData(I, 3),
EleNodeData(I, 4)

Next I

^{&#}x27; index, the element node numbers and the equation coefficients Dx, Dy,

^{&#}x27; G and Q

Module - InputDerivBC

Sub InputDerivBC(NumDerivBC, NumBdyNodes, BdyNode(), SubDerivBC(), BoundaryType())

'This module slightly modified from a module by Dr. Larry Segerlind - Michigan State University

'This subprogram inputs the subscripts and coefficients for the

```
For I = 1 To NumDerivBC
Input #1, SubDerivBC(I, 1), SubDerivBC(I, 2), BoundaryType(I)
```

Next I

For I = 1 To NumBdyNodes Input #1, BdyNode(I)

Next I

^{&#}x27; derivative boundary condition

Module - BuildGAM

```
Sub BuildGAM(BandWidth, GAM(), GCM(), GSM(), GAM_M(), GCM_M(), GSM_M(), GAM_F(), GCM_F(), GSM_F(), timestep, NumNodes)
```

'This module calculates the A matrix for the finite difference time solution using the central ' difference method

```
For X = 1 To NumNodes
```

```
For Y = 1 To BandWidth GAM(X, Y) = GCM(X, Y) + (GSM(X, Y) * (timestep / 2)) GAM\_M(X, Y) = GCM\_M(X, Y) + (GSM\_M(X, Y) * (timestep / 2)) GAM\_F(X, Y) = GCM\_F(X, Y) + (GSM\_F(X, Y) * (timestep / 2)) Next Y
```

Next X

Module - SolveBandMatrix

```
Sub SolveBandMatrix(NumNodes, BandWidth, GSV(), GFV(), GSM())
```

'This module provide by Dr. Larry Segerlind - Michigan State University

This subprogram solves the system of banded equations using the method

- ' of Gaussian elimination. The stiffness matrix has been decomposed
- ' prior to entering this subprogram using DecomposeBandMatrix.
- ' This subprogram decomposes the column vector GFV(NumNodalVal%) before
- ' solving the system using backward substitution

'Decompose the global force vector

```
For I = 1 To (NumNodes - 1)
        MJ = I + BandWidth - 1
        If (MJ > NumNodes) Then
                MJ = NumNodes
        End If
        NJ = I + 1
        L = 1
        For J = NJ To MJ
                L = L + 1
                GFV(J) = GFV(J) - GSM(I, L) * GFV(I) / GSM(I, 1)
        Next J
Next I
'Solution by backward substitution
GSV(NumNodes) = GFV(NumNodes) / GSM(NumNodes, 1)
For K = 1 To (NumNodes - 1)
        I = NumNodes - K
        MJ = BandWidth
        If ((I + BandWidth - 1) > NumNodes) Then
                MJ = NumNodes - I + 1
        End If
        Sum = 0!
        For J = 2 To MJ
                n = I + J - 1
                Sum = Sum + GSM(I, J) * GSV(n)
        GSV(I) = (GFV(I) - Sum) / GSM(I, 1)
Next K
```

Module - BuildBandedSystem

```
Sub BuildBandedSystem(NumEleSub, EleSub(), EFV(), ESM(), GFV(), GSM(), ECM(), GCM(), EFV_M(), ESM_M(), GFV_M(), GSM_M(), ECM_M(), GCM_M(), EFV_F(), ESM_F(), GFV_F(), GSM_F(), ECM_F(), GCM_F())
```

'This module modified from a module provided by Dr. Larry Segerlind - Michigan State University

This subprogram incorporates the element force vector and the element

- ' stiffness matrix into the global force matrix and the global stiffness
- ' matrix.

'This subprogram ASSUMES that the global stiffness matrix is symmetrical

' and stored in a rectangular format.

The direct stiffness method for a banded system of equations

```
For I = 1 To NumEleSub
        II = EleSub(I)
        'Force vector
        GFV(II) = GFV(II) + EFV(I)
        GFV M(II) = GFV M(II) + EFV M(I)
        GFV F(II) = GFV F(II) + EFV F(I)
        For J = 1 To NumEleSub
                JJ = EleSub(J)
                JJ = JJ - II + 1
                If (JJ > 0) Then
                         'Stiffness matrix
                         GSM(II, JJ) = GSM(II, JJ) + ESM(I, J)
                         GSM M(II, JJ) = GSM M(II, JJ) + ESM M(I, J)
                         GSM F(II, JJ) = GSM F(II, JJ) + ESM F(I, J)
                         'Capacitance matrix
                        GCM(II, JJ) = GCM(II, JJ) + ECM(I, J)
                         GCM M(II, JJ) = GCM M(II, JJ) + ECM M(I, J)
                        GCM F(II, JJ) = GCM F(II, JJ) + ECM F(I, J)
                End If
        Next J
```

Next I

Module – BuildGPM

```
Sub BuildGPM(BandWidth, GPM(), GCM(), GSM(), GPM_M(), GCM_M(), GSM_M(), GPM_F(), GCM_F(), GSM_F(), timestep, NumNodes)

'This module calculates the P matrix for the finite difference time solution using the central ' difference method
```

```
For X = 1 To NumNodes
```

```
For Y = 1 To BandWidth GPM(X, Y) = GCM(X, Y) - (GSM(X, Y) * (timestep / 2)) GPM\_M(X, Y) = GCM\_M(X, Y) - (GSM\_M(X, Y) * (timestep / 2)) GPM\_F(X, Y) = GCM\_F(X, Y) - (GSM\_F(X, Y) * (timestep / 2)) Next Y
```

Next X

Module - ModifyGFV

```
Sub ModifyGFV(GFV(), GFV_A(), GFV_Star(), GFV_M(), GFV_M_A(), GFV_M_Star(), GFV_F_A(), GFV_F_Star(), GFV_F(), timestep, NumNodes)
```

'Modify the global force vector for the finite difference time solution

```
For X = 1 To NumNodes

GFV\_Star(X) = (GFV\_A(X) + GFV(X)) * (timestep / 2)

GFV\_M\_Star(X) = (GFV\_M(X) + GFV\_M(X)) * (timestep / 2)

GFV\_F\_Star(X) = (GFV\_F\_A(X) + GFV\_F(X)) * (timestep / 2)
```

Next X

Module - EleCapMatrix

```
Sub EleCapMatrix(ElePhyData(), EleNodeData(), ECM(), ECM M(), ECM F(), Coord(), KK)
'Compose the element capacitance matrix
If (EleNodeData(KK, 4) = 0) Then
        'Triangular Element
          [c]=lamda*A/3*[100]
                   010
                   011]
       EleNode1 = EleNodeData(KK, 1)
       EleNode2 = EleNodeData(KK, 2)
       EleNode3 = EleNodeData(KK, 3)
        'Calculate the element area
       Ri = Coord(EleNode1, 1)
       R_j = Coord(EleNode2, 1)
       Rk = Coord(EleNode3, 1)
       Rbar = (Ri + Rj + Rk) / 3
       XLengthSide1 = Coord(EleNode2, 1) - Coord(EleNode1, 1)
       YLengthSide1 = Coord(EleNode2, 2) - Coord(EleNode1, 2)
       XLengthSide2 = Coord(EleNode3, 1) - Coord(EleNode2, 1)
       YLengthSide2 = Coord(EleNode3, 2) - Coord(EleNode2, 2)
       XLengthSide3 = Coord(EleNode3, 1) - Coord(EleNode1, 1)
       YLengthSide3 = Coord(EleNode3, 2) - Coord(EleNode1, 2)
       Side1Length = Sqr(XLengthSide1 ^ 2 + YLengthSide1 ^ 2)
       Side2Length = Sqr(XLengthSide2 ^ 2 + YLengthSide2 ^ 2)
       Side3Length = Sqr(XLengthSide3 ^ 2 + YLengthSide3 ^ 2)
       HalfP = (Side1Length + Side2Length + Side3Length) / 2
       Area = Sqr(HalfP * (HalfP - Side1Length) * (HalfP - Side2Length) * (HalfP - Side3Length))
       Lamda = ElePhyData(1, 5)
       Lamda_M = ElePhyData(1, 10)
       Lamda F = ElePhyData(1, 15)
       ECM(1, 1) = 2 * 3.14 * Rbar * Lamda * Area / 3
       ECM(2, 2) = 2 * 3.14 * Rbar * Lamda * Area / 3
       ECM(3, 3) = 2 * 3.14 * Rbar * Lamda * Area / 3
       ECM M(1, 1) = 2 * 3.14 * Rbar * Lamda M * Area / 3
       ECM M(2, 2) = 2 * 3.14 * Rbar * Lamda M * Area / 3
       ECM_M(3, 3) = 2 * 3.14 * Rbar * Lamda_M * Area / 3
       ECM F(1, 1) = 2 * 3.14 * Rbar * Lamda F * Area / 3
```

```
ECM F(2, 2) = 2 * 3.14 * Rbar * Lamda F * Area / 3
       ECM F(3, 3) = 2 * 3.14 * Rbar * Lamda F * Area / 3
Else
        'Rectangular element
        ' [c]=lamda*A/4*[ 1 0 0 0
                   0100
                   0010
                   0001]
       EleNode1 = EleNodeData(KK, 1)
       EleNode2 = EleNodeData(KK, 2)
       EleNode3 = EleNodeData(KK, 3)
       EleNode4 = EleNodeData(KK, 4)
        'Calculate the element area
       Side1 = Coord(EleNode1, 2) - Coord(EleNode1, 2)
       Side2 = Coord(EleNode2, 1) - Coord(EleNode1, 1)
       Area = Side1 * Side2
       Lamda = ElePhyData(1, 5)
       Lamda M = ElePhyData(1, 10)
       Lamda_F = ElePhyData(1, 15)
        For J = 1 To 4
               ECM(J, J) = Lamda * Area / 4
               ECM M(J, J) = Lamda M * Area / 4
               ECM_F(J, J) = Lamda_F * Area / 4
       Next J
```

End If

Module - ConvertHtoTemp

```
Sub ConvertHtoTemp(heat_capacity_f, GSV(), GSV_M(), GSV_F(), temperature(), NumNodes,
InitialM,
        Solid, frozenH, latentW, latentF, heat capacity, LevelOne, LevelTwo, LevelThree,
LevelFour,
        LevelFive)
'Convert enthalpy to temperature data
For K = 1 To NumNodes
         If GSV(K) < LevelOne Then
                 temperature(K) = GSV(K) / heat_capacity_f - 273
        ElseIf GSV(K) >= LevelOne And <math>GSV(K) <= LevelTwo Then
                 temperature(K) = -2
        ElseIf GSV(K) > LevelTwo And <math>GSV(K) \le LevelThree Then
                 temperature(K) = ((GSV(K) - (frozenH + latentW)) / 3.35) - 2
        ElseIf GSV(K) > LevelThree And <math>GSV(K) \le LevelFour Then
                 temperature(K) = 45
        ElseIf GSV(K) > LevelFour Then
                 temperature(K) = ((GSV(K) - (frozenH + latentW + latentF)) / 3.35) - 2
        End If
Next K
End Sub
```

Module – CalculateProperties

```
Sub CalculateProperties(Meat, Solid, NumEle, EleNodeData(), ElePhyData(), temperature(), GSV M,
                   GSV F(), moisture capacity, density)
For I = 1 To NumEle
                    'Calculate element average temperature, moisture, and fat
                   If EleNodeData(I, 4) = 0 Then
                                     ElementAverageT = (1 * temperature(EleNodeData(I, 1)) + 1 *
                                                       temperature(EleNodeData(I, 2)) + 1 * temperature(EleNodeData(I, 3))) / 3
                                     ElementAverageM = (1 * GSV M(EleNodeData(I, 1)) + 1 *
GSV_M(EleNodeData(I, 2))
                                                         + 1 * GSV_M(EleNodeData(I, 3))) / 3
                                     ElementAverageFP = (1 * GSV F(EleNodeData(I, 1)) + 1 * GSV F(EleNodeData(I,
2))
                                                        + 1 * GSV F(EleNodeData(I, 3))) / 3
                  Else
                                     ElementAverageT = (1 * temperature(EleNodeData(I, 1)) + 1 *
                                                        temperature(EleNodeData(I, 2)) + 1 * temperature(EleNodeData(I, 3)) + 1
                                                         temperature(EleNodeData(I, 4))) / 4
                                     ElementAverageM = (1 * GSV M(EleNodeData(I, 1)) + 1 *
GSV M(EleNodeData(I, 2))
                                                         + 1 * GSV M(EleNodeData(I, 3)) + 1 * GSV M(EleNodeData(I, 4))) / 4
                                     ElementAverageFP = (1 * GSV_F(EleNodeData(I, 1)) + 1 * GSV_F
2))
                                                        + 1 * GSV F(EleNodeData(I, 3)) + 1 * GSV_F(EleNodeData(I, 4))) / 4
                  End If
                  moisture = ElementAverageM / 100
                                                                                                                          'Element average moisture, decimal wb
                  MP = Solid
                                                                                                     'Mass protein
                  MF = ElementAverageFP * Solid
                                                                                                                         'Mass fat
                  MM = (moisture * MF + moisture * MP) / (1 - moisture) 'Mass moisture
                  Total = MP + MM + MF
                                                                                                                   'Mass total
                  Fat = MF / Total
                                                                                                       'Percent fat
                  Protein = MP / Total
                                                                                                          Percent protein
                   'Beef
                  If Meat = 1 Then
                                    If ElementAverageT <= -2 Then
                                                       heat capacity = 1.9 * moisture + 1.711 * Protein + 1.298 * Fat
                                    Else
                                                        heat_capacity = 0.9 * (4.18 * moisture + 1.711 * Protein + 1.298 * Fat)
'(4.18 *
                                                                         moisture + 1.711 * Protein + 1.298 * Fat)
                                    End If
                                    moisture capacity = 0.003
                                                                                                                                       'g/g
```

```
'g/cm^3
                 density = 1 / (moisture + Fat / 0.9 + Protein / 1.4)
                 Vmoisture = moisture / 1 'Volume moisture
                 Vprotein = Protein / 1.4 'Volume protein
                 V fat = Fat / 0.9
                                       'Volume fat
                 Vtotal = Vmoisture + Vprotein + Vfat 'Total volume
                 VFm = Vmoisture / Vtotal 'Volume fraction moisture
                 VFp = Vprotein / Vtotal 'Volume fraction protein
                 VFf = Vfat / Vtotal
                                         'Volume fraction fat
                  'thermal conductivity
                 ElePhyData(1, 1) = ((0.602 * VFm + 0.18 * VFf + 0.2 * VFp) / 100)
                 ElePhyData(1, 2) = ((0.602 * VFm + 0.18 * VFf + 0.2 * VFp) / 100)
                                                                                'density*heat
                 ElePhyData(1, 5) = heat capacity * density
capacity
                  'Coefficient for Mittal moisture diffusivity equation
                 A = 0.003
                 ElePhyData(1, 6) = 10000 * A * (0.003 * Exp(-0.442 * ElementAverageFP - 4829.7)
/
                          (ElementAverageT + 273) + 11.55 * moisture)) * moisture_capacity *
                          density 'moisture conductivity
                 ElePhyData(1, 7) = 10000 * A * (0.003 * Exp(-0.442 * ElementAverageFP - 4829.7)
                          (ElementAverageT + 273) + 11.55 * moisture)) * moisture_capacity *
                          density 'moisture conductivity
                 ElePhyData(1, 10) = density * moisture_capacity
                                                                              'density*moisture
capacity
                  If ElementAverageT <= 45 Then
                                                         'fat diffusivity r-direction zero below
                          ElePhyData(1, 11) = 0
melting
                                                         'fat diffusivity z-direction zero below
                          ElePhyData(1, 12) = 0
melting
                 Else
                          ElePhyData(1, 11) = 0.0008
                                                           'fat diffusivity r-direction
                                                           'fat diffusivity z-direction
                          ElePhyData(1, 12) = 0.0008
                 End If
                 ElePhyData(1, 15) = 1
                                                  'Variable not used for fat trasfer equations
        'Pork
        ElseIf Meat = 2 Then
                 If ElementAverageT <= -2 Then
                          heat capacity = 1.9 * moisture + 1.711 * Protein + 1.298 * Fat
                 Else
                          heat capacity = (4.18 * moisture + 1.711 * Protein + 1.298 * Fat) '(4.18 *
                                  moisture + 1.711 * Protein + 1.298 * Fat)
                 End If
```

```
moisture capacity = 0.003
                                                                'g/g
                 density = 1 / (moisture + Fat / 0.9 + Protein / 1.4) 'g/cm<sup>3</sup>
                 Vmoisture = moisture / 1 'Volume moisture
                 Vprotein = Protein / 1.4 'Volume protein
                 V fat = Fat / 0.9
                                       'Volume fat
                 Vtotal = Vmoisture + Vprotein + Vfat Total volume
                 VFm = Vmoisture / Vtotal 'Volume fraction moisture
                 VFp = Vprotein / Vtotal 'Volume fraction protein
                 VFf = Vfat / Vtotal
                                         'Volume fraction fat
                 'thermal conductivity
                 ElePhyData(1, 1) = ((0.602 * VFm + 0.18 * VFf + 0.2 * VFp) / 100)
                 ElePhyData(1, 2) = ((0.602 * VFm + 0.18 * VFf + 0.2 * VFp) / 100)
                 ElePhyData(1, 5) = heat_capacity * density
                                                                                'density*heat
capacity
                  'Coefficient for Mittal moisture diffusivity equation
                 A = 0.003
                 ElePhyData(1, 6) = 10000 * A * (0.003 * Exp(-0.442 * ElementAverageFP - 4829.7)
/
                          (ElementAverageT + 273) + 11.55 * moisture)) * moisture_capacity *
                 density
                           'moisture conductivity 0.000000129 '
                 ElePhyData(1, 7) = 10000 * A * (0.003 * Exp(-0.442 * ElementAverageFP - 4829.7)
                          (ElementAverageT + 273) + 11.55 * moisture)) * moisture capacity *
                 density
                           'moisture conductivity 0.0000000129 '
                 ElePhyData(1, 10) = density * moisture capacity
                                                                             'density*moisture
capacity
                 If ElementAverageT <= 45 Then
                          ElePhyData(1, 11) = 0
                                                         'fat diffusivity r-direction zero below
melting
                          ElePhyData(1, 12) = 0
                                                         'fat diffusivity z-direction zero below
melting
                 Else
                                                            'fat diffusivity r-direction
                          ElePhyData(1, 11) = 0.00125
                                                            'fat diffusivity z-direction
                          ElePhyData(1, 12) = 0.00125
                 End If
                 ElePhyData(1, 15) = 1
                                                  'Variable not used for fat trasfer equations
         'Turkey
         ElseIf Meat = 3 Then
                  If ElementAverageT <= -2 Then
```

```
heat capacity = 1.9 * moisture + 1.711 * Protein + 1.298 * Fat
                 Else
                          heat capacity = (4.18 * moisture + 1.711 * Protein + 1.298 * Fat) '(4.18 *
                          moisture + 1.711 * Protein + 1.298 * Fat)
                 End If
                 moisture capacity = 0.003
                 density = 1 / (moisture + Fat / 0.9 + Protein / 1.4) 'g/cm<sup>3</sup>
                 Vmoisture = moisture / 1 'Volume of moisture
                 Vprotein = Protein / 1.4 'Volume of protein
                 V fat = Fat / 0.9
                                       'Volume of fat
                 Vtotal = Vmoisture + Vprotein + Vfat Total volume
                 VFm = Vmoisture / Vtotal 'Volume fraction moisture
                 VFp = Vprotein / Vtotal 'Volume fraction protein
                 VFf = Vfat / Vtotal
                                         'Volume fraction fat
                 'thermal conductivity
                 ElePhyData(1, 1) = ((0.602 * VFm + 0.18 * VFf + 0.2 * VFp) / 100)
                 ElePhyData(1, 2) = ((0.602 * VFm + 0.18 * VFf + 0.2 * VFp) / 100)
                                                                                'density*heat
                 ElePhyData(1, 5) = heat_capacity * density
capacity
                 'Coefficient for Mittal moisture diffusivity equation
                 A = 0.003
                 ElePhyData(1, 6) = 10000 * A * (0.003 * Exp(-0.442 * ElementAverageFP - 4829.7)
                          (ElementAverageT + 273) + 11.55 * moisture)) * moisture capacity *
                 density
                          'moisture conductivity
                 ElePhyData(1, 7) = 10000 * A * (0.003 * Exp(-0.442 * ElementAverageFP - 4829.7
                          (ElementAverageT + 273) + 11.55 * moisture)) * moisture capacity *
                 density
                          'moisture conductivity
                 ElePhyData(1, 10) = density * moisture capacity
                                                                              'density*moisture
capacity
                 If ElementAverageT <= 45 Then
                          ElePhyData(1, 11) = 0
                                                         'fat diffusivity r-direction zero below
melting
                                                         'fat diffusivity z-direction zero below
                          ElePhyData(1, 12) = 0
melting
                 Else
                          ElePhyData(1, 11) = 0.00125
                                                            'fat diffusivity r-direction
                                                            'fat diffusivity z-direction
                          ElePhyData(1, 12) = 0.00125
                 End If
                                                  'Variable not used for fat trasfer equations
                 ElePhyData(1, 15) = 1
        End If
```

Next I

Module - CalculateElementAverage

```
This module calculates a weighted volume average of the nodal values.
ReDim VolumeRatio(NumEle)
ReDim ElementAverage(NumEle)
WeightedAverage = 0
For KK = 1 To NumEle
        TotalVolume = TotalVolume + Volume(KK)
        'Calculate the element average of the nodal values
        If (EleNodeData(KK, 4) = 0) Then
                                                                             'Triangular
element
                Node1 = EleNodeData(KK, 1)
                Node2 = EleNodeData(KK, 2)
                Node3 = EleNodeData(KK, 3)
                ElementAverage(KK) = (Phi(Node1) + Phi(Node2) + Phi(Node3)) / 3
                                                                             'Rectangular
        Else
element
                Node1 = EleNodeData(KK, 1)
                Node2 = EleNodeData(KK, 2)
                Node3 = EleNodeData(KK, 3)
                Node4 = EleNodeData(KK, 4)
                ElementAverage(KK) = (Phi(Node1) + Phi(Node2) + Phi(Node3) + Phi(Node4)) / 4
        End If
Next KK
'Calculate the volume weighted average
For KK = 1 To NumEle
        VolumeRatio(KK) = Volume(KK) / TotalVolume
        ElementAverage(KK) = ElementAverage(KK) * VolumeRatio(KK)
Next KK
For I = 1 To NumEle
        WeightedAverage = WeightedAverage + ElementAverage(I)
Next I
End Sub
```

Sub CalculateElementAverage(Volume(), NumEle, EleNodeData(), Phi(), WeightedAverage)

Module-Input Oven Conditions

```
Sub InputOvenConditions(OvenConditions(), NumTimeSteps)
```

'Input oven conditions from file

```
For I = 1 To NumTimeSteps
Input #2, OvenConditions(I, 1), OvenConditions(I, 2), OvenConditions(I, 3)
If OvenConditions(I, 2) = 0 Then OvenConditions(I, 2) = 1
```

Next I

Module - CalculateSurfaceFatContent

Sub CalculateSurfaceFatContent(InitialF, T, GSV_F(), NumBdyNodes, BdyNode(), temperature(), timestep)

'This soubroutine calculates the fat content at the surface of the meat as functions

- ' of time and temperature. Experimental fat holding data was utilized to determine
- ' the relationship between time, temperature and fat content. Fat content is expressed
- ' in terms of Fat/Protein ratio.

'Calculate FP at each boundary node

Module - CalculateSurvivors

End Sub

```
logreduction(), logreductionW, Dvalue, Tref, Z, TimeToLimit, TR)
'Calculate the number of surviving microorganisms for eanch node at each time step
'Log-linear inactivation equation
For X = 1 To NumNodes
        If logreduction(X) < 9 Then
                                      'limit solution to 9 log reduction in order to avoid
                                       'computer overload from low numbers as well as because a
                                       '9-log reduction is well above the legal requirement
        If ((Tref - temperature(X)) / Z) > -2 Then
                 d = Dvalue * 10 ^ ((Tref - temperature(X)) / Z)
        Else
                 d = 0.05
        End If
        Nnew(X) = No(X) / (10 ^ (timestep / d))
        If Nnew(X) < 1 Then Nnew(X) = 1
                 No(X) = Nnew(X)
                 logreduction(X) = -Log(No(X) / Ninitial) / Log(10)
        Else
                 logreduction(X) = 9
        End If
        If logreduction(X) > 9 Then
                 logreduction(X) = 9
        End If
'Weibull inactivation equation
        If logreductionW < 9 Then
                 b = 0.00000000011047 * Exp(0.41758 * temperature(1)) '0.03 * (temperature(1)) ^
                     (2.7 * temperature(1)) + 72.19
                 n = 1.12
                 NnewW(X) = NW(X) * (10 ^ (-b * ((timestep / 60) ^ n)))
                 If Nnew(X) < 1 Then Nnew(X) = 1
                          NW(X) = NnewW(X)
                          logreductionW = -Log(NW(X) / Ninitial) / Log(10)
                 Else
                          logreductionW = 9
        End If
Next X
If logreduction(1) <= TR Then
        TimeToLimit = TimeToLimit + timestep
End If
```

Sub CalculateSurvivors(NumNodes, timestep, temperature(), Ninitial, No(), NW(), Nnew(), NnewW(),

Module - CalculateInitialProperties

Sub CalculateInitialProperties(heat capacity f, Meat, Solid, InitialT, InitialM, InitialF, heat capacity, latentW, frozenH, latentF)

'Calculate the initial thermal properties of the product before time-stepping.

moisture = InitialM / 100 'Moisture, decimal wb Fat = InitialF / 100'Fat content, decimal wb Protein = Solid / 100 'Protein content, decimal wb

'Beef

If Meat = 1 Then

If InitialT <= -2 Then heat capacity f = 1.9 * moisture + 1.711 * Protein + 1.298 * FatfrozenH = (1.9 * moisture + 1.711 * Protein + 1.298 * Fat) * 271

'Enthalpy tied up 'in frozen meat 'Latent heat of

water

latentF = 64.4 * Fat

'Latent heat of fat

Else

heat capacity f = 1.9 * moisture + 1.711 * Protein + 1.298 * Fat heat capacity = (4.18 * moisture + 1.711 * Protein + 1.298 * Fat)

frozenH = (1.9 * moisture + 1.711 * Protein + 1.298 * Fat) * 271'Enthalpy tied up 'in frozen meat

latentW = 337.78 * moisture

latentW = 337.78 * moisture

'Latent heat of

water

latentF = 64.4 * Fat

End If

'Pork

ElseIf Meat = 2 Then

If InitialT <= -2 Then

heat capacity f = 1.9 * moisture + 1.711 * Protein + 1.298 * FatfrozenH = (1.9 * moisture + 1.711 * Protein + 1.298 * Fat) * 271

'Enthalpy tied up 'in frozen meat

latentW = 337.78 * moisture

'Latent heat of

water

latentF = 64.4 * Fat

latentF = 64.4 * Fat

'Latent heat of fat

Else

heat_capacity_f = 1.9 * moisture + 1.711 * Protein + 1.298 * Fat heat capacity = (4.18 * moisture + 1.711 * Protein + 1.298 * Fat)

frozenH = (1.9 * moisture + 1.711 * Protein + 1.298 * Fat) * 271

'Enthalpy tied up 'in frozen meat 'Latent heat of

latentW = 337.78 * moisture

'Latent heat of fat

End If

'Turkey

water

ElseIf Meat = 3 Then

If InitialT <= -2 Then

heat_capacity_f = 1.9 * moisture + 1.711 * Protein + 1.298 * Fat frozenH = (1.9 * moisture + 1.711 * Protein + 1.298 * Fat) * 271

rozenH = (1.9 * moisture + 1.711 * Protein + 1.298 * Fat) * 271 'Enthalpy tied up 'in frozen meat

latentW = 337.78 * moisture

'in frozen meat 'Latent heat of

water

latentF = 64.4 * Fat

'Latent heat of fat

Else

 $\begin{aligned} & \text{heat_capacity_f} = 1.9 \text{ * moisture} + 1.711 \text{ * Protein} + 1.298 \text{ * Fat} \\ & \text{heat_capacity} = (4.18 \text{ * moisture} + 1.711 \text{ * Protein} + 1.298 \text{ * Fat}) \end{aligned}$

frozenH = (1.9 * moisture + 1.711 * Protein + 1.298 * Fat) * 271

'Enthalpy tied up 'in frozen meat 'Latent heat of

water

latentF = 64.4 * Fat

latentW = 337.78 * moisture

'Latent heat of fat

End If

End If

Module - CalcBandwidth

Sub CalcBandwidth(NumEle, EleNodeData(), BandWidth)

'This module provided by Dr. Larry Segerlind - Michigan State University

This subprogram evaluates the bandwidth for any group of elements.

- ' The subprogram assumes that triangular elements have as many data
- ' values as rectangular elements. The extra data values are zeros.

```
'Evaluate the bandwidth
```

```
NumEleNodes = 4
MaxDiff = 0
For I = 1 To NumEle
        For J = 1 To (NumEleNodes - 1)
                JJ = EleNodeData(I, J)
                If (JJ = 0) Then Exit For
                For K = (J + 1) To NumEleNodes
                        KK = EleNodeData(I, K)
                        If (KK = 0) Then Exit For
                        Diff = Abs(JJ - KK)
                        If (Diff > MaxDiff) Then
                                 MaxDiff = Diff
                                 Element = I
                        End If
                Next K
        Next J
Next I
BandWidth = (MaxDiff + 1)
```

Module - DecompBandMatrix

Sub DecompBandMatrix(NumNodes, BandWidth, GAM())

'This module provided by Dr. Larry Segerlind - Michigan State University

This subprogram decomposes a symmetric banded matrix into an upper

- ' triangular form using the method of Gaussian elemination. The
- ' matrix is stored in the rectangular array GSM(NumNodalVal%,BandWidth%).
- ' Only the upper part of the banded matrix is stored.

End Sub

'Decompose the global stiffness matrix stored in a rectangular format

```
NumNodalVal = NumNodes * 1
For I = 1 To (NumNodalVal - 1)
       MJ = I + BandWidth - 1
        If (MJ > NumNodalVal) Then
               MJ = NumNodalVal
       End If
       NJ = I + 1
       MK = BandWidth
       If ((NumNodalVal - I + 1) < BandWidth) Then
               MK = NumNodalVal - I + 1
       End If
       ND = 0
       For J = NJ To MJ
               MK = MK - 1
               ND = ND + 1
               NL = ND + 1
               For K = 1 To MK
                       NK = ND + K
                       GAM(J, K) = GAM(J, K) - GAM(I, NL) + GAM(I, NK) / GAM(I, 1)
               Next K
       Next J
Next I
```

Module - ZeroGlobalMatrices

```
Sub ZeroGlobalMatrices(NumNodalVal, BandWidth, GFV(), GSM(), GFV M(), GSM M(),
GFV_F(),
       GSM F(), GCM(), GCM M(), GCM F())
```

'This module modified from a module by Dr. Segerlind - Michigan State University

```
For I = 1 To NumNodalVal
       GFV(I) = 0
        GFV M(I) = 0
       GFV_F(I) = 0
        For J = 1 To BandWidth
               GSM(I, J) = 0
               GSM_M(I, J) = 0
               GSM_F(I, J) = 0
               GCM(I, J) = 0
               GCM_M(I, J) = 0
               GCM F(I, J) = 0
       Next J
Next I
```

^{&#}x27;This subprogram fills the global stiffness matrix and force vector

^{&#}x27; with zero values. This subprogram assumes that the global stiffness

^{&#}x27; matrix is symmetrical and stored in a rectangular format.

9 BIBLIOGRAPHY

- AMI. 2003. AMI Process Lethality Determination Spreadsheet. American Meat Institute. Arlington VA.
- AOAC. 2000. Official Methods of Analysis of AOAC International. AOAC International. Arlington, VA.
- ASHRAE. 1998. ASHRAE Handbook: Fundamentals. American Society of Heating, Refrigerating, and Air-conditioning Engineers. Atlanta, GA.
- Badiani, A., Stipa, S., Bitossi, F., Gatta, P.P., Vignola, G., and R. Chizzolini. 2002. Lipid composition, retention, and oxidation in fresh and completely trimmed beef muscles as affected by common culinary practices. *Meat Science*. 60:169-186.
- Barbut, S. 1996. Determining water and fat holding. *Methods of Testing Protein Functionality*. Blackie Academic and Professional. New York.
- Bejan, A. 1995. Convection Heat Transfer 2nd Ed. John Wiley and Sons. New York.
- Bengtsson, N.E., Jakobsson, B., and M. Dagerskog. 1976. Cooking of beef by oven roasting: a study of heat and mass transfer. *Journal of Food Science*. 41:1047-1053.
- Bimbenet, J.J., Loncin, M., and H. Brusset. 1971. Heat and mass transfer during air drying of solids. *Canadian Journal of Chemical Engineering*. 49:860-865.
- Bird, R.B., Stewart, W.E., and E.N. Lightfoot. 1960. *Transport Phenomena*. John Wiley and Sons. New York
- Bodwell, C.E. and P.E. McClain. 1978. Proteins. *The Science of Meat and Meat Proteins*. Food and Nutrition Press. Westport, CT.
- Chen, H., Marks, B.P., and R.Y. Murphy. 1999. Modeling coupled heat and mass transfer for convection cooking of chicken patties. *Journal of Food Engineering*. 42:139-146.
- Choi, Y., and M. Okos. 1985. Effects of temperature and composition on the thermal properties of foods. Food Engineering and Process Applications, Transport Phenomena vol. 1. Elsevier. London.
- Dagerskog, M. 1979 a. Pan frying of meat patties I. A study of heat and mass transfer. Lebensmittel-Wissenschaft und Technologie. 12:217-224.

- Dagerskog, M. 1979 b. Pan frying of meat patties II. Influence of processing conditions on heat transfer, crust color formation, cooking losses, and sensory quality. Lebensmittel-Wissenschaft und Technologie. 12:225-230.
- Dagerskog, M. and N.E. Bengtsson. 1974. Pan frying of meat patties relationship among crust formation, yield, composition, and processing condition. Lebensmittel-Wissenschaft und Technologie. 7:202-207.
- Datta, A. 2002. Biological and Bioenvironmental Heat and Mass Transfer. Marcel Dekker. New York. pp. 199-215.
- Dincer, I. 1996. Modeling of thermal and moisture diffusions in cylindrically shaped sausages during frying. *Journal of Food Engineering*. 28:35-43.
- Erdogdu, F., Balaban, M.O., and K.V. Chau. 1999. Mathematical model to predict yield loss of medium and large tiger shrimp (*Penaues monodon*) during cooking. *Journal of Food Process Engineering*. 22:383-394.
- Farkas, B.E., Singh, R.P., and T.R. Rumsey. 1996 a. Modeling heat and mass transfer in immersion frying. I., model development. *Journal of Food Engineering*. 29:211-226.
- Farkas, B.E., Singh, R.P., and T.R. Rumsey. 1996 b. Modeling heat and mass transfer in immersion frying. II, model solution and verification. *Journal of Food Engineering*. 29:227-248.
- Fellows, P. 1988. Food Processing Technology: Principals and Practice. Ellis Horwood. New York.
- FSIS. 1999. Performance standards for the production of certain meat and poultry products. *Federal Register*. January 6, 1999. 732-749.
- FSIS. 2001. Performance standards for the production of processed meat and poultry products; proposed rule. *Federal Register*. February 27, 2001. 12590-12636.
- FSIS. 2002. Use of microbial pathogen computer modeling in HACCP plans. FSIS Notice 55-02. December 2, 2002.
- Gardon, R., and J.C. Akfirat. 1966. Heat transfer characteristics of impinging twodimensional air jets. *Journal of Heat Transfer*. 88:101-108.
- Geankopolis, C.J. 1993. *Transport Processes and Unit Operations* 3rd Ed. Prentice Hall. Englewood Cliffs, NJ.

- Hallström, B. 1990. Mass transport of water in foods a consideration of the engineering aspects. *Journal of Food Engineering*. 12:45-52.
- Hayakawa, K. 1970. Experimental formulas for accurate estimation of transient temperature of food and their application to thermal process evaluation. *Food Technology*. 24:89-100.
- Holtz, E. and C. Skjöldebrand. 1986. Simulation of the temperature of a meat loaf during the cooking process. *Journal of Food Engineering*. 5:109-121.
- Housová, J. and P. Topinka. 1985. Heat transfer during contact cooking of minced meat patties. *Journal of Food Engineering*. 4:169-188.
- Huang, E. and G.S. Mittal. 1995. meatball cooking modeling and simulation.

 Journal of Food Engineering. 24:87-100.
- Hung, C.C., Davis, E.A., Gordon, J., and H.T. Davis. 1978. Mechanisms of water loss of bovine semitendinosus muscle dry cooked from the frozen state. *Journal of Food Science*. 43:1191-1195.
- Ikediala, J.N., Correia, L.R., Fenton, G.A., and N. Ben-Abdallah. 1996. Finite element modeling of heat transfer in meat patties during single-sided panfrying. *Journal of Food Science*. 61:796-802.
- Juneja, V.K. and B.S. Eblen. 1999. Predictive thermal inactivation model for *Listeria monocytogenes* with temperature, pH, NaCl, and sodium pyrophosphate as controlling factors. *Journal of Food Protection*. 62:986-993.
- Levy, F.L. 1979. Enthalpy and specific heat of meat and fish in the freezing range. Journal of Food Technology. 14:549-560.
- Mallikarjunan, P., Hung, Y.C., and S. Gundavarapu. 1996. Modeling microwave cooking of cocktail shrimp. *Journal of Food Process Engineering*. 19:97-111.
- Maroulis, Z.B., Kiranoudis, C.T., and D. Marinos-Kouris. 1998. Heat and mass transfer modeling in air-drying foods. *Journal of Food Engineering*. 26:113-130.
- Martin, H. 1977. Heat and mass transfer between impinging gas jets and solid surfaces. *Advances in Heat Transfer*. 13:1-60.
- Mattick, K.L., Legan, J.D., Humphrey, T.J., and M. Peleg. 2001. Calculating Salmonella inactivation in non-isothermal heat treatments from isothermal nonlinear survival curves. Journal of Food Protection. 64:606-613.

- McProud, L.M. and D.B. Lund. 1983. Thermal properties of beef loaf produced in foodservice systems. *Journal of Food Science*. 48:677-680.
- Millsap, S.C. and B.P. Marks. 2002. Modeling condensing/convective heat transfer to food products in moist air impingement ovens. ASAE Paper No. 026045.
- Mannapperuma, J.D. and R.P. Singh. 1989. A computer-aided method for the Prediction of properties and freezing/thawing times of foods. *Journal of Food Engineering*. 9:275-304.
- Mittal, G.S. and J.L. Blaisdell. 1982. Moisture mobility in frankfurter during thermal processing: analysis of moisture profile. *Journal of Food Processing and Preservation*. 6:111-126.
- Mittal, G.S. and J.L. Blaisdell. 1984. Heat and mass transfer properties of meat emulsion. Lebensmittel-Wissenschaft und Technologie. 17:94-98.
- Mittal, G.S. and J. Zhang. 2000. Prediction of temperature and moisture content of frankfurters during thermal processing using neural network. *Meat Science*. 55:13-24.
- Mittal, G.S. and J. Zhang. 2001. Artificial neural network for the prediction of temperature, moisture, and fat contents in meatballs during deep-fat frying. *International Journal of Food Science and Technology*. 36:489-497.
- Mittal, G.S., Blaisdell, J.L., and F.L. Herum. 1982. Moisture mobility in meat emulsion during cooking. *Journal of Food Technology*. 17:709-717.
- Mittal, G.S., Blaisdell, J.L., and F.L. Herum. 1983. Moisture mobility in meat emulsion during thermal processing: analysis of slab moisture profile. *Meat Science*. 8:15-32.
- Murphy, R.Y., Marks, B.P., and J.A. Marcy. 1998. Apparent specific heat of chicken breast patties and their constituent proteins by differential scanning calorimetry. *Journal of Food Science*. 63:88-91.
- Murphy, R.Y., Johnson, L.K., Duncan, L.K., Davis, M.D., Johnson, M.G., and J.A. Marcy. 2001a. Thermal inactivation of *Salmonella* spp. and *Listeria innocua* in chicken breast patties processed in a pilot-scale air-convection oven. *Journal of Food Science*. 66:734-741.
- Murphy, R.Y., Duncan, L.K., Johnson, E.R., and M.D. David. 2001b. Process lethality and product yield for chicken patties processed in a pilot-scale airsteam impingement oven. *Journal of Food Protection*. 64:1549-1555.

- Murphy, R.T., Duncan, L.K., Johnson, E.R., Davis, M.D., and J.A. Marcy. 2002. thermal inactivation of *Salmonella seftenberg* and *Listeria innocua* in beef/turkey blended patties cooked via fryer and/or air convection oven. *Journal of Food Science*. 67:1879-1885.
- Murphy, R.Y., Duncan, L.K., Beard, B.L., and K.H. Driscoll. 2003. D and z values of Salmonella, Listeria innocua, and Listeria monocytogenes in fully cooked poultry products. Journal of Food Science. 68:1443-1447.
- Ngadi, M.O. and L.R. Correia. 1995. Moisture diffusivity during deep-fat frying of chicken drum muscle. J. CSAE. 37:339-344.
- Ngadi, M.O., Watts, K.C., and L.R. Correia. 1997. Finite element method modeling Of moisture transfer in chicken drum during deep fat frying. *Journal of Food Engineering*. 32:11-20.
- Pan, Z. 1998. Predictive modeling and optimization of hamburger patty contact-cooking process. PhD. Dissertation. University of California Davis. Davis, CA.
- Pan, Z., Singh, R.P., and T.R. Rumsey. 2000. Predictive modeling of contact heating process for cooking a hamburger patty. *Journal of Food Engineering*. 46:9-19.
- Pan, Z. and R.P. Singh. 2001. Physical and thermal properties of ground beef during cooking. Lebensmittel-Wissenschaft und Technologi. 34:437-444.
- Peleg, M. and M.B. Cole. 1998. Reinterpretation of microbial survival curves. Critical Reviews in Food Science. 38:353-380.
- Perez, M.G.R. and A. Calvelo. 1984. Modeling the thermal conductivity of cooked meat. *Journal of Food Science*. 49:152-156.
- Roberts, T.A. 1997. Microbial growth and survival: developments in predictive modeling. *Food Technology*. 51:88-99.
- Sanz, P.D., Alonso, M.D., and R.H. Mascheroni. 1987. Thermophysical properties of meat products: general bibliography and experimental values. *Transactions of the ASAE*. 30:283-296.
- Sarkin, R.S. 1978. Computerized cooking simulation of meat products. *Journal of Food Science*. 43:1140-1143.
- Segerlind, L.J. 1984. Applied Finite Element Analysis. John Wiley and Sons. New York.

- Sereno, A.M. and G.L. Medeiros. 1990. A simplified model for the prediction of drying rates for foods. *Journal of Food Engineering*. 12:1-11.
- Shilton, N., Mallikarjunan, P., and P. Sheridan. 2002. Modeling of heat transfer and evaporative mass losses during the cooking of beef patties using far-infrared radiation. *Journal of Food Engineering*. 55:217-222.
- Singh, R.P. 2000. Moving boundaries in food engineering. *Food Technology*. 54:44-53.
- Singh, N., Akins, R.G., and L.E. Erickson. 1984. Modeling heat and mass transfer during the oven roasting of meat. *Journal of Food Process Engineering*. 7:205-220.
- Skala, D., Bastic, M., Bastic, L.J., Remberg, G., and J. Jovanovic. 1989. Thermal behavior of different hog and cattle tissue lipids by DSC analysis.

 Proceedings. 35th International Congress of Meat Science and Technology.

 Roskilde, Denmark. Danish Meat Research Institute.
- Skjöldebrand, C. 1980. Convection oven frying: heat and mass transfer between air and product. *Journal of Food Science*. 45:1354-1362.
- Skjöldebrand, C. and B. Hallström. 1980. Convection oven frying: heat and mass transport in the product. *Journal of Food Science*. 45:1347-1353.
- Smith, S.E., Maurer, J.L., Orta-Ramirez, A., Ryser, E.T., and D.M. Smith. 2001. thermal inactivation of *Salmonella* spp., *Salmonella typhimurium* DT104, and *Escherichia coli* O157:H7 in ground beef. *Journal of Food Science*. 66:1164-1168.
- Stroshine, R. and D. Hamann. 1996. Physical Properties of Agricultural Materials

 And Food Products.
- Thorvaldsson, K. and C. Skjöldebrand. 1995. Water transport in meat during reheating. *Journal of Food Engineering*. 29:13-21.
- Tocci, A.M. and R.MH. Mascheroni. 1998. Characteristics of differential scanning calorimetry determination of thermophysical properties of meats. *Lebensmittel-Wissenschaft und Technologie*. 31:418-426.
- Tsai, S.J., Unklesbay, N., Unklesbay, K., and A. Clarke. 1998. Thermal properties of restructured beef products at different isothermal temperatures. *Journal of Food Science*. 63:481-484.
- USDA. 2002.Pathogen Modeling Program Version 5.1. United States Department of Agriculture

- Van Impe, J.F., Nicoli, B.M., Schellekens, M., Martens, T., and J. DeBaerdemaeker. 1995. Predictive microbiology in a dynamic environment: a system theory approach. *International Journal of Food Microbiology*. 25:227-249.
- Vijayan, J. and R.P. Singh. 1997. Heat transfer during immersion frying of frozen foods. *Journal of Food Engineering*. 34:293-314.
- Voller, V. and M. Cross. 1981. Accurate solutions of moving boundary problems using the enthalpy method. *International Journal of Heat and Mass Transfer*. 24:545-556.
- Whiting, R.C. 1995. Microbial modeling in foods. Critical Reviews in Food Science and Nutrition. 35:467-494.
- Whiting, R.C. and R.L. Buchanan. 1994. Scientific status summary: microbial modeling. *Food Technology*. 48:113-120.
- Young, L.L., Garcia, J.M., Lillard, H.S., Lyon, C.E., and C.M. Papa. 1991. Fat content effects of yield, quality, and microbial characteristics of chicken patties. *Journal of Food Science*. 56:1527-1528, 1541.
- Zanoni, B., Peri, C., Garzaroli, C., and S. Pierucci. 1997. A dynamic mathematical model of the thermal inactivation of *Enterococcus faecium* during bologna sausage cooking. *Lebensmittel-Wissenschaft und Technologie*. 30:727-734.
- Zogzas, N.P., Maroulis, Z.B., and D. Marinos-Kouris. 1996. Moisture diffusivity data compilation in foodstuffs. *Drying Technology*. 14:2225-2253.